

IN THE HIGH COURT OF DELHI AT NEW DELHI
(EXTRA ORDINARY ORIGINAL WRIT JURISDICTION)
I.A. NO. _____ OF 2022

IN
WRIT PETITION (C) NO. 6632 OF 2022

IN THE MATTER OF:

ASHWINI KUMAR UPADHYAY ...PETITIONER

VERSUS

UNION OF INDIA & ORS. ...RESPONDENTS

AND IN THE MATTER OF:

PATANJALI RESEARCH INSTITUTE
(PATANJALI RESEARCH FOUNDATION TRUST)
OPP. PATANJALI YOGPEETH-1,
MAHARISHI DAYANAND GRAM,
DELHI-HARIDWAR NATIONAL HIGHWAY,
HARIDWAR-249405,
UTTRAKHAND, INDIA

....INTERVENOR/
APPLICANT

**APPLICATION UNDER ORDER 1 RULE 8A READ WITH
SECTION 151 OF THE CODE OF CIVIL PROCEDURE, 1908
SEEKING INTERVENTION IN THE PRESENT WRIT PETITION**

MOST RESPECTFULLY SHOWETH

1. That the Applicant/Intervenor is a world class Research Institute backed up with advanced scientific technology and a highly qualified scientists' team and has been set up and is governed by

the Patanjali Research Foundation Trust. The Applicant/Intervenor believes in Nationalism, Ayurved and Yoga as its pillars to create a healthier society and country. The mission of the Applicant/Intervenor is to make India an ideal launch pad for the growth and development of Ayurveda backed with modern scientific evidence and thereby become a pioneer in the said field for the betterment of health and living for the rest of the world.

2. That with the mission of providing scientific evidence for the Ayurvedic practices and treatments, the mandate of Patanjali Research Institute (PRI) is to conduct research using the modern techniques to establish the scientific authenticity of Ayurveda for its global acceptance. Establishing the scientific authenticity of Ayurveda requires research on several aspects, and in order to address this issue, the Applicant/Intervenor has dedicated divisions, namely: (1) Drug Discovery and Development Division (hereinafter “D4”), (2) Herbal Research Division (hereinafter “HRD”), and (3) Ayurveda and Sanskrit Division (hereinafter “ASD”). With the objective of achieving global

scientific acceptance for Ayurveda, the besides engaging in R&D for Ayurvedic drug development, backs up the scientific rationales of Ayurveda with mechanistic studies. The D4 department is an interdisciplinary research unit with four departments: Chemistry, in-vitro biology, in-vivo biology and Microbiology whereas the HRD is mainly involved in taxonomical identification and documentation of the endemic medicinal flora of India, and world and the ASD is engaged in reviving the ancient scientific texts and documents on Ayurveda, and their preservation and translation into modern languages, to fill up the gaps created in our traditional knowledgebase over past few centuries. Despite being in its infancy, with just 5 years since its establishment, the Applicant/Intervenor has already established a compelling body of scientific evidence to explain the rationales behind Ayurvedic principles. These research works of the Applicant/Intervenor are published in different high impact peer reviewed international journals and have received critical appreciation from the scientific community across the world. An exhaustive list of these scientific articles published by the Applicant/Intervenor can be accessed through the link:

<https://patanjali.res.in/research-paper.php> and can be placed before this Hon'ble Court as and when directed.

3. That the Applicant/Intervenor works on a disease driven approach to provide remedial solutions, through Ayurvedic drug development, and scientific evidence for safety and efficacy of these drugs through meticulous experimental studies using cutting-edge technologies in a state-of-the-art research facility. The main disease areas currently targeted by the Applicant/Intervenor are inflammation, metabolic disorders, cancer, neuroscience and infectious diseases. The scientific validations of the functioning of the Ayurvedic formulations and deciphering of their mode-of-actions are done through a combination of different experimental approach, uniquely designed for each formulation. These combinations include chemical characterizations (for functional and safety traceability), in-vitro biological evaluations using cell lines (for understanding the mode-of-action), in-vivo biological evaluations through different scientifically authenticated disease models of animals (rats, mice and zebrafish), and microbiological evaluations (in

case of studies involving formulations against infectious diseases).

4. That the Applicant/Intervenor has had the exalted vision to bring Ayurveda to the society in a more contemporary form and to unravel the mystery behind this haloed and revered ancient Indian system of medicine by exploring and selecting indigenous herbs, ancient Ayurvedic literatures and subjecting the formulations to modern pharmacological, toxicological safety tests and clinical trials as mandated by the concerned Government agencies from time to time so as to create new drugs and therapies for society, with a specific focus on the poor and down-trodden who can't avail modern medical facilities. Furthermore, Ayurveda is one of the oldest Indian system of medicine which means 'Science of life' with an integrated way of dealing with health and nature derived medicine, the very basic method of the said science is to ensure that any individual can achieve a strong and robust natural immunity which is the most certain method to ensure better health and a robust response in case of any infection. Unfortunately, due to lack of scientific evidences, this valuable treasure handed over to us by our progenitors has not

been extensively explored. As such the Applicant/Intervenor herein has specifically worked to ensure that the science of Ayurveda, backed up with scientific data as mandated for allopathic interventions, is made available to showcase the benefits of Ayurveda to one and all.

5. That in order to ensure the efficacy of ancient Indian knowledge and Ayurveda the Applicant/Intervenor has been set up as the Patanjali Research Foundation Trust, wherein till date an investment of more than Rs. 100 Crore has been made towards setting up the state of art infrastructure therein to conduct research in relation to ancient Indian knowledge of Ayurveda and subsequent testing of the products so developed on its basis. Such efforts have gone a long way in developing various medicinal products which are manufactured without using harmful chemicals. In addition to this, the said approach has also lead to the said ancient Indian knowledge being recognized globally as evidence based science rather than being mere anecdotal in nature.

6. That furthermore, the Applicant/Intervenor has been established to bring scientific fervor to the ancient art of Ayurveda. It is not an institute which has been set up for profit or for gain but is an institute set up for the greater good of human kind wherein the long lost traditions of Ayurveda have been used and subjected to scientific manufacturing methods leading to integration of home remedies with scientific studies of contemporary healing practices. It is further tasked with the onerous duty of breakthrough research in the field of Ayurveda to further consolidate on the already vast knowledge in the field of Ayurveda.
7. That the Applicant/Intervenor has consistently worked towards the upliftment of the society. In the current pandemic, the Applicant/Intervenor has made a contribution of about Rs. 25 Crores towards the PM-Cares Fund as its contribution towards helping people affected with the novel Coronavirus i.e. COVID-19. The Applicant/Intervenor has also further taken the initiative to teach Yoga across various health centers, provide free food and water to the poor, as well as provide Free Food and water to the

frontline workers in the state of Uttarakhand including the state Police as well as the CRPF personnel deployed in the state.

8. That for the purpose of the present Application, the Applicant/Intervenor endeavors to enliven the aspect of Ayurveda and how Ayurveda should be used in consonance with modern medicine under various heads while also highlighting the lacunae within the current healthcare system of India, the challenges being faced by the allopathic field of medicine, general medical management using Ayurveda and the desirous outcome of using Ayurveda with Allopathy.

9. That the Applicant/Intervenor has made key scientific contributions towards authentication of Ayurvedic treatments for different diseases as specified below in brief detail :

A. Inflammatory disorders - Rheumatoid Arthritis, Arthritis, Ashthma, Psoriasis and Dermatitis. The Applicant/Intervenor has researched and formulated the following :

- i. Herbo-mineral Formulation Ashwashila
- ii. Divya Amvatari Ras

- iii. Peedanil Gold
- iv. Divya-Swasari-Kwath/ Divya-Swasari-Ras
- v. Sahastraputi-Abhrak-Bhasma
- vi. Malla Sindoor
- vii. Biotite-Calx Based Traditional Indian Medicine
Sahastraputi-Abhrak-Bhasma

B. Psoriasis and Dermatitis.

- i. Divya-Kayakalp-Vati
- ii. Divya-Kayakalp-Oil – derived from oil extracted
from *Withania somnifera* (Ashwagandha)

Lifestyle Disorders

C. Cardiac Hypertrophy/ High Blood Pressure/ Hypertension

- i. Yogendra Ras

D. Liver dysfunction

- ii. Divya Sarva-Kalp-Kwath' also known as
'Livogrit' - A Herbal Formulation of *Boerhavia
diffusa*, *Phyllanthus niruri* and *Solanum nigrum*

E. Infertility.

- i. Oils obtained through SCFE from the seeds of

Putranjiva roxburghii Wall. (Putrajeevak) and
Bryonopsis laciniosa (Shivlingi)

- ii. Fluid Extract of Bryonopsis laciniosa (Shivlingi) Seeds
- iii. Immunity boosters

F. Overall Immunity

- i. Chyawanprash,
- ii. Divya-Herbal-Peya

G. Cancer

- i. Pistacia integerrima (Kakrasinghi) containing
phytocompound, penta-O-Galloyl- β -D-Glucose,

H. Neuroscience

- i. Divya-Peedantak-Vati
- ii. Herbal Decoction Divya-Peedantak-Kwath

I. Infectious diseases

- i. Withanone, present in Coronil
- ii. Tinospora cordifolia (Giloy)
- iii. Divya-Swasari-Vati
- iv. Anu taila
- v. Denguenil Vati for treatment of Dengue
- vi. Roots of Ashwagandha

A detailed write-up with relevant citations and studies is annexed herewith and marked as ANNEXURE A-1.

STRUCTURE OF HEALTHCARE SYSTEM IN INDIA

10. That the healthcare delivery in India is classified under three categories – primary, secondary and tertiary care. All three levels need to work in a cohesive manner to help delivery of healthcare on all the four pillars. In the healthcare system (HCS) of India, Sub-Centres and Primary Health Centres form the primary level of Healthcare system; Community Health Centre contribute to the secondary level of HCS while hospitals and medical colleges are considered in the Tertiary level of the Healthcare system.

11. That the Primary Health Care Infrastructure has been developed as a three-tier system with Sub Centre, Primary Health Centre (PHC) and Community Health Centre (CHC) being the three pillars of Primary Health Care System in India. As of 31.03.2021, there are 25,140 PHCs and 5,481 CHCs along with 1,56,101 sub-centres in Rural areas and 5,439 PHCs, 470 CHCs and 1,718 sub-centres in Urban areas as per the Rural Health Statistics Report, 2020-21 by the Government of India, Ministry of Health & Family Welfare. Over

the years, a number of PHCs have been upgraded to the level of CHCs in many States. The factual position in urban areas is that the Sub-centres are not envisaged in the urban areas as distances and mode of transportation are much better there and also has a closer proximity and accessibility of health facilities. Per the said report, only in PHCs, where there was a requirement of a minimum of 5,439 doctors, more than 1,530 positions remained vacant and despite sanctioning of 8229 doctors, there was a shortfall of 537 doctors.

STATUS OF HEALTH CARE PROFESSIONALS

12. That before the Applicant/Intervenor avers to the subject matter of the present Petition, it is important to look at the status of healthcare professionals in the country subsisting as on date. The Union Minister of State Health and Family Welfare stated that as per information provided by the Indian Nursing Council (INC) records, there are around 8,92,829 Auxiliary Nurse Midwives (ANM), 21,51,850 Registered Nurses and Registered Midwives (RN&RM) and 56,644 Lady Health Visitors (LHV) in the Country and there is availability of 1.4 bed per 1000 people. All these estimates are well below the WHO threshold of 44.5 doctor, nurses and midwives per

10,000 people whereas the current situation is 20.6 health workers per 10,000 people.

13. That a recent study published in March, 2021 titled “Size, composition and distribution of health workforce in India” reported that a substantial proportion of active healthcare workers were found to be not adequately qualified while on the other hand more than 20% of qualified health professionals were not active in labor markets.

14. That the above mentioned data effectively reflects a highly skewed distribution of health workforce across states meaning thereby that a significant majority of people are not able to receive quality medical treatment at rural level where the majority of population resides. This situation, in view of the dire need for medical care that is more accessible and of a better standard, is highly un-ethical and illegal and results in depriving diseased individuals from receiving the necessary medical care and attention due to their inability to pay exorbitant health expenses.

15. That as per information provided by the Board of Governors in supersession of Medical Council of India (MCI), a total of 12,55,786

allopathic doctors are registered in the Medical Council. Out of these, 3,71,870 allopathic doctors have registered their specialist/post-graduate qualification with Medical Council of India/State Medical Council. As per the Report of High Level Group on Health Sector of 2019 submitted to the Fifteenth Finance Commission of India, the current doctor-population ratio in India is 1:1511. However, the World Health Organization (hereinafter “WHO”) has promulgated the desirable doctor–population ratio as 1:1,000. This further evidences why our Country is facing various such obstacles in becoming a medically sound super nation.

16. That contrastingly, under the alternative methods of medicine, there are an approx. 7.88 lakh Ayurveda, Unani and Homeopathy (AUH) doctors in the country. Even assuming an 80% availability of such practitioners, it is estimated that around 6.30 lakh Ayurveda, Unani and Homeopathy (AUH) doctors are available for service. Such numbers when considered along with allopathic doctors allows for a much improved doctor-population ratio of 1:834, as propounded by Dr. Bharati Pravin Pawar, the Ld. Health Minister of India on December 1, 2021 . Such an improved predicted ratio is in consonance with the desirable ratio laid down by the WHO. In view

of such compelling data, it is pertinent that the Respondent No. 1 be directed to take into consideration the lacunae in the current medical system resulting in the detriment to the health of the general public and with the possibility of bettering the access of the common man to a medical health care system with a higher standard and efficacy by bringing the practitioners of both allopathic and alternative medicines under the same roof.

LACKING HEALTHCARE INFRASTRUCTURE

17. That according to the recent Report on Rural Health Statistics, 2020-21 published by the Ministry of Health and Family Welfare, while the number of allopathic doctors at Primary Health Centres (hereinafter “PHC”) increased from 20308 in 2005 to 31716 in 2021, which is about 56.2% increase, there is shortfall of 4.3% of allopathic doctors at PHCs. Further, specialist doctors at CHCs have increased from 3550 in 2005 to 4405 in 2021. However, as compared to requirement for existing infrastructure, there is a shortfall of 83.2% of Surgeons, 74.2% of Obstetricians & Gynecologists, 82.2% of Physicians and 80.6% of Pediatricians. Overall, there is a shortfall of 79.9% specialists at the CHCs as

compared to the requirement for existing CHCs. Most functioning rural health facilities were further found to be deficient in essential medical equipment/ medicine as nearly 30% of the Sub Centres did not have regular water supply, 26% lacked electricity and 11% did not have all-weather connecting roads. While, 63% PHCs did not have an operation theatre, 29% even lacked a labor room. According to data supplied by the Health Management Information System of Respondent No. 1, there was a huge shortfall of surgeons (83.4%), obstetricians & gynecologists (76.3%), physicians (83.0%) and pediatricians (82.1%). Overall, there was a shortfall of 81.2% specialists at the CHCs vis-a-vis the requirement for existing CHCs. Finally, as per the Rural Health Statistics 2019-20, there is a total shortfall of 2,65,551 rural health care workers in India.

18. That when it comes to treatment preferences of people in India, more than 70% of the population (72% in rural areas and 79% in urban areas) with spells of ailment were treated in the private sector, consisting of private doctors, nursing homes, private hospitals and charitable institutions. Furthermore, in rural India, 42% of hospitalized treatment was carried out in public hospitals while in urban India, the corresponding figure was 32%.

19. That since both rural and urban India depend mostly on private hospitals for treatment, the general spending for hospitalization has also been higher as a result. The NITI Aayog's Report titled Health Insurance for India's Missing Middle dated October, 2021 stated that almost 60% of all hospitalizations, and 70% of out-patient services are delivered by the private sector (NSSO's 75th Round survey on Social Consumption of Health, 2017-18). Furthermore, highest expenditure was recorded for treatment of cancer which, excluding the cost of consultations and diagnostics, ranges anywhere from Rs. 1-6 lakh for surgery, Rs. 2.5 – 22 lakh for radiation therapy, Rs. 5-50 lakh for chemotherapy and targeted/immunotherapy and post treatment costs being exorbitant as well depending on the stage and remission of the same. Similarly, on an average, for cardiovascular diseases the cost for treatment would range anywhere from Rs. 30,000 to Rs. 8 lakh in private hospitals. To address this skewed treatment, policy frameworks in several states have mandated compulsory rural service of 1-5 years during postgraduate medical studies. Further, some states require medical officers to practice medicine in rural areas for a particular period after postgraduate studies. However, poor living and working

conditions, irregular drug supply, weak infrastructure, professional isolation and the burden of administrative work are just some of the challenges faced by doctors on rural postings, stated a 2017 study by the Public Health Foundation of India.

20. Hence, in the present scenario, modern medicine has remained to be a chief medical source to treat several illnesses but being the only solution, has enhanced our dependency on this medicinal practice. It has led to significant loss of both our health and simultaneously wealth also as we are solely dependent to adopt the medicinal strategies proposed by modern medicine.

21. That additionally, the reliance on pharmacies makes a big dent in family budgets for medical treatment in India. As per the Household Health Expenditures in India Report released in 2016, pharmacies accounted for 52% of the out-of-pocket expenses incurred for buying medicines, 18 times more than the expenses incurred in general government hospitals (3%), more than two times the expenses in private general hospitals (22%). In India, 65 per cent of health expenditure is out-of-pocket, and such expenditures push some 57 million people into poverty each year.

22. That the Applicant/Intervenor now refers to the grass root level which is responsible for creating a base for the medical industry in India. As of 2018, India had 497 medical colleges registered with the Medical Council of India that together offer an intake capacity of only 60,680 seats for MBBS all over the country. Trends in India, as well as other BRICS nations such as South Africa, suggest that most doctors prefer to sign up for hospital-based specializations in urban areas than get into general practice at PHCs.

AYURVEDA AND ITS SCOPE

23. That among all the cultures of the world, Indian civilization is not only ancient but also unique. The Vedas are the root and basis of our culture and civilization and are one of the oldest scriptures in the world. Ayurveda is the oldest treatise related to treatment and health and is believed to be a part of the Atharvaveda, one of the four Vedas. Ancient learned sages described Ayurveda as ‘immortal’ in support which there are three reasons: “Soya, māyurvedaḥ śāśvato nirdīśyate, anāditvāt, Svabhāvasaṁsidhalakṣaṇatvāt, bhāvasvabhāvanityatvācca” (Caraka Samhitā- Sūtra Sthāna 30/26) which translates to ‘That which is Ayurveda, in itself is complete, eternal and immortal. It regulates the behavior of the mind and

emotions'. In Indian culture, the four most valuable objectives of human life are dharma, artha, kāma and mokṣa - duty, wealth, desire and liberation, which helps to attain self-realization and gain freedom from the cycle of birth and death and come closer to God. The actual resource and base for the attainment and accomplishment of these four great values is a healthy body which is entrenched in the sanskriti shloka "Śarīrmādhyam khalu dharma sādhanam", meaning 'the means by which one can achieve one's own duty resides only in a healthy body'. Ayurveda propounds that a healthy person who is free from all ailments can work harder, follow a balanced routine in a proper manner and perform his/her daily work more efficiently and serve the family, society and his/her nation in a better way.

24. That the importance and utility of an Ayurveda treatise has been questioned and subsequently answered as: "Prayojanam cāsyā svasthasya svāsthyarakṣaṇamāturaṣya vikārapraśamanam ca" (Caraka Samhitā Sūtra Sthāna 30/26) meaning 'the objective of Ayurveda is to protect the health of a healthy person and cure all the ailments of a sick person'. Ayurveda therefore, is a practice of principles of high idealism and is an exceptional system of medicine

which lays significant emphasis on diet, what to eat and what not to eat, and explains that eradicating the cause of a disease is the first step to cure it. “Samkṣepataḥ kriyāyogo nidana parivarjanam” which means 'first of all eliminate the cause of the disease.' To prove its objective Ayurveda describes the ways and means to safeguard the health and also the reasons due to which diseases develop in the body. The most significant of all such shlokas is: “Hitāhitam sukham duḥkhamāyustasya hitāhitam. mānam ca tacca yatroktamāyurvedaḥ sa ucyate” (Caraka Samhitā Sūtra Sthāna 1/41) which means ‘the science that describes the diet to be taken and not to be taken, as well as the good duration of life, bad duration of life, happy span of life and unhappy span of life is termed as Āyurveda.’ In view of the above therefore, Ayurveda is the name given to an optimal and healthy lifestyle. It is the knowledge of life and the science which makes human life healthy and happy on all levels and is not merely the science that gives knowledge of treatment of disease through herbal medicines but it is a complete guide, an overview and a life philosophy leading to a healthy human life. Ayurveda not only describes the medicines for the well-being of a patient but it also maintains and safeguards the health of a healthy person.

25. That in India, Ayurveda is brought forward to the public domain by some important players and their products are very popular as therapeutics with the general population. Since, these Ayurvedic medicines come under schedule E drugs, they are available over the counter and can be prescribed by any system of medicine. In fact, the Applicant/Intervenor's own medicinal formulations like that have been found to protect liver ischemia reperfusion through the modulation of redox homeostasis and anti-oxidant levels.

26. That only because allopathy is accepted worldwide, it does not render our natural and ancient remedies as ineffective. It essentially only signifies that the rest of the world did not adapt to what it never had. Indian culture being one of the oldest in the world had always relied on natural remedies and the Applicant/Intervenor even today is in the business of keeping that tradition alive. At the cost of repetition, it is being stated again that the Applicant/Intervenor is not advocating for usage of Ayurvedic medicine only, it is just to bring to the notice of the Hon'ble Court that the science of Ayurveda needs to run in tandem with the modern science.

**BENEFICIAL AND EFFECTIVE USE OF AYURVEDA IN
MANAGEMENT OF VARIOUS AILMENTS**

27. That Ayurveda has also proven to be beneficial for various other diseases. It has been used for helping in the management of acute and chronic dermal, respiratory, liver, cardiac, and neuronal diseases.

28. That in chronic reoccurring dermal and joint inflammatory disease like psoriasis or eczema (atopic dermatitis), caused by growth of keratinocytes, and influx of inflammatory cells into the dermal region releasing pro-inflammatory mediators, evidence has shown that herbal formulation application can provide significant prolonged relief. In a single-blind, placebo-controlled study involving adult (>18 years old) psoriasis patients, treatment with Seabuck thorn (*Hippophae rhamnoides*) extract improved their 'Psoriasis Area Severity Index' (PASI) scores and 'Dermatology Life Quality Index' (DLQI) scores, compared to the baseline values. The Seabuck thorn extract treatment significantly reduced the dermal inflammatory lesions present in the patients within a time period of four and eight weeks. Oil derived from the pulp of Seabuck thorn fruit was found to high in nutrient value with the presence of several essential fatty

acids. Using psoriasis animal model, it was observed that Seabuck thorn oil significantly reduced the pro-inflammatory cytokine production and generation of reactive nitrogen species reducing the associated inflammatory lesion levels. Similarly, other traditional herbal medicines belonging to ancient medicinal systems have also been found to be effective in healing Psoriasis like inflammation, for example, *Curcuma amada* (Ayurvedic medicine), *Humulus lupulus* (Occidental Monastic Medicine and Ayurvedic medicine) and *Hypericum perforatum* (Occidental Monastic Medicine) inhibited inflammation markers and reduced growth of keratinocytes. Ashwagandha (*Withania somnifera*) has been recommended as a magic bullet plant in healing inflammation and having anti-viral effects. Pre-clinical analysis of fatty acids extracted from Ashwagandha (*Withania somnifera*) plant have been observed to ameliorate psoriasis like dermal inflammatory lesions through the reduction of pro-inflammatory cytokines in psoriasis-like disease animal models. A copy of the medical literature with relation to benefits of Ayurveda is annexed herewith as ANNEXURE A-2 (copy).

29. That furthermore, traditional Indian plants, Ashwagandha (*Withania somnifera*) and Indian Echinacea (*Andrographis paniculata*),

Turmeric (*Curcuma longa*), Neem (*Azadirachta indica*) have been found to have anti-viral efficacy against influenza virus and reduce associated cough and cold. Through molecular docking/ simulation, Withaferin, a compound present in the *Withania somnifera* was found to bind and inhibit the neuraminidase activity of H1N1 influenza virus. That Andrographolide present in *Andrographis paniculata* and curcumin present in *Curcuma longa* has been observed to reduce the respiratory inflammation in the lung cells through the modulation of associated pathways such as NF- κ B, and JAK-STAT. *Azadirachta indica* contains a Hyperoside that binds to the influenza virus nucleoprotein. Ayurveda based herbal decoction of Divya-Swasari-Kwath has been found to reduce inflammation induced in the lung of mouse model using ovalbumin through the increase in Nrf-2 mediated antioxidant levels. Furthermore, research showed that the anti-inflammatory activity of the Divya-Swasari-Kwath has been attributed phyto components and linked to the presence of phytochemical such as Rutin, Glycyrrhizin, Gallic acid, Cinnamic acid, Chlorogenic acid, Caffeic acid and Piperine. A copy of the medical literature with relation to benefits of Ayurveda is annexed herewith as **ANNEXURE A-3.**

30. That traditional herbal formulations have been found to have anti-viral efficacy against other viral diseases. Dengue virus is a prominent arbovirus in Southeast Asia which is an enveloped positive-sense ssRNA virus of the Flaviviridae family. The virus is transmitted through mosquito bites and classical clinical manifestations can include fever, headache, myalgias, joint pains, nausea, vomiting, skin rash, and life-threatening hemorrhagic diseases, specifically dengue hemorrhagic fever/dengue shock syndrome (DHF/DSS) in severe cases. Ayurveda based pentaherbal medicine Denguenil Vati developed using traditionally described herbs Giloy (*Tinospora cordifolia*), Aloe vera (*Aloe barbadensis*), Papaya (*Carica papaya*), Anardana (*Punica granatum*) and Tulsi (*Ocimum tenuiflorum*) was found to inhibit Dengue viral propagation along with hepatocyte necrosis, liver inflammation and red blood cell (RBC) infiltration. The formulation also inhibited the disease-induced expression of apoptotic marker Angiopoetin2 (Ang-2) and pro-inflammatory chemokine marker CCL3 in a novel Zebrafish model. The anti-viral effect of Denguenil Vati formulation was found to originate from gallic acid, ellagic acid, palmetin, and berberine molecules in the Denguenil formulation. *Terminalia*

chebula has also been shown to function as broad-spectrum antiviral agents against several viruses including Dengue virus. The anti-viral activity of the *Terminalia chebula* plant has been attributed to the presence of phytochemicals such as chebulagic acid and punicalagin that interfere with the free Dengue virus particles and interfere with their attachment and fusion events during early viral entry. Using molecular docking based evidence, Gedunin and Pongamol present in the plant Neem (*Azadirachta indica*) has been found as a potential candidate for inhibition Dengue virus host attachment and propagation through interaction with its proteins NS3 RNA polymerase, NS3 protease helicase, capsid and envelope proteins. A copy of the medical literature with relation to benefits of Ayurveda is annexed herewith as **ANNEXURE A-4**.

31. That additionally, traditional herbal formulations have been found to heal different diseases and injuries relating to the liver. Traditional herbal tri-herbal formulation Divya-Sarvakalp-Kwath composed of *Boerhavia diffusa*, *Phyllanthus niruri*, and *Solanum nigrum* has been found to reduce industrial chemical carbon tetrachloride induced liver damages in human liver cell lines and animal models. Additional research has showed that Divya-Sarvakalp Kwath also

inhibited alcohol and non-alcoholic (fatty acid) induced liver steatosis in human liver hepatocyte. Divya-Sarvakalp-Kwath treatment reduced inflammation, lipogenesis processes along with reduction in intracellular lipid contents.

32. That furthermore, the heart is a major organ involved in the perfusion of blood and oxygen demands to the distal organs. Cardiac hypertrophy is induced through physiological stress, which produces stimuli to the cardiomyocytes to grow in length and width. Physiologically, this leads to an increase in cardiac pump function while decreasing ventricular wall tension. It is also accompanied by an increase in the left ventricular wall thickness as a response for reducing systolic and diastolic stress on the left cardiac wall. Long-term persistence of Cardiac Hypertrophy leads to heart failure arrhythmia and sudden death. Ayurveda has proposed several herbal formulations for the treatment of heart-based abnormalities. Arjuna (*Terminalia arjuna*) plant has been found to present one of the finest evidence of plant based herbal remedy for cardiac morbidities. *Terminalia arjuna* bark extract has been found to provide protection against drug induced toxicities and induction of cardiac hypertrophy through amelioration of inflammation and oxidative stress. Recently,

Ayurveda polyherbal formulation Divya-HridyAmrit-Vati containing *Terminalia arjuna* bark extract has been found to inhibit drug induced cardiac hypertrophy. Also, Divya-HridyAmrit-Vati reduced cardiac hypertrophy through rebalancing of redox homeostasis and modulation of cardiac hypertrophy related genes.

33. That Ayurvedic herbal medicines have also been applied for the treatment of neurological disorders. Sankhpushpi (*Convolvulus prostrates*) has been found to function as a cognitive enhancer that helps in various neurodegenerative etiologies. The plant contains bioactive phytoconstituents, such as, alkaloid (convolamine), flavonoid (kaempferol) and phenolics (scopoletin, β -sitosterol and ceryl alcohol), that have been ascribed to its medicinal properties. Other plants that have been attributed with neuroprotective and neurogenerative properties are *Bacopa monnieri*, *Terminalia chebula*, *Woodfordia fruticose*, and *Acorus calamus*.

34. That in lieu of the above plant based research, it is also important to mention that commonly preferred allopathic medicines are also chiefly comprised of approximately 40% plant derived components. Such constitution of general allopathic medicines of constituents of Ayurveda, Unani and Siddha traditional medicines, then it only

flows naturally that the Respondent No. 1 as also the general medical community accept Ayurveda as part of the regular medicinal support system. Choice of plant-based material as raw constituents to prepare medicine also stands to benefit the Indian farmer as also better their current plight by way of consequent increase of cultivation of such by generating income, as well as generating revenue for the State and ultimately reduce the state of the overburdened medicinal system.

INTERNATIONAL SCOPE OF TRADITIONAL MEDICINE

35. That there is now a startling new research aligned with data that truly necessitates the use of certain herbs for Covid-19 prevention and treatment. On the data front, it can be seen that China and Madagascar controlled/eliminated the Coronavirus by mandating the use of certain herbal formulas. China mandated the use of a Traditional Chinese Medicine (TCM formula containing *Hypericums*, *Inula racemosa*, *Andrographis* and *Glycyrhizza*) which saw such startling positive results with the Covid virus dying within a period of two months in China. Also, Madagascar promoted the use of organics containing *Artemisia* and neem. Not only did the

mortality rate in their country shoot down but went below 0.5 % for every country that used Covid Organics.

36. That the Applicant/Intervenor is of the thought that the best way to encounter these problems is by adoption of the proposed holistic integrated medicinal approach mentioned hereinabove, which will comprise of a combination of modern medicine along with traditional and complementary medicine at level of education, training, practice and policies & regulations to enhance status of health care sector in India It may also be stated that this is not the first time that an integrated health system has been proposed in the world. These practices have remained in existence from past more than 70 years in different countries of world for example China, Japan, Korea and Germany. In these countries traditional and contemporary medicines run parallel in accordance with modern medicine. They have specific framework to integrate it along with modern medicine as part of their regular educational curriculum, training program and status of these traditional practitioners have been legalized by the respective Governments. These practitioners are honoured with equal rights to that of modern medicine unlike

India where inspite of having nearly thousand years of history is still not being recognised as a competent mode of treatment.

37. That continuing with the advantages of Ayurveda, it is also a relevant factor to note that the World Health Organisation recognizes Ayurveda as a Traditional Medicine(TM) being one of the oldest existing therapeutic system used by humanity for health and wellbeing. The WHO also clearly states that TM is being formally used within existing health-care systems and when practised correctly, TM can help protect and improve citizens' health and well-being.

38. That planning and execution of policies for mainstreaming of traditional medicines (TRM) of respective countries along with conventional system of medicine (allopathy), first in the country of origin followed by the international arena, is the priority agenda of operations of WHO. Within the Indian context, WHO accorded prime focus to Ayurveda in its activities related to Traditional Medicines. Sponsorship and encouragement of studies substantiating parameters of standardization, safety and efficacy of herbal medicines of Ayurveda are under chief consideration of WHO. That Respondent No. 2 and Central Council of Research in Ayurveda and

Siddha are several collaborative centers of WHO in India which are assigned with Appraisal Project Work (APW) and Direct Financial Cooperation (DFC) projects that are set to strengthen Ayurveda as evidence-based medicine for its global acceptance. Implementation of pharmacovigilance program in Ayurveda, publication of documents for rational use and initiatives to prepare consumer guidelines for appropriate use of Ayurvedic medicines are some other contributions of WHO toward advancement of Ayurveda at national as well as global level.

39. That WHO to accomplish its duties regarding Traditional Medicines, in 2003, at the 56th Session of the WHO Regional Committee for South-East Asia, decided that measures should be taken to protect, preserve and improve traditional knowledge and medicinal plant resources for sustainable development of Traditional Medicines. Subsequently, WHO Commission on Intellectual Property Rights, Innovation and Public Health (CIPIH) was formed. This Commission is examining contribution of Traditional Medicines in improving healthcare and suggesting developmental measures for the same. The role for WHO has been identified which is as follows:

- i. To facilitate the efforts of interested member states in formulating national policies and regulations on traditional, complementary and alternative medicine, and promoting the exchange of information and collaboration on national policy and regulation of TRM among member states;
- ii. To provide technical support for the development of methodologies to monitor or ensure product quality, efficacy and safety, preparation of guidelines, and promotion of exchange of information; and
- iii. To provide technical support to member states in defining indications for the treatment of diseases and conditions by means of TM.

40. That to put matters in context, the demand for herbal products worldwide has increased at an annual rate of 8% during the period of 1994–2001, and according to WHO forecast, the global herbal market would be worth \$5 trillion by the year 2050. As of today, Europe and the United States are two major herbal product markets in the world, with a market share of 41% and 20%, respectively. This data is in consonance with the emerging interest surrounding

the international potential for Ayurvedic products. From the foregoing, it is clear that Ayurveda is undergoing a phase of resurgence and revival “in the world” similar to the one in India and yet the Respondent No. 1 fails to take note of the same.

41. That Likewise, in countries of the South-East Asia Region, although modern medicines are now increasingly available throughout different levels of health care, Traditional Medicine has maintained its popularity since it has been used for generations in the past and hence there is increase in trade among countries in medicinal plants and traditional remedies as well. All Member Countries of the SouthEast Asia Region (SEAR) have been developing and strengthening their TM programmes in primary Traditional Medicine in the WHO South-East Asia Region health care. Traditional systems of medicine in South-East Asia Region Countries of SEAR have a rich heritage of various systems of traditional medicine. Bangladesh, India, Nepal and Sri Lanka have people practising Ayurveda, Unani and /or Siddha Medicine(s). Traditional Medicine known as Jamu has flourished in Indonesia. The traditional medicine in DPR Korea is Koryo medicine while the Traditional Medicine of Maldives is called Dhjivehi Beys. Bhutan, Myanmar and Thai traditional

medicines also are practised in their respective countries. Thus, systems of traditional medicine in various countries of the Region have a significant role to play in the provision of health care as they are being used by those living in the cities as well as by the majority of the population who live in the rural areas. Apart from these systems, homoeopathy, nature cure and yoga are also practised in a number of countries of the Region.

42. Thus, the Ayurvedic medicines are not only documented in our ancient texts, but there is a large body of scientific evidence accumulating that testifies the effectiveness of these medicines against several chronic, lifestyle and communicable diseases. With the second wave of COVID-19 pushing the healthcare infrastructure of our country to a precipice, it is time that traditional forms of medicine with scientific evidence are integrated with modern medicine. That the ministry of AYUSH with the minimal resources available to it has still managed to make some development in the field of propagating traditional methods of medicine. That despite the Respondent No. 2's attempt over the years to popularize Ayurveda, Yoga or Naturopathy Unani, Siddha and homoeopathy practices, the people at large are still inclined towards allopathy

treatment both in rural and urban India for various ailments that could be dealt with effectively by ayurveda. One major reason for such preferences is the negligence of AYUSH practitioner in providing the necessary substantiation to their medicinal protocol. A number of educational institutes, training centres, as well as current infrastructure is not upto mark to make people believe in this therapeutic solution. Modern medicine practitioners have remained confined to their own niche which has restricted them to avail knowledge of other medicinal practices and thereby cannot benefit the diseased individuals by using other therapeutic regimens. Moreover, the established provisions regarding their practice doesn't permit them to collectively practice available medicinal systems in order to provide maximum health benefits. Henceforth, it is highly needed to establish integrated medicinal system to enable those practitioners who are willing to prescribe medicines of other domains too.

ROLE OF AYURVEDA IN COVID-19

43. That having examined various facts about the present healthcare system, the Applicant/Intervenor relies on how Covid-19 should have changed India's outlook towards medical infrastructure. That in

December 2019, the entire world witnessed the initiation of the novel Coronavirus or Covid-19. The virus originated from a single point and spread rapidly to all countries in a matter of few weeks inasmuch as majority of the countries witnessed a total and nationwide lockdown by March 2020 to curb the spread of the Covid-19 virus.

44. That for that matter even India witnessed a nationwide lockdown in March 2020 with the Government of India warning the Indian population against the deadly effects of Covid-19 vide Notification dated 06.03.2020. To combat the said disease, the Ministry of Ayush was also tasked by the Government of India to ascertain how the field of Ayurveda can be of assistance in the fight against the pandemic. Thus the Ministry of Ayush formulated guidelines on the said aspect and itself defined COVID-19 as a virus that causes fever/flu and respiratory illness and published various notifications regarding the same. Keeping the same in view, the Applicant/Intervenor had already started conducting tests of its medicines/ ayurvedic formulations/ herbal remedies to fight the symptoms of Covid-19 by seeking to ensure an immune response in the body by boosting the immunity levels of an individual. It is

relevant to mention that various allopathic interventions for treatment of COVID-19 also use this method of generating an immune response in some form or the other, however the same was sought to be attained through drugs/steroids.

45. Predicated on the above belief, the Applicant/Intervenors also took a conscious decision to undertake a clinical trial to develop a medicine to fight flu like symptoms identical to that of Covid-19. It is also relevant to mention that the said Ministry is a recognized Ministry under the Government of India and is purposed with developing education, research and propagation of indigenous alternative medicine systems in India.

46. That upon the onset of Covid-19 in 2020, a circular was issued by the Ministry of AYUSH which advised Ayurvedic remedies and promoted medicines like Samshamani Vati, Ayush-64, Agasthya Hareetaki, Anuthaila/Sesame Oil and promoted use of ingredients like Haldi (turmeric), Jeera (cumin), Dhaniya (coriander), Lahsun (Garlic), Herbal tea, Tulsi (Basil), Dalchini(Cinnamon), Kalimirch (Black Pepper), Shunthi (Dry Ginger) and Munakka (Raisin) which was dated 06.03.2020. The said Notification further encouraged various AYUSH systems of medicine for promotion of immunity

and also improving the respiratory symptoms of individuals by using basic home based time-tested remedies. Copy of the Circular dated 06.03.2020 is annexed herewith as ANNEXURE A-5.

47. That subsequently, the Ministry of AYUSH also issued a Notification dated 02.04.2020 to all the State Licensing Authorities for expediting the process for grant of approval/licenses/renewal of licenses for manufacturing Ayurvedic, Siddhi and Unani immunity boosting healthcare products and sanitizers. It is important to note that the stand of the Ministry of AYUSH is to promote Ayurvedic medicines by expediting the manufacturing licenses as it believes that ayurvedic medicines boost immunity and can help in either prevention of COVID-19 like illnesses or treatment/management of the same. Copy of the Notification dated 02.04.2020 is annexed herewith as ANNEXURE A-6.

48. That subsequently, the Ministry of AYUSH also issued a Notification dated 21.04.2020 wherein it was stated as there were no specific guidelines in place for verifying the efficacy of Ayurvedic formulation for Covid-19 management, a certain set of guidelines had to be created so that the data generated can be ascertained and verified. The same was necessary to validate the efficacy of the

herbal intervention. Thus certain guidelines were laid down which had to be followed by any organization undertaking a research to find a possible treatment of Covid-19. The said set of guidelines are similar to ones for allopathic formulation and are verified by the Clinical Trials Registry of India (CTRI) which comes under the ICMR (Nodal Central Government agency dealing with COVID response in India). It is noteworthy to mention that currently more than 900 clinical trials have been registered with the CTRI for study on Covid-19 while there are near about 150 clinical trials which have been registered with the CTRI for the study of ayurvedic medicine in treating Covid-19. Copy of the Notification dated 21.04.2020 is annexed herewith as **ANNEXURE A-7**.

49. That the above noted guidelines mentioned in the notification dated 21.04.2020 provide that the proposals should be approved by the scientific advisory bodies and Institutional Ethics Committee of the institution undertaking such a trial, registration with CTRI, the sample size should be based on statistical justification and compliance with Bio-medical and Health Research, Good Clinical Practice Guidelines and other relevant regulations in force. This effectively means that any medicine or drug undergoing trial, once

finalized, shall be subject to human consumption and can be attributed at par with other remedies for a particular disease. At the same time, it is also important to mention that there are no specific regulatory provisions in the Drugs and Cosmetics Rules, 1945, for conduct of clinical trials of Ayurveda, Siddha, Unani and Homeopathy drugs.

50. That it is an admitted position that the Respondent No. 2 was set up to promote the usage of Ayurveda and other remedies and that Respondent No. 1 accepts and gives due regard to the same. It is also an admitted position of fact that Respondent No. 2 in collaboration with Respondent No. 1 came out with their own remedies and prescribed medicines and home based remedies to tackle covid-19 initially. That at the same time it is also important to mention that the said remedies of Ayurvedic medicines, when prescribed by trained and authorized practitioners, tend to increase the bodily immunity without having any side effects.

51. That after the first wave of Covid-19 in 2020, the country witnessed the lifting of the lockdown with the situation getting better and the number of recoveries far outreaching the number of covid positive patients. That the said fact only was possible as people had

developed anti-bodies and the immunity of the human body formed resistance against the said virus. However, in layman terms, if the said immunity was not enhanced or kept at a high rate, it was not unforeseen that the virus would attack again. Therefore, it becomes important to address the issue of strengthening immunity for general betterment of public health as also to combat specific diseases.

DRAWBACKS OF ALLOPATHY

52. That various systems of treatment that are prevalent in the modern medical systems have been used and misused and have resulted in emerging of unprecedented issues and side-effects. A prime example of the same is the over-use of antibiotics. Overuse and misuse of antibiotics are the first risk factors for the development of antibiotics resistance. Inadequate professional competence of health care physicians might worsen the complications associated with antibiotics resistance. Antibiotic resistance is a global issue; however, the epicenter of this misfortune is Asian regions due to the easy accessibility of the strongest antibiotics without prescriptions or diagnoses. High effectiveness and easy accessibility of antibiotics lead to overuse/misuse and encouraging bacteria to develop the resistance. The over-usage and mis-usage of antibiotics are antibiotic

abuse, which increase the potentially serious impact on human health. Bestowing to WHO guidelines, the resistance has led to spread worldwide and classifying resistance is a serious health problem. Furthermore, resistance claims uncertainty to predict the future.

53. That further, the use of opioids, which is done generally for severe and acute pain, has major side-effects. Of particular importance in this respect are clinicians treating chronic musculoskeletal pain that results in opioid-induced hyperalgesia, the activation of pronociceptive pathways by exogenous opioids that results in central sensitization to pain. This phenomenon results in an increase in pain sensitivity and can potentially exacerbate pre-existing pain. Opioids also have powerful positive effects on the reward and reinforcing circuits of the brain that might lead to continued drug use, even if there is no abuse or misuse. While opioids commonly have side effects such as constipation, nausea or vomiting, pruritus, somnolence or cognitive impairment, dry mouth, tolerance or dependence and urinary retention, the societal risk of increased opioid prescription associated with increased nonmedical use, can lead to serious adverse events, even death.

54. That the second wave of Covid-19 virus besieged the Country in April 2021 with a much alarming and deadlier rate than before. However, the same could have been avoided had the bodily immunity of the people not gone down and that is where the indigenous methods of medicine would have come into play thereby seeking to work on the methodology that an asymptomatic patient did not become a mild case and similarly a mild case did not become a moderate case and escalating up to a severe or thereafter critical or fatal case. The role of the Respondent No. 2 becomes very important here so as to streamline the usage of Ayurveda medicines with the scientific methods and suggested therapies for tackling Covid-19.

55. That after the first wave in 2020, the Respondent No. 1 suggested various therapies to tackle the Corona virus as laid down by the World Health Organization. However, many such treatments/therapies were advised to be discontinued after taking into consideration their redundancy or non-efficacy in effectively battling Covid-19 while also demonstrating various side effects, the Respondent No. 1 has still not done away with those outdated therapies.

56. That despite its initial popularity, the WHO issued a conditional recommendation against the use of Remdesivir in hospitalized patients, regardless of disease severity, as there was found to be no evidence that Remdesivir improved survival or other positive outcomes in Covid-19 patients. That furthermore, WHO in November 2020 also suspended Remdesivir from its so-called prequalification list however the same was evidently ignored by the Indian medical fraternity as well as the Respondent No. 1 for the longest time. The usage of the said drug in the country was only stopped once the death toll amongst patients being administered Remdesivir reached an alarming toll, that too in the middle of the lethal Covid second wave. That it is also a fact that the common adverse event noted during compassionate use of Remdesivir in patients with COVID-19 included rashes, diarrhea, hypotension, abnormal liver function and renal impairment. Serious adverse events (acute kidney injury, septic shock, multi-organ failure) were also noted when Remdesivir was administered. Despite such statistics as well as the recommendation by the WHO to the contrary, Remdesivir is still listed as a treatment for Covid-19 in the latest notification dated 14.01.2022. A copy of the medical literature on Remdesivir and its suspension from WHO list are annexed herewith

as ANNEXURE A-8 (COLLY). A copy of Notification dated 14.01.2022 issued by Ministry of Health and Family Welfare, Government of India is annexed herewith ad ANNEXURE A-9.

57. That apart from the usage of Remdesivir, the Respondent No. 1 also notified the convalescent plasma therapy as a possible remedy for countering the Corona virus. However Convalescent plasma therapy was proven to have no benefit in treatment of Covid-19 patients. The ICMR's own trial found weak evidence to support any meaningful use out of transfusing plasma from a Covid-19 recovered patient to a recovering one. A big cause of worry that also emerged was that plasma therapy's unchecked use could potentially create new virus variants. But despite evidence, Respondent No. 1 continues to cautiously keep plasma on its guidelines and endanger the lives of the people one day at a time.

58. Further, the Respondent No. 1 had earlier allowed for prescribing drugs such as Hydroxychloroquine(HCQ) and Ivermectin, which showed early promise but were quickly found to be ineffective in Covid-19 treatment. Anti-malarial drug Hydroxychloroquine suggested by ICMR in its guideline has shown no impact on death outcomes in Covid-19. In fact, it is said to have severe cardiac side-

effects when given to Covid-19 patients. Even the European Union has banned its usage in its countries. However in spite of the same, Respondent No. 1 had allowed to prescribe HCQ for home isolation cases as a “prophylaxis” or preventive measure even when there is no proof that HCQ works in such circumstances. With complete disregard to the established researches and guidelines by International bodies, the Respondent No. 1 had proceeded to distribute about 100 million tablets of HCQ in various Indian states. Subsequently ICMR removed both HCQ and Ivermectin as a treatment for Covid-19.

59. That apart from the above mentioned drugs/treatments, the same holds true even for Ivermectin, an anti-parasitic that was initially believed to help reduce the viral load. There is not enough proof in any research or medical literature to support the claim that the said drug has any real benefit for Covid-19 patients and is yet being prescribed openly to the patients. Respondent No. 1 must not act in utter disregard to the lives of the patients and at the same time without even giving a seconds’ thought to the usage of Ayurvedic medicines which are said to be devoid of any such complexities or side effects.

60. That the real purpose to bring before this Hon'ble Court, the details of the said drugs and remedies for Covid-19 is to show that allopathy although complete in itself is not devoid of frailties especially in light of a pandemic such as Covid-19 and that is where the usage of Ayurveda and other indigenous remedies should be seriously considered. It is not untoward to mention here that Ayurveda medicines are devoid of any side effects when properly prescribed.

61. That moreover, the issue of promotion of steroids freely is another issue that needs to be addressed by Respondent No. 1 however is not being given the attention it deserves. There have been countless cases where irrational usage of steroids has led to surge in the number of cases for related diseases. Many hospitals in Delhi itself have reported a rise in the number of Black Fungus cases or Mucormycosis among people recovering from COVID-19 and it can be ascribed to irrational use of steroids.

62. That Dr Rommel Tickoo, the director of Internal Medicine at Max Hospital, New Delhi, when questioned about the new disease Black Fungus had fairly stated that such a disease was attributable to the indiscriminate use of steroids and further stated that such diseases are more common in people who are immuno-compromised like

cancer patients, transplant recipients, those suffering from diabetes etc. Dr Tickoo went onto add that Azithromycin and doxycycline, which were being used extensively for Covid patients really have no role in reality and yet these were prescribed because there was nothing else to prescribe. In lieu of such statements, it is indeed an imminent necessary for the Respondent No. 1 to re-evaluate the strategy with regard to allopathy and to consider complimenting the same with Ayurvedic medicines which does boosts the metabolism as well as the immunity of the human body without having to address the problem of such side effects.

63. That furthermore, apart from the problems allopathic medicines face during such times of a pandemic, the factual and ground reality relating to Quacks is not being dispelled by the Respondent No. 1. In layman terms, a Quack is a fake doctor or a doctor impostor who claims to have knowledge, skill, qualification with relation to medical science.

64. That there are numerous reports from all over the country regarding sprouting of Quacks in various states and that due to lack of a proper qualified doctor in a village, people are turning to Quacks in times of need which in turn is endangering the lives of the people.

65. That the Applicant/Intervenor herein therefore, by way of the instant Application, prays that the Respondent No. 1 be directed to take the disease seriously and consider all opportunities available at its hands and not blindly follow the path of allopathic medicine even if there is evidence contravening the same, without any further delay.

66. That globally, according to the FDA, there was a 123% per capita increase in deaths from prescription drug overdoses between 2006 and 2014. That there was a sharp increase from 264,227 in 2006 to 807,270 in 2014 for serious but nonfatal prescription drug overdose outcomes (e.g., hospitalization, brain damage) which constitutes a death rate of 67.26%.

67. That despite the knowledge of the linkage between antibiotic use and resistance, there is significant worldwide misuse and overuse of antibiotics. The IMS Institute for Healthcare Informatics has estimated that this problem is costing health systems US\$ 54 billion per year, equivalent to 0.9% of global total health expenditure whereas, as per the World Health Organization's (WHO) data on global health expenditures reveals that when it comes to out-of-pocket expenditure as a proportion of current health expenditure, India is much worse in comparison to the world average (65% for

India versus world average of around 20% in 2016). That the World Health Organization (WHO) also warned that more than 138 million patients were harmed every year by doctors' errors, just a few days before celebrating the first World Patient Safety Day, with which it sought to raise awareness of this ongoing tragedy.

68. That while overall antibiotic prescribing rates have increased over the past 10 years, a current key concern is rapid growth in drug resistant strains of E. coli, a microbe often responsible for urinary tract and bloodstream infections. Also, some drugs can't help but trigger side effects because of their chemical structure. The common allergy drug diphenhydramine (also known by the brand name Benadryl) is one. Though it eases allergy symptoms, it also blocks the chemical acetylcholine, and that leads to drowsiness and a host of other side effects, including dry mouth. In 2014, Tamil Nadu lost more than 200 lives to drug overdose, followed Punjab which saw 186 deaths. It often results in a short-lived treatment of a symptom, rather than removal of the disease.

AYURVEDA : A WAY FORWARD

69. That as such, principles of common sense and logic support the ageless quality of Ayurveda knowledge for healthcare. Ayurvedic

institutions including teachers, students and practitioners are in despair and are encountering a crisis similar to that faced by contemporary Western medicine compatriots. To cope up with this situation as well as the ongoing healthcare crisis, *Vaidya*-scientists, who form a scholarly group of change agents and are well versed in the richness of the Ayurveda classics as well as with the details and insights of modern biology are the need of the hour. It is imminent therefore that the Respondents No. 1 takes the necessary next steps to promote and capitalize on the popularity and efficacy of the Ayurvedic science and mainstream the same with the modern science.

70. That it is also a matter of fact that the essence of WHO resolutions for development and mainstreaming Traditional Medicines are reasonably applicable to the Respondent No. 1 and state governments of India, which require the said Respondents to frame more concrete policies and proceed for their execution through every sincere stakeholder of Ayurveda and to organize and recognize Ayurveda as an authentic system of medicine worldwide however the Respondents have miserably failed to take cognizance of the same.

71. That however in continuation of the above, seeing the promising results of Ayurveda, many a states in collaboration with Respondent No. 2 have also issued orders with respect to the usage and doses of Ayurveda medicines. This has been done in addition to the therapies as suggested in modern science and is to be used as a complimenting treatment to the allopathic treatment. 7. That although, the State of Maharashtra also issued guidelines and advisory for Covid-19 for Ayurveda, Unani and Homeopathy Practitioners but however the nothing concrete was done or implemented by the State Government and neither overseen by the Respondent No. 1. The approach of the Respondent No. 1 towards the ancient remedies of Ayurveda needs to be improved in this regard.

72. That however the State of Haryana has made a proactive effort during the second wave of Covid-19 by including and giving due importance to the Ayurvedic medicines as per its Letter No. NHM/MH/Home Isolation/21-22/2437-2480 dated 08.05.2021 which is for provision of medical kits for those quarantining at home and which includes *inter alia* a mix of allopathic medicines and ayurvedic medicines.

73. That even the state of Madhya Pradesh issued an Order No/Covid-19 control/IDSP/202071868 dated 05.11.2020 which relies on ayurvedic treatment of mild and asymptomatic Covid positive patients.

74. That it is also a matter of fact that the entire campaign of the Applicant/Intervenor is to educate the public about the benefits of ayurvedic science along with the usage of modern science. The Applicant/Intervenor has intended to only allow usage of ayurvedic medicine even along with the vaccination being administered by the Respondent No. 1 throughout the country to safeguard the population against Covid-19. The Applicant/Intervenor has neither stated any ill will against modern science nor against the developed vaccines to combat Covid-19. The Applicant/Intervenor only insists that the Respondent No. 1 take cognizance of the ancient science of Ayurveda and to put it to maximum usage along with modern science in the current pandemic to increase bodily immunity and to reduce the threat of side effects.

75. That while India is still classified as a third world country, in terms of lifestyle and health Indians have the same morbidity profile as that of a first world country. It is humbly submitted that today's

lifestyle diseases like cardiovascular diseases, diabetes, hypertension, asthma and respiratory afflictions as well as cancers are on the rise. It is worth noting that India has the highest number of diabetics at 5 crore 8 lakhs according to the World Health Organization which accounts for a significant percentage of its total population and unfortunately, it is predicted that the aforementioned figure could rise up to 7 crore people by the year 2025. Further, 2 crore Indians suffer from cardiovascular diseases which amounts to a whopping 60% of the global figure. Many factors such as overcrowding, poor living conditions, lack of equitable distribution of resources also increase stress levels among the Indian population leading to coronary heart diseases, asthma and cancers. The ever-growing urban population contributes to an increasingly sedentary lifestyle leading to increase in cases of obesity as well. In view of the abovementioned conditions that are on the rise in our country, it is important to keep an open mind towards all medical resources and treatments that can possibly help change such unhealthy lifestyles with the least impact on the human body and ensure longevity and healthier living conditions for all persons irrespective of their status in the society.

76. Some of the most common types of lifestyle diseases prevailing amongst the Indian population include the following:

- (i) **Obesity:** Numerous factors such as unhealthy eating habits, stressful lifestyle, reduced physical activity, etc. result in obesity. Obesity in turn has a significant negative impact on the body, including breathing and pulmonary issues, irregular blood pressure, cardiovascular diseases, diabetes etc. It is seen as one of the first health issues that bring on further lifestyle diseases and afflictions. According to the National Family Health Survey, India has the second highest obese population with 15.5 crore obese people which is further predicted to increase dramatically over the years going by the trend in the past few years.
- (ii) **Type II diabetes:** Type II diabetes is the non-insulin form of diabetes that tends to develop in adults due to poor eating habits and unhealthy lifestyle conditions. At the cost of repetition it is submitted that today India has the largest number of diabetics with type II diabetes at approximately 4 crores. This figure is on the rise as well with children also being at risk of contracting this form of diabetes merely as a

result of unhealthy lifestyles. Since Type II diabetes does not require insulin, it is easy to treat the same by way of Ayurvedic medicines and treatments. This is possible because Ayurveda through various measures which can help counter the effects of Type II diabetes in a sustainable way and without as many side effects as other heavier medicines may have on the human body.

- (iii) High blood pressure or Hypertension: One of the most prevailing health condition prevailing mostly among adults, it is estimated that about 10 crore Indians suffer from high blood pressure or hypertension today. Many reasons for high blood pressure exist today including increasing stress, obesity, genetic factors and poor eating habits. High blood pressure can also be rectified by way of Ayurveda and the milder treatments laid down in the Ayurvedic science.
- (iv) Cirrhosis: Cirrhosis is a group of liver disorders. The liver can be affected by heavy alcohol consumption and chronic hepatitis. Unfortunately, due to the massive increase in the number of people consuming alcohol, as well the increase of alcohol consumption amongst existing drinking adults,

cirrhosis has become a common lifestyle disease as many people consume alcohol on a daily basis to deal with the increasing stress mentioned hereinabove. Ayurveda can greatly help in recovering and coping with cirrhosis by many treatments that don't have major side effects.

77. The abovementioned conditions are few among the many conditions that afflict the citizens of our country. It has been seen that the lack of care imparted towards our health in general has results in these conditions becoming life threatening. Particularly in the background of Covid-19, the existence of co-morbidities, some of which have been mentioned hereinabove, has proven to be especially fatal and life-threatening and has resulted in unfortunate deaths of lakhs of Indians. Therefore, it is imminent that the focus of our citizens is shifted back to improving and taking care of our health, body and mind. These lifestyle diseases, in threatening and unforeseeable circumstances like the Covid-19 pandemic can turn into life-threatening conditions and result in painful situations and untimely demise. Therefore, as evidenced in the present application, it is submitted that it is high time that health and lifestyle needs to be given much more importance than before. It is emphasized that

timely and effective treatment of such health issues and can help prevent bigger health risks. It is submitted that with the way the world is progressing, we are moving further away from our roots and the way of living that has been proven to be most beneficial by our ancestors and forefathers and the same is resulting in bigger health issues than ever before, and in the threat of further pandemics that may afflict the populations worldwide, it is imperative that as many efficacious treatments, especially Ayurveda which is based on real science and natural treatments, are explored and implemented among the Indian population so as to timely rectify today's health issues and help prevent the unfortunate and tragic loss of lives that was witnessed due to the Covid-19 pandemic in the years 2020 and 2021. That keeping in mind all the aforementioned facets of allopathy and its harmful side effects coupled with the advantages of ayurvedic form of medicine, it is clear that the Respondent No. 1 have failed to provide impetus to Respondent No. 2 whereby the ancient science of Ayurveda needs to be integrated with the modern science of medicine to tackle the fatal second wave of the deadly disease of Covid-19.

78. That in view of the aforementioned submissions, it is imperative that the Respondents herein be directed to mandatorily include Ayurveda

in the curriculum of medical students pursuing M.B.B.S. and other medical courses. The objective of the same would be to allow each and every upcoming health practitioner in India to familiarize themselves with the concepts of alternative medicines such as Ayurveds and to build their knowledge base on the said issue, along with the current curriculum on modern medical sciences. A benefit of such an inclusion, in due course of time, would be to allow a practitioner to provide a potential patient with the option of opting for treatments under ayurvedic medical systems along with the current medical treatments commonly prescribed.

GROUND

- A. BECAUSE** providing correct medical treatments to an individual is a fundamental right of every citizen enshrined under Article 21 of the constitution of India;
- B. BECAUSE** the Right to Life enshrined in Article 21 of the Constitution of India includes protection of health, and access to good healthcare and the Respondent No. 1 has a constitutional obligation to serve the fundamental rights of the citizenry by providing correct, easy and all access to health resources.

C. BECAUSE right to Livelihood and Right to Health are recognised as Fundamental Rights. The Hon'ble Supreme Court of India, in Suo Motu Writ Petition (Civil) No.7/2020 vide Order dated 18.12.2020, has observed Right to Health being a fundamental right.

D. BECAUSE the medical universe does not constitute allopathy alone and to deal with the pandemic which has risen exponentially in India, hence it is incumbent upon the Respondent No. 1 to provide every remedy available to mankind to uphold the fundamental rights as guaranteed under Article 14 and Article 21 of the Constitution.

E. BECAUSE the preservation of human life is of paramount importance, and that the Respondents being the Government has a duty to act in public interest by providing large scale access to all remedies which may cure the disease which in turn guarantees the Fundamental Rights of Citizens enshrined under Article 14 and Article 21 of the Constitution.

F. BECAUSE Covid-19 is a disease which can be broadly classified into three categories : Mild, Moderate and Severe. Further, none of these categories involve surgical intervention, however, mild and moderate covid patients do not require hospitalization and can be

treated with natural remedies without having to undergo the pain and trauma of side effects which can further lead to hospitalization.

G. BECAUSE every day delay in fighting Covid-19 without the ancient science of Ayurveda only endangers the lives of the people at large.

H. BECAUSE Ayurveda has proved its multi faceted usage even in such modern times.

I. BECAUSE Ayurveda has no known side effects on usage whereby the Allopathic medicines have known to cause side effects which have turned out to be fatal for the general public at large

J. BECAUSE the Respondent No. 1 has not sufficiently promoted or recognized the usage of Ayurveda and other indigenous and natural remedies and is still not able to contain the deadly virus.

K. BECAUSE the initiatives taken by the Respondent No. 2 become only a lip service and do not count unless and until Respondent No. 1 accept the usage of Ayurvedic medicines and propagate the same to the general public.

L. BECAUSE the indiscriminate use of steroids and other allopathic medicines have given rise to other diseases like the black fungus, yellow fungus and white fungus.

M. BECAUSE the World Health Organisation took Remdisivir off the list of prescribed medicines in November 2020 and the Respondent No. 1 is still propagating the same when instead the Respondents should be advancing the knowledge of Ayurvedic medicines

N. BECAUSE the Respondent No. 1 has allowed the existence of QUACKS in numerous villages, towns and cities of various states in the country instead of allowing the existence of Ayurvedic medicines in each and every household.

O. BECAUSE the Respondents need to work in tandem to integrate the science of ancient and natural ayurvedic medicine with modern science

79. That the Applicant/Intervenor also craves leave of the Hon'ble Court to amend/add any or fssurther grounds.

80. That the present Application has been filed bona fide and in the interest of justice.

81. That the annexures filed along with the present Application are true copies of their respective originals.

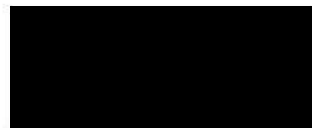
PRAYER

In the facts and circumstances mentioned above and in the interest of justice, it is the humble prayer of the Applicant/Intervenor above named that this Hon'ble Court may be graciously pleased to:

- a. Allow the present Application and allow the Applicant/Intervenor to be impleaded and participate in the present proceedings;
- b. Direct the Respondents to take effective steps for the inclusion of Ayurveda in the curriculum for M.B.B.S; and
- c. Pass any such other and further orders as this Hon'ble Court may deem fit and proper under the facts and circumstances of the present case.

AND FOR THIS ACT OF KINDNESS, THE APPLICANT/
INTERVENOR AS IN DUTY BOUND SHALL EVERY PRAY:

Through:



[ATHENA LEGAL]

Advocates for the Applicant/Intervenor
37, Link Road, 1st Floor,
Lajpat Nagar – III,
New Delhi- 11002
011-42004400

Place: New Delhi
Dated: 10.10.2022



IN THE HIGH COURT OF DELHI AT NEW DELHI
EXTRA ORDINARY ORIGINAL WRIT JURISDICTION
I.A. NO. _____ OF 2022
IN
WRIT PETITION (C) NO. 6632 OF 2022

IN THE MATTER OF:

ASHWINI KUMAR UPADHYAY

...PETITIONER

VERSUS

UNION OF INDIA & ORS.

...RESPONDENTS

AND IN THE MATTER OF:

PATANJALI RESEARCH INSTITUTE

....INTERVENOR/
APPLICANT

I, Acharya Balkrishna, aged about 50 years, [REDACTED]

[REDACTED] the deponent
abovenamed, do hereby solemnly affirm and declare as under:

1. I am the General Secretary of Patanjali Research Institute (Patanjali Research Foundation Trust) and as such am competent to swear this affidavit.
2. I have read and understood the accompanying application under Order 1 Rule 8A read with Section 151 of the Code of Civil Procedure, 1908 and state and verify that the averments made in the same are based on the records of the Intervenor/Applicant and based on legal advice received from the Intervenor/Applicant and are believed by me to be true and the averments made in the last non-numerated paragraph are in the nature of humble prayers of the Intervenor/Applicant before this Hon'ble Court.

3. That the documents filed herewith are copies of their respective originals.



DEPONENT



VERIFICATION:

I, Acharya Balkrishna, verify that the averments made in Paragraphs 1-3 of my affidavit are true to my knowledge, that no part of it is false and nothing material has been concealed therefrom.

Verified at Haridwar on this 9th day of November, 2022.



I. INFLAMMATORY DISORDERS - RHEUMATOID ARTHRITIS, ARTHRITIS, ASHTHMA, PSORIASIS AND DERMATITIS

The scientists at PRI have proved that the herbo-mineral Ayurvedic formulation 'Ashwashila' reduced the pro-inflammatory cytokines responsible for severe symptoms of Rheumatoid arthritis. The effectivity of this Ayurvedic medicine was verified in rats suffering from Rheumatoid arthritis (Scientific Reports, 2019, 9, 8025, doi: 10.1038/s41598-019-44485-9). Another herbo-mineral Ayurvedic formulation that was scientifically proven to effective against arthritis is 'Divya Amvatari Ras'. This formulation provides relief from arthritis by targeting the inflammation generating pathway. All these scientific details were obtained from studying the anti-arthritic effects of Divya Amvatari Ras in mice suffering from arthritis (Frontiers in Pharmacology, 2019, 10: 659. doi: 10.3389/fphar.2019.00659). Likewise, the herbo-mineral formulation 'Peedanil Gold' was found to relieve pain and other symptoms of osteoarthritis in experiment rats by targeting inflammation (Frontiers in Pharmacology, 2022, 13: 883475. doi: 10.3389/fphar.2022.883475).

A. Herbo-mineral Formulation 'Ashwashila' Attenuates Rheumatoid Arthritis Symptoms in Collagen-antibody-induced Arthritis (CAIA) Mice Model. (2019) Acharya Balkrishna, Sachin Shridhar Sakat, Kheemraj Joshi, Sandeep Paudel, Deepika Joshi, Kamal

Joshi, Ravikant Ranjan, Abhishek Gupta, Kunal Bhattacharya, Anurag Varshney. *Scientific Reports*. 9, 8025, doi: 10.1038/s41598-019-44485-9. (IF 4.379)

- B. Anti-Inflammatory and Anti-Arthritic Efficacies of An Indian Traditional Herbo-Mineral Medicine “Divya Amvatari Ras” in Collagen Antibody-Induced Arthritis (CAIA) Mouse Model Through Modulation of IL-6/IL-1 β /TNF- α /NF κ B Signalling. (2019) Acharya Balkrishna, Sachin Shridhar Sakat, Kheemraj Joshi, Sandeep Paudel, Deepika Joshi, Kamal Joshi, Ravikant Ranjan, Abhishek Gupta, Kunal Bhattacharya, Anurag Varshney. *Frontiers in Pharmacology*. 10: 659. doi: 10.3389/fphar.2019.00659. (IF 5.988)
- C. Peedanil Gold, Herbo-Mineral Formulation, Moderates Cytokine Levels and Attenuates Pathophysiology in Monosodium Iodoacetate Induced Osteoarthritis in SD Rat Model. (2022) Acharya Balkrishna, Sandeep Sinha, Shadrak Karumuri, Jyotish Srivastava, Swati Haldar, Anurag Varshney. *Frontiers in Pharmacology*. 13: 883475. doi: 10.3389/fphar.2022.883475. (IF 5.988)
- D. Asthma. PRI has provided compelling scientific evidence proving the efficacies of the Ayurvedic formulations, ‘Divya-Swasari-

Kwath' (herbal) (Phytomedicine. 2020, 78: 153295. doi: 10.1016/j.phymed.2020.153295) and 'Divya-Swasari-Ras' (herbo-mineral) (Biomedicine & Pharmacotherapy. 2020, 126: 110063. doi: 10.1016/j.biopha.2020.110063) against allergic asthma. Both these formulations suppressed the underlying inflammation that leads to undesirable changes in the airway passage that ultimately results in asthma. Divya-Swasari-Kwath provided this protection to the airway passage by activating anti-oxidant-mediated defense mechanism. 'Malla Sindoor', a herbo-metallic Ayurvedic formulation was also proved to be equally effective against asthma by targeting oxidative stress and inflammation causing cytokines (Journal of Ethnopharmacology. 292: 115120. doi: 10.1016/j.jep.2022.115120). The biotite-calc based traditional Ayurvedic formulation 'Sahastraputi-Abhrak-Bhasma' could also prevent allergic asthma in experimental mice (Journal of Inflammation Research. 2021, 14: 4743. doi: 10.2147/JIR.S313955).

- E. Herbal Decoction Divya-Swasari-Kwath Attenuates Airway Inflammation and Remodelling Through Nrf-2 Mediated Antioxidant Lung Defence in Mouse Model of Allergic Asthma. (2020) Acharya Balkrishna, Siva Kumar Solleti, Hoshiyar Singh,

Sudeep Verma, Niti Sharma, Pradeep Nain, Anurag Varshney.
Phytomedicine. 78: 153295. doi: 10.1016/j.phymed.2020.153295.
(IF 6.656)

F. Calcio-Herbal Formulation, Divya-Swasari-Ras, Alleviates Chronic Inflammation and Suppresses Airway Remodelling in Mouse Model of Allergic Asthma by Modulating Pro-Inflammatory Cytokine Response. (2020) Acharya Balkrishna, Siva Kumar Solleti, Hoshiyar Singh, Meenu Tomer, Niti Sharma, Anurag Varshney. Biomedicine & Pharmacotherapy. 126: 110063. doi: 10.1016/j.biopha.2020.110063. (IF 7.419)

G. Herbo-Metallic Ethnomedicine 'Malla Sindoor' Ameliorates Lung Inflammation in Murine Model of Allergic Asthma by Modulating Cytokines Status and Oxidative Stress. (2022) Acharya Balkrishna, Siva Kumar Solleti, Hoshiyar Singh, Rani Singh, Kunal Bhattacharya, Anurag Varshney. Journal of Ethnopharmacology. 292: 115120. doi: 10.1016/j.jep.2022.115120. (IF 5.195)

H. Biotite-Calx Based Traditional Indian Medicine Sahastraputi-Abhrak-Bhasma Prophylactically Mitigates Allergic Airway Inflammation in a Mouse Model of Asthma by Amending Cytokine Responses. (2021) Acharya Balkrishna, Siva Kumar Solleti, Hoshiyar Singh, Rani Singh, Niti Sharma, Anurag

Varshney. *Journal of Inflammation Research*. 14: 4743. doi: 10.2147/JIR.S313955. (IF 6.532)

II. PSORIASIS AND DERMATITIS.

A. The scientists at PRI proved that the classical Ayurvedic formulation, in the form of tablet, 'Divya-Kayakalp-Vati' and oil 'Divya-Kayakalp-Oil' could treat Psoriatic-like skin ailments in experimental mice by targeting inflammation, when used in combination (*Journal of Traditional and Complementary Medicine*. 2021, 12: 335. doi: 10.1016/j.jtcme.2021.09.003). This combination of Divya-Kayakalp-Vati and Oil was also effective against atopic dermatitis in mice, shown in a another study published from PRI (*Clinical, Cosmetic and Investigational Dermatology*. 2022, 15: 293. doi: 10.2147/CCID.S342227). The chemists at PRI optimized a process to get oil from the seeds of *Withania somnifera* (Ashwagandha) using carbon dioxide (CO₂) at a very low temperature under very high pressure conditions. These conditions are called super-critical conditions and the process is called Super Critical Fluid Extraction (SCFE). SCFE Ashwagandha seed oil provided relief from Prosiasis-like skin lesions in mice by controlling inflammation (*Biomolecules*. 2020, 10: 185; doi: 10.3390/biom10020185). Besides, the scientists at PRI also proved the anti-inflammatory and anti-psoriatic effects of Sea Buckthorn (*Hippophae rhamnoides*) oil in mice (*Frontiers*

in Pharmacology. 2019, 10: 1186. doi: 10.3389/fphar.2019.01186).

- **Modulation of Psoriatic-like Skin Inflammation by Traditional Indian Medicine Divya-Kayakalp-Vati and Oil Through Attenuation of Pro-inflammatory Cytokines.** (2021) Acharya Balkrishna, Sachin Sakat, Kheemraj Joshi, Rani Singh, Sudeep Verma, Pradeep Nain, Kunal Bhattacharya, Anurag Varshney. *Journal of Traditional and Complementary Medicine*. 12: 335. doi: 10.1016/j.jtcme.2021.09.003. (IF 4.425)
- **Modulation of Psoriatic-like Skin Inflammation by Traditional Indian Medicine Divya-Kayakalp-Vati and Oil Through Attenuation of Pro-inflammatory Cytokines.** (2021) Acharya Balkrishna, Sachin Sakat, Kheemraj Joshi, Rani Singh, Sudeep Verma, Pradeep Nain, Kunal Bhattacharya, Anurag Varshney. *Journal of Traditional and Complementary Medicine*. 12: 335. doi: 10.1016/j.jtcme.2021.09.003. (IF 4.425)
- **Super Critical Fluid Extracted Fatty Acids from *Withania somnifera* Seeds Repair Psoriasis-Like Skin Lesions and Attenuate Pro-Inflammatory Cytokines (TNF- α and IL-6) Release.** (2020) Acharya Balkrishna, Pradeep Nain, Anshul Chauhan, Niti Sharma, Abhishek Gupta, Ravikant Ranjan, Anurag Varshney. *Biomolecules*. 10: 185; doi: 10.3390/biom10020185. (IF 4.569)

- **Cytokines Driven Anti-Inflammatory and Anti-Psoriasis Like Efficacies of Nutraceutical Sea Buckthorn (*Hippophae rhamnoides*) Oil.** (2019) Acharya Balkrishna, Sachin Shridhar Sakat, Kheemraj Joshi, Kamal Joshi, Vinay Sharma, Ravikant Ranjan, Kunal Bhattacharya, Anurag Varshney. *Frontiers in Pharmacology*. 10: 1186. doi: 10.3389/fphar.2019.01186. (IF 5.988)

LIFESTYLE DISORDERS

III. CARDIAC HYPERTROPHY. HIGH BLOOD PRESSURE/ HYPERTENSION

A. Chronic hypertension can lead to thickening of heart muscles, resulting in inefficient pumping of blood to the organs. This condition is called Cardiac hypertrophy. Oxidative stress is a major underlying cause of hypertension. In a study using zebrafish model of the disease, scientist at PRI had shown that the classical Ayurvedic formulation, 'Yogendra Ras' could oxidative stress and consequently, relief from cardiac hypertrophy (Biomolecules. 2020, 10: 600. doi: 10.3390/biom10040600).

- **Application of Zebrafish Model in the Suppression of Drug-Induced Cardiac Hypertrophy by Traditional Indian Medicine Yogendra Ras.** (2020) Acharya Balkrishna, Yashika Rustagi, Kunal Bhattacharya, Anurag Varshney *Biomolecules*. 10: 600.

doi: 10.3390/biom10040600. (IF 4.569)

IV. LIVER DYSFUNCTION.

A. Lifestyle-mediated liver dysfunctions, resulting from exposure to environmental pollutants or consumption of too much alcohol are very common these days. The Ayurvedic formulation, ‘Divya Sarva-Kalp-Kwath’ also known as ‘Livogrit’ was shown to be effective against carbon tetrachloride-mediated liver impairments in mice (**Frontiers in Pharmacology. 2020, 11: 288. doi: 10.3389/fphar.2020.00288**) and thioacetamide-induced liver toxicity in zebrafish (**Toxicology Reports. 2022, 9: 1056. doi: 10.1016/j.toxrep.2022.03.053**). Besides, Livogrit was also effective in treating non-alcoholic Steatosis by targeting oxidative stress in spheroid primary rat hepatocyte cultures (**Bioengineered. 2022, 13: 10811 doi: 10.1080/21655979.2022.2065789**) and alcoholic steatosis by reducing intracellular triglycerides and extracellular glycerol levels (**Molecules 2020, 25: 4849. doi:10.3390/molecules25204849**). Carbon tetrachloride and thioacetamide are common industrial pollutants released in the environment, whereas, high levels of fatty acids (triglycerides and glycerol in the body) is an indication of alcoholism.

B. Polyherbal Medicine Divya Sarva-Kalp-Kwath Ameliorates Persistent Carbon Tetrachloride Induced Biochemical and Pathological Liver Impairments in Wistar Rats and in HepG2 cells. (2020) Acharya Balkrishna, Sachin Shridhar Sakat, Ravikant Ranjan, Kheemraj

Joshi, Sunil Shukla, Kamal Joshi, Sudeep Verma, Abhishek Gupta, Kunal Bhattacharya, Anurag Varshney. *Frontiers in Pharmacology*. 11: 288. doi: 10.3389/fphar.2020.00288. (IF 5.988)

➤ **Livogrit, A Herbal Formulation of Boerhavia diffusa, Phyllanthus niruri and Solanum nigrum Reverses the Thioacetamide Induced Hepatocellular Toxicity in Zebrafish Model. (2022) Acharya Balkrishna, Savita Lochab, Anurag Varshney. *Toxicology Reports*. 9: 1056. doi: 10.1016/j.toxrep.2022.03.053. (IF 4.807)**

➤ **Livogrit Prevents Methionine-Cystine Deficiency Induced Nonalcoholic Steatohepatitis by Modulation of Steatosis and Oxidative Stress in Human Hepatocyte-Derived Spheroid and in Primary Rat Hepatocytes. (2022) Acharya Balkrishna, Vivek Gohel, Priya Kumari, Moumita Manik, Kunal Bhattacharya, Rishabh Dev, Anurag Varshney. *Bioengineered*. 13: 10811 doi: 10.1080/21655979.2022.2065789. (IF 3.269)**

C. Tri-Herbal Medicine Divya Sarva-Kalp-Kwath (Livogrit) Regulates Fatty Acid-Induced Steatosis in Human HepG2 Cells through Inhibition of Intracellular Triglycerides and Extracellular Glycerol Levels. (2020) Acharya Balkrishna, Vivek Gohel, Rani Singh, Monali Joshi, Yash Varshney, Jyotish Srivastava, Kunal Bhattacharya, Anurag Varshney. *Molecules* 25: 4849. doi:10.3390/molecules25204849. (IF 4.148)

V. INFERTILITY

A. Ayurveda already has solutions for infertility, which have now been scientifically proven by the studies conducted at PRI. Oils obtained through SCFE from the seeds of **Putranjiva roxburghii Wall. (Putrajeevak)** (**Molecules. 2021, 26: 1020. doi: 10.3390/molecules26041020**) and **Bryonopsis laciniosa (Shivlingi)** (**Journal of Ovarian Research. 2022, 15: 46. doi: 10.1186/s13048-022-00982-6**) when tested on both male and female infertile zebrafish, showed significant improvement in fertility.

- **Supercritical Fluid Extract of Putranjiva roxburghii Wall. Seeds Mitigates Fertility Impairment in a Zebrafish Model. (2021) Acharya Balkrishna, Pradeep Nain, Monali Joshi, Lakshmi pathi Khandrika, Anurag Varshney. Molecules. 26: 1020. doi: 10.3390/molecules26041020. (IF 4.148)**
- **Super-critical Fluid Extract of Bryonopsis laciniosa (Shivlingi) Seeds Restores Fertility in Zebrafish Models Through Revival of Cytological and Anatomical Features. (2022) Acharya Balkrishna, Pradeep Nain, Monali Joshi, Brijesh Kumar, Anurag Varshney. Journal of Ovarian Research. 15: 46. doi: 10.1186/s13048-022-00982-6. (IF 4.234)**

VI. IMMUNITY BOOSTERS

Our overall immunity has become significantly compromised due to our lifestyle choices and practices. Ayurveda already had specific recommendations for overall immunity boosting of the body. Chyawanprash, a classical Ayurvedic food, has been used for centuries for protection against general infection and for boosting the overall immunity and vigor of the body. Inflammation is like a general process that gets active during several metabolic and infectious diseases. In a study on zebrafish with bacterial toxin induced inflammation indicating infection, Chyawanprash relieved all disease symptoms and restored strength and vigor (Frontiers in Pharmacology. 2021, 12: 751576. doi: 10.3389/fphar.2021.751576). Likewise, the Ayurvedic drink, Divya-Herbal-Peya, also exerted inflammation balancing effects in bacterial-toxin induced zebrafish disease model (**Journal of Experimental Pharmacology. 2021, 13: 937. doi: 10.2147/JEP.S328864**).

- **Chyawanprash, An Ancient Indian Ayurvedic Medicinal Food, Regulates Immune Response in Zebrafish Model of Inflammation by Moderating Inflammatory Biomarkers. (2021) Acharya Balkrishna, Meenu Tomer, Moumita Manik, Jyotish Srivastava, Rishabh Dev, Swati Haldar, Anurag Varshney. Frontiers in Pharmacology. 12: 751576. doi: 10.3389/fphar.2021.751576. (IF 5.988)**
- **Divya-Herbal-Peya Decoction Harmonizes the Inflammatory**

Response in Lipopolysaccharide-Induced Zebrafish Model. (2021)

Acharya Balkrishna, Savita Lochab, Monali Joshi, Jyotish Srivastava, Anurag Varshney. Journal of Experimental Pharmacology. 13: 937. doi: 10.2147/JEP.S328864. (IF 2.24)

VII. CANCER

This disease has occupied a special category, different from all other diseases. There are several types of cancers, that affect different organs to different extent. In a very interesting study on *Pistacia integerrima* (Kakrasinghi), cancer biologists at PRI has shown that the phytochemical, penta-O-Galloyl- β -D-Glucose, present in the extract of this plant could specifically kill human lung cancer cells (**Frontiers in Pharmacology. 2022, 13:889335. doi: 10.3389/fphar.2022.889335**). Anti-cancer potentials of several other Ayurvedic formulations/extracts are being currently studied by the team of cancer biologists at PRI.

- **Penta-O-Galloyl- β -D-Glucose in *Pistacia integerrima* Targets AMPK-ULK1 and ERK/STAT3 Signaling Axes to Induce ROS-Independent Autophagic Cell Death in Human Lung Cancer Cells. (2022) Acharya Balkrishna, Vallabh Prakash Mulay, Sudeep Verma, Jyotish Srivastava, Savita Lochab, Anurag Varshney. Frontiers in Pharmacology. 13:889335. doi: 10.3389/fphar.2022.889335. (IF 5.988)**

VIII. NEUROSCIENCE

The field of neuroscience encompasses a wide variety of study prospects, ranging from neuropathologies (occurring as adverse side-effects of treatments of other diseases) to neural functioning, memory and cognition. PRI also already generated scientific evidence to prove the effectivity of Ayurvedic formulations, ‘Divya-Peedantak-Vati’ (**Phytomedicine Plus. 2022, 2: 100229. doi: 10.1016/j.phyplu.2022.100229**) and ‘Divya-Peedantak-Kwath’ (**Frontiers in Pharmacology. 2020; 11: 566490. doi: 10.3389/fphar.2020.566490**) in providing relief from chemotherapy induced neuropathy and pain. Several other studies are currently on-going to scientifically establish the abilities of Ayurvedic formulations in treating memory and cognitive issues.

- **Anti-oxidant Profile of Divya-Peedantak-Vati Abates Paclitaxel-induced Hyperalgesia and Allodynia in CD-1 Mice Model of Neuropathic Pain. (2022) Acharya Balkrishna, Shadrak Karumuri, Sachin S Sakat, Swati Haldar, Anurag Varshney. Phytomedicine Plus. 2: 100229. doi: 10.1016/j.phyplu.2022.100229. (IF ~ 3.000)**
- **Herbal Decoction Divya-Peedantak-Kwath Alleviates Allodynia and Hyperalgesia in Mice Model of Chemotherapy-Induced Peripheral Neuropathy via Modulation in Cytokine Response. (2020) Acharya Balkrishna, Sachin S Sakat, Shadrak Karumuri, Hoshiyar Singh, Meenu Tomer, Ajay Kumar, Niti Sharma, Pradeep Nain, Swati Haldar, Anurag Varshney. Frontiers in Pharmacology. 11: 566490.**

doi: 10.3389/fphar.2020.566490. (IF 5.988)

IX. INFECTIOUS DISEASES

Infections can occur anytime, anywhere and to anybody. Ayurveda has a very strategic rationale for handling infections. The first aspect of this rationale is to keep the body as much prepared for such external assaults as possible. The other aspects of this strategy includes the application of Ayurvedic formulations known for their anti-microbial properties. There are several medicinal plants which are exclusively known for their strong anti-microbial potentials, and Ayurveda has recommendations for using them as per requirements. The best example has been the Ayurvedic formulations, **Coronil (Journal of Inflammation Research. 2021,14: 869. doi: 10.2147/JIR.S298242)** and **Divya-Swasari-Vati (Frontiers in Pharmacology. 2022, 13:1024830. doi: 10.3389/fphar.2022.1024830)**, which were proven to be effective inhibitors of SARS-CoV-2 pseudovirus entry into the human lung cells. Prior computational and biochemical validations of a major phytochemical, Withanone, present in Coronil, helped us understand the exact mechanism by which it could prevent interaction of SARS-CoV-2 virus with the receptors on human lung cells, and thus, inhibit virus entry into these cells. Such anti-SARS-CoV-2 activity of Withanone deduced from computational and biochemical studies was validated in zebrafish model of the disease (**Drug Design, Development and Therapy. 2021, 15: 1111. doi: 10.2147/DDDT.S292805**). In a similar study in zebrafish,

anti-SARS-CoV-2 activity of the extract of **Tinospora cordifolia (Giloy)**, one of the herbal ingredients of Coronil, was validated (**Frontiers in Pharmacology. 2021, 12: 635510doi: 10.3389/fphar.2021.635510**). The anti-SARS-CoV-2 efficacies of Coronil (**Molecules. 2020, 25: 5091. doi: 10.3390/molecules25215091**) and Divya-Swasari-Vati (**Journal of Inflammation Research. 2020, 13:1219. doi: 10.2147/JIR.S286199**) were pre-clinically validated through similar zebrafish models.

In the wake of the second COVID-19 wave in India, COVID-associated Mucormycosis (CAM) became prevalent. Being a rare but highly invasive fungal infection with no established treatment regime, Mucormycosis became endemic to India in no time. The team of microbiologists at PRI assessed the anti-fungal effect of the classical Ayurvedic nasal drop, Anu taila, one of the components of the Coronil Kit, against *Mucor* spp, the causative microbe of Mucormycosis. This study clearly showed that Anu taila very effectively inhibited *Mucor* growth and its spore germination. Anu taila also triggered an infection-combat state in the human lung cells (**Journal of Applied Microbiology. 2022, 132: 3355. doi: 10.1111/jam.15451**). PRI has also provided a solution for Dengue in the form of ‘Denguenil Vati’, the anti-viral efficacy of which was established using zebrafish model of the disease (**Biomolecules. 2020, 10: 971. doi: 10.3390/biom10070971**). The SCFE oil from Ashwagandha, besides being a potent anti-psoriatic agent, was found to

have strong anti-biofilm activity against the Gram-negative food borne pathogen, *Salmonella enterica*, known to cause Salmonellosis (**Phytomedicine Plus. 2021, 4: 100047. doi: 10.1016/j.phyplu.2021.100047**). Roots of Ashwagandha, besides several other medicinal properties, are also associated with anti-microbial effect. In an interesting effort to validate the anti-microbial property of the aerial parts of this plant, the microbiologists at PRI discovered that the whole plant extract of Ashwagandha has a significant anti-fungal effect against the rare skin pathogen, *Sporothrix globosa*, which is known to cause a chronic skin infection, Sporotrichosis (**PLoS Neglected Tropical Diseases. 2022, 16: e0010484. doi: org/10.1371/journal.pntd.0010484**). In yet another study, it was shown that the phytochemicals, withanolides from Ashwagandha reduced neutrophil infiltration by curbing oxidative stress and inflammation in bacterial-endotoxin induced peritonitis in experimental mice (**Planta Medica. 2021, 88: 466. doi: 10.1055/a-1438-2816**).

- **Coronil, a Tri-Herbal Formulation, Attenuates Spike-Protein-Mediated SARS-CoV-2 Viral Entry into Human Alveolar Epithelial Cells and Pro-Inflammatory Cytokines Production by Inhibiting Spike Protein-ACE-2 Interaction. (2021) Acharya Balkrishna, Swati Haldar, Hoshiyar Singh, Partha Roy, Anurag Varshney. Journal of Inflammation Research. 14: 869. doi: 10.2147/JIR.S298242. (IF 6.532.**
- **Herbo-mineral formulation, Divya-Swasari-Vati averts SARS-CoV-2**

pseudovirus entry into human alveolar epithelial cells by interfering with spike protein-ACE 2 interaction and IL-6/TNF- α /NF- κ B signaling. (2022) Acharya Balkrishna, Sudeep Goswami, Hoshiyar Singh, Vivek Gohel, Rishabh Dev, Swati Haldar, Anurag Varshney. *Frontiers in Pharmacology*. 2022, 13:1024830. doi: 10.3389/fphar.2022.1024830. (IF 5.988)

- **Withanone from *Withania somnifera* Attenuates SARS-CoV-2 RBD and Host ACE2 Interactions to Rescue Spike Protein Induced Pathologies in Humanized Zebrafish Model.** (2021) Acharya Balkrishna, Subarna Pokhrel, Hoshiyar Singh, Monali Joshi, Vallabh Prakash Mulay, Swati Haldar, Anurag Varshney. *Drug Design, Development and Therapy*. 15: 1111. doi: 10.2147/DDDT.S292805. (IF 4.162)
- **Giloy Ghanvati (*Tinospora cordifolia* (willd.) Hook.f. & Thomson) Reversed SARS-CoV-2 Viral Spike-protein Induced Disease Phenotype in the Xenotransplant Model of Humanized Zebrafish.** (2021) Acharya Balkrishna, Lakshmipathi Khandrika, Anurag Varshney. *Frontiers in Pharmacology*. 12: 635510doi: 10.3389/fphar.2021.635510. (IF 5.988)
- **Calcio-Herbal Medicine Divya-Swasari-Vati Ameliorates SARS-CoV-2 Spike Protein-Induced Pathological Features and Inflammation in Humanized Zebrafish Model by Moderating IL-6**

- and TNF- α Cytokines. (2020) Acharya Balkrishna, Sudeep Verma, Siva Kumar Solleti, Lakshmipathi Khandrika, Anurag Varshney. *Journal of Inflammation Research*. 13:1219. doi: 10.2147/JIR.S286199. (IF 6.532)
- **Application of Humanized Zebrafish Model in the Suppression of SARS-CoV-2 Spike Protein Induced Pathology by Tri-Herbal Medicine Coronil via Cytokine Modulation. (2020) Acharya Balkrishna, Siva Kumar Solleti, Sudeep Verma, Anurag Varshney. *Molecules*. 25: 5091. doi: 10.3390/molecules25215091. (IF 4.148)**
- **Anu Taila, An Herbal Nasal Drop, Suppresses Mucormycosis by Regulating Host TNF- α Response and Fungal Ergosterol Biosynthesis. (2022) Acharya Balkrishna, Shubhangi Rastogi, Bhawana Kharayat, Meenu Tomer, Yash Varshney, Kanchan Singh, Priya Kumari, Rishabh Dev, Jyotish Srivastava, Swati Halder, Anurag Varshney. *Journal of Applied Microbiology*. 132: 3355. doi: 10.1111/jam.15451. (IF 4.059)**
- **Validation of a Novel Zebrafish Model of Dengue Virus (DENV-3) Pathology Using the Pentaherbal Medicine Denguenil Vati. (2020) Acharya Balkrishna, Siva Kumar Solleti, Sudeep Verma, Anurag Varshney. *Biomolecules*. 10: 971. doi: 10.3390/biom10070971. (IF 4.569)**
- **Effects of Fatty Acids in Super Critical Fluid Extracted Fixed Oil**

- from *Withania somnifera* Seeds on Gram-Negative *Salmonella enterica* Biofilms. (2021) Acharya Balkrishna, Ashish Kumar Gupta, Kanchan Singh, Swati Haldar, Anurag Varshney. *Phytomedicine Plus*. 4: 100047. doi: 10.1016/j.phyplu.2021.100047. (IF ~ 3.000)
- *Withania somnifera* (L.) Dunal Whole-plant Extracts Exhibited Anti-Sporotrichotic Effects by Destabilizing Peripheral Integrity of *Sporothrix globosa* Yeast Cells. (2022) Acharya Balkrishna, Sudeep Verma, Vallabh Prakash Mulay, Ashish Kumar Gupta, Swati Haldar, Anurag Varshney. *PLoS Neglected Tropical Diseases*. 16: e0010484. doi: org/10.1371/journal.pntd.0010484. (IF 4.781)
- Withanolides from *Withania somnifera* Ameliorate Neutrophil Infiltration in Endotoxin-Induced Peritonitis by Regulating Oxidative Stress and Inflammatory Cytokines. (2021) Acharya Balkrishna, Siva Kumar Solleti, Hoshiyar Singh, Niti Sharma, Anurag Varshney *Planta Medica*. 88: 466. doi: 10.1055/a-1438-2816. (IF 3.352)

Toxicological Studies. Although there are no guidelines mandating the regulatory toxicological studies for Ayurvedic drugs, PRI, in an unprecedented attempt to charter a roadmap for Ayurvedic drug development in alignment with that of the modern drugs, have started conducting non-clinical safety assessments for herbal extracts and Ayurvedic formulations in compliance with

regulatory guidelines, like OECD-407. In this series, so far, two studies have been published: both were 28-day repeated dose toxicological evaluations with 14-day recovery regime conducted in Sprague-Dawley rats for Coronil (**Drug and Chemical Toxicology. 2022, doi: 10.1080/01480545.2022.2036183**) and whole plant extract of *Withania somnifera* (Ashwagandha) (**Scientific Reports. 2022, 12: 11047. doi: 10.1038/s41598-022-14944-x**).

- **28-Day Repeated Dose Toxicological Evaluation of Coronil in Sprague Dawley Rats: Behavioral, Hematological, Biochemical and Histopathological Assessments Under GLP Compliance. (2022) Acharya Balkrishna, Sandeep Sinha, Anurag Varshney. Drug and Chemical Toxicology. doi: 10.1080/01480545.2022.2036183. (IF 3.356)**
- ***Withania somnifera* (L.) Dunal Whole plant Extract Demonstrates Acceptable Non clinical Safety in Rat 28 day Subacute Toxicity Evaluation Under GLP compliance. (2022) Acharya Balkrishna, Sandeep Sinha, Jyotish Srivastava, Anurag Varshney. Scientific Reports. 12: 11047. doi: 10.1038/s41598-022-14944-x. (IF 4.379)**

Chemical Characterizations. Ayurvedic formulations are of natural origin, with medicinal herbs being major ingredients. Therefore, the phytochemical compositions of Ayurvedic formulations are affected by several environmental

factors which directly influence bioactive components of the plant raw materials. Heterogeneity of the phytoconstititional composition of the Ayurvedic formulations, and consequently, their therapeutic efficacy, therefore, raise a major concern in the global acceptability of these drugs. Thus, a traceability with respect to the phytoconstituent compositions of the Ayurvedic formulations is a prime requirement. In order to address this issue, the team of analytical chemists at PRI is engaged in optimizing batteries of analytical processes to consistently and reproducibly identify certain marker phytocompounds in different Ayurvedic formulations. So far they have optimized the processes for classical Ayurvedic formulation, Mahayograj Guggul (**Journal of Separation Science. 2022, 45:1616. doi: 10.1002/jssc.202100935**), Divya-Kayakalp-Vati and Divya-Kayakalp-Oil (**Clinical, Cosmetic and Investigational Dermatology. 2022, 15: 293. doi: 10.2147/CCID.S342227**), Coronil (**Journal of Separation Science. 2021, 44: 4064. doi: 10.1002/jssc.202100499**) and Divya-Swasari-Vati (**Journal of Separation Science. 2021, 44: 3146. doi: 10.1002/jssc.202100096**).

- **Standardization and Validation of Phytometabolites by UHPLC and High-performance Thin Layer Chromatography for Rapid Quality Assessment of Ancient Ayurvedic Medicine, Mahayograj Guggul. (2022) Acharya Balkrishna, Meenu Tomer, Monali Joshi, Seema Gujral, Rajesh Kumar Mishra, Jyotish Srivastava, Anurag**

Varshney. *Journal of Separation Science*. 45:1616. doi: 10.1002/jssc.202100935. (COVER PAGE) (IF 3.645)

- **Comprehensive Phytochemical Profiling of Polyherbal Divya-Kayakalp-Vati and Divya-Kayakalp-Oil and Their Combined Efficacy in Mouse Model of Atopic Dermatitis-Like Inflammation Through Regulation of Cytokines. (2022) Acharya Balkrishna, Sudeep Verma, Sachin Sakat, Kheemraj Joshi, Siva K Solleti, Kunal Bhattacharya, Anurag Varshney. *Clinical, Cosmetic and Investigational Dermatology*. 15: 293. doi: 10.2147/CCID.S342227. (IF 2.489)**
- **Phyto-metabolite Profiling of Coronil, A Herbal Medicine for COVID-19, Its Identification by Mass-spectroscopy and Quality Validation on Liquid Chromatographic Platforms. (2021) Acharya Balkrishna, Meenu Tomer, Sudeep Verma, Monali Joshi, Priyanka Sharma, Jyotish Srivastava, Anurag Varshney. *Journal of Separation Science*. 44: 4064. doi: 10.1002/jssc.202100499. (COVER PAGE) (IF 3.645)**
- **Development and Validation of a Rapid High-performance Thin-layer Chromatographic Method for Quantification of Gallic acid, Cinnamic acid, Piperine, Eugenol, and Glycyrrhizin in Divya-Swasari-Vati, An Ayurvedic Medicine for Respiratory Ailments. (2021) Acharya Balkrishna, Priyanka Sharma, Monali Joshi, Jyotish**

Srivastava, Anurag Varshney. *Journal of Separation Science*. 44: 3146. doi: 10.1002/jssc.202100096. (IF 3.645)

Clinical and Psychosomatic Studies. In a regular drug development process, clinical studies are a must. However, Ayurvedic drugs being in use for several centuries, do not raise questions regarding clinical safety. Regardless of that, as mentioned above, in order to align the Ayurvedic drug development process with that of modern drugs, the team of clinical researchers have conducted and are conducting several ethical approved registered clinical trials; the one on the herbal ingredients effective against SARS-CoV-2 infection has been published (*Phytomedicine*. 2021, 84: 153494. doi: 10.1016/j.phymed.2021.153494). It is of utmost importance that patient compliance and post-marketing surveys be conducted on newly launched drugs. Along these lines, PRI has also initiated quite a few psychosomatic studies, a couple of which have been already completed and published, like the one on extent of satisfaction and associated improvement of the quality of life of the patients who received Ayurvedic COVID-19 treatment (***Patient Preference and Adherence*. 2021, 15: 899. doi: 10.2147/PPA.S302957**). In a peripheral study, the effect of hospital COVID-19 policies on treatments of other diseases was captured for dental patients (***Psychology Research and Behavior Management*. 2022, 15: 913. doi: 10.2147/PRBM.S351948**).

➤ **Randomized Placebo-controlled Pilot Clinical Trial on The Efficacy**

of Ayurvedic Treatment Regime on COVID-19 Positive Patients.

(2021) Ganpat Devpura, Balvir S Tomar, Deepak Nathiya, Abhishek Sharma, Deepak Bhandari, Swati Haldar, Acharya Balkrishna, Anurag Varshney. Phytomedicine. 84: 153494. doi: 10.1016/j.phymed.2021.153494. (IF 6.656)

- **Influence of Patient-Reported Treatment Satisfaction on Psychological Health and Quality of Life Among Patients Receiving Divya-Swasari-Coronil-Kit Against COVID-19: Findings from a Cross-Sectional “SATISFACTION COVID” Survey. (2021) Acharya Balkrishna, Preeti Raj, Pratima Singh, Anurag Varshney. Patient Preference and Adherence. 15: 899. doi: 10.2147/PPA.S302957. (IF 2.711)**
- **Psychological Impacts of COVID-19 in Dental Patients Are Moderated and Mediated by Hospital-Infection-Control-Policy and Satisfaction-with-Life: A Prospective Observational DENTAL-COVID Study. (2022) Acharya Balkrishna, Kuldeep Singh, Gurpreet Oberoi, Pratima Singh, Preeti Raj, Anurag Varshney. Psychology Research and Behavior Management. 15: 913. doi: 10.2147/PRBM.S351948. (IF 2.945)**



Contents lists available at ScienceDirect

Phytomedicine Plus

journal homepage: www.elsevier.com/locate/phyplu

Effects of fatty acids in super critical fluid extracted fixed oil from *Withania somnifera* seeds on Gram-negative *Salmonella enterica* biofilms



Acharya Balkrishna^{a,b}, Ashish Kumar Gupta^a, Kanchan Singh^a, Swati Haldar^a, Anurag Varshney^{a,b,*}

^a Drug Discovery and Development Division, Patanjali Research Institute, Roorkee-Haridwar Road, Haridwar-249405, Uttarakhand, India

^b Department of Allied and Applied Sciences, University of Patanjali, NH-58, Haridwar-249405, Uttarakhand, India

ARTICLE INFO

Keywords:

WSSO
Salmonella enterica
 Antibacterial
 Fatty acids
 Potassium efflux
 Nucleotide efflux
 Biofilm
 Bacterial motility.

ABSTRACT

Background: Biofilms are responsible for the growing resistance of bacteria to antibiotics, preventing the antibiotic accessibility to bacterial cells. As an alternative to antibiotics, fatty acids (FAs) have been explored for their antibiofilm activities due to their diffusible nature and ability to modulate the membrane fluidity of the bacteria. Fatty acids have been shown as anti-biofilm agents mostly for Gram-positive pathogens. Therefore, we chose to explore the anti-biofilm activity of FAs from *Withania somnifera* (L.) Dunal (Solanaceae) seeds fixed oil (WSSO) on the Gram-negative pathogen, *Salmonella enterica*. Biofilm formation in *Salmonella* spp enhances its resistance to antibiotics and host immune response, with consequent increase in its virulence and chronicity of infection. FAs from WSSO was reported for their effectivity against Psoriasis-like skin inflammation. Biofilms are implicated in Psoriasis pathology and anti-biofilm therapy can provide new treatment options. In view of its biological importance, we have explored the activity of WSSO against planktonic and biofilm forms of *S. enterica*.

Purpose: The purpose of the current study is to evaluate the potentials of fixed fatty acids from an important medicinal plant (*W. somnifera*) as antibiofilm agents against a Gram-negative bacterium (*S. enterica*).

Methods: Antibacterial activity of WSSO against planktonic form of *S. enterica* was evaluated through broth microdilution method. Antibiofilm activity in terms of prevention of biofilm initiation, inhibition of biofilm formation and disruption of mature biofilm were quantified through crystal-violet staining. WSSO induced loss of membrane integrity, and concomitant effect on *S. enterica* motility were assessed through quantification of intracellular potassium and nucleotide effluxes, and motility assays, respectively.

Results: The minimal inhibitory concentration of WSSO required for 50% reduction in the planktonic bacterial load (IC₅₀) was 5.78 mg/ml. Cells lost their motility when treated with WSSO at IC₅₀. At a similar concentration of 6.28 mg/ml, WSSO disrupted mature biofilm of *S. enterica*. Bacterial cell membrane was compromised after treatment with 5.40 mg/ml WSSO as evident from potassium (K⁺) ion and nucleotide effluxes.

Conclusion: WSSO not only prevented initiation of biofilm formation and but also efficiently disrupted mature biofilm of *S. enterica*. Taken together, these results indicated that WSSO has the potentials to be used as an alternative antibacterial agent against Gram-negative pathogenic *S. enterica*. The mode of action of WSSO seems to be linked to its ability to modulate membrane integrity and to restrain bacterial motility, most likely by its abundant and trace fatty acid contents.

Introduction

Discovery of penicillin in 1928, closely followed by that of sulfonamide in 1935, marked the beginning of a new era in clinical microbiology. However, the emergence of penicillinase producing *Staphylococcus aureus* almost soon after the first clinical application of penicillin in 1940s marked the inception. As an alternative, the use of

plant materials is currently recognized as an effective approach for handling this issue, one that was to make the medical system struggle despite its advancements some 90 years down the line (Saga and Yamaguchi, 2009). Antibiotics have evolved significantly over the next six decades from 1930s-1990s, and so did the bacterial resistance to them. During this time, aminoglycosides, chloramphenicol, tetracycline, macrolides, vancomycin, methicillin, nalidixic acid, first, second and

* Corresponding author at: Drug Discovery and Development Division, Patanjali Research Institute, Roorkee-Haridwar Road, Haridwar-249405, Uttarakhand, India. E-mail address: anurag@prft.co.in (A. Varshney).

third generation cepheims, carbapenem, monobactams and quinolones were developed. Indiscriminate use of these drugs led to the emergence of penicillin interfering *Streptococcus pneumonia* (PISP), penicillin resistant *S. pneumonia* (PRSP), penicillinase producing, β -lactamase negative, ampicillin resistant (BLNAR) *Haemophilus influenza*, extended spectrum β -lactamase (ESBL) producing Gram-negative bacilli, vancomycin resistant enterococci (VREs) emerged, resistant gonococci, multidrug resistant *Pseudomonas aeruginosa* (MDRP) and quinolone resistant *Escherichia coli*. Only during the past two decades this unselective use of antibiotics has been reduced (Saga and Yamaguchi, 2009). However, drug resistance developed by different bacterial strains till now, prevents effective treatments.

Drug resistance is conferred due to changes in bacterial genome that enhances their fitness in the face of selection pressure from the evolving antibiotics. Changes in bacterial genomes facilitate quorum sensing and biofilm formation through diffusible signal factors (DSFs). Biofilms constitutes physical barriers made of extra-cellular polymeric substance (EPS) containing polysaccharides, proteins, extracellular DNA and lipids (Kumar et al., 2020). Bacterial cells embedded within the biofilm become inaccessible to the antibiotics, thus, making them highly resistant to antibiotic treatment. This quite often results in recurrent infections (D'Ambrosia et al., 2013). As an alternative, the use of plant materials is currently recognized as an effective approach for handling this issue.

Several studies proved long chain fatty acids (LCFAs) to be bactericidal for Gram-positive bacteria and that they affect the integrity of the bacterial cell wall (Galbraith and Miller, 1973a; Sheu et al., 1975). The significant difference in the sensitivities of Gram-positive and Gram-negative bacteria towards LCFAs was believed to be due to the structure of the cell wall of the latter that prevented LCFAs from reaching the lipid bilayer of the cell membrane (Galbraith and Miller, 1973b; Greenway and Dyke, 1979; Sheu et al., 1975). This was experimentally proved in case of *Salmonella typhimurium*, where the outer lipid bilayer was significantly resistant to hydrophobic substances while, the protoplasts devoid of this layer were sensitive to them (Nikaido, 1976). Most of the earlier reports emphasize that effectivity of FAs as antibacterial against Gram negative bacteria is either non-existent or meager. All these studies have been conducted with single FAs (Yoon et al., 2018).

Withania somnifera (L.) Dunal (Solanaceae), a popular medicinal herb, is extensively used in traditional Indian medicine. It is a rich source of phytochemicals like steroids (withanolides) and alkaloids many of which has been identified and extracted (Balkrishna et al., 2020; Mwitari et al., 2013; Vyas et al., 2011). Roots, leaves, and fruits of *W. somnifera* exhibited potent antibacterial activities against *Salmonella enterica* and other pathogenic bacteria which are attributed to the withanolides present in them (Alam et al., 2012; Owais et al., 2005). In an earlier study from our group, *W. somnifera* seeds fixed oil (WSSO) showed to be effective against psoriasis. In the light of a previous study demonstrating that innate immune system of human skin has antimicrobial lipids as an indispensable component, this observation led us to think that WSSO could be a potential antibacterial agent (Yoon et al., 2018). WSSO was obtained using CO₂ as supercritical solvent, which offers the advantages of possessing low viscosity and high diffusivity into the seeds, thus ensuring improved extractions of FAs present in trace amount. Linoleic, oleic, palmitic and stearic acids were identified as the major long chain fatty acids (LCFAs) in WSSO while ecosatrienoic and nervonic acids, which are also LCFAs, were present in trace amounts (Fig. 1) (Balkrishna et al., 2020). Thus, WSSO, being a mixture of abundant and trace FAs, is anticipated to be effective against Gram negative bacteria. *S. enterica* infection and antibiotic resistance are results of biofilm formation, which in turn is dependent on bacterial motility and quorum sensing. Biofilm forms through several stages. Therefore, the present study was designed to evaluate the effect of WSSO at the following stages of *S. enterica* biofilm development: (1) initial stages of biofilm formation (when bacterial cells attach to the substratum), (2) at the maturation stage (when the agglomerated bacterial cells secrete extracellular polymeric substance or EPS to fortify the biofilm) and (3)

on mature biofilm (from which bacterial cells disperse to recolonize new surfaces). Besides, we have explored the possible mode of action of WSSO as an antibacterial and antibiofilm agent.

Material and methods

Chemicals, bacteriological media, and bacterial strain

Chemicals used in this study were from Sigma-Aldrich (St Louis, MO, USA) unless otherwise mentioned. Bacteriological media were procured from Difco (BD Biosciences, San Jose, CA, USA). The pathogenic strain of *S. enterica* (MTCC1165) was obtained from Microbial Type Culture Collection (MTCC), CSIR-Institute of Microbial Technology (Chandigarh, India). Henceforth, we will refer this strain as *S. enterica*. Bacterial cells were reactivated from glycerol stock, first by streaking on nutrient agar plate for the single colony and subsequently, followed by overnight growth in nutrient broth at 37 °C.

Antibacterial assay

Determination of inhibitory concentration through microbroth dilution method

The antibacterial potency of WSSO against *S. enterica* was evaluated through microbroth dilution method as per the standard guidelines of the Clinical and Laboratory Standards Institute (CLSI, 2015). WSSO was emulsified in an equal volume of 5% DMSO containing 0.1% v/v polysorbate-80. Stock solution (180 mg/ml) was further two-fold serially diluted with 5% DMSO along with 0.1%v/v polysorbate-80 which resulted in test dilutions ranging from 0.70–90 mg/ml with reference to WSSO and 0.01–1.25% wrt to DMSO. After dispersing 125 μ l of each test dilution of WSSO in triplicate in the wells of a 96-well plate, an equal volume of bacterial suspension of *S. enterica* prepared in 2x Mueller Hinton Broth (MHB), containing $\sim 10^5$ CFU/ml was added to each well so that the final volume per well reached 250 μ l. A control set having bacterial cells incubated in amount of DMSO corresponding to each dilution (0.01–1.25%) was included to ensure that the observed inhibitory effects were not due to DMSO. The maximum concentration of DMSO to which the cells got exposed was 2.5%. The plates were incubated for 18 h at 37°C with shaking at 195 xg. Post-incubation, absorbance of these cultures was measured at 600 nm using a microplate reader (Envision, Perkin Elmer, Waltham, MA, USA). Chloramphenicol (Lupin, Mumbai, India) was used as a positive control. A negative control containing 5% DMSO along with 0.1%v/v polysorbate-80 was used. Percent bacterial growth inhibition by WSSO was calculated using the following equation:

$$\% \text{ Bacterial Growth Inhibition} = [(A_c - A_t) / A_c] \times 100$$

Where A_c: Absorbance of the control; A_t: Absorbance of test extract

Percent growth inhibition was represented graphically as a function of increasing WSSO concentrations. Using the inbuilt option of Graph-Pad Prism software 7.05 (San Diego, CA, USA), IC₅₀ value which inhibited 50% percent of the organism tested was determined (Van Dijk et al., 2018).

Determination of bactericidal potency of WSSO

Different concentrations of WSSO 0.70–90 mg/ml were inoculated with a fixed concentration of *S. enterica* bacterial cells (10⁵ CFU/ml) in sterile Mueller Hinton broth and incubated at 37°C for 24 h. Subsequently, 50 μ l of each incubated mix was spread on sterile Mueller Hinton Agar plates (without WSSO). Colony-forming units (CFU) were counted after 24 h incubation at 37°C and plotted as CFU/plate versus concentration of WSSO. The lowest concentration of WSSO which prevented bacterial growth was identified as the minimum bactericidal concentration (MBC) (Bertelloni et al., 2020). Chloramphenicol (Lupin) was used as a positive control.

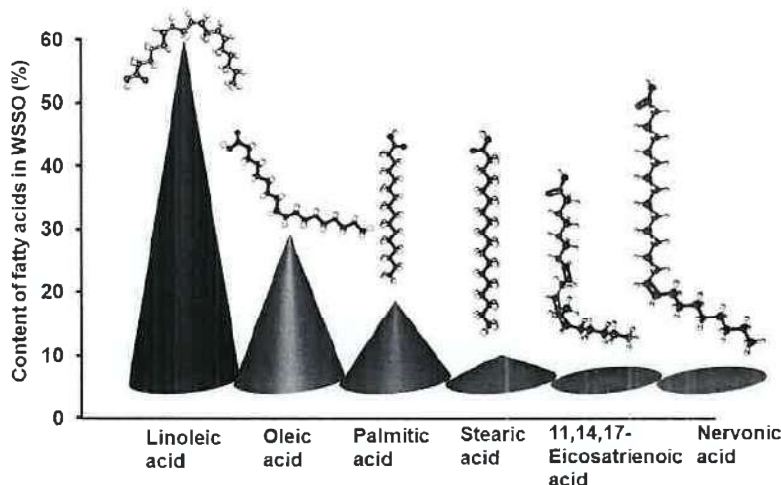


Fig. 1. Chemical composition of WSSO on GC-FID quantification.

A schematic showing the composition of WSSO in terms of percentages of different fatty acids present along with their chemical structures [Adapted from Fig 2 and Table 1 of (Balkrishna et al., 2020)].

Mechanism of action

Potassium (K^+) cation leakage

The K^+ leakage from *S. enterica* was estimated in the presence of WSSO. K^+ leakage was quantified by using a spectrophotometric method (Rajawat et al., 2014). Bacterial cells from an overnight culture were centrifuged at 8600xg for 10 min, washed twice with 1x PBS (pH 7.2) and resuspended in 1x PBS at a density of 1×10^8 cells/ml. 1 ml aliquots of the cell suspension were mixed with 0.90, 3.60, 5.40 and 10.8 mg/ml and incubated at 37°C for 0, 2, 4, 6, and 8 h. At each point, the supernatant was collected by centrifugation and mixed with 25% sodium cobaltinitrite. The sodium cobaltinitrite precipitate formed was kept at room temperature for 45 min and subsequently washed with 95% ethanol. After adding concentrated HCl to the precipitates, samples were incubated at room temperature for 20 min for deep green color formation that was quantified at 623 nm by using a UV-VIS spectrophotometer (Shimadzu, Kyoto, Japan). Chloramphenicol (30 µg/ml) (Lupin) was used as a positive control. The intensity of the green coloration was proportional to the amount of K^+ ions present in the supernatant and quantified using a standard curve.

Nucleotide efflux

Cells from logarithmic phase culture of *S. enterica* were washed and resuspended as 1 ml aliquots in 1x PBS buffer (pH 7.2) at a density of 1×10^8 cells/ml, followed by incubation with different concentrations (0.90, 3.60, 5.40 and 10.8 mg/ml) of WSSO for 12 h. Every 3 h, an aliquot was filtered and absorbance of the filtrate measured at 260 nm using a UV-VIS spectrophotometer (Shimadzu) (Da Silva et al., 2014). Chloramphenicol (30 µg/ml) (Lupin) was used as positive control.

Antibiofilm activity

Determination of biofilm forming capacity of *S. enterica* (MTCC1165)

S. enterica biofilms were grown in 96-well plates, containing 200 µl of cell suspension in MHB containing 1×10^6 cells/ml. MHB without any bacterial inoculum was included as negative control. Plates were incubated for 24 and 48 h at 37 °C. Subsequently, biofilm biomass was stained with crystal violet, the stain extracted with acetic acid and absorbance measured at 570 nm. Critical OD value (ODc) was defined according to Christensen et al. (1985) and Gomes et al. (2019) as three standard deviations above the mean OD of the negative control and the biofilm production was scored as: [strong biofilm producers {(+++), OD > 4 x ODc}, moderate biofilm producers {(++), 2 x ODc < OD

< 4 x ODc}, weak biofilm producers {(+), ODc < OD ≤ 2 x ODc} and non-biofilm producers {(−), OD ≤ ODc}] (Christensen et al., 1985; Gomes et al., 2019).

Determination of inhibitory effect of wssO on biofilm formation

S. enterica cell suspension aliquots of 125 µl in MHB containing 1×10^6 cells/ml were mixed with different concentrations of WSSO (0.70, 1.40, 2.80, 5.62, 11.25, 22.5, 45 and 90 mg/ml) and incubated for 24 h at 37 °C. Biofilm biomass was determined through crystal violet staining as described above. Percent inhibition of biofilm formation was calculated with respect to the untreated control.

Determination of preventive effect of WSSO on biofilm maturation

Cells were first allowed to incubate for 24 h at 37 °C without shaking following which they were mixed with different concentrations of WSSO (0.70, 1.40, 2.80, 5.62, 11.25, 22.5, 45 and 90 mg/ml) and incubated for another 24 h at 37 °C. Biofilm biomass was determined through crystal violet staining as described above and percent preventive efficiency of biofilm maturation was calculated with respect to the untreated negative control.

Determination of disruptive effect of WSSO on mature biofilm

In this case, the cells at same density as mentioned earlier were allowed to form mature biofilm by incubating them at 37 °C for 48 h without shaking. The mature biofilms were then treated with different concentrations of WSSO (0.70, 1.40, 2.80, 5.62, 11.25, 22.5, 45 and 90 mg/ml) for another 24 h at 37 °C. The biofilm biomass degradation was assayed by the crystal violet staining method (Famuyide et al., 2019).

Staining of biofilm

Crystal violet staining

After following the above incubation periods, biofilms were stained according to a previous report (Gomes et al., 2019). All planktonic cells were carefully removed, and adhered/biofilm cells were washed twice with NaCl 0.9% (w/v), and then fixed for 15 min at 37 °C by adding 250 µl of methanol, and subsequently, cells were air-dried after discarding the excess methanol. 250 µl of 1% (v/v) crystal violet (CV) was added to each well for 5 min. The stained adherent/biofilm cells were air-dried for 2 h, following which, 250 µl of 33% (v/v) acetic acid was added to extract the dried CV stain. Absorbances of the resulting violet solutions were measured at 570 nm. Un-inoculated wells stained with CV were

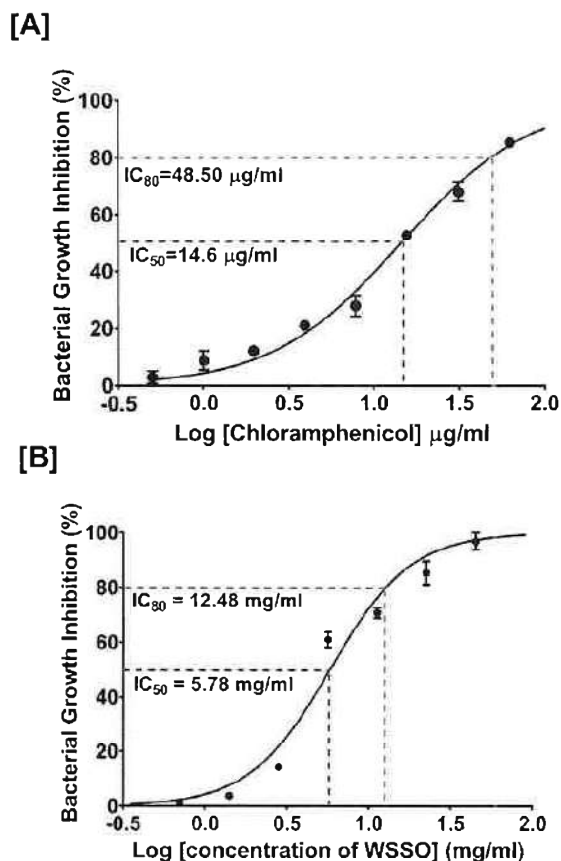


Fig. 2. Antibacterial effect of WSSO on *S. enterica* [A, B] Dose-response curves showing a normalized dose-dependent inhibitory effect of positive control chloramphenicol (A) and WSSO (B) on the growth of *S. enterica* cells as evaluated through microbroth dilution method. Concentrations responsible for 50 (IC_{50}) and 80 (IC_{80})% growth inhibitions, as determined through non-linear regression analysis, are mentioned.

used as blank controls. Percent inhibition of biofilm formation and maturation and percent disruption of mature biofilm were determined using the following equation

$$\% \text{ bacterial biofilm inhibition} = [(A_c - A_t) / A_c] \times 100$$

where A_c : Absorbance of the untreated sample; A_t : Absorbance of treated sample

Data represented as percent inhibition of bacterial biofilm formation (BIC or biofilm inhibition concentration) or percent disruption of the mature biofilm (BEC or biofilm eradication concentration) as a function of increasing concentrations of WSSO (Van Dijck et al., 2018). 50% inhibitory (BIC_{50} or BEC_{50}) concentrations for each assay was determined using an in-built option provided in GraphPad Prism 7.0.

Gram staining of biofilm

Gram staining of microbial biofilms was performed as reported earlier (Haney et al., 2018). For staining of biofilms, control cells and test cells were grown on coverslips placed in 35 mm petri plates. 125 μ l of bacterial suspension in MBH containing 1×10^6 cells/ml, was added on the coverslips and incubated at 37 °C for 48 h without any shaking, following which 0.70, 1.40, 2.80, 5.62, 11.25, 22.5, 45 and 90 mg/ml of

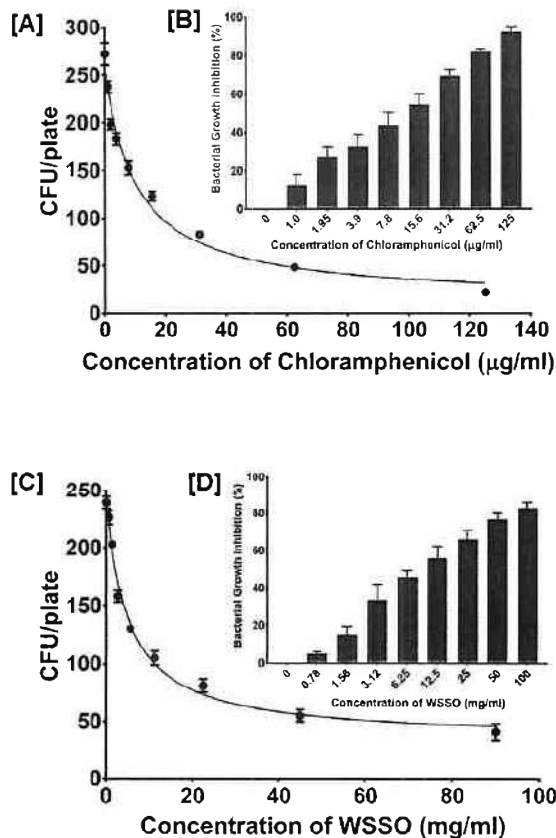


Fig. 3. Bactericidal potency of WSSO against *S. enterica* [A, C] Rectangular hyperbolic plots of CFU/plate versus different concentrations of positive control chloramphenicol and WSSO. [B, D] Percent growth inhibition versus concentration bar graphs showing the effects of increasing concentrations of chloramphenicol (B) and WSSO (D) on *S. enterica* growth.

WSSO was added and incubated further at 37 °C for 24 h without agitation. The coverslips were Gram-stained, to verify the effect of WSSO on the viable cells embedded within the biofilm. Stained coverslips were mounted on clean glass slides by applying 40% glycerol and imaged using a bright field microscope (AxioScope A1, Carl Zeiss Microimaging GmbH, Oberkochen, Germany) under 100x objective.

Bacterial motility assay

Motility inhibition of *S. enterica* in the presence of WSSO was determined through swimming and swarming assays. Lauria Bertani (LB) plates enriched with 0.5% (w/v) glucose, and containing 0.20% and 0.50% bacteriological agar, respectively, were used for swimming and swarming assays (Chelvam et al., 2014). 5 μ l of an overnight culture of *S. enterica* with 5.89 mg/ml and without WSSO were placed on the agar surface of the specific plates. Both types of plates were kept for incubation at 37 °C for 24 h. Uninhibited motility of the bacteria was visible as expanded circular bacterial surface around the initial spot of application of the bacterial culture. The radius of this expanding circle, measured as the distance traveled by the bacteria, depicted the extent of bacterial motility. The plates were imaged and distances measured from three independent experiments for each type of motility were represented as mean \pm SE.

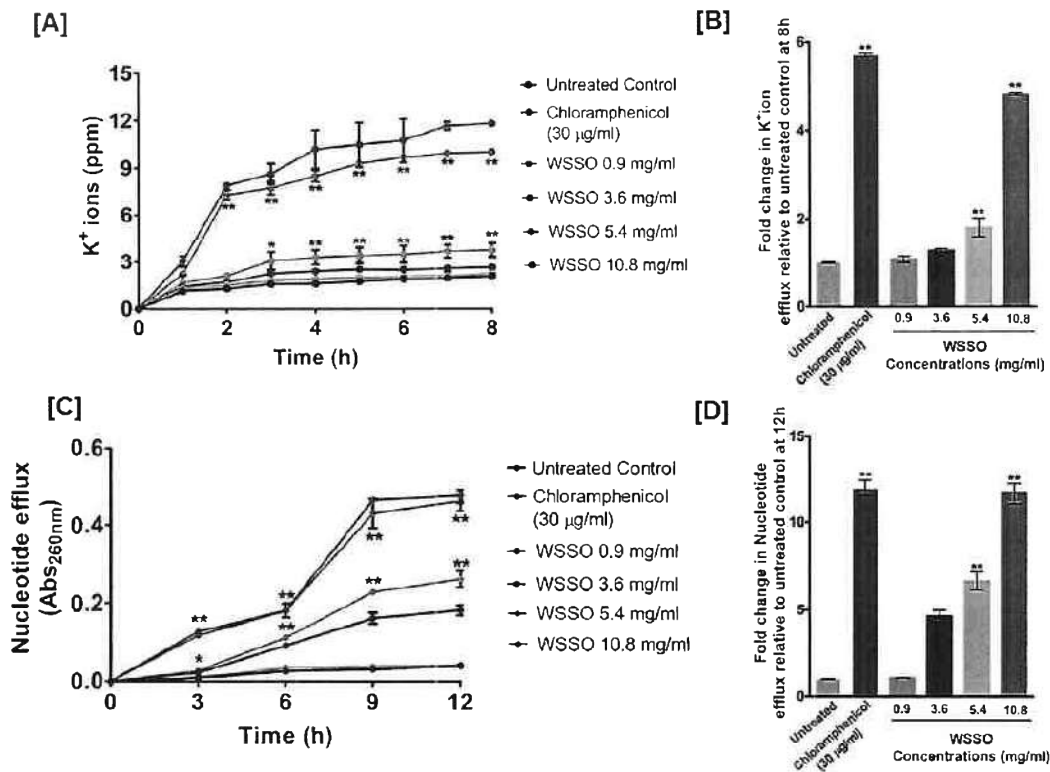


Fig. 4. WSSO treatment promotes efflux of intracellular ions and nucleotides from the bacterial cells [A, C] Comparative line graphs showing concentration and time dependent effect of WSSO on intracellular K^+ (A) and nucleotide (C) leakage/efflux. [B, D] The observed fold change in intracellular K^+ (B) and nucleotide (D) leakage/efflux after 8 and 12 h, respectively, of treatment with different concentrations of WSSO. Data represented as mean \pm SE. Statistical significance determined through one-way ANOVA with Dunnett's multiple comparison test where * and ** represent $p < 0.01$ and 0.001 , respectively, when compared to untreated control in case of (A & C) and chloramphenicol in case of (B & D).

Statistical analysis

Statistical significance of the observed differences between the average potassium ion and nucleotide effluxes of various groups was analyzed through one-way ANOVA followed by Dunnett's post-hoc test and indicated with ** for $p < 0.01$ when compared to control. Paired t-test was used to evaluate the statistical significance of the observations for motility assays and indicated with * and ** for $p < 0.05$ and $p < 0.01$, respectively. Two-way ANOVA with Bonferroni's post-hoc test was used to assess the statistical significance of the observations regarding inhibitory effect of WSSO on biofilm formation and were represented with ** and *** for $p < 0.01$ and $p < 0.001$, respectively. All statistical analyses were done using GraphPad Prism 7.0.

Results

Determination of IC_{50} and IC_{80}

Concentrations of Chloramphenicol and WSSO against *S. enterica* MTCC1165 that inhibited 50 and 80% of bacterial growth was determined through microbroth dilution method. Chloramphenicol at $14.6 \mu\text{g/ml}$ (IC_{50}) and $48.5 \mu\text{g/ml}$ (IC_{80}) (Fig. 2A) while WSSO at concentration 5.78 mg/ml (IC_{50}) and 12.41 mg/ml (IC_{80}) (Fig. 2B) inhibited 50 and 80% of the bacterial growth, respectively. Bactericidal potency of WSSO was evaluated as the efficiency with which colony forming units (CFU) were formed after WSSO treatment. The CFU was counted

and plotted against different concentrations of the positive control, chloramphenicol concentrations (Fig. 3A) or WSSO (Fig. 3C). We observed that even at 90 mg/ml , a few CFUs were still visible, suggesting a high MBC value for WSSO (Fig. 3C) which reflected as $\sim 80\%$ inhibition in the bacterial growth at 100 mg/ml of WSSO (Fig. 3D). Bactericidal activity of chloramphenicol was observed at higher concentration (Fig. 3A & B).

Intracellular potassium (K^+) ion leakage

The mechanism behind the antibacterial effect of WSSO on *S. enterica* was evaluated by investigating the effect of WSSO treatment on the bacterial cell membrane. Leakage of intracellular ions is indicative of damage in the cell membrane which can be detected through the presence of K^+ ions in the medium. So, growth media of cells treated with different concentrations of WSSO were tested for the presence of K^+ ions. Untreated cells were taken as negative control while cells treated with chloramphenicol (that is known to disrupt the bacterial membrane), were included as a positive control. An indirect quantification method involving the colorimetric measuring of acid precipitates of potassium cobaltinitrite was employed. The amount of the precipitated K^+ ions were determined in parts per million (ppm) using a standard curve. We did not detect any K^+ ion in the medium of untreated cells throughout the experiment even after 8 h. Lower concentrations of WSSO 0.9 and 3.6 mg/ml also did not show any K^+ ions leakage in the media. However, K^+ ions were detectable 3 h onwards in the medium from

cells treated with near IC_{50} concentration 5.40 mg/ml of WSSO and the measured levels were significantly higher when compared to untreated cells. K^+ ion efflux in chloramphenicol treated cells was nearly 4 times higher than the untreated within 2 h of treatment, kept on increasing till 8 h, and became almost 6 times that of untreated. K^+ ion efflux in cells treated with 10.8 mg/ml (double to the determined IC_{50} concentration) followed a trajectory almost overlapping that of the positive control (Fig. 4A). The fold change in K^+ ions after 8 h in positive control calculated concerning untreated showed 5.7 times more efflux of these cells. Cells treated with different concentrations of WSSO exhibited dose-dependent fold increase in K^+ ion efflux; treatment with 10.8 mg/ml of WSSO showing comparable (4.8) fold change to that of positive control (Fig. 4B).

Nucleotide efflux

Along with the K^+ leakage quantification, nucleotide efflux is also one of the most common methods for monitoring the damages to cell membranes. Therefore, if WSSO damages the cell membrane in *S. enterica*, the presence of nucleotides will be evident in the medium. Growth media of cells treated with different concentrations of WSSO were tested for the efflux of nucleotides. Untreated cells were taken as negative control while cells treated with chloramphenicol were included as a positive control. Lower concentration of WSSO (0.9 mg/ml) did not show any nucleotide efflux in the medium. However, nucleotide efflux was detectable 6 h onwards in the medium from cells treated with near IC_{50} concentrations (3.60 and 5.40 mg/ml) of WSSO and the measured levels were significantly higher when compared to untreated cells. Nucleotide efflux in chloramphenicol treated cells was nearly 7 times higher than the untreated within 6 h of treatment, kept on increasing till 12 h, and became almost 12 times that of untreated. Nucleotide efflux in cells treated with 10.8 mg/ml (double the determined IC_{50} concentration) followed a trajectory almost overlapping that of the positive control (Fig. 4C). The fold change in nucleotide efflux after 12 h in positive control calculated concerning untreated showed 12 times more efflux of these cells. Cells treated with different concentrations of WSSO exhibited dose-dependent fold increase in nucleotide efflux; treatment with 10.8 mg/ml of WSSO showing fold change (11.7) comparable to the positive control (Fig. 4D).

Inhibitory effect of WSSO on the motility of *S. enterica*

Effect of WSSO on the motility of *S. enterica* was measured for their surface swimming (media with 0.2% agar) and swarming (media with 0.5% agar) ability. A 24 h incubation resulted in distinct circular bacterial zones in both swimming and swarming plates with untreated cells indicating unhindered motility of bacteria. However, following treatment with 5.78 mg/ml WSSO, no bacterial zones were observed showing that the motility of the cells has been jeopardized (Fig. 5A). By measuring the radius of the bacterial zones, we determined the extent of motility inhibition WSSO could inflict. We found at 50% microbial inhibitory concentration (IC_{50}) of 5.78 mg/ml, WSSO reduced swimming and swarming almost equally (~ 2.7 and ~ 3.0 folds, respectively) (Fig. 5B).

Antibiofilm activity

For the determination of the antibiofilm activity of WSSO, it was necessary to test the biofilm formation tendency of *S. enterica* strain used. We observed that *S. enterica* MTCC1165 can form moderate to strong biofilms depending on the duration of incubation. With an incubation of 24 h, the biomass of the formed biofilm as determined according to Gomes et al., 2019, who qualifies it to be a moderate one, while, an incubation of 48 h resulted in a strong biofilm (Gomes et al., 2019) (Table 1).

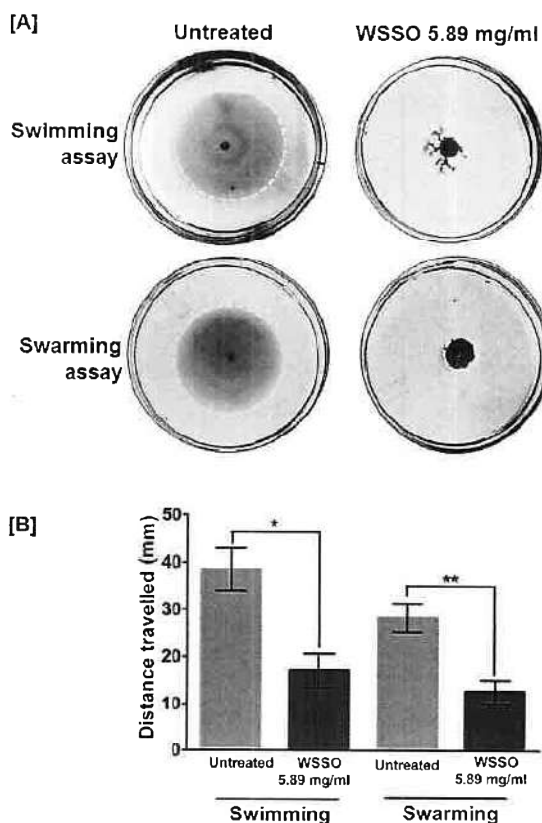


Fig. 5. Detrimental effect of WSSO treatment on bacterial motility [A] Representative digital images (inverted) of swimming and swarming assay plates showing the effect of WSSO (at 5.89 mg/ml) on *S. enterica* motility. [B] The observed attenuation of bacterial motility in response to WSSO treatment is represented as distance travelled by the bacteria as determined by measuring the radius of the circular bacterial zone formed by treated and untreated cells. Data represents the mean \pm SE from three independent experiments. Statistical significance determined through paired *t*-test where * and ** represent $p < 0.05$ and 0.01 , respectively, when compared to untreated to respective controls.

We first checked whether WSSO treatment is capable of inhibiting biofilm formation, for which, we allowed the bacterial cells to adhere to the bottom of the wells before incubating them with different concentrations of the oil for 24 and 48 h without shaking. At designated time points, the biofilm biomasses were CV stained and quantified. We observed that WSSO prevented biofilm formation in a dose-dependent manner. Apparently, longer incubation did not have any visible advantage; rather, it seemed to be unnecessary as evident from statistically significant increased inhibitory effects, for concentrations 2.80, 22.5 and 45 mg/ml. However, the concentrations near IC_{50} did not show difference for 24 and 48 h incubations (Fig. 6A). We plotted a normalized dose-response curve to determine the corresponding BIC_{50} values for 24 and 48 h incubations. Although the values were in the same range, the one for 24 h (5.56 mg/ml) was lesser than that for 48 h (6.87 mg/ml), implying that a 24 h incubation might be sufficient to prevent the biofilm formation. In order to prevent biofilm formation with an efficiency of 80% by 24 h, one might need to incubate with 19.24 mg/ml (BIC_{80}) of WSSO (Fig. 6B). Next, we checked whether WSSO can prevent biofilm maturation. From our experiments to determine the biofilm forming capacity of the *S. enterica* strain under study, we figured out that following a 24 h incubation, the cells formed mod-

Table 1
S. enterica (MTCC1165) biofilm formation after 24 and 48 h cultivation.

| Time | Control Mean ^a (OD±SD) | Biofilm Mean ^b (OD±SD) | Ratio (b/a) | Biofilm formation ^c |
|------|-----------------------------------|-----------------------------------|-------------|--------------------------------|
| 24h | 0.104±0.045 | 0.364±0.050 | 3.5 | ++ |
| 48h | 0.101±0.021 | 0.420±0.067 | 4.15 | +++ |

OD, optical density; SD, Standard deviation.

^a Gradation of biofilm formation as moderate biofilm producer (++) and strong biofilm producer(+++)are as per Gomes et al., 2019; Gomes et al., 2019.

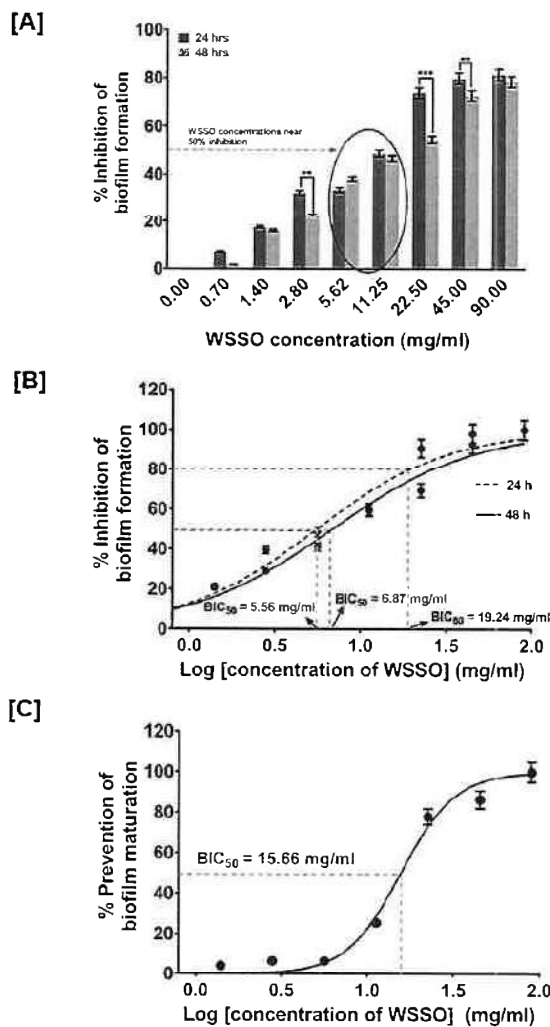


Fig. 6. WSSO inhibits initiation of biofilm formation more efficiently than preventing its maturation

[A] Comparative graphical representation of dose-dependent responses of WSSO on inhibition of initiation of biofilm formation over 24 and 48 h incubation. Doses near 50% inhibition of bacterial growth are encircled in red open circle. ** and *** respectively denote $p < 0.01$ and 0.001 from two-way ANOVA with Bonferroni's post-hoc test. [B] Normalized dose-response curve of the above showing the doses sufficient for 50 and 80% inhibitions of the inhibition of biofilm formation after 24 (broken line) and 48 h (solid line) incubations. [C] Normalized dose-response curve exhibiting the preventative effect of WSSO on biofilm maturation with the dose required for 50% effect.

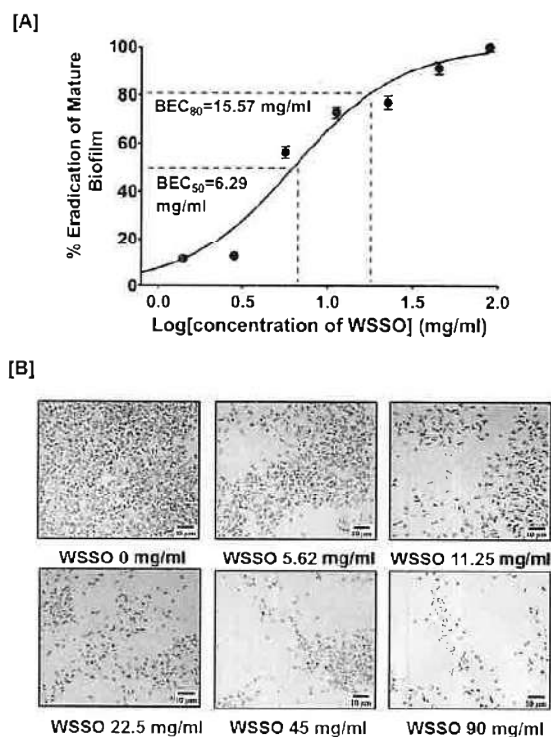
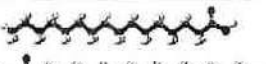

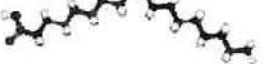
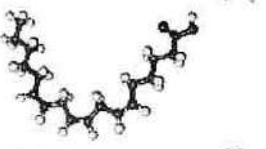




Fig. 7. WSSO efficiently disrupts mature biofilm

[A] Normalized dose-response curve showing the efficiency of WSSO in disrupting mature biofilm. Dose required for 50% disruption of mature biofilm was calculated through linear regression and marked accordingly in the graph. [B] Representative microscopic images of Gram stained WSSO treated and untreated mature biofilms.

erate biofilm which after another 24 h becomes strong. This indicated that by 24 h, the biofilm reaches the maturation phase. Therefore, our experimental design allowed the cells to form biofilm for 24 h before treatment with WSSO for another 24 h. WSSO could prevent biofilm maturation in a dose-dependent manner. However, its efficiency of preventing biofilm maturation was less compared to its efficiency in inhibiting the initiation of biofilm formation. This was evident from a higher BIC_{50} value of 15.66 mg/ml for prevention of biofilm maturation (compared to 5.56 mg/ml for 24 h or 6.87 mg/ml for 48 h incubation for inhibition of biofilm initiation study) (Fig. 6C). We further evaluated whether WSSO could disrupt and eradicate mature biofilms. For this strong mature biofilm formed through 48 h incubation of bacterial cells was treated with WSSO for 24 h. A treatment with 6.29 mg/ml of WSSO calculated from the normalized dose-response curve was enough to eradicate 50% of the mature biofilm (BEC_{50}) (Fig. 7A). Similarly, for an 80% biofilm eradication (BEC_{80}), 15.57 mg/ml of the oil. WSSO treated and

Table 2
Fatty acids present in WSSO detected through gas chromatography-flame ionized detector (GC-FID).

| WSSO Component | Molecular Formula | Chemical Structure | Content (% w/w) |
|--------------------------------------|--|--|-----------------|
| Palmitic acid (Hexadecanoic acid) | C ₁₆ H ₃₂ O ₂ |  | 12.64 |
| Stearic acid (Octadecanoic acid) | C ₁₈ H ₃₆ O ₂ |  | 4.07 |
| Oleic acid (Cis-9-Octadecanoic acid) | C ₁₈ H ₃₄ O ₂ |  | 23.16 |
| Linoleic acid | C ₁₈ H ₃₂ O ₂ |  | 54.15 |
| 11,14,17-Eicosatrienoic acid | C ₂₀ H ₃₄ O ₂ |  | 0.66 |
| Nervonic acid | C ₂₄ H ₄₆ O ₂ |  | 0.38 |

Note: These data were obtained and published in our previous research paper Balkrishna et al. (2020)(Balkrishna et al., 2020).

untreated mature biofilms were Gram stained and imaged and our observations from these images could be corroborated with our quantitative data mentioned above (Fig. 7B).

Discussion

The alarming rate at which drug resistance is rising in *Salmonella* spp necessitates identification of alternatives to the current antibiotics against this bacterium, particularly, when most of the current therapies seem to be inadequate in managing *Salmonella* infection (Britto et al., 2018). Through this study, we have observed that WSSO could not only prevent growth but also efficiently inhibit initiation of biofilm formation and disrupt mature biofilms of *S. enterica*. However, its ability to prevent biofilm maturation was rather less pronounced. Delving into the possible underlying mechanisms behind these WSSO activities, we discovered that this oil significantly increased the bacterial membrane permeability. In fact, a double dose of the IC₅₀ was equally efficient as the antibiotic chloramphenicol in increasing the membrane permeability. Since, FAs are already known to mimic different DSFs responsible for biofilm formation through affecting the motility of the bacteria, therefore, we checked the effect of WSSO on the communal locomotion of *S. enterica* through swimming and swarming assays. We noticed significant reduction, achieving almost no bacterial motility.

The observed IC₅₀ of WSSO against *S. enterica* (5.78 mg/ml) falls in the range of minimum inhibitory concentrations reported for different plant extracts and natural compounds (Mostafa et al., 2011). WSSO was observed to be toxic against different mammalian cell lines, like, THP-1, A431, and RAW264.7 only at concentrations above 27 mg/ml, thereby, indicating suitability of its usage in humans and livestock, the main targets of *Salmonella* infections (Balkrishna et al., 2020). WSSO treatment increases membrane permeability clearly suggesting that the bacterial membrane is compromised. FAs are known to interact with bacterial cell membrane to reduce its integrity. Most of the natural compounds from herbal extracts disrupt the bacterial membranes (Lou et al., 2011).

WSSO is a mixture of long chain both saturated and unsaturated FAs with carbon chains ranging from C-16 to C-24. It is enriched in linoleic (54%), oleic (23%), palmitic (13%), and stearic (4%) acids as evident

from gas chromatography-flame ionized detection (GC-FID) analysis. Eicosatrienoic and nervonic acids were also present, but in very small quantities (Fig. 1; Table 2)(Balkrishna et al., 2020). While palmitic and stearic acids are saturated FAs, the others are unsaturated ones. Linoleic, stearic and oleic acids are already reported for their bactericidal activity against different forms of *Helicobacter. pylori* and is found to be associated with *H. pylori* cell membrane (Jung et al., 2015). Palmitic, oleic and stearic acids were individually potent against *Salmonella* spp. (Zhang et al., 2016). Our observations also suggest that WSSO disrupts bacterial membrane with resultant leakage of K⁺ and nucleotides. Overall these reports support our observations that FAs destabilize bacterial cell membranes which, in turn, leads to the leakage of intracellular components (Yoon et al., 2018). FAs as alternatives to antibiotics are attractive because of their non-specific targets, unlike antibiotics. Non-specific targets minimize the risk of developing resistant bacterial strains (Desbois and Smith, 2010). The observed antibacterial effect of WSSO is attributed to the FAs present in it. Single chain FAs, like the ones present in WSSO, when get incorporated into the cell membrane, decrease interactions between intra-membrane phospholipids. This, in turn, results in increased membrane fluidity and permeability. Besides, linoleic acid is known to inhibit enzymes involved in FA synthesis, thereby, exerting a negative effect on the membrane formation (Yoon et al., 2018).

Biofilm formation in *Salmonella* spp. significantly enhances its drug resistance (González et al., 2018). We evaluated the biofilm forming capacity in *S. enterica* strain and observed a moderate to strong biofilm forming propensity that matched earlier reports (Beshiru et al., 2018; Trncic et al., 2018). Biofilm formation facilitates effective colonization of the luminal wall of the intestine leading to enhanced bacterial virulence, at the same time, imparting tolerance in the bacteria against hostile enteric environment. These chain of events are known to perpetuate into severe gastro-enteric infections in humans and have been recognized, over the past decade, as factors behind failure in infection management (MacKenzie et al., 2017). Transition to a sessile biofilm dominated lifestyle was associated with increase in the levels of saturated fatty acids in the cell membrane of *Salmonella* spp. (Dubois-Brissonnet et al., 2016). It is quite possible that in the presence of

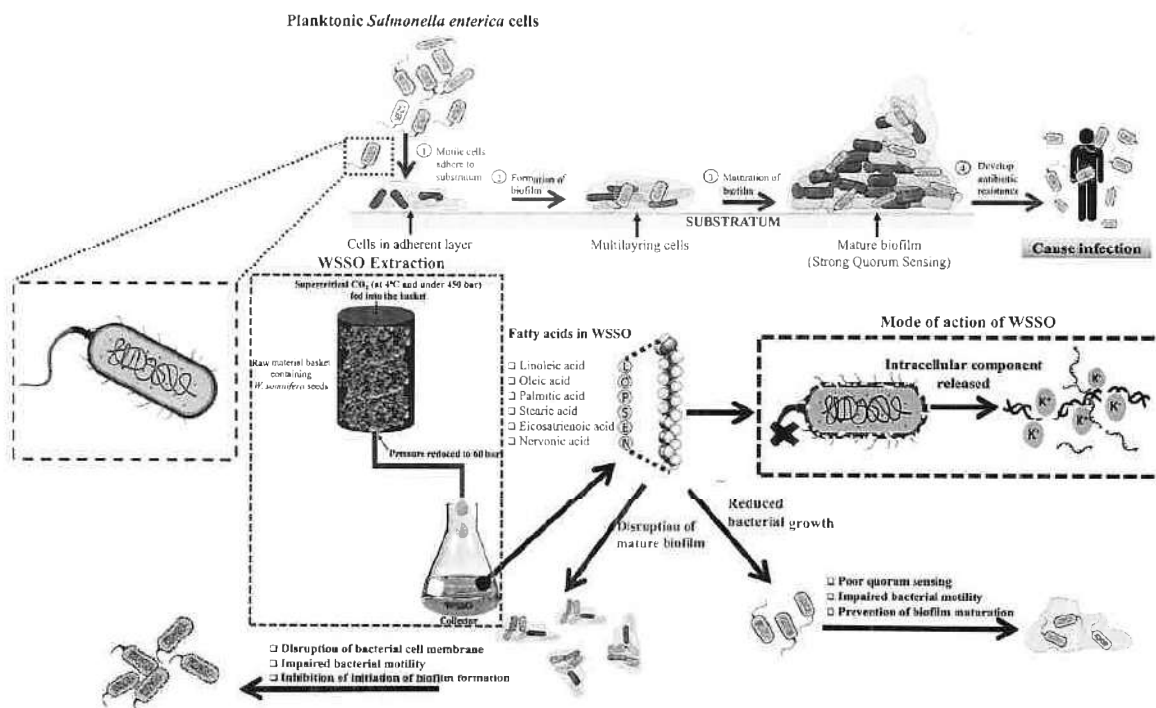


Fig. 8. WSSO efficiently disrupts mature biofilm

Schematic of a hypothetical model, as proposed based on the observations of this study, depicting a plausible mode of action of WSSO as an antibacterial and antibiofilm agent against Gram-negative pathogen, *S. enterica*.

WSSO, that contains mainly unsaturated FAs, the bacterial membrane gets more populated with these single chain unsaturated FAs that eventually increase its permeability as already mentioned above (Yoon et al., 2018). The IC₅₀ and BIC₅₀ of WSSO were comparable, indicating equivalent antibacterial and antibiofilm efficacies. WSSO effectively inhibited motility in *S. enterica*. Biofilm formation depends on bacterial motility and efficient quorum sensing communication system within the bacterial colony. Unsaturated FAs are reported to jeopardize both of these in *Acinetobacter baumannii*, another Gram-negative pathogen popular for its nosocomial acquisition (Nicol et al., 2018). A hexane extract from ground beef containing a blend of palmitic, stearic, oleic and linoleic acids inhibited biofilm formation in *Vibrio harveyi* and *E. coli*. Similarly, palmitic and oleic acids are known to affect the expressions of motility and quorum sensing related genes (Kumar et al., 2020). Based on these reports together with our observations, we speculate that a similar method is likely, to be employed by WSSO in inhibiting biofilm formation in *S. enterica*. It is worth to note that FAs act as signals for dispersion of mature biofilms, under normal conditions, to seed the formation of new biofilms (Davies and Marques, 2009). This is yet another caveat in the bacterial biofilm formation that is very effectively targeted by FAs to destroy mature biofilms when they are used at therapeutic doses (Marques et al., 2015). Putting all our observations in perspective, we proposed a hypothetical model describing the possible modes of action of WSSO as an anti-bacterial and anti-biofilm agent (Fig. 8)

Bacterial outer membrane is an evolving antibacterial barrier in Gram-negative bacteria which plays a significant role in imparting resistance against several antibiotics which are otherwise effective against Gram-positive bacteria (MacNair and Brown, 2020). Outer membrane disruptors are being increasingly recognized as an important component of combinatorial treatment, which is based on the principle of membrane perturbation followed by antibiotic treatment (Ma et al.,

2019; MacNair and Brown, 2020; Vaara, 1992). Our observations implicate that WSSO is capable of perturbing the outer membrane of *S. enterica*. The outer leaflet of the membrane of enteric bacteria, including that of *S. enterica*, lacks glycerophospholipids, thereby preventing diffusion of hydrophobic solutes across it. This leaflet is a highly ordered quasi-crystalline structure composed of only lipopolysaccharide (LPS) (Vaara, 1992). Such lipid asymmetry of the outer membrane imparts its barrier function, fortifying it against antibiotics and bile salts (May and Grabowicz, 2018). The LPS sequestered in the outer leaflet of the outer membrane facilitates bridging via their negatively charged saccharide portions through divalent cations. Colistin, from polymyxin group of antibiotics, that disrupts these intermolecular bridging reactions, is used as an outer membrane disruptor. Unfortunately, colistin is not spared from antibiotic resistance due to evolved LPS with less negative charges on their saccharide portions (May and Grabowicz, 2018). Therefore, lipophilic substances that can disrupt LPS-mediated fortification, without specifically targeting any step of out membrane biosynthesis, is likely to survive the rapidly evolving resistance. While, we are short of insight into the antibacterial effect of WSSO, nevertheless, intuitive thinking points towards a possibility that this oil, being rich in long chain FAs (saturated and unsaturated, alike) is presumably allowed to diffuse into the outer membrane and consequently, disrupt its compactness.

Conclusion

There have been several reports on antibacterial FAs. But, a mix of such antibacterial FAs obtained from an herbal source is probably reported for the first time in this study. The effective dose of WSSO is significantly lower than the one that showed inhibition of mammalian cells. This implies that WSSO would be a safe alternative to current

antibiotics for systematic development into a therapeutic against drug-resistant bacteria. In conclusion, this study offers the preliminary evidences in favor for developing WSSO it into a clinically usable antibacterial agent.

Funding source

This work has been conducted using internal research funds from Patanjali Research Foundation Trust, Haridwar, India.

Declaration of Competing Interest

The author(s) declare no competing interests and that this research was conducted with no commercial or financial relationships that can be construed as a potential conflict of interest.

CRedit authorship contribution statement

Acharya Balkrishna: Conceptualization, Funding acquisition, Resources. **Ashish Kumar Gupta:** Investigation, Methodology, Validation, Visualization, Writing – original draft. **Kanchan Singh:** Investigation, Methodology, Validation, Visualization. **Swati Haldar:** Supervision, Investigation, Visualization, Writing – review & editing. **Anurag Varshney:** Conceptualization, Supervision, Project administration, Writing – review & editing.

Acknowledgment

We thank Mr. Vallabh Mulay and Mr. Sudeep Verma for chemistry support. We extend our gratitude to Ms. Priyanka Kandpal, Ms. Babita Chandel, Mr. Tarun Rajput, Mr. Gagan Kumar and Mr. Lalit Mohan for their swift administrative supports.

References

- Alam, N., Hossain, M., Mottalib, M.A., Sulaiman, S.A., Gan, S.H., Khalil, M.I., 2012. Methanolic extracts of *Withania somnifera* leaves, fruits and roots possess antioxidant properties and antibacterial activities. *BMC Complement. Altern. Med.* 12, 2–9. doi:10.1186/1472-6882-12-175.
- Balkrishna, A., Nain, P., Chauhan, A., Sharma, N., Gupta, A., Ranjan, R., Varshney, A., 2020. Super critical fluid extracted fatty acids from *Withania somnifera* seeds repair psoriasis-like skin lesions and attenuate pro-inflammatory cytokines (TNF- α and IL-6) release. *Biomolecules* 10. doi:10.3390/biom10020185.
- Bertelloni, F., Cilita, G., Fratini, F., 2020. Bacteriostatic and bactericidal effect of figecycline on *Leptospira* spp. *Antibiotics* 1–7. doi:10.3390/antibiotics9080467.
- Beshiru, A., Igbinoza, I.H., Igbinoza, E.O., 2018. Biofilm formation and potential virulence factors of *Salmonella* strains isolated from ready-to-eat shrimps. *PLoS ONE* 13, 1–22. doi:10.1371/journal.pone.0204345.
- Britto, C.D., Wong, V.K., Dougan, G., Pollard, A.J., 2018. A systematic review of antimicrobial resistance in *Salmonella enterica* serovar Typhi, the etiological agent of typhoid. *PLoS Negl. Trop. Dis.* 12, 1–15. doi:10.1371/journal.pntd.0006779.
- Chelvam, K.K., Chai, L.C., Thong, K.L., 2014. Variations in motility and biofilm formation of *Salmonella enterica* serovar Typhi. *Gut Pathog* 6, 1–10. doi:10.1186/1757-4749-6-2.
- Christensen, G.D., Simpson, W.A., Younger, J.J., Baddour, L.M., Barrett, F.F., Melton, D.M., Beachey, E.H., 1985. Adherence of coagulase negative staphylococci to plastic tissue culture plates: a quantitative model for the adherence of staphylococci to medical devices. *J. Clin. Microbiol.* 22, 996–1006. doi:10.1128/jcm.22.6.996-1006.1985.
- D'Ambrosio, B., Buommino, E., D'Angelo, G., Coretti, L., Scognamiglio, M., Severino, V., Pacifico, S., Donnarumma, G., Fiorentino, A., 2013. Spectroscopic identification and anti-biofilm properties of polar metabolites from the medicinal plant *Helichrysum italicum* against *Pseudomonas aeruginosa*. *Bioorg. Med. Chem.* 21, 7038–7046. doi:10.1016/j.bmc.2013.09.019.
- Da Silva, I.F., De Oliveira, R.G., Mendes Soares, I., Da Costa Alvim, T., Donizeti Ascêncio, S., De Oliveira Martins, D.T., 2014. Evaluation of acute toxicity, antibacterial activity, and mode of action of the hydroethanolic extract of *Piper umbellatum* L. *J. Ethnopharmacol.* 151, 137–143. doi:10.1016/j.jep.2013.10.011.
- Davies, D.G., Marques, C.N.H., 2009. A fatty acid messenger is responsible for inducing dispersion in microbial biofilms. *J. Bacteriol.* 191, 1393–1403. doi:10.1128/JB.01214-08.
- Desbois, A.P., Smith, V.J., 2010. Antibacterial free fatty acids: activities, mechanisms of action and biotechnological potential. *Appl. Microbiol. Biotechnol.* 85, 1629–1642. doi:10.1007/s00253-009-2355-3.
- Dubois-Brissonnet, F., Trotier, E., Briandet, R., 2016. The biofilm lifestyle involves an increase in bacterial membrane saturated fatty acids. *Front. Microbiol.* 7, 1–8. doi:10.3389/fmicb.2016.01673.
- Famuyide, I.M., Aro, A.O., Fasina, F.O., Eloff, J.N., McGaw, L.J., 2019. Antibacterial and antibiofilm activity of acetone leaf extracts of nine under-investigated south African *Eugenia* and *Syzygium* (Myrtaceae) species and their selectivity indices. *BMC Complement. Altern. Med.* 19, 1–13. doi:10.1186/s12906-019-2547-z.
- Galbraith, H., Miller, T.B., 1973a. Effect of long chain fatty acids on bacterial respiration and amino acid uptake. *J. Appl. Bacteriol.* 36, 659–675. doi:10.1111/j.1365-2672.1973.tb04151.x.
- Galbraith, H., Miller, T.B., 1973b. Effect of metal cations and pH on the antibacterial activity and uptake of long chain fatty acids. *J. Appl. Bacteriol.* 36, 635–646. doi:10.1111/j.1365-2672.1973.tb04149.x.
- Gomes, F., Martins, N., Ferreira, I.C.F.R., Henriques, M., 2019. Anti-biofilm Activity of Hydromethanolic Plant Extracts Against *Staphylococcus aureus* Isolates from Bovine Mastitis. *5. Heliyon* doi:10.1016/j.heliyon.2019.e01728.
- González, J.F., Alberts, H., Lee, J., Doolittle, L., Gunn, J.S., 2018. Biofilm formation protects salmonella from the antibiotic ciprofloxacin in vitro and in vivo in the mouse model of chronic carriage. *Sci. Rep.* 8, 1–8. doi:10.1038/s41598-017-18516-2.
- Greenway, D.L.A., Dyke, K.G.H., 1979. Mechanism of the inhibitory action of linoleic acid on the growth of *Staphylococcus aureus*. *J. Gen. Microbiol.* 115, 233–245. doi:10.1099/00221287-115-1-233.
- Haney, E.F., Trimble, M.J., Cheng, J.T., Vallé, Q., Hancock, R.E.W., 2018. Critical assessment of methods to quantify biofilm growth and evaluate antibiofilm activity of host defence peptides. *Biomolecules* 8, 1–22. doi:10.3390/biom8020029.
- Jung, S.W., Thamphiwatana, S., Zhang, L., Obonyo, M., 2015. Mechanism of antibacterial activity of liposomal linolenic acid against *Helicobacter pylori*. *PLoS ONE* 10, 1–13. doi:10.1371/journal.pone.0116519.
- Kumar, P., Lee, J.H., Beyenal, H., Lee, J., 2020. Fatty acids as antibiofilm and antivirulence agents. *Trends Microbiol.* 28, 753–768. doi:10.1016/j.tim.2020.03.014.
- Lou, Z., Wang, H., Zhu, S., Ma, C., Wang, Z., 2011. Antibacterial activity and mechanism of action of chlorogenic acid. *J. Food Sci.* 76. doi:10.1111/j.1750-3841.2011.02213.x.
- Ma, B., Fang, C., Lu, L., Wang, M., Xue, X., Zhou, Y., Li, M., Hu, Y., Luo, X., Hou, Z., 2019. The antimicrobial peptide thanatin disrupts the bacterial outer membrane and inactivates the NDM-1 metallo- β -lactamase. *Nat. Commun.* 10. doi:10.1038/s41467-019-11503-3.
- MacKenzie, K.D., Palmer, M.B., Köster, W.L., White, A.P., 2017. Examining the link between biofilm formation and the ability of pathogenic *Salmonella* strains to colonize multiple host species. *Front. Vet. Sci.* 4, 1–19. doi:10.3389/fvets.2017.00138.
- MacNair, C.R., Brown, E.D., 2020. Outer membrane disruption overcomes intrinsic, acquired, and spontaneous antibiotic resistance. *MBio* 11, 1–15.
- Marques, C.N.H., Davies, D.G., Sauer, K., 2015. Control of biofilms with the fatty acid signaling molecule cis-2-decenoic acid. *Pharmaceuticals* 8, 816–835. doi:10.3390/ph8040816.
- May, K.L., Grabowicz, M., 2018. The bacterial outer membrane is an evolving antibiotic barrier. *Proc. Natl. Acad. Sci. U.S.A.* 115, 8852–8854. doi:10.1073/pnas.1812779115.
- Mostafa, M.G., Rahman, M., Karim, M.M., 2011. Antimicrobial activity of *Terminalia chebula*. *Int. J. Med. Arom. Plants* 1, 175–179.
- Mwitari, P.G., Ayeka, P.A., Ondicho, J., Matu, E.N., Bii, C.C., 2013. Antimicrobial activity and probable mechanisms of action of medicinal plants of Kenya: *withania somnifera*, *Warbugia ugandensis*, *Prunus africana* and *Plectranthus barbatus*. *PLoS ONE* 8, 4–12. doi:10.1371/journal.pone.0065619.
- Nicol, M., Alexandre, S., Luizet, J.B., Skogman, M., Jouenne, T., Salcedo, S.P., Dé, E., 2018. Unsaturated fatty acids affect quorum sensing communication system and inhibit motility and biofilm formation of *Acinetobacter baumannii*. *Int. J. Mol. Sci.* 19. doi:10.3390/ijms19010214.
- Nikaido, H., 1976. Outer membrane of *Salmonella typhimurium*: transmembrane diffusion of some hydrophobic substances. *Biochim. Biophys. Acta* 433, 118–132.
- Owais, M., Sharad, K.S., Shehbaz, A., Saleemuddin, M., 2005. Antibacterial efficacy of *Withania somnifera* (Ashwagandha) an indigenous medicinal plant against experimental murine salmonellosis. *Phytomedicine* 12, 229–235. doi:10.1016/j.phymed.2003.07.012.
- Rajawat, M.V.S., Singh, S., Saxena, A.K., 2014. A new spectrophotometric method for quantification of potassium solubilized by bacterial cultures. *Indian J. Exp. Biol.* 52, 261–266.
- Saga, T., Yamaguchi, K., 2009. History of antimicrobial agents and resistant bacteria. *Japan Med. Assoc. J.* 52, 103–108.
- Sheu, C.W., Salomon, D., Simmons, J.L., Sreevalsan, T., Freese, E., 1975. Inhibitory effects of lipophilic acids and related compounds on bacteria and mammalian cells. *Antimicrob. Agents Chemother.* 7, 349–363. doi:10.1128/AAC.7.3.349.
- Trmcić, A., Chen, H., Trzaskowska, M., Tamber, S., Wang, S., 2018. Biofilm-forming capacity of five *Salmonella* strains and their fate on postharvest mini cucumbers. *J. Food Prot.* 81, 1871–1879. doi:10.4315/0362-028X.JFP-18-180.
- Vaara, M., 1992. Agents that increase the permeability of the outer membrane. *Microbiol. Rev.* 56, 395–411.
- Van Dijk, P., Sjollem, J., Cammue, B.P.A., Lagrou, K., Berman, J., d'Enfert, C., Andes, D.R., Arendrup, M.C., Brakhage, A.A., Calderone, R., Cantón, E., Coenye, T., Cos, P., Cowen, L.E., Edgerton, M., Espinel-Ingroff, A., Filler, S.G., Ghannoum, M., Gow, N.A.R., Haas, H., Jabra-Rizk, M.A., Johnson, E.M., Lockhart, S.R., Lopez-Ribot, J.L., Maertens, J., Munro, C.A., Nett, J.E., Noble, C.J., Pfaller, M.A., Ramage, G., Sanglard, D., Sanguinetti, M., Spriet, I., Verweij, P.E., Warris, A., Wauters, J., Yeaman, M.R., Zaat, S.A.J., Thevissen, K., 2018. Methodologies for in vitro and in vivo evaluation of efficacy of antifungal and antibiofilm agents and surface coatings against fungal biofilms. *Microb. Cell* 5, 300–326. doi:10.15698/mic2018.07.638.

A. Balkrishna, A.K. Gupta, K. Singh et al.

Phytomedicine Plus 1 (2021) 100047

Vyas, V.K., Bhandari, P., Patidar, R., 2011. A comprehensive review on *Withania somnifera* Dunal. *J. Nat. Remedies* 11, 1–13.

Yoon, B.K., Jackman, J.A., Valle-González, E.R., Cho, N.J., 2018. Antibacterial free fatty acids and monoglycerides: biological activities, experimental testing, and therapeutic applications. *Int. J. Mol. Sci.* doi:10.3390/ijms19041114.

Zhang, X., Ashby, R., Solaiman, D.K.Y., Uknalis, J., Fan, X., 2016. Inactivation of *Salmonella* spp. and *Listeria* spp. by palmitic, stearic, and oleic acid sophorolipids and thiamine dilauryl sulfate. *Front. Microbiol.* 7, 1–11. doi:10.3389/fmicb.2016.02076.

PROOF COVER SHEET

Journal: *Drug Design, Development and Therapy*
Author(s): Acharya Balkrishna, Subarna Pokhrel, Hoshiyar Singh, Monali Joshi, Vallabh Prakash Mulay, Swati Haldar and Anurag Varshney
Article title: Withanone from *Withania somnifera* Attenuates SARS-CoV-2 RBD and Host ACE2 Interactions to Rescue Spike Protein Induced Pathologies in Humanized Zebrafish Model
Submission no: 292805
Paper citation: Balkrishna A, Pokhrel S, Singh H, Joshi M, Mulay VP, Haldar S, Varshney A. Withanone from *Withania somnifera* Attenuates SARS-CoV-2 RBD and Host ACE2 Interactions to Rescue Spike Protein Induced Pathologies in Humanized Zebrafish Model. *Drug Design, Development and Therapy*. In Press 2021

Dear Dr Varshney,

1. Please check these proofs carefully. It is the responsibility of the contact person to check these and approve or amend them as a second proof is not normally provided. This is your chance to highlight any errors or omissions in your paper before it is published.

Please limit changes at this stage to the correction of errors (we would not expect corrections to exceed 30 changes). You should not make minor changes, improve prose style, add new material, or delete existing material at this stage.

2. Please review the table of contributors below and confirm that the names are structured correctly and that the authors are listed in the correct order. This check is to ensure that all author names will appear correctly online and when the article is indexed.

| Sequence | First name/given name | Family name/last name |
|----------|-----------------------|-----------------------|
| 1. | Acharya | Balkrishna |
| 2. | Subarna | Pokhrel |
| 3. | Hoshiyar | Singh |
| 4. | Monali | Joshi |
| 5. | Vallabh Prakash | Mulay |
| 6. | Swati | Haldar |
| 7. | Anurag | Varshney |

PubMed Citation: Balkrishna A, Pokhrel S, Singh H, Joshi M, Mulay VP, Haldar S, Varshney A

Google Citation: Acharya Balkrishna, Subarna Pokhrel, Hoshiyar Singh, Monali Joshi, Vallabh Prakash Mulay, Swati Haldar, Anurag Varshney

To change your PubMed or Google citation please contact Sandi McIver (sandi@dovepress.com).

AUTHOR QUERIES

Please complete the following steps:

1. Read your entire proof and respond to all the Author Queries (AQs) and make necessary amendments directly in the text (avoid leaving instructions/comments unless essential). All AQs must be answered before you submit the corrections to your proof.
 2. Please ensure your corrections (if any) are kept to a minimum.
 3. Please submit corrections when you are sure you have answered all of the AQs, and have proofread the entire article (including figures and tables).
- AQ1** Dear author, we present genus and species in italics, but not the family or group. This applies to viruses when used in a taxonomic sense. Please advise if anything should be changed into italics, or into non-italics according to this rule.
- AQ2** Dear author, please check your paper carefully for any errors that may have been introduced during typesetting of your manuscript.
- AQ3** **REDUCE TIME TO PUBLICATION**
Dear author, before you send corrections back, please download the PDF proof (see “View Original PDF” on left hand side of correction tool), check with each of the authors that all corrections will be submitted. Please pay special attention to authors names and affiliations, funding/acknowledgments, and table and figure presentation on the PDF proof.
- AQ4** Dear author, we present genus and species in italics, but not the family or group. This applies to viruses when used in a taxonomic sense. Please advise if anything should be changed into italics, or into non-italics according to this rule.
- AQ5** Dear author, we italicize gene names (DNA, mRNA), but not protein names. Please advise if anything should be changed into italics, or into non-italics according to this rule.
- AQ6** Dear author, please check and advise if the heading levels are correct.
- AQ7** Dear author, this web address no longer seems to be current. Please provide an updated link.
- AQ8** Dear author, we present genus and species in italics, but not the family or group. This applies to viruses when used in a taxonomic sense. Please advise if anything should be changed into italics, or into non-italics according to this rule.
- AQ9** Dear author, we italicize gene names (DNA, mRNA), but not protein names. Please advise if anything should be changed into italics, or into non-italics according to this rule.
- AQ10** Dear author, figures in this article have been renumbered as follows such that they are cited sequentially in the text: Fig. 9 -> Fig. 2; Fig. 2 -> Fig. 3; Fig. 3 -> Fig. 4; Fig. 4 -> Fig. 5; Fig. 5 -> Fig. 6; Fig. 6 -> Fig. 7; Fig. 7 -> Fig. 8; Fig. 8 -> Fig. 9. Please carefully check all the figures, their captions, and their citations and confirm that all are correct.
- AQ11** Dear author, please could you check that the figures have the correct captions and notes. Many thanks.
- AQ12** Dear author, the editor is unsure what this means. Please can you revise for clarity?
- AQ13** Dear author, these commonly known abbreviations (H&E, PBS) did not require defining by the journal and the definitions have been removed.
- AQ14** Dear author, tables in this article have been renumbered as follows such that they are cited sequentially in the text: Table 3 -> Table 1; Table 4 -> Table 2; Table 5 -> Table 3; Table 1 -> Table 4; Table 2 -> Table 5. Please carefully check all the tables, their captions, and their citations and confirm that all are correct.
- AQ15** Dear author, please confirm that our rewording retains your intended meaning.
- AQ16** Dear author, your figures/tables may have been redrawn/edited to align with PubMed specifications and journal house style, please check each one carefully.

- AQ17 Dear author, please confirm that our rewording retains your intended meaning.
- AQ18 Dear author, the editor has rephrased this sentence for clarity. Please check to see that they haven't inadvertently altered your intended meaning.
- AQ19 Dear author, italic has been removed as we only use it for gene names, genus and species.
- AQ20 Dear author, please confirm that our rewording retains your intended meaning.
- AQ21 Dear author, please confirm that our rewording retains your intended meaning.
- AQ22 Dear author, please confirm that our rewording retains your intended meaning.
- AQ23 Dear author, please confirm that our rewording retains your intended meaning.
- AQ24 Dear author, please confirm that our rewording retains your intended meaning.
- AQ25 Dear author, please confirm that our rewording retains your intended meaning.

Comprehensive Phytochemical Profiling of Polyherbal Divya-Kayakalp-Vati and Divya-Kayakalp-Oil and Their Combined Efficacy in Mouse Model of Atopic Dermatitis-Like Inflammation Through Regulation of Cytokines

Acharya Balkrishna^{1,2}, Sudeep Verma¹, Sachin Sakat¹, Kheemraj Joshi¹, Siva K Solleti¹, Kunal Bhattacharya¹, Anurag Varshney^{1,2}

¹Drug Discovery and Development Division, Patanjali Research Institute, Haridwar, 249 405, Uttarakhand, India;

²Department of Allied and Applied Sciences, University of Patanjali, Patanjali YogPeeth, Haridwar, 249 405, Uttarakhand, India

Correspondence: Anurag Varshney, Drug Discovery and Development Division, Patanjali Research Institute, NH-58, Haridwar, 249405, Uttarakhand, India, Tel +91 1334-244107 x7458, Fax +91 1334 244805, Email anurag@prft.co.in



Purpose: Atopic dermatitis (AD) is a chronic inflammatory disease that varies in signs and symptoms in different individuals. General symptoms include dryness of the skin, itching, and development of red to brownish-gray patches. Divya-Kayakalp-Vati (DKV) and -Oil (DKO) are Indian polyherbal compositions prescribed for treating inflammatory skin diseases. In the present study, we evaluated the anti-inflammatory efficacy of DKV and DKO co-treatment (DKV-O) in ameliorating Oxazolone (OXA)-stimulated AD-like inflammation and pro-inflammatory cytokine release in a Swiss albino mouse model.

Methods: Phytochemical profiling of the DKV and DKO were done using Liquid Chromatography-Mass Spectroscopy (LC-MS) QToF. Swiss albino mice were sensitized for 7 days and treated with OXA in their ear region. Stimulated and control animals were orally treated with DKV and topically with DKO. Anti-inflammatory efficacy of DKV-O was determined in OXA-treated animals through physiological, histopathological, and biochemical parameter analysis.

Results: DKV and DKO formulations individually contained 39 and 59 phytochemicals, respectively. Many of the phytochemicals have been reported to have anti-inflammatory activities. In the OXA-sensitized Swiss albino mice, combined treatment with DKV-O, and separately with Dexamethasone (positive control) significantly reduced the OXA-stimulated ear edema, biopsy weight, and epidermal thickness. DKV-O further reduced OXA-stimulated induction of inflammatory lesions, neutrophil influx, and release of Interleukin (IL)-1 β , IL-6, tumor necrosis factor- α , and myeloperoxidase.

Conclusion: Finally, DKV-O co-treatment showed good pharmacological effects in ameliorating AD-like inflammation through the modulation of inflammatory cell influx and release of soluble mediators. Therefore, DKV-O treatment can be used as a suitable polyherbal therapeutic against AD-like inflammatory diseases.

Keywords: inflammation, oxazolone, phytochemical profile, pro-inflammatory cytokines, histopathological analysis, biochemical analysis

Introduction

Atopic Dermatitis (AD) is a dermal inflammatory condition varying in symptoms for individual patients. Common symptoms associated with the disease include skin dryness and itching, red to brownish-gray scaly patches on limbs,



neck, upper chest, and eyelid regions. AD often occurs in children ≥ 6 years persisting until adolescence and adulthood.^{1,2} The disease may flare up occasionally and then clear up by itself after some time.

Exaggerated T helper-2 (Th2) cells-mediated immune-pathway activation in combination with exposure to environmental factors, neuropsychological factors, epidermal barrier deficiency, and microbial pathogens lead to the inception of AD.^{3–5} Incidences of AD have increased several times over the past 30 years affecting 20% of children and 2% of adults.⁶ Approximately, 70–80% of AD patients, show an elevated serum IgE level with high sensitization towards environmental allergens. While remaining 20–30% of patients show an “intrinsic” form of AD with low serum IgE levels.⁷ Early development of AD during infancy can be attributed to IgE sensitization to food allergens. Sharing of inflammatory pathways between AD and other immunomodulatory diseases may also lead to the development of allergic rhinitis and asthma in later part of patient's life.^{8–10} At a molecular level, AD is associated with gene mutations affecting epidermal differentiation, and skin barrier formation.^{11–13}

Based on age, ethnicity, and biological mechanism, AD presents varying clinical pathologies. In an Italian multi-centric retrospective cohort clinical study, Nettis et al showed the prevalence of lichenified/ exudative flexural AD in children often associated with head, neck, and hand eczema.¹⁴ In adults, besides the presence of lichenified/ exudative flexural dermatitis, they also showed the presence of prurigo nodularis-like AD characterized by distinct, intensely itching papules and nodules dominant in the limbs and back parts of the body, and nummular eczema-like phenotype presents with eczematous, sometimes “weeping” lesions and is often associated with cutaneous xerosis.¹⁴

Due to the chronic and recurrent nature of AD, long-term therapies and medications are necessary for treating the disease. Tofacitinib and Baricitinib act as inhibitors for JAK-based immune responses.¹⁵ Calcineurin inhibitors, and cAMP-specific 3',5'-cyclic phosphodiesterase-4 inhibitors, and biologics like Lebrikizumab, Apremilast, Crisaborole, Dupilumab, and IL-31 are generally applied as immunomodulators against AD.^{16–22} However, some of them may have unwanted health-related side effects.²³ Divya-Kayakalp-Vati (DKV) and -Oil (DKO) are polyherbal Ayurvedic formulations, suggested having efficacy in treating skin inflammatory disorders. DKV and DKO, formulated according to the ancient Indian texts of *Charak Samhita*, are composed of 18 different plants detailed under Table 1.^{24–26} Earlier, a combined DKV and DKO (DKV-O) treatment has shown immunomodulatory activity in λ -carrageenan-stimulated Wistar rats paw edema model and 12-O-tetradecanoylphorbol 13-acetate (TPA)-treated CD-1 mouse ear edema model.²⁷ Anti-inflammatory efficacy of DKV-O was observed to originate from the phytochemical constituents present within.

Different experimental mouse models have been employed for the study of AD, such as 1) animals stimulated with the epicutaneous application of sensitizers, 2) transgenic mice overexpressing or lacking selective molecules, and 3) mice showing spontaneous development of AD-like skin lesions.⁵ Oxazolone (OXA) is a Hapten that is used for evoking AD-like inflammation primarily through an epidermal barrier breach, and Th1-dominated initial response that later shifts to Th2-type response, similar to human AD.²⁸ OXA challenge has been reported to induce the development of epidermal hyperplasia and reduce expression of the skin differentiation proteins- filaggrin, loricrin, and involucrin.⁵

The present study investigates the pharmacological effects of DKV-O at a human equivalent dose in Swiss Albino mice challenged with OXA and eliciting AD-like dermal inflammation. Histological analysis parameters included ear edema, biopsy weight, epidermal thickness, and modulation of inflammatory lesions. Additionally, circulating serum biomarkers for inflammation were also analyzed. We precluded the study with an in-depth phytochemical analysis of DKV and DKO and correlated those findings to the biological study outcomes.

Materials and Methods

Reagents

Divya-Kayakalp-Vati (Batch no. A-KKVE090) and Divya-Kayakalp-Oil (Batch no. BKKT056) were sourced from Divya Pharmacy (Haridwar, Uttarakhand, India). Their herbal compositions were provided by the manufacturer (Table 1). Oxalozone (OXA; Purity 99.9%), Dexamethasone (DEXA; Purity 99.9%), and 3,3',5,5'-Tetramethylbenzidine were purchased from Sigma-Aldrich (St. Louis, MO, USA). ELISA reagents for IL-1 β , IL-6, and TNF- α analysis were purchased from BD Biosciences (San Jose, CA, USA). HPLC grade acetonitrile, ortho-phosphoric acid, and diethylamine

Table 1 Complete Herbal Composition of Divya-Kayakalp-Vati (DKV) and Divya-Kayakalp-Oil (DKO)

| S.No. | English Name | Latin Name (Family) | DKV (mg) | DKO (mg) | DKO (mL) |
|-------------------|------------------------------|--|----------|----------|----------|
| 1 | Ringworm plant | <i>Cassia tora</i> L. (Caesalpinaceae) | 30 | 30 | |
| 2 | Turmeric | <i>Curcuma longa</i> L. (Zingiberaceae) | 30 | 30 | |
| 3 | Indian laburnum | <i>Hemidesmus indicus</i> (L.) R. Br. (Periplocaceae) | 30 | 30 | |
| 4 | Indian barberry | <i>Berberis aristata</i> DC. (Berberidaceae) | 30 | 30 | |
| 5 | Margosa | <i>Azadirachta indica</i> A. Juss. (Meliaceae) | 30 | 30 | |
| 6 | Indian Gooseberry | <i>Emblica officinalis</i> Gaertn. (Euphorbiaceae) | 30 | 30 | |
| 7 | Indian Madder | <i>Rubia cordifolia</i> L. (Rubiaceae) | 25 | 25 | |
| 8 | Heart-leaved moonseed | <i>Tinospora cordifolia</i> (Willd.) Hoof. f. and Thomson (Menispermaceae) | 20 | | |
| 9 | Spider wort | <i>Leucas cephalotes</i> (Roth) Spreng. (Lamiaceae) | 10 | 10 | |
| 10 | Mexican poppy yellow thistle | <i>Argemone Mexicana</i> L. (Papaveraceae) | 10 | | |
| 11 | Cutch tree | <i>Acacia catechu</i> (Lf.) Willd. (Leguminosae) | 5 | | |
| 12 | Sandalwood white | <i>Santalum album</i> L. (Santalaceae) | | 10 | |
| 13 | Colocynth/ Bitter Apple | <i>Citrullus colocynthis</i> (L.) Schrad. (Cucurbitaceae) | | 10 | |
| 14 | Himalayan deodar | <i>Cedrus deodara</i> (Roxb. ex D. Don) G. Don (Pinaceae) | | 10 | |
| 15 | Sarsaparilla | <i>Smilax ornate</i> Lem. (Smilacaceae) | | 10 | |
| 17 | Mustard oil | <i>Brassica campestris</i> L. (Brassicaceae) | | | 100 |
| 18 | Ironweed | <i>Centratherum anthelminticum</i> (L.) Kuntze (Asteraceae) | | 10 | |
| Excipients | | | | | |
| 1 | Gum arabica (Exudate) | <i>Acacia arabica</i> (Lam.) Willd. (Fabaceae) | 12.5 | | |
| 2 | Talcum (Powder) | | 2.5 | | |
| 3 | Aerosil (Powder) | | 2 | | |

along with hematoxylin and Eosin (H&E) stains were purchased from Merck (Kenilworth, NJ, USA). All other chemicals and reagents purchased for the study were of the highest commercial grade.

Sample Preparation for DKO and DKV

Ninety grams of DKO were suspended in 200 mL of 90% aqueous methanol. The solution was stirred for 1 h using a magnetic stirrer and stored at -20°C for 2 days. Following separation of the methanol from the frozen oil layer, it was removed manually. Finally, the DKO sample was thawed, filtered, and dried using Rotavapor. Obtained DKO residue (0.66 g) was resuspended in 90% aqueous methanol at the final volume of 10 mL and filtered through a $0.45\ \mu\text{m}$ PTFE membrane filter (Millipore, Burlington, MA, USA), and stored until further use for LC-MS QToF analysis. One gram of DKV powder was dissolved in 40 mL of hydromethanolic solution and sonicated for 15 min. The hydromethanolic DKV suspension was centrifuged at 5000 rpm for 5 min. Approximately, 0.50 mL of the clear upper layer was collected and diluted further for LC-MS QToF analysis.

Liquid Chromatography (LC-MS) QToF Analysis

LC-MS QToF analysis was performed on a Xevo G2-XS QToF with Acquity UPLC- I Class and analyzed using Unifi Scientific Information System software (Waters Corporation, Milford, MA, USA). Separation was carried out using Acquity UPLC HSS -T3 column (100 x 2.10 mm, 1.70 μ m) maintained at 50°C. The sample temperature was kept at 10°C during the analysis. Elution was carried out at a flow rate of 0.40 mL/min using gradient elution of mobile Phase 0.1% formic acid in water (mobile phase A) and 0.1% formic acid in acetonitrile (mobile phase B). 1 μ L of test solution (either DKV or DKO) was injected and the chromatograph was recorded for 55 min.

Experimental Animals

Swiss albino mice (6–8 weeks) were procured from Charles River Laboratory licensed supplier Hylasco Biotechnology Pvt. Ltd. (Hyderabad, India). All the animals were placed under a controlled environment with 60–70% relative humidity and 12:12 h light and dark cycle in a registered animal house (1964/PO/RC/S/17/CPCSEA) of Patanjali Research Institute, India. The animals were fed a standard pellet diet (Golden Feed, India) and sterile filtered water *ad libitum*. The animal study protocol was approved by the Institutional Animal Ethical Committee (IAEC) of Patanjali Research Institute vide approval number: PRIAS/LAF/IAEC-023. Experimental procedures and animal husbandry practices were strictly conformed to the CPCSEA standards.²⁹ The study was conducted in compliance with The ARRIVE guidelines.³⁰ Eight animals were randomly allocated to each study group.

In-vivo Evaluation of DKV-O Against Atopic Dermatitis (AD)-Like Inflammation Mice Model of Oxazolone Induced AD-Like Inflammation

The combined therapeutic effect of DKV and DKO was analyzed in the OXA-stimulated AD-like inflammation mice model at human equivalent doses as described earlier.³¹ Briefly, 1.5% OXA solution was prepared by mixing it in acetone (vehicle). Mice were sensitized in their clipped abdomen to 1.5% OXA by applying 100 μ L solution for 7 days. The mice were then challenged with 1.5% OXA (20 μ L T.A.) in the ear region. Ear thickness was measured at 0, 6, 24, 48, and 72 h using a digital Vernier caliper (Mitutoyo, Tokyo, Japan) (Figure 1). Treatment group mice were given vehicle alone (acetone, P.O.), or DKV (150 mg/kg; P.O.) and DKO (20 μ L T.A.), or DEXA (0.2 mg/kg; P.O.) throughout the experimental period. Unchallenged OXA-sensitized mice were considered normal control (NC), and untreated OXA challenged mice were considered disease

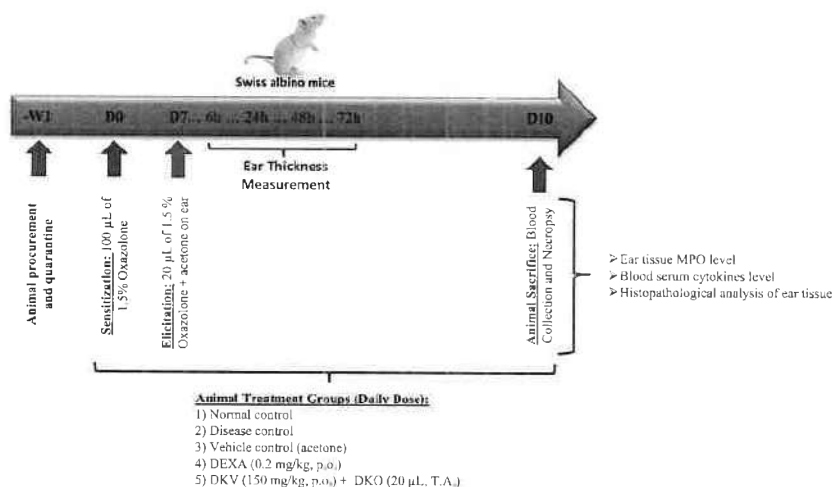


Figure 1 Study design for pharmacology study of Divya-Kayakalp-Vati (DKV) and Oil (DKO). Swiss albino mice were procured and acclimatized for one week. Mice were sensitized in their clipped abdomen against 1.5% Oxazolone (OXA; 100 μ L) for 7 days. Later, mice were challenged with 1.5% OXA (T.A.) on their ear (20 μ L/ear). Ear thickness was measured at 0, 6, 24, 48, and 72 h using a digital Vernier caliper. Animals were treated daily with DKV (150 mg/kg; P.O.) and DKO (20 μ L T.A.), or Dexamethasone (DEXA; 0.2 mg/kg). Animals were sacrificed on day 10, and tissue and blood samples were collected for histopathological and biochemical parameters analysis.

control (DC) in the study. Changes in ear thickness were calculated by subtracting ear thickness measure per hour from ear thickness measured at 0 h (Figure 1).

Histopathological Analysis

On day 10, mice were humanely sacrificed at 6 h post-treatment. Ear biopsy samples were weighed and fixed in 10% (v/v) neutral buffered formalin, embedded in paraffin, and sectioned at 3–5 μm thickness using a Leica RM2245 microtome (Wetzlar, Germany). Tissue sections were transferred to a glass slide and stained with H&E stain. Epidermal thickness from the basal to *stratum corneum* layer was measured using MagVision image analysis software attached to Magcam DC5 microscopic camera. Severity of inflammatory lesions was recorded as: NAD = No abnormality detected, 1 = minimal (<1%), 2 = mild (1–25%), 3 = moderate (26–50%), 4 = moderately severe/marked (51–75%), 5 = severe (76–100%). Distribution of the lesions was recorded as focal, multifocal, and diffused. Other parameters considered for histopathological examination were extent, hyperkeratosis, number, and size of pustules, epidermal hyperplasia (measured in the interfollicular epidermis), an influx of inflammatory cells in the dermis and soft tissue.

Immuno-Biochemical Parameters

Enzyme-linked immunosorbent assay (ELISA) was performed for determining the levels of interleukin (IL)-1 β , IL-6, and tumor necrosis factor-alpha (TNF- α) in circulating animal serum samples following the manufacturer's protocol. Myeloperoxidase level in the ear biopsy samples was analyzed following the protocol mentioned by Suzuki et al, using 3,3',5,5'-tetramethylbenzidine (TMB) dye.³² Briefly, 10 μL of ear biopsy homogenized samples were combined with 80 μL of 0.75 mM H₂O₂ and 110 μL of 2.9 mM TMB solution (prepared in 14.5% dimethyl sulphoxide) and 150 mM sodium phosphate buffer (pH 5.4) in a 96 well plate. Plate was incubated at 37°C for 5 min and the assay was stopped by adding 2 M H₂SO₄. Absorbance was obtained at 450 nm using the Envision microplate reader (Perkin Elmer, Waltham, MA, USA).

Statistical Analysis

Results have been presented as Mean \pm Standard Error of Mean (SEM). Statistical analysis was done using GraphPad Prism version 7.03 software (GraphPad Software Inc., San Diego, CA, USA). Two-way analysis of variance (ANOVA) followed by Newman-Keuls multiple comparison tests was used for ear edema parameter. A one-way analysis of variance (ANOVA) followed by Dunnett's multiple comparisons post-hoc tests were used for calculating statistical significance in cytokine(s) analysis, ear biopsy weights, epidermal thickness, and lesion scores parameters. Values with a p-value <0.05 were considered significant.

Results

A total of 39 phytochemicals in DKV and 59 phytochemicals in DKO were identified based on their retention time (RT) and mass-charge ratio (m/z) using LC-MS QToF assay. In DKV, 33 phytochemicals were identified in positive mode and 18 phytochemicals in negative mode. Twelve non-polar phytochemicals were observed in both positive and negative modes (Table 2, Figure 2A and B). In DKO, 26 phytochemicals were observed in positive mode and 31 phytochemicals in negative mode. Six phytochemicals were present in both the positive and negative modes (Table 2; Figure 3A and B). Major phytochemicals commonly detected in both DKV and DKO were 1,8-Dihydroxy-6-methoxy-3-methylanthraquinone (Physcion), Berberine, Berberine, Catechin, Columbin, Curcumin, Ellagic acid, Gallic acid, Kaempferol, Obtusin, Palmatine, Quercetin, and Swertiamarin. Physcion has been shown to inhibit the formation of AD-related skin lesions through the blocking of thymic stromal lymphopoietin.³³ Berberine has also been shown to regulate T-cell activation and inhibit NF- κB and MAPK (JNK and ERK1/2) signaling pathways in LPS-stimulated macrophages.^{34,35} Similarly, other individually identified phytochemicals in DKV and DKO have reported anti-inflammatory activities.

Our in-vivo study showed a significantly elevated level of ear edema in the OXA sensitized DC mice following challenge with 1.5% OXA, as compared to NC mice (p-value <0.01) (Figure 4A). OXA-treated DC mice showed maximum swelling at 24 h (0.54 ± 0.02 mm) post-treatment, reaching a plateau stage that continued to be elevated with a minor change up to 72 h (0.42 ± 0.04 mm). Co-treatment of the OXA-stimulated mice with DKV (150 mg/kg, P.O.) and

Table 2 Identified Phytochemicals Present in the Divya-Kayakalp-Vati (DKV) and Divya-Kayakalp-Oil (DKO) Using LC-MS QToF Analysis

| S.No. | Name of Phytochemical Detected | DKV | | | DKO | | |
|-------|---|---------|----------------|--------------------|---------|----------------|--------------------|
| | | Mode | Retention time | Mass/ Charge (m/z) | Mode | Retention time | Mass/ Charge (m/z) |
| 1 | 1,8-Dihydroxy-3-methylantraquinone (Chrysophanol) | -ve | 9.4 | 253.05 | | | |
| 2 | 1,8-Dihydroxy-6-methoxy-3-methylantraquinone (Physcion) | -ve | 12.44 | 283.06 | +ve/-ve | 12.45/ 12.42 | 285.08/ 283.06 |
| 3 | 3-Methoxy-4-hydroxybenzoic acid | | | | +ve/-ve | 5.27/ 5.22 | 169.05/ 167.04 |
| 4 | Afzelechin | +ve/-ve | 5.9 | 275.09/ 273.08 | | | |
| 5 | Alizarin | +ve/-ve | 11.48 | 241.05/ 239.03 | | | |
| 6 | Alizarin | | | | +ve/-ve | 11.51/ 11.48 | 241.05/ 239.03 |
| 7 | Androsin | +ve | 4.82 | 351.1 | | | |
| 8 | Apocynin | | | | +ve | 7.05 | 167.07 |
| 9 | Arbutin | +ve | 8.72 | 273.1 | | | |
| 10 | Arjunetin | | | | +ve/-ve | 23.1 | 651.41/ 649.39 |
| 11 | Arjunic acid | | | | -ve | 14.01 | 487.34 |
| 12 | Bavachinin | | | | -ve | 17.44 | 337.14 |
| 13 | Bavachromanol | | | | -ve | 12.55 | 339.12 |
| 14 | Bavachromene | | | | -ve | 12.82 | 321.11 |
| 15 | Benzoic acid | | | | -ve | 7.6 | 121.03 |
| 16 | Berberamine | +ve | 6.98 | 609.3 | +ve | 6.96 | 609.3 |
| 17 | Berberine | +ve | 8.97 | 336.12 | +ve | 8.98 | 336.12 |
| 18 | Bisdemethoxylcurcumin | | | | +ve | 13.04 | 309.11 |
| 19 | Butin | | | | -ve | 9.94 | 271.06 |
| 20 | Catalpol | +ve | 14.74 | 363.13 | | | |
| 21 | Catechin | +ve/-ve | 4.84/ 4.89 | 291.09/ 289.07 | -ve | 4.84 | 289.07 |
| 22 | Citric acid | +ve/-ve | 1.25 | 215.02/ 191.02 | | | |
| 23 | Columbamine | +ve | 8.23 | 338.14 | | | |
| 24 | Columbin | +ve | 10.1 | 359.15 | +ve | 10.02 | 359.15 |
| 25 | Corylidin | | | | -ve | 10.04 | 367.08 |
| 26 | Corylifolin | | | | +ve/-ve | 15.4 | 325.14/ 323.13 |
| 27 | Corylin | | | | -ve | 13.96 | 319.1 |
| 28 | Courmaric acid | +ve/-ve | 7.56/ 7.57 | 149.06/ 147.04 | | | |
| 29 | Curcumin | +ve | 13.6 | 369.13 | +ve/-ve | 13.62 | 369.13/ 367.12 |
| 30 | Cyclocurcumin | +ve | 4.66 | 369.13 | | | |

(Continued)

Table 2 (Continued).

| S.No. | Name of Phytochemical Detected | DKV | | | DKO | | |
|-------|--------------------------------|---------|------------|----------------|-----|-------|----------------|
| | | | | | | | |
| 31 | Cyclopamine | | | | +ve | 11.45 | 412.32 |
| 32 | Demethoxycurcumin | | | | +ve | 13.32 | 339.12/ 337.11 |
| 33 | Ellagic acid | -ve | 7.18 | 301 | -ve | 7.16 | 301 |
| 34 | Emodin | -ve | 10.16 | 269.04 | | | |
| 35 | Ethyl gallate | | | | -ve | 4.21 | 197.05 |
| 36 | Euxanthone | | | | +ve | 8.96 | 229.05 |
| 37 | Ferulic acid | -ve | 8.31 | 193.05 | | | |
| 38 | Gallic acid | +ve/-ve | 2.17/ 2.19 | 171.03/ 169.01 | -ve | 2.17 | 169.01 |
| 39 | Gentianine | +ve | 6.66 | 198.05 | | | |
| 40 | Gentiopicroside | +ve | 2.42 | 379.1 | | | |
| 41 | Isobavachalcone | | | | +ve | 12.28 | 325.14 |
| 42 | Isorhamnetin | +ve/-ve | 9.67/ 9.69 | 317.07/ 315.05 | | | |
| 43 | Jatrorrhizine | | | | +ve | 8.26 | 338.14 |
| 44 | Kaempferol | +ve/-ve | 10.3 | 287.06/ 285.04 | +ve | 10.34 | 287.06 |
| 45 | Lofoline | | | | +ve | 9.29 | 308.22 |
| 46 | Mangiferin | +ve/-ve | 5.74/ 5.76 | 423.09/ 421.08 | | | |
| 47 | Matairesinol | | | | -ve | 10.25 | 357.13 |
| 48 | Obtusifolin | +ve | 9.52 | 285.08 | | | |
| 49 | Obtusin | +ve | 13.37 | 345.1 | +ve | 13.39 | 345.10/ 343.08 |
| 50 | Oxyberberine | +ve | 7.63 | 352.12 | | | |
| 51 | Palmitine | +ve | 8.91 | 352.15 | +ve | 8.92 | 352.15 |
| 52 | Palmitamide | | | | +ve | 20.13 | 256.26 |
| 53 | p-Cresol | | | | -ve | 6.02 | 107.05 |
| 54 | Phenol | | | | -ve | 7.79 | 93.036 |
| 55 | Phenylacetic acid | | | | -ve | 6.32 | 135.05 |
| 56 | p-Hydroxybenzoic acid | | | | -ve | 7.78 | 137.02 |
| 57 | Protopine | | | | -ve | 9.99 | 352.12 |
| 58 | Psoralen | | | | -ve | 7.91 | 185.02 |
| 59 | Psoralenol | | | | -ve | 10.72 | 337.11 |
| 60 | Psoralidin | | | | -ve | 14.32 | 335.09 |
| 61 | Purpurin | +ve | 1.2 | 279.03 | | | |
| 62 | Quercetin | +ve/-ve | 9.29/ 9.31 | 303.05/ 301.03 | -ve | 9.29 | 301.03 |
| 63 | Quercetin 3,4'-dimethyl Ether | | | | +ve | 11.5 | 331.08 |

(Continued)

Table 2 (Continued).

| S.No. | Name of Phytochemical Detected | DKV | | | DKO | | |
|-------|--------------------------------|---------|------------|-----------------|-----|-------|--------|
| | | | | | | | |
| 64 | Rubiadin | +ve | 5.83 | 255.06 | | | |
| 65 | Rubrofusarin | +ve/-ve | 5.83/ 5.86 | 273.08/ 271.06 | | | |
| 66 | Shikimic acid | -ve | 0.87 | 173.04 | | | |
| 67 | Stigmasterol | | | | +ve | 14.28 | 413.38 |
| 68 | Sweroside | +ve | 4.9 | 395.13 | | | |
| 69 | Swertiamarin | +ve | 4.85 | 375.13 | -ve | 4.81 | 373.11 |
| 70 | Syringaresinol | +ve | 16.29 | 419.17 | | | |
| 71 | Terminolic acid | | | | -ve | 11.26 | 503.34 |
| 72 | Uridine | | | | +ve | 13.62 | 245.08 |
| 73 | Ursolic acid | | | | -ve | 20.5 | 455.35 |
| 74 | Vanillin | +ve/-ve | 5.82/ 5.85 | 153.057/ 151.04 | | | |
| 75 | Veratramine | | | | +ve | 12.72 | 410.3 |
| 76 | Veronicoside | +ve | 4.85 | 467.15 | | | |
| 77 | β -Amyrin | | | | +ve | 23.96 | 427.39 |

Note: Spectra were collected in the positive and negative modes (see Figures 2A and B, 3A and B).

DKO (20 μ L, T.A.) (DKV-O) significantly (p -value <0.01) reduced ear edema at 24 h (0.30 ± 0.02 mm), and 72 h (0.19 ± 0.02 mm) compared to DC animal (Figure 4A). DEXA (0.2 mg/kg, P.O.) treatment also significantly reduced the OXA-stimulated ear edema in the mice at 24 h (0.15 ± 0.01 mm) and 72 h (0.11 ± 0.01 mm) (Figure 4A). OXA-challenge also induced a significant (p -value <0.01) increase in the ear biopsy weight (11.74 ± 2.64 mg) of DC mice compared to NC animals (5.76 ± 0.44 mg) (Figure 4B). Vehicle control (VC) treated animals did not show any change (5.41 ± 0.86 mg) in their ear biopsy weight. Treatment of the OXA-stimulated mice with DKV-O significantly (p -value <0.01) reduced the induced biopsy weight (7.44 ± 1.09 mg) increase compared to the DC animals (Figure 4B). DEXA treatment also significantly (p -value <0.01) reduced the OXA-stimulated increase in the ear biopsy weight (4.44 ± 0.86 mg) (Figure 4B).

Histopathological analysis of NC and VC mice ears showed the presence of normal tissue condition with continuous epidermal, dermal, and cartilage layers containing sebaceous glands (Figure 5A and B). Stimulation of the mice ears with OXA induced pustule formation, hyperkeratosis, and hyperplasticity in the epidermal region along with the influx of neutrophils in the dermis region (Figure 5C). This was ameliorated through treatment with DEXA showing a reduction in the epidermal region pustule formation and a reduced presence of neutrophils in the dermis region (Figure 5D). Similarly, DKV-O treatment also reduced pustule formation in the epidermal region of the OXA stimulated animals. A minor change was observed in the presence of neutrophils within the dermis region, and pustule formation in the epidermal region of the DKV-O treated OXA-stimulated animals (Figure 5E).

Based on the histopathological tissue section analysis, OXA-stimulation of the animal ears induced a significant (p -value <0.01) $41.5 \pm 14.4\%$ increase in the ear epidermal thickness compared to the NC animals (Figure 6). No change was observed in the epidermal thickness of the mice treated with the VC only (Figure 6). DKV-O treatment of the OXA-stimulated animals for 10 days significantly (p -value <0.01) reduced ($27.58 \pm 4.26\%$) the induced ear epidermal thickness increase compared to the DC mice (Figure 6). DEXA treatment also significantly (p -value <0.01) reduced ($8.58 \pm 1.67\%$) the OXA-induced epidermal thickness in the mouse ear compared to the DC mice (Figure 6).

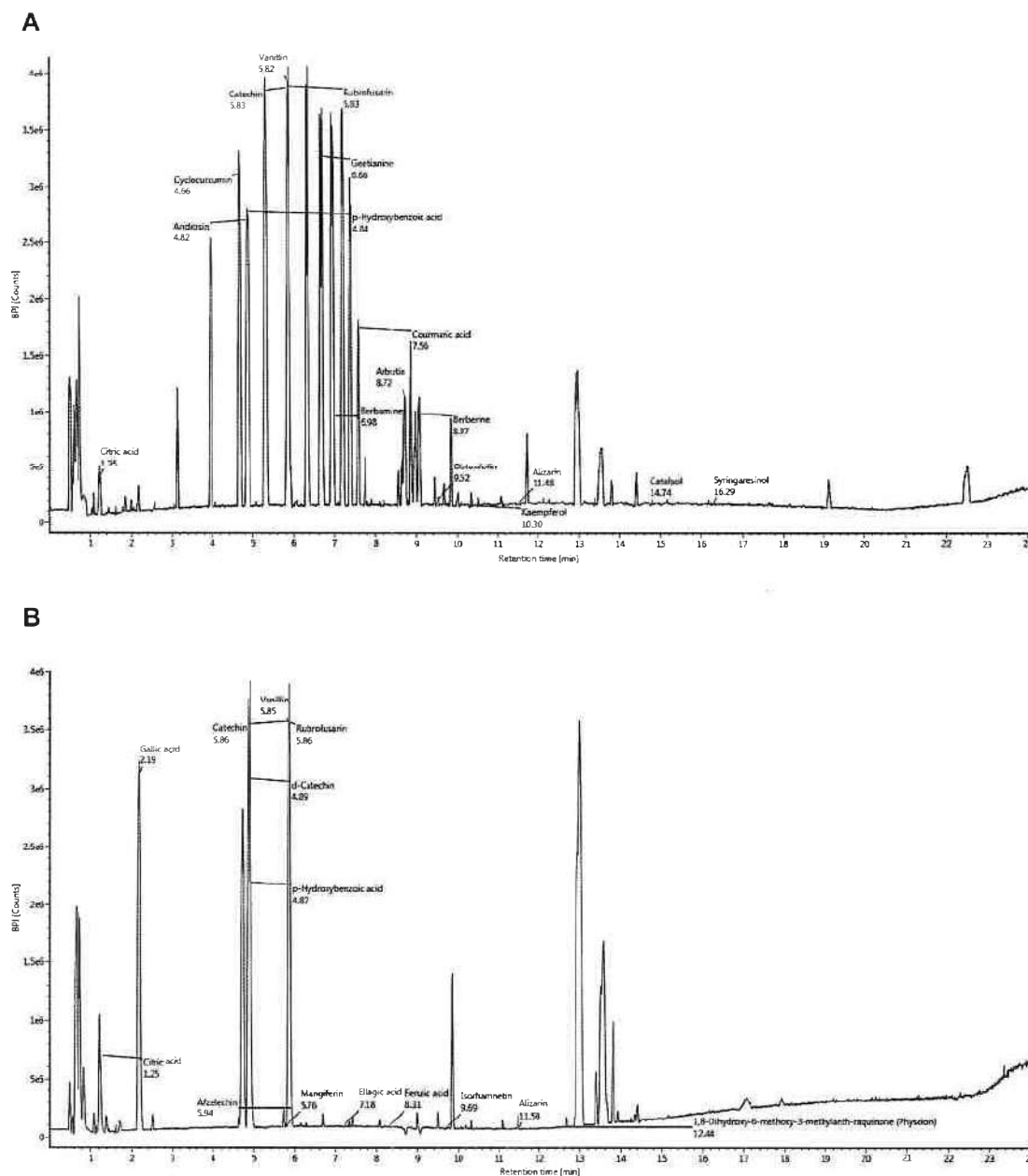


Figure 2 Phytochemical profiling of Divya-Kayakalp-Vari (DKV). Phytochemical composition of the DKV was identified using liquid chromatography–mass spectroscopy (LC-MS) QToF analysis in (A) positive mode, and (B) negative mode, based on their mass-to-charge ratio and retention time (min). Details of the phytochemicals identified in positive and negative mode are given in Table 2.

Total lesion score analysis in the OXA-stimulated mice showed a steep (9.50 ± 1.30 folds) and significant (p -value < 0.01) increase compared to the control animals (Figure 7A). Individual lesion score analysis in the OXA-stimulated mice showed a significant increase for epidermal hyperplasia (2.25 ± 0.88 folds), hyperkeratosis (1.75 ± 0.70 folds), and pustule formation (2.62 ± 1.06 folds), along with neutrophil influx (2.87 ± 0.83 folds) in the dermal region compared to NC mice (Figure 7A–E). DKV-O treatment of the OXA-simulated mice significantly (p -value < 0.01) reduced the total lesion score (4.37 ± 1.76 folds)

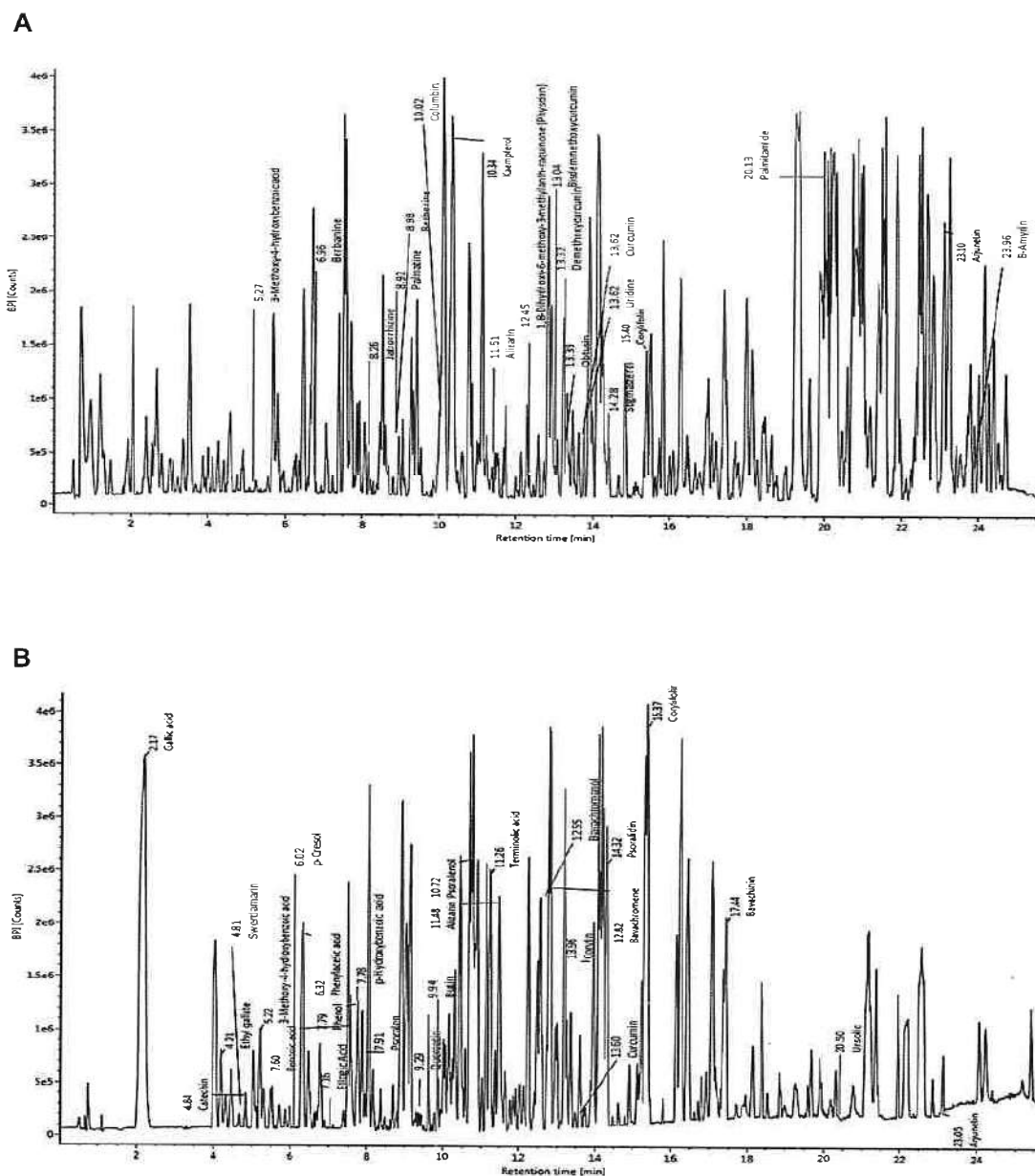


Figure 3 Phytochemical profiling of Divya-Kayakalp-Oil (DKO). Phytochemical composition of the DKO was identified using liquid chromatography-mass spectrometry (LC-MS) QToF analysis in **(A)** positive mode, and **(B)** negative mode, based on their mass-to-charge ratio and retention time (min). Details of the phytochemicals identified in positive and negative mode are given in Table 2

(Figure 7A). Individual lesion scores in the DKV-O treated mice showed significant reduction (p -value < 0.01) for epidermal hyperplasia (1.62 ± 0.51 folds), epidermal hyperkeratosis (0.75 ± 0.70 folds), epidermal pustule formation (0.37 ± 0.74 folds) and neutrophil influx in dermis region (1.5 ± 0.53 folds) (Figure 7B–E). DEXA treatment also showed significant (p -value < 0.01) effects in reducing the OXA-stimulated total and individual inflammatory lesion scores (Figure 7A–E).

Induction of inflammation in the OXA-stimulated mice was analyzed through measurement of pro-inflammatory cytokines- interleukin (IL)- 1β , IL-6, and TNF- α . In the blood serum of the DC animals stimulated with OXA

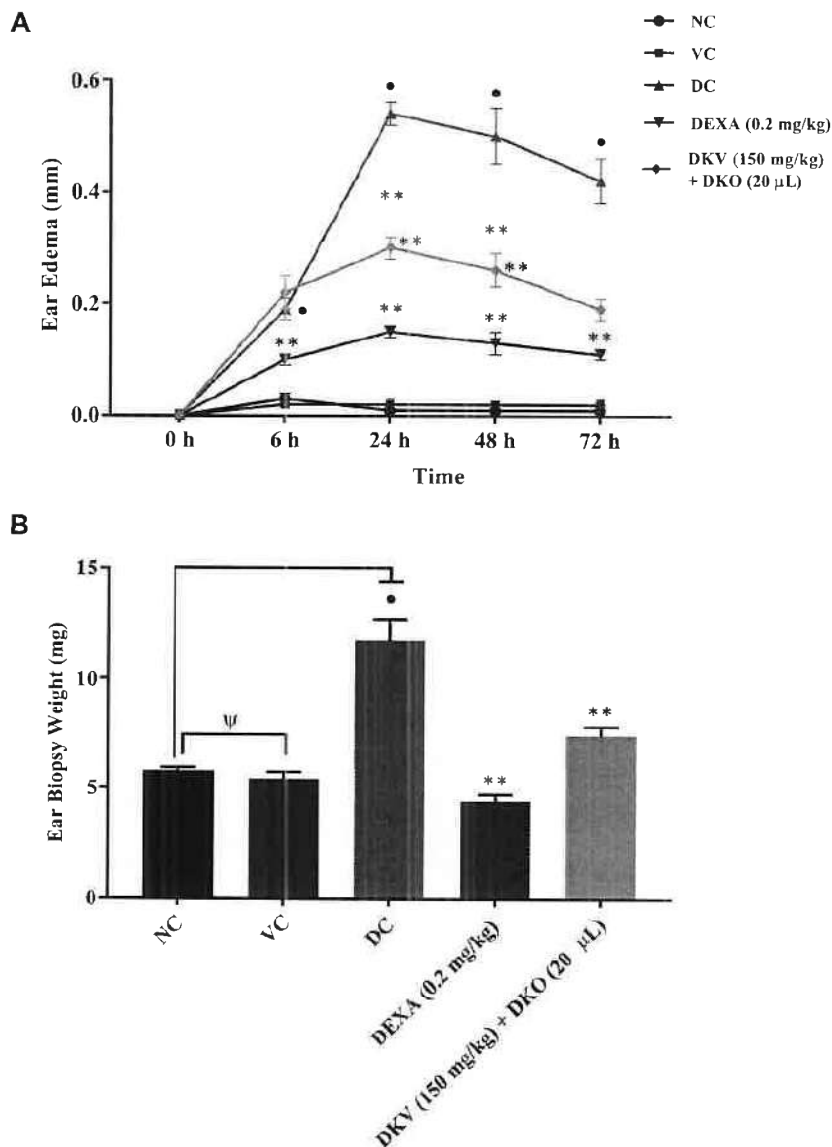


Figure 4 Ear edema and biopsy weight analysis in Oxazolone (OXA)-stimulated mice. Physiological parameters, such as (A) ear edema, and (B) ear biopsy weight changes were analyzed in 1.5% OXA-stimulated mice following co-treatment with Divya-Kayakalp-Vati (150 mg/kg; P.O.) and Divya-Kayakalp-Oil (20 µL, T.A.) (DKV-O), or treatment with Dexamethasone (DEXA; 0.2 mg/kg; T.A.) alone. Acetone treatment was given as vehicle control (VC). p-values ● <0.01 (normal control (NC) versus disease control (DC)); ** <0.01 (DC versus DKV-O treatment; DC versus DEXA); Ψ = Not significant.

a significant (p -value <0.01) induction of IL-1 β (5.27 ± 0.66 pg/mL), IL-6 (18.87 ± 6.25 pg/mL), TNF- α (8.84 ± 2.01 pg/mL) was observed (Figure 8A–C). Treatment with DKV-O significantly (p -value <0.01) reduced the presence of inflammatory cytokines in the blood serum of OXA-stimulated mice. The level of cytokines was determined at s IL-1 β : 3.21 ± 1.00 pg/mL, IL-6: 13.07 ± 1.61 pg/mL and TNF- α : 7.1 ± 0.81 pg/mL in the mice blood serum (Figure 8A–C). DEXA treatment of the OXA-stimulated mice also significantly (p -value <0.01) reduced the levels of pro-inflammatory cytokines to IL-1 β : 2.44 ± 0.58 pg/mL, IL-6: 10.20 ± 0.84 pg/mL and TNF- α : 4.55 ± 0.29 pg/mL (Figure 8A–C). Myeloperoxidase (MPO) is the most abundant protein produced by

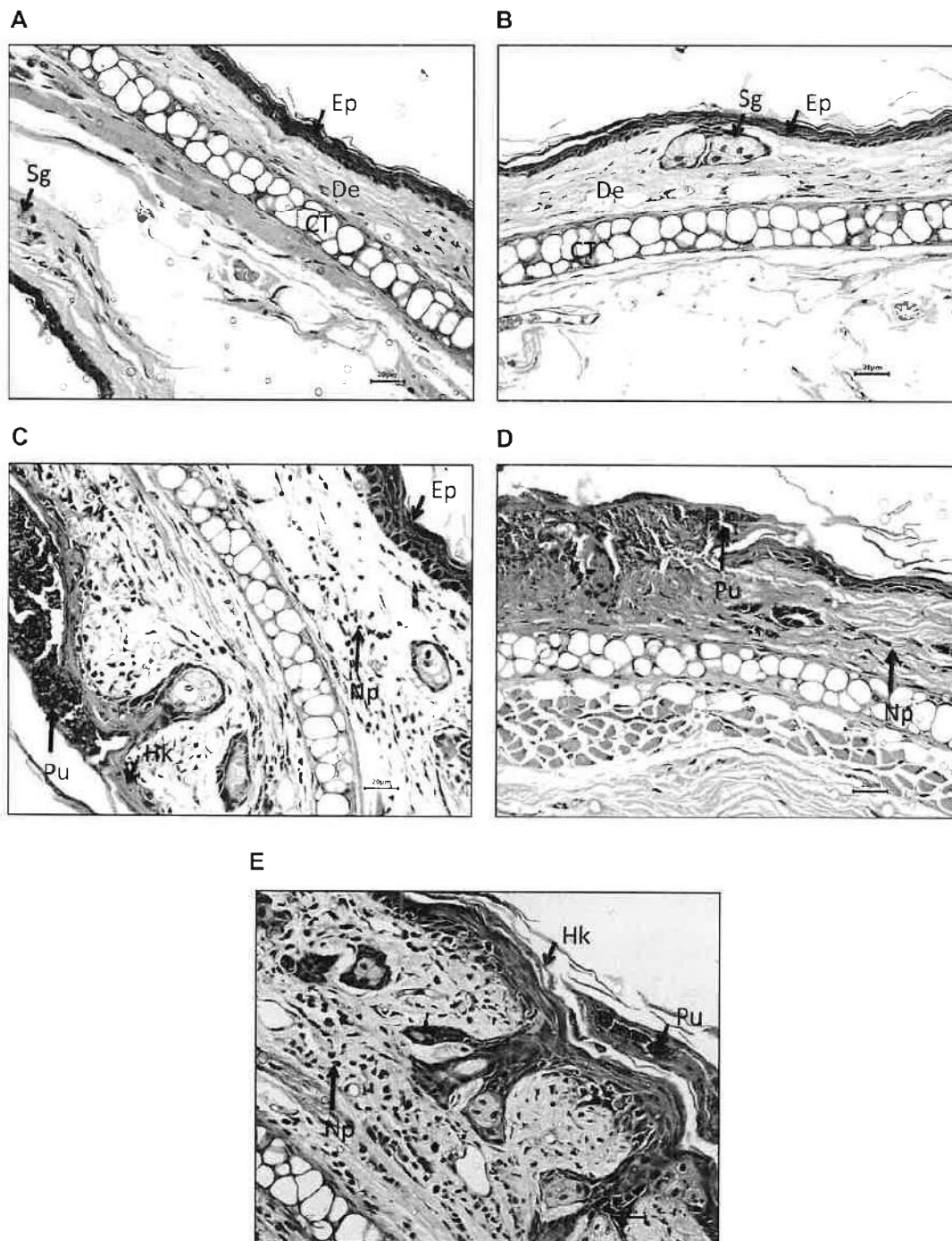


Figure 5 Histopathological analysis of ear tissue in Oxazolone (OXA)-stimulated mice. Histopathological images based lesion score (LS) analysis was performed in ear tissue obtained from (A) normal control (No OXA challenge) mice, (B) vehicle control (acetone) treated mice, (C) 1.5% OXA challenged DC mice, (D) 1.5% OXA challenged mice treated with Dexamethasone (DEXA; 0.2 mg/ear), and (E) 1.5% OXA challenged mice co-treated with DKV (150 mg/kg; P.O.) and DKO (20 μ L, T.A.). Tissue parts identified were epidermis (Ep), dermis (De), sebaceous gland (Sg), and cartilage (Ct) regions. Inflammatory lesions observed were hyperkeratosis (Hk), pustule formation (Pu), and the influx of neutrophils (Np).

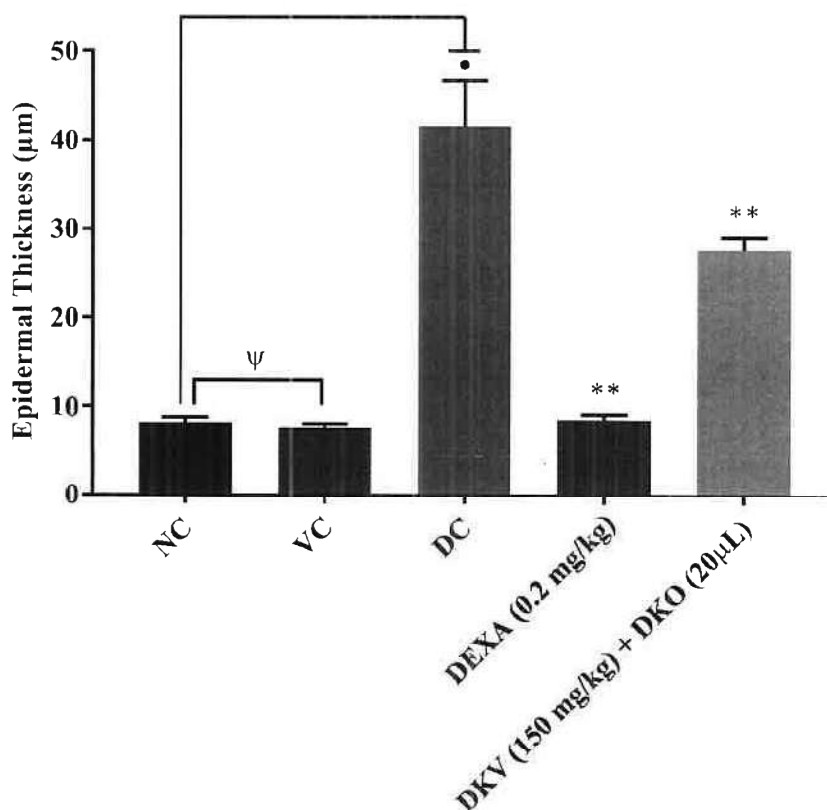


Figure 6 Ear epidermal thickness analysis in Oxazolone (OXA)-stimulated mice. Ear epidermal thickness was analyzed in 1.5% OXA-stimulated mice following treatment with Divya-Kayakalp-Vadi (150 mg/kg; P.O.) and Divya-Kayakalp-Oil (20 µL, T.A.) (DKV-O) co-treatment, or Dexamethasone (DEXA; 0.2 mg/kg) treatment. Acetone treatment was given as vehicle control (VC). Statistical analysis was performed using the one-way analysis of variance (ANOVA) method followed by Dunnett's multiple comparison t-test. p-values • <0.01 (normal control (NC) versus disease control (DC)); ** ≤0.01 (DC versus DKV-O treatment; DC versus DEXA); Ψ = Not significant.

neutrophilic granulocytes. In the present study, MPO was significantly (p -value <0.001) elevated in the OXA-treated mouse-ear (5.38 ± 1.12 U/mg fw) compared to NC mice MPO level (1.34 ± 0.61 U/mg fw) (Figure 8D). In the OXA-stimulated mice treated with DKV-O, the MPO level was found to be attenuated to 4.29 ± 1.68 U/mg fw. DEXA treatment also significantly (p -value <0.01) reduced the MPO levels (1.67 ± 0.67 U/mg fw) in the OXA-stimulated mice ears compared to the DC animal (Figure 8D).

Thus, the combined treatment of DKV-O was observed to show potential anti-inflammatory and antioxidant potentials in the AD-like inflammation in mice. DKV-O effectively reduced the OXA-stimulated ear edema, lesion formations, and associated influx of inflammatory cells and soluble factors such as cytokines and myeloperoxidase. These anti-inflammatory attributes for DKV-O could be related to the presence of phytochemicals in the poly-herbal formulations.

Discussion

Atopic Dermatitis (AD) is a common chronic relapsing inflammatory skin disease that is represented by the infiltration of the inflammatory cells and production of pro-inflammatory cytokines.³⁶ The disease is often accompanied by the development of inflammatory skin lesions. AD has also been associated with an increased risk of developing other inflammatory diseases like arthritis, inflammatory bowel disease, and vitiligo.^{4,37} While, therapeutics for curing AD are directed towards immunomodulation with the objective of prevention and cure, the existence of endotypic disease complexity makes it difficult to exploit a final solution. Temporary relief from AD is acquired through anti-histamine and immunosuppressive agents, moisture care therapy, corticosteroids, or localized immuno-regulatory agents.³⁸ However,

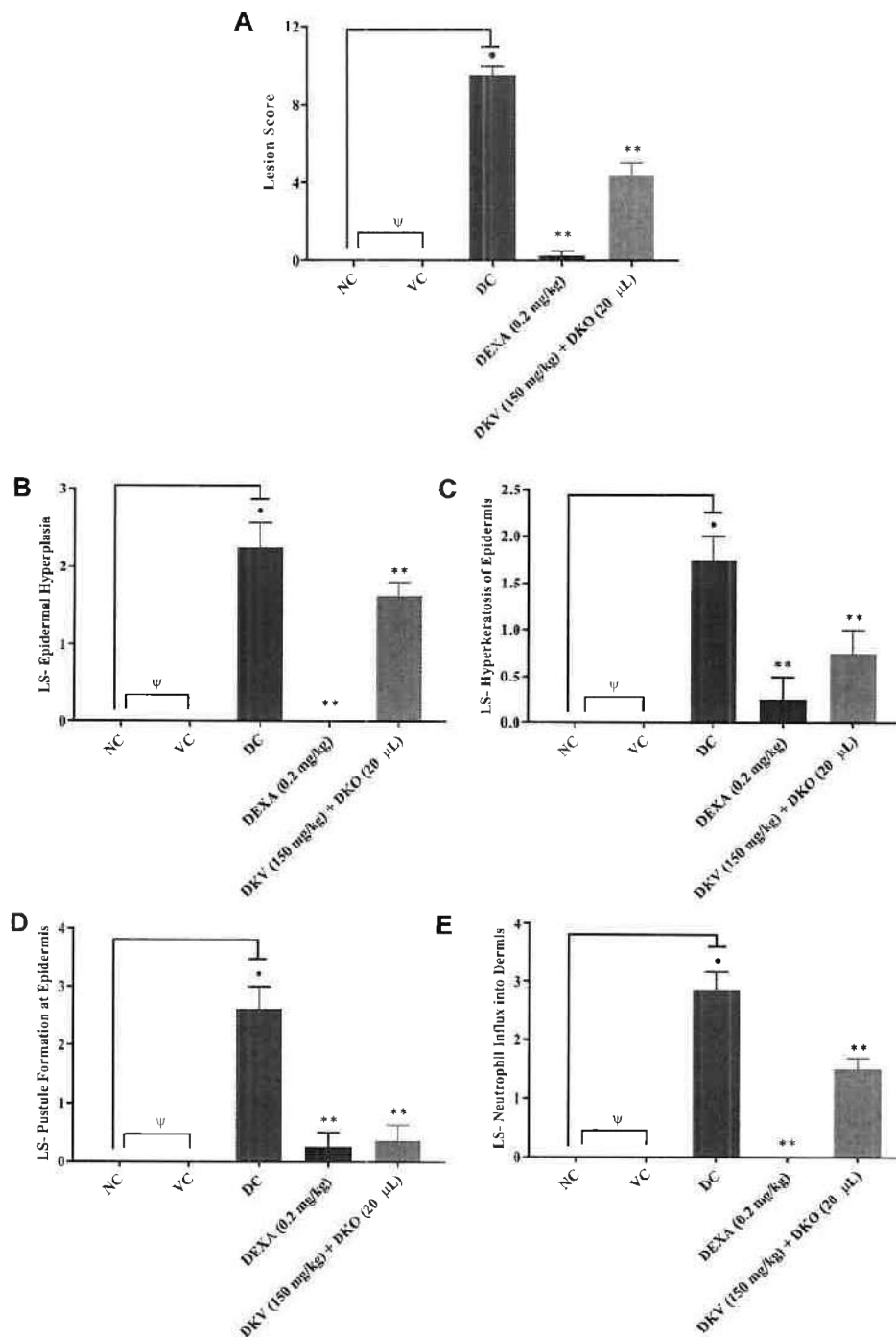


Figure 7 Inflammatory lesion score analysis in ear tissue obtained from Oxazolone (OXA)-stimulated mice. Histopathological lesion scoring (LS) was performed for (A) Total Lesion Score, (B) Epidermal hyperplasia, (C) Hyperkeratosis of the epidermis, (D) Pustule formation in the epidermis and (E) Neutrophil influx into the dermis in normal control (No OXA-challenge) mice, vehicle control (Acetone) treated mice, 1.5% OXA challenged DC mice, 1.5% OXA-challenged mice treated with Dexamethasone (DEXA; 0.2 mg/ear), and 1.5% OXA challenged mice co-treated with DKV (150 mg/kg; P.O.) and DKO (20 µL, T.A.). Statistical analysis was performed using one-way analysis of variance (ANOVA) followed by Dunnett's multiple comparison t-test was applied. p-value ≤ 0.01 (normal control (NC) versus disease control (DC)), ** ≤ 0.01 (DC versus DKV-O treatment; DC versus DEXA); Ψ = Not significant.

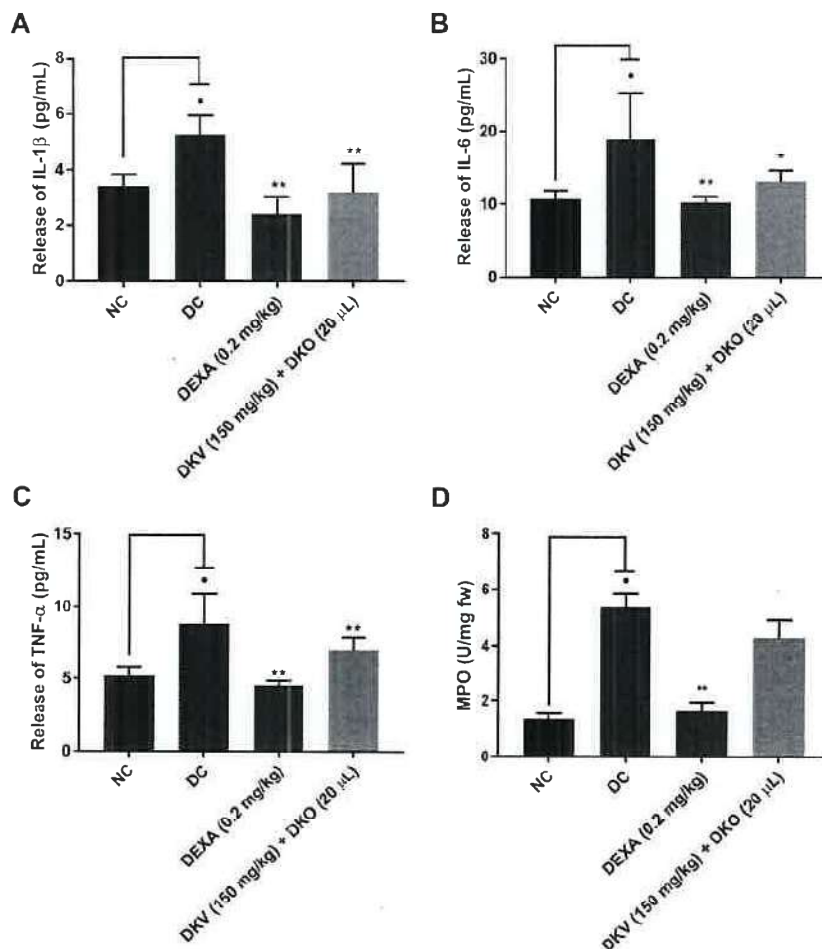


Figure 8 Inflammatory marker analysis in samples obtained from Oxazolone (OXA)-stimulated mice. Inflammatory markers- (A) Interleukin (IL)-1 β , (B) IL-6, (C) tumor necrosis factor-alpha (TNF- α) in the blood serum, and (D) myeloperoxidase (MPO) analysis was done in ear tissue stubs obtained from normal control (No OXA-challenge) mice, vehicle control (Acetone) treated mice, 1.5% OXA challenged DC mice, 1.5% OXA challenged mice treated with Dexamethasone (DEXA; 0.2 mg/ear), and 1.5% OXA challenged mice co-treated with DKV (150 mg/kg; P.O.) and DKO (20 μ L, T.A.). Statistical analysis was performed using one-way analysis of variance (ANOVA) followed by Dunnett's multiple comparison t-test was applied. p-value \bullet ≤ 0.01 (normal control (NC) versus disease control (DC)); \ast ≤ 0.05 $\ast\ast$ ≤ 0.01 (DC versus DKV-O treatment; DC versus DEXA).

prolonged use of these medications can lead to other health-related side effects and drug intolerances.³⁹ Phototherapy using UltraViolet radiation "A" (UVA) is not recommended for acute AD and other dermal inflammatory diseases like Psoriasis.⁴⁰ Furthermore, UVA therapy can lead to photo-aging of skin and in some cases dermal carcinogenesis.⁴⁰

Therefore, there is an increased necessity to discover more effective therapies against AD with minimum or no side effects. Medicinal plants play an important role in folk medicines with minimum side effects and some have been reported to have anti-AD applications.⁴¹⁻⁴³ Tradition Indian medicine system is known as "Ayurveda" has been widely applied as an alternative or additive therapeutics.⁴⁴⁻⁴⁶ Herbal components of DKV-O such as *Berberis aristata* DC., *Curcuma longa* L., *Caesalpinia bonducella* F., *Azadirachta indica* A. Juss., *Santalum album* L., and *Acacia catechu* (L.F.) Willd. has shown efficacy in treating various dermal and non-dermal maladies.⁴⁷⁻⁵¹ Therapeutic properties of the mono- and poly-herbal formulations have been attributed to their phytochemical contents including phenol, polyphenol, alkaloid, terpenoid, and glycoside classes of molecules.⁵² Phytochemicals identified in DKV-O have been reported to play a major role in regulating inflammation, prevention of allergen, and platelet-activating factors.⁵³⁻⁵⁶ Berbamine and Catechin attenuate the allergen-stimulated release

of pro-inflammatory cytokines (IL-1 β , IL-6, and TNF- α), the neutrophil influx into the affected site, and activation of NF κ B, matrix metalloproteinase (MMP)-9, and acetylcholine esterase.⁵⁷⁻⁶¹ Additionally, Berberine exhibits anti-inflammatory activity through modulation of T cell activation and inhibition of NF κ B and MAPK signaling pathways.^{34,35} Hence, the AD-like inflammation amelioration properties of DKV-O can be attributed to the reported immunomodulatory activity of these phytochemicals.

Activation of keratinocytes, inflammatory cells, and release of pro-inflammatory cytokines have been implicated as a major event in the induction of dermal inflammatory diseases like AD and psoriasis. Clinical studies have confirmed elevated levels of inflammatory cells along with the release of IL-1 β , IL-6, and TNF- α cytokines in the dermal tissues of AD and psoriasis patients.^{62,63} DKV-O treatment was found capable of altering the OXA-stimulated ear edema, and associated inflammation through the modulation of inflammatory cells influx into the dermis and release of pro-inflammatory cytokines. During AD, IL-1 β and TNF- α are released by inflamed keratinocytes and activated immune cells.⁶⁴ While serum IL-1 β and TNF- α levels stimulate the release of IL-6 cytokines from T-cells.^{65,66} Phytochemicals contents of DKV-O such as Curcumin, Berberine, and Gallic Acid possess excellent anti-inflammatory, anti-oxidant, chemo-preventive, and chemotherapeutic activities. Curcumin modulates T-cell secretion of pro-inflammatory cytokines including TNF-alpha responsible for the induction of inflammation and epidermal edema.^{67,68} Similarly, Gallic acid and Berberine are responsible for inhibiting allergen stimulated release of pro-inflammatory cytokine release from macrophages and in reducing induced epidermal edema.⁶⁹

Myeloperoxidase (MPO) is a well-known biomarker for skin inflammation originating from stimulated neutrophilic granulocytes.⁷⁰ In the present study, DKV-O treatment reduced the OXA-stimulated MPO levels in the inflamed ear tissue of mice directly indicating a reduced presence of activated neutrophils. Histopathological analysis confirmed the reduced influx of neutrophils in the DKV-O treated inflamed ear tissue dermis along with a moderated generation of inflammatory lesions such as hyperkeratosis, hyperplasticity, and pustule formation in the epidermis. The results correlate well with our previous finding showing DKV-O eliminated 12-O-tetradecanoyl phorbol 13-acetate (TPA) stimulated inflammatory lesion and the neutrophil influx into the dermal region.²⁷ 1,8-Dihydroxy-3-methylanthraquinone (Chrysophanol) is known as a multifaceted phytochemical that has anti-inflammatory, anti-cancer, hepatoprotective, and neuroprotective activities.⁷¹ Pretreatment of human mast cells (HMC-1) with Chrysophanol suppressed intracellular calcium levels and histamine release following phorbol 12-myristate 13-acetate and calcium ionophore treatments.⁷² Chrysophanol also reduced the overexpression of caspase-1, nuclear factor- κ B, and thymic stromal lymphopoietin in the stimulated HMC-1 cells.⁷² In human keratinocytes (HaCaT cells) pretreatment with chrysophanol significantly reduced stimulated expression of caspase-1 and thymic stromal lymphopoietin proteins.⁷² Similarly, Quercetin is a flavonoid that has been observed to inhibit neutrophil influx in affected regions during the onset of rheumatoid arthritis.⁷³ In addition, Quercetin leads the neutrophils to undergo apoptosis, reducing the incidences of neutrophilic extracellular trap formation and release of extracellular pro-inflammatory cytokines.⁷³ Additionally, Quercetin pre-treatment reduced oxidative stress through the generation of antioxidants within the in vitro model for AD using HaCaT cells treated with IL-4, IL-13, and TNF- α .⁷⁴ Quercetin also increased the mRNA expression of occludin and E-cadherin, while downregulating MMP1, MMP2, and MMP9 expression stimulating wound healing in stimulated HaCaT cells as well as, downregulated phosphorylation of MAPK, and NF- κ B reducing inflammation.⁷⁴

In the end, phytochemical constituents of the DKV-O are extensively responsible for the inhibition of inflammation through the modulation of the activated immune cells and the release of the pro-inflammatory cytokines. Though further analysis is still required for understanding the individual contribution of the herbal components and phytochemicals present in the DKV-O. It is important to note that the current study demonstrated the efficacy of DKV-O as a whole, where its herbal components functioned in synergy, and possibly in a multifocal manner in moderating the acute inflammation triggered by OXA. Also, species-wise variations exist for biological studies, due to which caution needs to be taken while translating the observed efficacy of DKV-O in mice to humans.

Conclusion

In short, combined treatment of DKV-O showed anti-inflammatory efficacy in ameliorating stimulated AD through the modulation of inflammatory neutrophilic influx, and release of pro-inflammatory cytokines. Suppression of inflammation in

the OXA-stimulated ear tissue also lessened the incidence of inflammatory lesion generation. The observed anti-AD efficacy of the DKV-O can be attributed to the rich presence of all the phytochemicals working in synergy. These phytochemicals directly function in reducing inflammation by modulating the inflammatory cells and activated keratinocytes and their multicentric synergistic effect in the modulation of AD-like inflammatory response needs further exploration. Taken together, DKV-O could well be a suitable healing option for atopic dermatitis-like inflammatory skin diseases.

Abbreviations

AD, Atopic Dermatitis; IL-1 β , Interleukin-1 beta; IL-6, Interleukin-6; TNF- α , Tumor necrosis factor-alpha; MPO, Myeloperoxidase; ELISA, Enzyme-Linked Immunosorbent Assay; DC, disease control; DKV, Divya-Kayakalp-Vati; DKO, Divya-Kayakalp-Oil; DKV-O, Divya-Kayakalp-Vati and Divya-Kayakalp-Oil co-treatment; DEXA, Dexamethasone; OXA, Oxazolone; CPCSEA, Committee for the Purpose of Control and Supervision of Experiments on Animals; IAEC, Institutional Animal Ethical Committee, ICH, International Conference on Harmonization; Na-CMC, Sodium-carboxymethyl cellulose, ANOVA, One-way analysis of variance; NC, normal control; LC-MS QToF, Liquid Chromatography-Mass Spectroscopy Quadrupole Time-of-Flight; Th2, T helper-2; IgE, Immunoglobulin E; T.A., Topical application; P.O., *per os* (orally); H&E stain, Haematoxylin and Eosin stain; TMB, 3,3',5,5'-tetramethylbenzidine; m/z, Mass-charge ratio; UVA, UltraViolet radiation "A"; NF κ B, Nuclear factor kappa B; MAPK, Mitogen-activated protein kinase; TPA, 12-O-tetradecanoyl phorbol 13-acetate; HMC-1, Human mast cells; HaCaT, Human Keratinocyte cells; mRNA, Messenger ribonucleic acid.

Acknowledgments

We thank Mr. Hoshiyar Singh and Dr. Niti Sharma for their support in conducting biochemical assays. We would also like to appreciate Mr. Bhanu Pratap, Mr. Pushpendra Singh, Mr. Vipin Kumar, and Mr. Sonit Kumar for the excellent animal handling and maintenance support. We extend our gratitude to Mr. Brij Kishore, Mr. Pardeep Nain, Mr. Tarun Rajput, Mr. Gagan Kumar, and Mr. Lalit Mohan for their swift administrative support. This research work was funded internally by Patanjali Research Foundation Trust, Haridwar, India.

Disclosure

The test articles were sourced from Divya Pharmacy, Haridwar, Uttarakhand, India. Acharya Balkrishna is an honorary trustee in Divya Yog Mandir Trust, Haridwar, India; in addition, he holds an honorary managerial position in Patanjali Ayurved Ltd., Haridwar, India; he reports no other potential conflicts of interest for this work. Besides, providing the test article, Divya Pharmacy was not involved in any aspect of this study. All other authors report no conflicts of interest for this work.

References

1. Cork MJ, Thaci D, Eichenfield LF, et al. Dupilumab provides favourable long-term safety and efficacy in children aged ≥ 6 to < 12 years with uncontrolled severe atopic dermatitis: results from an open-label phase IIa study and subsequent Phase III open-label extension study. *Br J Dermatol*. 2021;184(5):857–870. doi:10.1111/bjd.19460
2. Paller AS, Siegfried EC, Thaci D, et al. Efficacy and safety of dupilumab with concomitant topical corticosteroids in children 6 to 11 years old with severe atopic dermatitis: a randomized, double-blinded, placebo-controlled Phase 3 trial. *J Am Acad Dermatol*. 2020;83(5):1282–1293. doi:10.1016/j.jaad.2020.06.054
3. Lin YT, Wang CT, Chiang BL. Role of bacterial pathogens in atopic dermatitis. *Clin Rev Allergy Immunol*. 2007;33(3):167–177. doi:10.1007/s12016-007-0044-5
4. Weidinger S, Beck LA, Bieber T, Kabashima K, Irvine AD. Atopic dermatitis. *Nat Rev Dis Primers*. 2018;4(1):1. doi:10.1038/s41572-018-0001-z
5. Jin H, He R, Oyoshi M, Geha RS. Animal models of atopic dermatitis. *J Invest Dermatol*. 2009;129(1):31–40. doi:10.1038/jid.2008.106
6. Maarouf M, Vaughn AR, Shi VY. Topical micronutrients in atopic dermatitis-An evidence-based review. *Dermatol Ther*. 2018;31(5):e12659. doi:10.1111/dth.12659
7. Leung DY, Boguniewicz M, Howell MD, Nomura I, Hamid QA. New insights into atopic dermatitis. *J Clin Invest*. 2004;113(5):651–657. doi:10.1172/JCI21060
8. Longo G, Berti I, Burks AW, Krauss B, Barbi E. IgE-mediated food allergy in children. *Lancet*. 2013;382(9905):1656–1664. doi:10.1016/S0140-6736(13)60309-8
9. van der Hulst AE, Klip H, Brand PL. Risk of developing asthma in young children with atopic eczema: a systematic review. *J Allergy Clin Immunol*. 2007;120(3):565–569. doi:10.1016/j.jaci.2007.05.042
10. Kapoor R, Menon C, Hoffstad O, Bilker W, Leclerc P, Margolis DJ. The prevalence of atopic triad in children with physician-confirmed atopic dermatitis. *J Am Acad Dermatol*. 2008;58(1):68–73. doi:10.1016/j.jaad.2007.06.041

11. Irvine AD, McLean WH, Leung DY. Filaggrin mutations associated with skin and allergic diseases. *N Engl J Med*. 2011;365(14):1315–1327. doi:10.1056/NEJMra1011040
12. Ellinghaus D, Baurecht H, Esparza-Gordillo J, et al. High-density genotyping study identifies four new susceptibility loci for atopic dermatitis. *Nat Genet*. 2013;45(7):808–812. doi:10.1038/ng.2642
13. Palmer CN, Irvine AD, Terron-Kwiatkowski A, et al. Common loss-of-function variants of the epidermal barrier protein filaggrin are a major predisposing factor for atopic dermatitis. *Nat Genet*. 2006;38(4):441–446. doi:10.1038/ng1767
14. Nettis E, Ortoncelli M, Pellacani G, et al. A multicenter study on the prevalence of clinical patterns and clinical phenotypes in adult atopic dermatitis. *J Investig Allergol Clin Immunol*. 2020;30(6):448–450. doi:10.18176/jiaci.0519
15. Tavakolpour S. Tofacitinib as the potent treatment for refractory pemphigus: a possible alternative treatment for pemphigus. *Dermatol Ther*. 2018;31(5):e12696. doi:10.1111/dth.12696
16. Brunner PM, Khattri S, Garcet S, et al. A mild topical steroid leads to progressive anti-inflammatory effects in the skin of patients with moderate-to-severe atopic dermatitis. *J Allergy Clin Immunol*. 2016;138(1):169–178. doi:10.1016/j.jaci.2015.12.1323
17. Danby SG, Chittock J, Brown K, Albenali LH, Cork MJ. The effect of tacrolimus compared with betamethasone valerate on the skin barrier in volunteers with quiescent atopic dermatitis. *Br J Dermatol*. 2014;170(4):914–921. doi:10.1111/bjd.12778
18. Nakahara T, Morimoto H, Murakami N, Furue M. Mechanistic insights into topical tacrolimus for the treatment of atopic dermatitis. *Pediatr Allergy Immunol*. 2018;29(3):233–238. doi:10.1111/pai.12842
19. Jensen JM, Weppner M, Dahnhardt-Pfeiffer S, et al. Effects of pimecrolimus compared with triamcinolone acetonide cream on skin barrier structure in atopic dermatitis: a randomized, double-blind, right-left arm trial. *Acta Derm Venereol*. 2013;93(5):515–519. doi:10.2340/00015555-1533
20. Zebda R, Paller AS. Phosphodiesterase 4 inhibitors. *J Am Acad Dermatol*. 2018;78(3 Suppl 1):S43–S52. doi:10.1016/j.jaad.2017.11.056
21. Garritsen FM, Brouwer MW, Limpens J, Spuls PI. Photo(chemo)therapy in the management of atopic dermatitis: an updated systematic review with implications for practice and research. *Br J Dermatol*. 2014;170(3):501–513. doi:10.1111/bjd.12645
22. Dattola A, Bennardo L, Silvestri M, Nistico SP. What's new in the treatment of atopic dermatitis? *Dermatol Ther*. 2019;32(2):e12787. doi:10.1111/dth.12787
23. Castela E, Archier E, Devaux S, et al. Topical corticosteroids in plaque psoriasis: a systematic review of risk of adrenal axis suppression and skin atrophy. *J Eur Acad Dermatol Venereol*. 2012;26(Suppl 3):47–51. doi:10.1111/j.1468-3083.2012.04523.x
24. AFI. Ayurvedic Formulary of India, Part 1 2 ed. Delhi; 2003.
25. UPI. The Unani Pharmacopoeia of India Ministry of AYUSH, Government of India; 2007.
26. Trikamji J. *Charaka Samhita* of Agnivesha, Chikitsa Sthana; Abhaya Amalaki Rasayana Pada. Vol 1. 1 ed. Varanasi: Chowkhamba Prakashan; 2007:378–379.
27. Balkrishna A, Sakat SS, Joshi K, et al. Modulation of psoriatic-like skin inflammation by traditional Indian medicine Divya-Kayakalp-Vati and Oil through attenuation of pro-inflammatory cytokines. *J Tradit Complement Med*. 2021. doi:10.1016/j.jtcm.2021.09.003
28. Man MQ, Hatano Y, Lee SH, et al. Characterization of a hapten-induced, murine model with multiple features of atopic dermatitis: structural, immunologic, and biochemical changes following single versus multiple oxazolone challenges. *J Invest Dermatol*. 2008;128(1):79–86. doi:10.1038/sj.jid.5701011
29. CPCSEA. Committee for the Purpose of Control and Supervision of Experiments on Animals (CPCSEA), Compendium of CPCSEA; 2018.
30. Percie du Sert N, Ahluwalia A, Alam S, et al. Reporting animal research: explanation and elaboration for the ARRIVE guidelines 2.0. *PLoS Biol*. 2020;18(7):e3000411. doi:10.1371/journal.pbio.3000411
31. Webb EF, Tzimas MN, Newsholme SJ, Griswold DE. Intralésional cytokines in chronic oxazolone-induced contact sensitivity suggest roles for tumor necrosis factor alpha and interleukin-4. *J Invest Dermatol*. 1998;111(1):86–92. doi:10.1046/j.1523-1747.1998.00239.x
32. Suzuki K, Ota H, Sasagawa S, Sakatani T, Fujikura T. Assay method for myeloperoxidase in human polymorphonuclear leukocytes. *Anal Biochem*. 1983;132(2):345–352. doi:10.1016/0003-2697(83)90019-2
33. Moon PD, Han NR, Lee JS, et al. Use of physcion to improve atopic dermatitis-like skin lesions through blocking of thymic stromal lymphopoietin. *Molecules*. 2019;24:8. doi:10.3390/molecules24081484
34. Jia XJ, Li X, Wang F, Liu HQ, Zhang DJ, Chen Y. Berbamine exerts anti-inflammatory effects via inhibition of NF-kappaB and MAPK signaling pathways. *Cell Physiol Biochem*. 2017;41(6):2307–2318. doi:10.1159/000475650
35. Luo CN, Lin X, Li WK, et al. Effect of berbamine on T-cell mediated immunity and the prevention of rejection on skin transplants in mice. *J Ethnopharmacol*. 1998;59(3):211–215. doi:10.1016/S0378-8741(97)00117-7
36. Nakagawa R, Yoshida H, Asakawa M, et al. Pyridone 6, a pan-JAK inhibitor, ameliorates allergic skin inflammation of NC/Nga mice via suppression of Th2 and enhancement of Th17. *J Immunol*. 2011;187(9):4611–4620. doi:10.4049/jimmunol.1100649
37. Acharya P, Mathur M. Association of atopic dermatitis with vitiligo: a systematic review and meta-analysis. *J Cosmet Dermatol*. 2020;19(8):2016–2020. doi:10.1111/jocd.13263
38. Kim JE, Lee YB, Lee JH, et al. Disease awareness and management behavior of patients with atopic dermatitis: a questionnaire survey of 313 patients. *Ann Dermatol*. 2015;27(1):40–47. doi:10.5021/ad.2015.27.1.40
39. Yang H, Jung EM, Ahn C, et al. Elemol from *Chamaecyparis obtusa* ameliorates 2,4-dinitrochlorobenzene-induced atopic dermatitis. *Int J Mol Med*. 2015;36(2):463–472. doi:10.3892/ijmm.2015.2228
40. Megna M, Napolitano M, Patruno C, et al. Systemic treatment of adult atopic dermatitis: a review. *Dermatol Ther*. 2017;7(1):1–23. doi:10.1007/s13555-016-0170-1
41. Karimi A, Majlesi M, Rafeian-Kopaei M. Herbal versus synthetic drugs; beliefs and facts. *J Nephroarmacol*. 2015;4(1):27–30.
42. Joo SS, Yoo YM, Ko SH, et al. Effects of essential oil from *Chamaecyparis obtusa* on the development of atopic dermatitis-like skin lesions and the suppression of Th cytokines. *J Dermatol Sci*. 2010;60(2):122–125. doi:10.1016/j.jdermsci.2010.08.008
43. Chen Y, Xian Y, Lai Z, Loo S, Chan WY, Lin ZX. Anti-inflammatory and anti-allergic effects and underlying mechanisms of Huang-Lian-Jie-Du extract: implication for atopic dermatitis treatment. *J Ethnopharmacol*. 2016;185:41–52. doi:10.1016/j.jep.2016.03.028
44. Ravishankar B, Shukla VJ. Indian systems of medicine: a brief profile. *Afr J Tradit Complement Altern Med*. 2007;4(3):319–337. doi:10.4314/ajtcam.v4i3.31226
45. Balkrishna A, Sakat SS, Joshi K, et al. Herbo-mineral formulation 'Ashwashila' attenuates rheumatoid arthritis symptoms in collagen-antibody-induced arthritis (CAIA) mice model. *Sci Rep*. 2019;9(1):8025. doi:10.1038/s41598-019-44485-9

46. Balkrishna A, Sakat SS, Joshi K, et al. Anti-inflammatory and anti-arthritis efficacies of an Indian traditional herbo-mineral medicine "Divya Amvatar Ras" in Collagen Antibody-Induced Arthritis (CAIA) mouse model through modulation of IL-6/TL-1beta/TNF-alpha/NFkappaB signaling. *Front Pharmacol*. 2019;10:659. doi:10.3389/fphar.2019.00659
47. Kumar R, Gupta YK, Singh S. Anti-inflammatory and anti-granuloma activity of Berberis aristata DC. in experimental models of inflammation. *Indian J Pharmacol*. 2016;48(2):155–161. doi:10.4103/0253-7613.178831
48. Shukla S, Mehta A. In vivo anti-inflammatory, analgesic and antipyretic activities of a medicinal plant, Caesalpinia bonducella F. *Pak J Pharm Sci*. 2015;28(4 Suppl):1517–1521.
49. Umar MI, Asmawi MZ, Sadikun A, et al. Multi-constituent synergism is responsible for anti-inflammatory effect of Azadirachta indica leaf extract. *Pharm Biol*. 2014;52(11):1411–1422. doi:10.3109/13880209.2014.895017
50. Moy RL, Levenson C. Sandalwood album oil as a botanical therapeutic in dermatology. *J Clin Aesthet Dermatol*. 2017;10(10):34–39.
51. Vaughn AR, Branum A, Sivamani RK. Effects of Turmeric (Curcuma longa) on skin health: a systematic review of the clinical evidence. *Phytother Res*. 2016;30(8):1243–1264. doi:10.1002/ptr.5640
52. Borokini TI, Omotayo FO. Phytochemical and ethnobotanical study of some selected medicinal plants from Nigeria. *J Med Plants Res*. 2012;6(7):1106–1118.
53. Kroes BH, van den Berg AJ, Quarles van Ufford HC, van Dijk H, Labadie RP. Anti-inflammatory activity of gallic acid. *Planta Med*. 1992;58(6):499–504. doi:10.1055/s-2006-961535
54. Kuo CL, Chi CW, Liu TY. The anti-inflammatory potential of berberine in vitro and in vivo. *Cancer Lett*. 2004;203(2):127–137. doi:10.1016/j.canlet.2003.09.002
55. Farhood B, Mortezaee K, Goradel NH, et al. Curcumin as an anti-inflammatory agent: implications to radiotherapy and chemotherapy. *J Cell Physiol*. 2019;234(5):5728–5740. doi:10.1002/jcp.27442
56. Dorsch W, Stuppner H, Wagner H, Gropp M, Demoulin S, Ring J. Antiasthmatic effects of Pterorhiza kurroa: androsin prevents allergen- and PAF-induced bronchial obstruction in Guinea pigs. *Int Arch Allergy Appl Immunol*. 1991;95(2–3):128–133. doi:10.1159/000235416
57. Wang X, Feng S, Ding N, et al. Anti-inflammatory effects of berberine hydrochloride in an LPS-induced murine model of mastitis. *Evid Based Complement Alternat Med*. 2018;2018:5164314. doi:10.1155/2018/5164314
58. Kim S, Kim Y, Kim JE, Cho KH, Chung JH. Berberine inhibits TPA-induced MMP-9 and IL-6 expression in normal human keratinocytes. *Phytochemistry*. 2008;15(5):340–347. doi:10.1016/j.phymed.2007.09.011
59. Balkrishna A, Pokhrel S, Tomer M, et al. Anti-acetylcholinesterase activities of mono-herbal extracts and exhibited synergistic effects of the phytoconstituents: a biochemical and computational study. *Molecules*. 2019;24:22. doi:10.3390/molecules24224175
60. Kim-Park WK, Allam ES, Palasuk J, Kowolik M, Park KK, Windsor LJ. Green tea catechin inhibits the activity and neutrophil release of Matrix Metalloproteinase-9. *J Tradit Complement Med*. 2016;6(4):343–346. doi:10.1016/j.jtcm.2015.02.002
61. Huang MT, Liu Y, Ramji D, et al. Inhibitory effects of black tea theaflavin derivatives on 12-O-tetradecanoylphorbol-13-acetate-induced inflammation and arachidonic acid metabolism in mouse ears. *Mol Nutr Food Res*. 2006;50(2):115–122. doi:10.1002/mnfr.200500101
62. Junghans V, Gutgesell C, Jung T, Neumann C. Epidermal cytokines IL-1beta, TNF-alpha, and IL-12 in patients with atopic dermatitis: response to application of house dust mite antigens. *J Invest Dermatol*. 1998;111(6):1184–1188. doi:10.1046/j.1523-1747.1998.00409.x
63. Oxholm A. Epidermal expression of interleukin-6 and tumour necrosis factor-alpha in normal and immunoinflammatory skin states in humans. *APMIS Suppl*. 1992;24:1–32.
64. Asahina R, Maeda S. A review of the roles of keratinocyte-derived cytokines and chemokines in the pathogenesis of atopic dermatitis in humans and dogs. *Vet Dermatol*. 2017;28(1):16–e15. doi:10.1111/vde.12351
65. Toshitani A, Ansel JC, Chan SC, Li SH, Hanifin JM. Increased interleukin 6 production by T cells derived from patients with atopic dermatitis. *J Invest Dermatol*. 1993;100(3):299–304. doi:10.1111/1523-1747.ep12469875
66. Hunter CA, Jones SA. Corrigendum: IL-6 as a keystone cytokine in health and disease. *Nat Immunol*. 2017;18(11):1271. doi:10.1038/ni1117-1271b
67. Kang D, Li B, Luo L, et al. Curcumin shows excellent therapeutic effect on psoriasis in mouse model. *Biochimie*. 2016;123:73–80. doi:10.1016/j.biochi.2016.01.013
68. Huang MT, Lysz T, Ferraro T, Abidi TF, Laskin JD, Conney AH. Inhibitory effects of curcumin on in vitro lipoxygenase and cyclooxygenase activities in mouse epidermis. *Cancer Res*. 1991;51(3):813–819.
69. Tsang MS, Jiao D, Chan BC, et al. Anti-inflammatory activities of pentaherbs formula, berberine, gallic acid and chlorogenic acid in atopic dermatitis-like skin inflammation. *Molecules*. 2016;21(4):519. doi:10.3390/molecules21040519
70. Trush MA, Egnor PA, Kensler TW. Myeloperoxidase as a biomarker of skin irritation and inflammation. *Food Chem Toxicol*. 1994;32(2):143–147. doi:10.1016/0278-6915(94)90175-9
71. Prateeksha S, Yusuf MA, Singh BN, et al. Chrysophanol: a natural anthraquinone with multifaceted biotherapeutic potential. *Biomolecules*. 2019;9(2):68. doi:10.3390/biom9020068
72. Jeong HJ, Kim HY, Kim HM. Molecular mechanisms of anti-inflammatory effect of chrysophanol, an active component of AST2017-01 on atopic dermatitis in vitro models. *Int Immunopharmacol*. 2018;54:238–244. doi:10.1016/j.intimp.2017.11.019
73. Yuan K, Zhu Q, Lu Q, et al. Quercetin alleviates rheumatoid arthritis by inhibiting neutrophil inflammatory activities. *J Nutr Biochem*. 2020;84:108454. doi:10.1016/j.jnutbio.2020.108454
74. Beken B, Sertas R, Yazicioglu M, Turkekul K, Erdogan S. Quercetin improves inflammation, oxidative stress, and impaired wound healing in atopic dermatitis model of human keratinocytes. *Pediatr Allergy Immunol Pulmonol*. 2020;33(2):69–79. doi:10.1089/ped.2019.1137

Clinical, Cosmetic and Investigational Dermatology

Dovepress

Publish your work in this journal

Clinical, Cosmetic and Investigational Dermatology is an international, peer-reviewed, open access, online journal that focuses on the latest clinical and experimental research in all aspects of skin disease and cosmetic interventions. This journal is indexed on CAS. The manuscript management system is completely online and includes a very quick and fair peer-review system, which is all easy to use. Visit <http://www.dovepress.com/testimonials.php> to read real quotes from published authors.

Submit your manuscript here: <http://www.dovepress.com/clinical-cosmetic-and-investigational-dermatology-journal>



Modulation of psoriatic-like skin inflammation by traditional Indian medicine Divya-Kayakalp-Vati and Oil through attenuation of pro-inflammatory cytokines

Acharya Balkrishna^{a, b}, Sachin Sakat^a, Kheemraj Joshi^a, Rani Singh^a, Sudeep Verma^a, Pardeep Nain^a, Kunal Bhattacharya^a, Anurag Varshney^{a, b, *}

^a Drug Discovery and Development Division, Patanjali Research Institute, NH-58, Haridwar, 249405, Uttarakhand, India

^b Department of Allied and Applied Sciences, University of Patanjali, Patanjali Yog Peeth, Haridwar, India

ARTICLE INFO

Article history:

Received 29 October 2020

Received in revised form

10 September 2021

Accepted 13 September 2021

Available online xxx

Keywords:

Divya-kayakalp-vati

Divya-kayakalp-oil

Skin psoriasis

Inflammation

Cytokine release

ABSTRACT

Background and aim: Psoriasis (Ps) is a chronic skin inflammatory disorder, that progresses to scaly-red dermal plaque formations associated with inflammation. Divya-Kayakalp-Vati (DKV) and Divya-Kayakalp-Oil (DKO) are traditional Ayurveda herbo-mineral formulations, that are prescribed for the treatment of inflammatory dermal ailments. In the present study, we evaluated the efficacy of Divya-Kayakalp-Vati and Divya-Kayakalp-Oil (DKV-O) combined treatment in ameliorating Ps-like skin inflammation under *in-vitro* and *in-vivo* conditions.

Experimental procedure: Efficacy of DKV-O was analyzed in λ -carrageenan-treated Wistar rats paw edema and 12-O-tetradecanoylphorbol 13-acetate (TPA)-treated CD-1 mouse ear edema models through physiological and histopathological analysis. Mode of action for the DKV-O was studied in LPS-stimulated THP-1 cells through pro-inflammatory cytokine analysis. Observed effects were correlated to the phytochemicals constituents of DKV-O analyzed using the HPLC method.

Result and conclusion: DKV and DKO formulations were individually found to contain phytochemicals Gallic acid, Catechin, Berberine, Curcumin, Phenol and Benzoic acid. DKV-O treatment significantly reduced the paw volume and edema in Wistar rats stimulated through λ -carrageenan-treatment. Furthermore, DKV-O treatment significantly reduced the ear edema and enhanced biopsy weight, epidermal thickness, inflammatory lesions and influx of neutrophils stimulated by TPA-treatment in CD-1 mice. DKV alone ameliorated the LPS-stimulated release of Interleukin (IL)-6, IL-17A, IL-23, and Tumor Necrosis Factor-alpha cytokines in the THP-1 cells.

Taken together, DKV-O showed good efficacy in ameliorating acute systemic inflammation stimulated by effectors such as, λ -carrageenan and TPA in animal models. Hence, Divya-Kayakalp-Vati and Divya-Kayakalp-Oil co-treatment can be further explored as an anti-inflammatory treatment against dermal diseases like psoriasis and atopic dermatitis.

© 2021 Center for Food and Biomolecules, National Taiwan University. Production and hosting by Elsevier Taiwan LLC. This is an open access article under the CC BY license (<http://creativecommons.org/licenses/by/4.0/>).

1. Introduction

Psoriasis (Ps) is an innate and adaptive autoimmune disorder, which affects approximately 125 million people worldwide.¹ Ps is a

systemic inflammatory disease represented by the activation of the innate and adaptive immune systems and increased release of pro-inflammatory cytokines.²⁻⁶ Onset of the disease can cause long-term damage to multiple tissues and organs. Dermal Ps cause a variety of lesion phenotypes with Ps vulgaris being the common manifestation represented by the occurrence of scaly-red inflammatory plaques having enhanced hyperkeratosis, parakeratosis and reduced stratum granulosum, and pain with tenderness.^{7,8} Currently, there is no permanent cure available for Ps; and anti-inflammatory drugs are applied to quell the Ps flaring.

* Corresponding author. Drug Discovery and Development, Patanjali Research Institute, NH-58, Haridwar, 249405, Uttarakhand, India.

E-mail address: anurag@prft.co.in (A. Varshney).

Peer review under responsibility of The Center for Food and Biomolecules, National Taiwan University.

<https://doi.org/10.1016/j.jtcm.2021.09.003>

2225-4110/© 2021 Center for Food and Biomolecules, National Taiwan University. Production and hosting by Elsevier Taiwan LLC. This is an open access article under the CC BY license (<http://creativecommons.org/licenses/by/4.0/>).

| Abbreviations | | | |
|---------------|--|---------------|---|
| ANOVA | One-way Analysis of Variance | ICH | International Conference on Harmonization |
| CPCSEA | Committee for the Purpose of Control and Supervision of Experiments on Animals | IL-17A | Interleukin 17A |
| DEXA | Dexamethasone | IL-23 | Interleukin 23 |
| DKO | Divya-Kayakalp-Oil | IL-6 | Interleukin-6 |
| DKV | Divya-Kayakalp-Vati | INDO | Indomethacin |
| DKV-O | Divya-Kayakalp-Vati and Divya-Kayakalp-Oil co-treatment | LPS | lipopolysaccharide |
| ELISA | Enzyme-Linked Immunosorbent Assay | Na-CMC | Sodium-carboxymethyl cellulose |
| HPLC | High-Performance Liquid Chromatography | NC | Normal Control |
| IAEC | Institutional Animal Ethical Committee | PPIA | Peptidyl-prolyl cis-trans isomerase (PPIase) family |
| | | Ps | Psoriasis |
| | | RT-PCR | Real-time polymerase chain reaction |
| | | TNF- α | Tumor necrosis factor-alpha |
| | | TPA | 12-O-tetradecanoylphorbol 13-acetate |

Recently, herbal formulations have gained popularity as 'cosmeceuticals' as they don't produce any side effects.⁹ Divya-Kayakalp-Vati (DKV) and Divya-Kayakalp-Oil (DKO) have been formulated following method prescribed in ancient India Ayurvedic textbooks *Bhavprakash Nighantu* and *Ayurved Saar Sangraha* for treatment of dermal etiologies.^{10,11} DKV is composed of herbo-mineral components- Panvad (*Cassia tora* L.), Haldi (*Curcuma longa* L.), Daru Haldi (*Berberis aristata* DC.), Khair (*Acacia catechu* (L.F.) Willd.), Karanj (*Caesalpinia bonducella* (L.) Fleming), Neem (*Azadirachta indica* A. Juss.), Amla (*Emblica officinalis* Gaertn.), Manjishta (*Rubia cordifolia* L.), Giloy (*Tinospora cordifolia* (Willd.) Hook. f. & Thomson), Chirayata (*Swertia chirata* Buch. -Ham. (ex. Wall)), Kutaki (*Picrorhiza kurroa* Royale ex. Benth.), Dronpushapi (*Leucas cephalotes* (Roth) Spreng.), Satyanashi (*Argemone Mexicana* L.), and Rasmanikya (Red Sapphire ash) (Suppl. Table 1). Several of the phytochemicals have been reported to display anti-inflammatory activities.¹²⁻²⁰

Animal models for λ -carrageenan-stimulated Wistar rat paw edema and 12-O-tetradecanoylphorbol 13-acetate (TPA)-stimulated CD-1 mouse ear edema represents acute systemic inflammation that is similar to Ps-like morbidities through the production of cytokine, reactive oxygen and nitrogen species.^{21,22} λ -carrageenan-treatment induces a bi-phasic inflammatory response, with the early response represented by an increase in vascular permeability, and the later-stage represented through an induction of edema.²³ TPA treatment stimulates the development of dermal inflammation including IL17/IL23 axis, edema, epidermal hyperplasia and has been used for studying the Ps-like disease modulating efficacy of different medicines.²⁴⁻²⁸

In the present study, using λ -carrageenan-stimulated Wistar rats paw-edema and TPA-stimulated CD-1 mice ear edema models, we analyzed the anti-inflammatory activity for combined treatment of DKV (oral) and DKO (topical) (DKV-O) in ameliorating Ps-like inflammation. We investigated the anti-inflammatory mode of action for DKV through modulation of cytokine release in bacterial lipopolysaccharide (LPS)-stimulated phorbol 12-myristate-13-acetate (PMA)-transformed THP-1 cells. We summed up this study with a chemical analysis of DKV and DKO; and appended those findings with observed biological efficacies.

2. Materials and methods

2.1. Chemicals and reagents used

DKV and DKO were procured from Divya Pharmacy, Haridwar, India. RPMI-1640 cell culture media, FBS, antibiotic/antimycotic were purchased from Gibco, USA. Bacterial origin endotoxin LPS (O111:B4), λ -carrageenan, TPA, indomethacin (INDO), DEXA, and

standard compounds (>95% by HPLC) such as Gallic acid, Catechin, Berberine, Phenol, Benzoic acid, and Curcumin were purchased from Sigma-Aldrich (St. Louis, MO, USA). ELISA kits for TNF- α and IL-6 were purchased from BD Biosciences, USA. Primers for the study of IL-17A and IL-23 were purchased from Eurofins, India. HPLC grade acetonitrile, ortho-phosphoric acid, and diethylamine along with hematoxylin, potassium aluminum sulfate dodecahydrate, and mercury (II) oxide red were purchased from Merck India Pvt. Ltd, India. Eosin yellow and ferric chloride were purchased from HiMedia Laboratories, India. All other chemicals and reagents purchased were of the highest commercial grade.

2.2. Herbal sample preparation

20 g of DKV (Batch no. A-KKVE090) was pulverized and refluxed for 6 h at 88 °C in 300 mL of 70% ethanol. The solution was filtered and dried at 45 °C through evaporation under vacuum in a rotary film evaporator and stored until further use.

90 g of DKO (Batch no. BKKTO56) was mixed in 200 mL of 90% methanol and stirred for 1 h. The prepared solution was stored at -20 °C for 2 days. Following, separation of methanol from the frozen oil layer, it was removed manually. DKO was thawed, filtered, and dried using a Rotavapor. The dried DKO residue was resuspended in 90% methanol, and stored for further experiments.

2.3. High-performance-liquid-chromatography (HPLC) analysis

Chemical analysis of the DKV and DKO was performed using the binary HPLC system (Waters Corporation, Milford, MA, USA). Clear separations of DKV and DKO were done using an aqueous 0.1% ortho-phosphoric acid (v/v) (pH 2.5), diethylamine, and acetonitrile mobile-phase. A reversed-phase C18 analytical column of 4.60 \times 250 mm and 5 μ m particle sizes (Sunfire, Waters, USA) set at 35 °C was utilized for the analysis of Gallic acid, Phenol, Benzoic acid, and Catechin at 275 nm, and Berberine and Curcumin at 475 nm. A gradient-based program was used for the analysis and was repeated six times to confirm repeatability (relative standard deviation of <2.5%).

2.4. Experimental animals

Male Wistar rats (8–10 weeks) and CD-1 mice (6–8 weeks) were procured from Liveon Biolabs Pvt. Ltd, India, and from Hylasco Biotechnology Pvt. Ltd, India (licensed supplier for Charles River Laboratory), respectively. Animals were placed under a controlled environment with a relative humidity of 60–70% and 12:12 h light and dark cycle in a registered animal house of Patanjali Research Institute, India (1964/PO/RC/S/17/CPCSEA). They were fed a

standard pellet diet (Golden Feed, India) and sterile filtered water *ad libitum*. The study protocols were approved by the Institutional Animal Ethical Committee (IAEC) of Patanjali Research Institute vide approval numbers: PRIAS/LAF/IAEC-008 and PRIAS/LAF/IAEC-022 and implementation of the study were performed following the UK Animals (Scientific Procedures) Act, 1986 and EU Directive 2010/63/EU guidelines and regulations for animal experimentation.²⁹

2.5. Evaluation of in-Vivo anti-inflammatory and anti-Ps like efficacies

2.5.1. λ -carrageenan-stimulated paw-edema Wistar rat model

λ -carrageenan-stimulated paw-edema test was performed following the procedure mentioned earlier.³⁰ Briefly, male Wistar rats were randomly divided into eight animals per group for studying the parameter basal paw volume using the Plethysmometer (Ugo Basile, Italy). Inflammation was stimulated by the subcutaneous injection of 0.1 ml λ -carrageenan (1% solution prepared in normal saline) into the plantar side of the left hind paw. The paw was marked with ink at the level of the lateral malleolus and the volume was measured every hour up to 5 h. Animals were treated with 75 mg/kg of DKV (p.o.) (1000 mg/day human equivalent dose) + 40 μ l of DKO (T.A.), or, with 10 mg/kg of INDO (positive control) (p.o.), 1 h before the λ -carrageenan challenge. Vehicle control animals were treated with normal saline only. The onset of paw edema and anti-inflammatory activity (%) was calculated for each animal/h using the formula:

$$\left[\frac{\text{Mean paw edema of control animals} - \text{Mean paw edema of each test animals}}{\text{Mean paw edema of control animals}} \right] \times 100 \quad (1)$$

2.5.2. TPA-stimulated Ps-like skin inflammation CD-1 mouse model

The inhibitory efficacy of DKV-O in ameliorating Ps-like etiologies was studied in the TPA-stimulated CD-1 mouse model as defined earlier.³⁰ Briefly, 20 μ L of TPA solution prepared in acetone was applied topically on the right ear of CD-1 mouse at the concentration of 2.5 μ g/ear every second day till the 10th day. The left ear was reserved as vehicle control and treated with 20 μ L of acetone alone during the study duration. Ear thickness was measured every day using a digital Vernier caliper (Mitutoyo, Tokyo, Japan) and changes were determined by subtracting the ear thickness of day 0 from the respective time points. Based on treatments, animal groups were divided as normal control, vehicle control, TPA only (disease control), 0.2 mg/kg of DEXA (T.A.), and 150 mg/kg of DKV (p.o.) + 20 μ l of DKO (T.A.).

2.6. Histopathological analysis

CD-1 mice were humanely sacrificed on day 10, exactly 6 h after the last drug treatment. Ear biopsy samples were fixed in 10% formalin and embedded in paraffin. The paraffin-embedded samples were sectioned using microtome to 5 μ m thickness. The tissue samples were stained with hematoxylin and eosin dyes. Epidermal thickness (from the basal layer to stratum corneum) of the ear tissue sample was measured using Magcam DC5 microscopic camera (Magnus Opto Systems India Pvt. Ltd., Noida, India) equipped with a stage micrometer and was analyzed using

MagVision image analysis software (Magnus Opto Systems India Pvt. Ltd., Noida, India). Distribution of the lesions was recorded as focal, multifocal, and diffused. Severity of the observed lesions and neutrophil influx was recorded as NAD= No abnormality detected, 1 = minimal (<1%), 2 = mild (1–25%), 3 = moderate (26–50%), 4 = moderately severe/marked (51–75%), and 5 = severe (76–100%). Other parameters such as the extent of lesions, severity of hyperkeratosis, number and size of pustules, epidermal hyperplasia (measured in the interfollicular epidermis), the severity of inflammation in the dermis and soft tissue, and any other lesion(s) were also recorded and scored.

2.7. Cell culture of human monocyte (THP-1) cells

THP-1 cells were obtained from the National Centre for Cell Science, Pune, India. THP-1 cells were cultured in RPMI-1640 media, supplemented with 10% heat-inactivated fetal bovine serum (FBS), 1% penicillin-streptomycin (100 U/mL), 1% sodium pyruvate (1 mM), and 1% L-glutamine (4 mM); and were maintained in a humid and sterile environment at 37 °C and 5% CO₂.

2.8. Real-time Polymerase Chain Reaction (RT-PCR) assay

THP-1 cells were seeded in 24 wells culture plates at the concentration of 5 x 10⁵ cells/well and stimulated with 20 ng/ml of PMA overnight. The next day, old media containing PMA was replaced and the transformed THP-1 cells were washed with lukewarm sterile PBS. THP-1 cells were replenished with fresh culture media and incubated for one day for stabilization. PMA-

transformed THP-1 cells were pre-exposed to varying concentrations of DKV for a period of 1 h. After incubation time was over, the THP-1 cells were stimulated with LPS (1 μ g/ml) for 24 h following completion of exposure time, cell culture media was separated and stored at -80 °C till further use. Cells were washed and total RNA was isolated using RNeasy mini kit (Qiagen, USA) including an on-column DNase digestion with the RNase-free DNase set (Qiagen, USA) and quantified using Nabi microdigital spectrophotometer. cDNA synthesis was performed using the Verso cDNA synthesis kit (Thermo Scientific™) and stored at -80 °C until further use.

RT-PCR was conducted using qTOWER3G RT-PCR machine (Analytik Jena, Germany). Primer sequences selected for the study were: IL-17A: F-5' TCACCCGATTGCCACCAT-3'/R-5' GAGTTAGTCCGAAATGAGGCTG-3'; IL-23: F- 5'-GCTTCAAAATCCTTCG-CAG-3'/R-5'GATCTGAGTGCCATCCTTGG-3'; Peptidyl-prolyl *cis*-trans isomerase (PPIA) (Housekeeping gene): F-5'-CCCACCGTCTTCGACATT-3'/R-5'-GGACCCGATGCITTAGGATGA-3'; Amplification of cDNA was carried out by mixing cDNA with PowerUp™ SYBR Green Master Mix (Applied Biosystems) at the ratio of 1:10 and values were normalized against the endogenous control gene (PPIA). RT-PCR cycling conditions were set at initial denaturation: 94 °C for 5 min, followed by 45 cycles of denaturation 94 °C for 30 s; annealing: 60 °C for 30 s; extension: 72 °C for 45 s and final extension: 72 °C for 5 min. All the experiments were performed in triplicates and the quantification was performed by calculating the 2^{- $\Delta\Delta$ Ct}.

2.9. Enzyme-linked immunosorbent assay

Stored cell culture media from the LPS stimulated THP-1 cells, treated with DKV was used for the analysis of TNF- α and IL-6 using ELISA. Assays were performed following the manufacturer's protocol and absorbance was recorded at 450 nm using the Envision microplate reader (PerkinElmer, USA).

2.10. Statistical analysis

The data are expressed as Mean \pm Standard Error of Mean (SEM) for each group. Statistical analysis was performed using GraphPad Prism version 7.03 (GraphPad Software, Inc., San Diego, CA, USA). A one-way analysis of variance (ANOVA) followed by Dunnett's multiple comparisons post-hoc test was used to calculate the statistical significance in-ear edema, biopsy weights, epidermal thickness, lesion scores, cytokine(s), and myeloperoxidase analysis. All analyses and comparisons were evaluated at a 95% level of confidence ($p < 0.05$).

3. Results

3.1. Phytochemical Profiling of DKV and DKO components

High-performance liquid chromatography (HPLC) analysis of the DKV and DKO using parameters of retention time (RT) and

individual phytochemical standard curve showed DKV samples to be composed of 9.05 $\mu\text{g}/\text{mg}$ Gallic acid (RT 6.3 min); 23.19 $\mu\text{g}/\text{mg}$ Catechin (RT 11.4 min); 0.02 $\mu\text{g}/\text{mg}$ Berberine (RT 17.6 min); and 0.0012 $\mu\text{g}/\text{mg}$ Curcumin (RT 30.5 min) (Suppl. Table 2, Suppl. Fig. 1A and 1B). DKO samples were composed of 0.0029 $\mu\text{g}/\text{mg}$ Gallic acid (RT 6.3 min); 0.0003 $\mu\text{g}/\text{mg}$ Catechin (RT 11.4 min); 0.0056 $\mu\text{g}/\text{mg}$ Berberine (RT 17.6 min); 0.002 $\mu\text{g}/\text{mg}$ Phenol (RT 17.9 min); Benzoic acid (RT 19.6 min); and Curcumin (RT 30.5 min) (Suppl. Table 2, Suppl. Fig. 1C and 1D).

3.2. Anti-inflammatory effects of DKV-O in λ -carrageenan stimulated wistar rats

Plantar injection of Wistar rats with λ -carrageenan (0.1 ml of 1% solution in normal saline) stimulated an increase in the absolute paw volume and edema up to 5 h (Fig. 1A and B). Treatment of the λ -carrageenan stimulated rats with 75 mg/kg of DKV (p.o.) + 40 μl /paw of DKO (T.A.) significantly reduced the absolute paw-volume and edema (Fig. 1A and B). Treatment of the λ -carrageenan stimulated rats with positive control INDO (10 mg/kg) (p.o.) significantly reduced both the paw volume and edema compared to the vehicle control animal (Fig. 1A and B).

3.3. Anti-Ps-like-inflammation activity of DKV-O in TPA-Stimulated CD-1 mice

Stimulation of the CD-1 mice right ear with TPA (2.5 $\mu\text{g}/\text{ear}$)

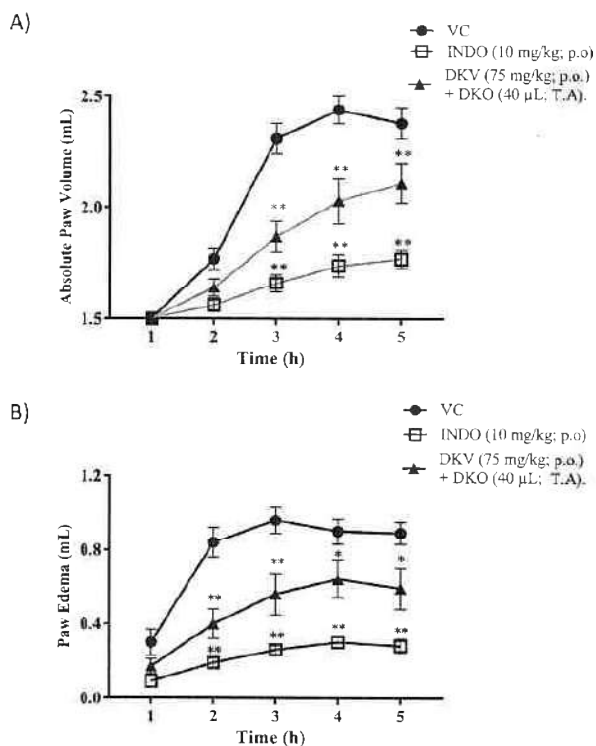


Fig. 1. Effect of DKV-O treatment on λ -Carrageenan Stimulated Paw-Edema Rat Model. Treatment of λ -carrageenan stimulated Wistar rats with 75 mg/kg DKV (p.o.) and 40 μL DKO (T.A.), or with INDO (10 mg/kg) (p.o.) significantly reduced their A) absolute paw volume, and B) paw edema indicating anti-inflammatory efficacy. Statistical analysis of the treatments was performed using a one-way analysis of variance (ANOVA) followed by Newman-Keuls multiple comparison test. p-values * <0.05 , ** <0.01 (DC versus DKV-O treatment; DC versus INDO treated animals).

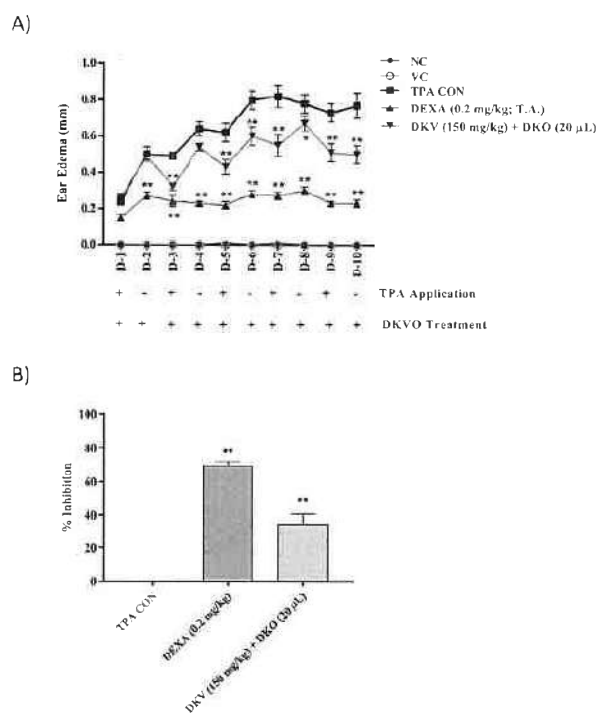


Fig. 2. Effect of DKV-O Treatment on TPA-Stimulated Ear Edema in Mice. A) Treatment of the TPA-stimulated Ps-like inflamed ear (TPA CON) with DKV-O, or with DEXA (T.A.) significantly reduced ear edema. Vehicle control (VC) did not induce any change. B) Both, DKV-O, and DEXA induced significantly high inhibition in the ear stimulated with TPA alone (TPA CON). Statistical analysis was performed using a two-way analysis of variance (ANOVA) followed by Newman-Keuls multiple comparison test. P-values # <0.01 (Normal Control (NC) versus TPA CON); * <0.05 , ** <0.01 (TPA CON versus DKV-O co-treatment; TPA CON versus DEXA).

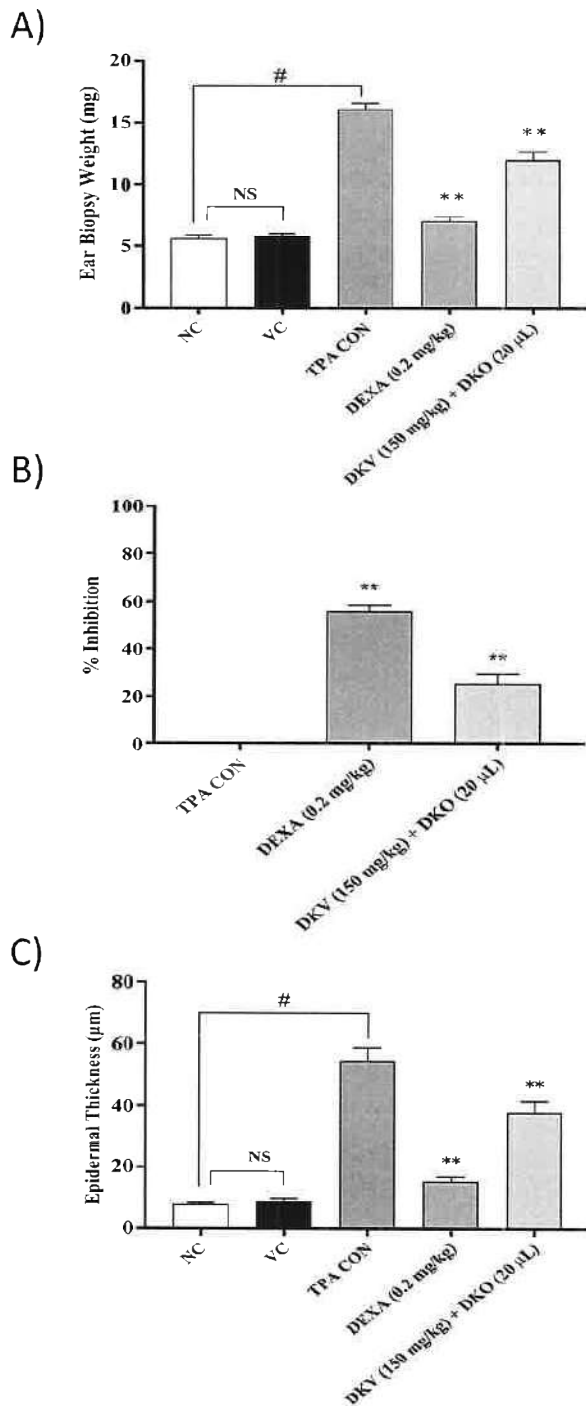


Fig. 3. Histopathological Analysis of DKV-O Treatment on TPA-Stimulated Mice Ear Biopsy. A) Treatment of the TPA-stimulated Ps-like inflamed ear with DKV-O, or with DEXA (T.A.) significantly decreased the ear biopsy weight, B) Percent inhibition of TPA (TPA CON) stimulated Ps-like ear biopsy weight by DKV-O, or DEXA were found significantly high, and C) Treatment of the Ps-like inflamed ear with DKV-O, or DEXA significantly reduced the ear epidermal thickness. Vehicle Control (VC) alone did not cause any modification in the ear biopsy-weight or epidermal thickness. Statistical analysis was performed using the One-way analysis of variance (ANOVA) method followed by Dunnett's multiple comparison *t*-test. P-values #<0.01 (Normal Control

induced Ps-like inflammation through an increase in ear edema, biopsy weight, and epidermal thickness (Figs. 2 and 3). Treatment of the stimulated CD-1 mice with 150 mg/kg DKV (p.o.) and 20 µL DKO (T.A.) significantly (*p*-value <0.01) reduced the ear edema with an inhibition percentage of $34.2 \pm 19.5\%$ (Fig. 2A and B).

Treatment of TPA-stimulated ear with DKV-O also significantly (*p*-value <0.01) reduced the elevated ear biopsy-weight with an inhibition percentage of $25.3 \pm 12.3\%$ and the epidermal layer thickness (Fig. 3A–C). DEXA treatment of the stimulated ear also significantly (*p*-value <0.01) reduced the TPA-stimulated ear edema, biopsy weight and epidermal thickness (Figs. 2 and 3).

3.4. Effect of DKV-O treatment on ear tissue histopathology in CD-1 mice

TPA-stimulation of the right ear in CD-1 mice induced epidermal hyperkeratosis, hyperplasticity, pustule formation, and neutrophils influx in the dermis region (Fig. 4A–C). Treatment of the TPA-stimulated mice with DKV-O, or DEXA significantly (*p*-value <0.01) reduced the incidences of inflammatory lesion formation in the epithelial region, pustule formation, and an influx of the neutrophils (Fig. 4D and E).

Quantification of the observed histopathological effects through lesion score analysis showed DKV-O treatment to significantly (*p*-value <0.01) reduce the TPA-induced inflammatory lesions with a percent inhibition of $37.05 \pm 10.52\%$ (*p*-value <0.01) (Fig. 5A and B). Individually, DKV-O treatment ameliorated TPA-induced hyperkeratosis, and hyperplasia (*p*-value <0.05) in the epidermis, and neutrophil influx (*p*-value <0.05) in the dermal region of the stimulated ear of mice (Fig. 5C, D and 5F). No effect was observed on TPA-induced pustule formation from the DKV-O treatment (Fig. 5E). DEXA treatment also showed high anti-inflammatory efficacy through inhibition for all histopathological parameters observed having a percent inhibition of $84.47 \pm 4.83\%$ (*p*-value <0.01) (Fig. 5A).

3.5. In-vitro anti-inflammatory activity of DKV

LPS-stimulation of the PMA-transformed THP-1 cells showed an upregulation of pro-inflammatory cytokines- IL-17A, IL-23, TNF- α , and IL-6 (Figs. 6 and 7). Pre-treatment of the THP-1 cells with varying concentrations of DKV showed a significant (*p*-value <0.01) reduction in the mRNA expression of IL-17A and IL-23 cytokines following LPS-stimulation (Fig. 6A and B). Similarly, DKV pre-treatment also reduced the LPS-stimulated release of TNF- α and IL-6 cytokines in the THP-1 cells (Fig. 2A and B). Statistically significant (*p*-value <0.01) reduction of TNF- α release from the LPS-stimulated THP-1 cells was only detectable at the DKV treatment concentrations of 3 mg/ml (47%) and 5 mg/ml (15%) (Fig. 7A). Similarly, a statistically significant (*p*-value <0.01) reduction in IL-6 cytokine release from the THP-1 cells was observed following pre-treatment with DKV at the concentrations 0.3–5 mg/ml (Fig. 7B).

Based on the obtained results, DKV-O treatment showed anti-inflammatory activity in Ps-like systemic inflammation through modulation of neutrophils influx, pro-inflammatory cytokine release and lesion formation.

4. Discussion

Skin is the outermost physical protective barrier of the body

(NC) versus TPA CON); * <0.05, ** <0.01 (TPA CON versus DKV and DKO co-treatment; TPA CON versus DEXA).

providing protection and maintaining physiological homeostasis. Initiation of Ps-like inflammation is represented by infiltration of the innate immune cells such as macrophages, neutrophils, TH17 and dendritic cells in the dermal region of the affected site. This is accompanied by the production of cytokines and chemokines, and proliferation of the keratinocytes leading to thickening of the epidermal region.³¹

Herbal formulations play an important role in the treatment of human diseases without any known side effects.³² Their therapeutic properties have been attributed to the presence of a wide variety of phytochemicals acting together in synergy and through a multicentric approach towards diseases.^{32,33} Herbal components of DKV such as *Phyllanthus emblica* L., *Curcuma longa* L. contain phytochemicals that have anti-inflammatory and antioxidant activities

against skin inflammation.^{34–36} In our study, phytochemicals such as Gallic acid, Catechin, Berberine, Curcumin, Phenol, and Benzoic acid were found to be present in both DKV and DKO. Gallic acid can modulate the NADPH-oxidase activity in polymorphonuclear leukocytes associated with induction of oxidative stress through reactive oxygen species generation.³⁷ Curcumin has been well-known for ages to have antioxidant and anti-inflammatory activity.³⁸ Similarly, Catechin, Berberine, and Curcumin have been found to have anti-inflammatory and antioxidant abilities through modulation of inflammatory cells and mediators.^{39–46}

Macrophages play an important role in the pathogenicity of Ps through the release of pro-inflammatory cytokines and modulating the IL-23/IL-17 pathway.⁶ During the onset of Ps lesions, macrophages are present in large quantities and involved in the release of

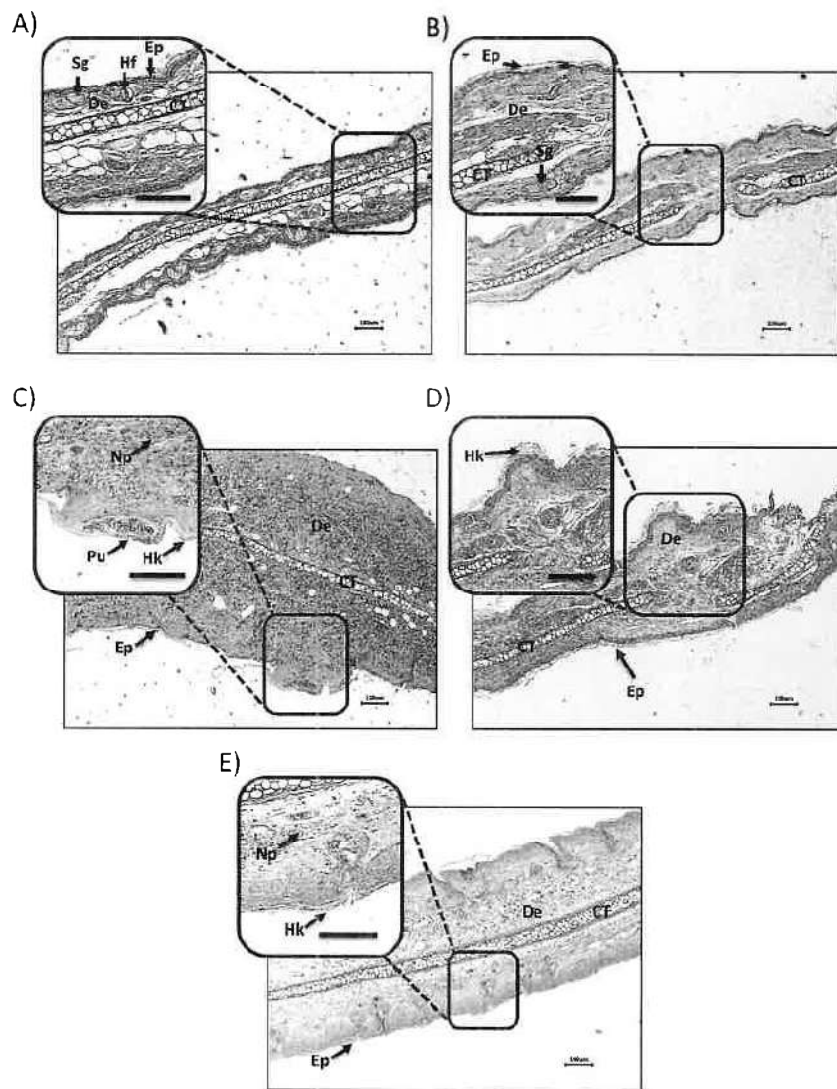


Fig. 4. Histopathological Analysis of DKV-O Treatment on TPA-Stimulated Ear Ps in Mice. Histopathological analysis of the CD-1 mouse-ear dermal region showed A) Normal epidermis (Ep), dermis (De), sebaceous gland (Sg), cartilage (CT) and hair follicle (Hf) in the normal control animals; B) Normal Ep, De, Sg, CT in the vehicle control animals; C) Induction of hyperkeratosis (Hk) and hyperplastic Ep, pustule formation (Pu), and presence of neutrophils (Np) in dermis (De) region of TPA stimulated animal; D) Reduced hyperkeratosis (Hk) and hyperplastic Ep, and absence of neutrophils in the dermis (De) region of DEXA treated ear of TPA-stimulated animal and E) Reduced Hk and hyperplastic Ep, the reduced presence of neutrophils (Np) in the dermis (De) region of the DKV-O treated ear of TPA-stimulated animal.

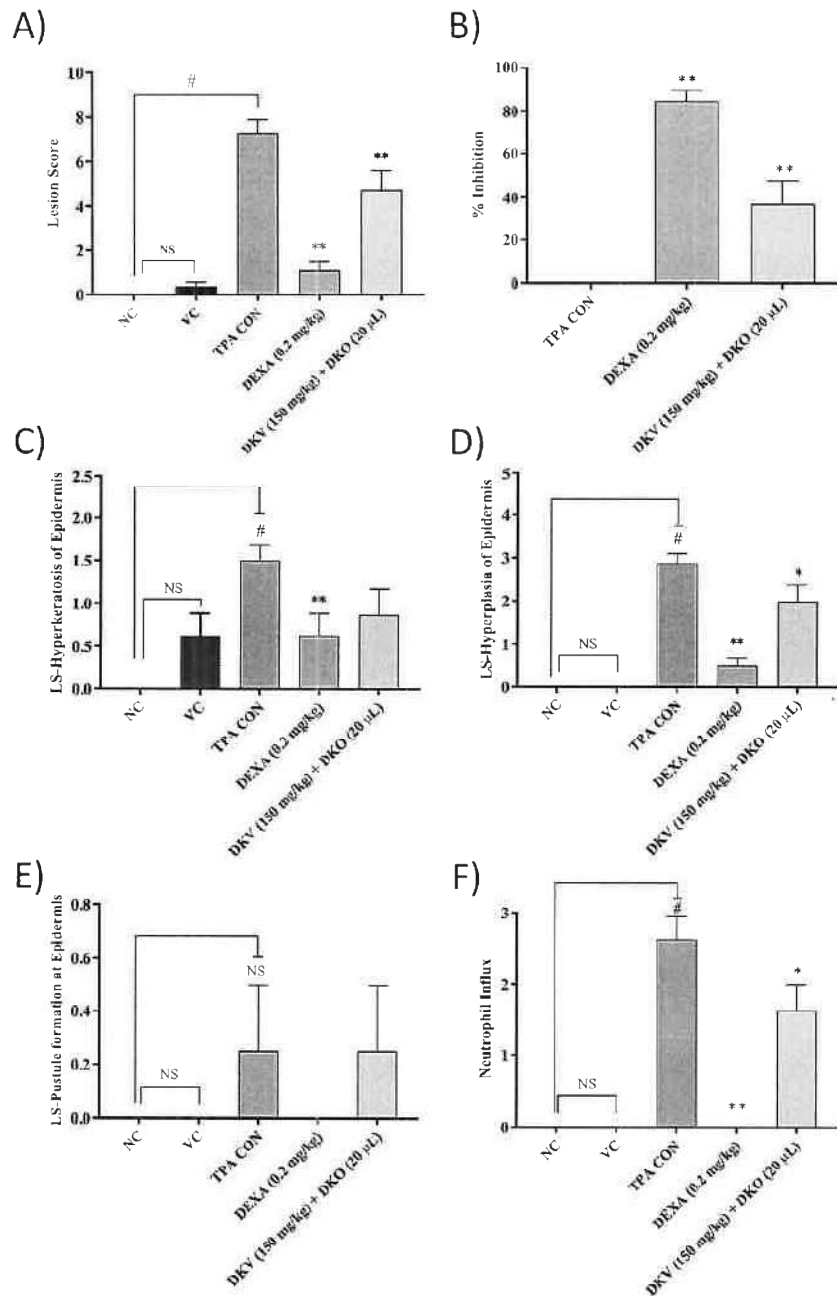


Fig. 5. Inflammatory Lesion Scores in the DKV-O Treated and TPA-Stimulated Mice Ear. Treatment of the Ps-like inflamed ear with DKV-O, or with DEXA (T.A.) showed a reduction in TPA (TPA CON) stimulated- A) Total lesion score; B) Percentage inhibition of total lesion score in TPA CON versus DKV-O, or DEXA treated animals; C) Hyperkeratosis of the epidermis; D) Hyperplasia of the epidermis; E) Pustule formation in epidermis region; F) Neutrophil influx in dermis region. For statistical analysis, a one-way analysis of variance (ANOVA) followed by Dunnett's multiple comparison t-test was applied. P-value # <0.01 (Normal Control (NC) versus TPA CON). * <0.05, ** <0.01 (TPA CON versus DKV and DKO treatments; TPA CON versus DEXA treatment).

pro-inflammatory cytokines.⁶ In our study, LPS-stimulation of the PMA-transformed THP-1 cells showed an increase in the levels of IL-17A, IL-23, TNF- α and IL-6 that was ameliorated by DKV treatment. These soluble mediators are considered biomarkers of Ps disease as they process the inter- and intracellular signaling between the innate cells and affected dermal keratinocytes.^{47,48} [L-17

and IL-23 are produced by the innate and adaptive immune cells, and keratinocytes lead to the formation of epidermal hyperplasia. In our study, pro-inflammatory macrophage activity modulation by DKV indicated the anti-inflammatory contribution of the phytochemicals present in the herbal formulations.^{49,50}

In-vivo efficacy of the DKV-O was observed in systemic acute

A. Balkrishna, S. Sakat, K. Joshi et al.

Journal of Traditional and Complementary Medicine xxx (xxxx) xxx

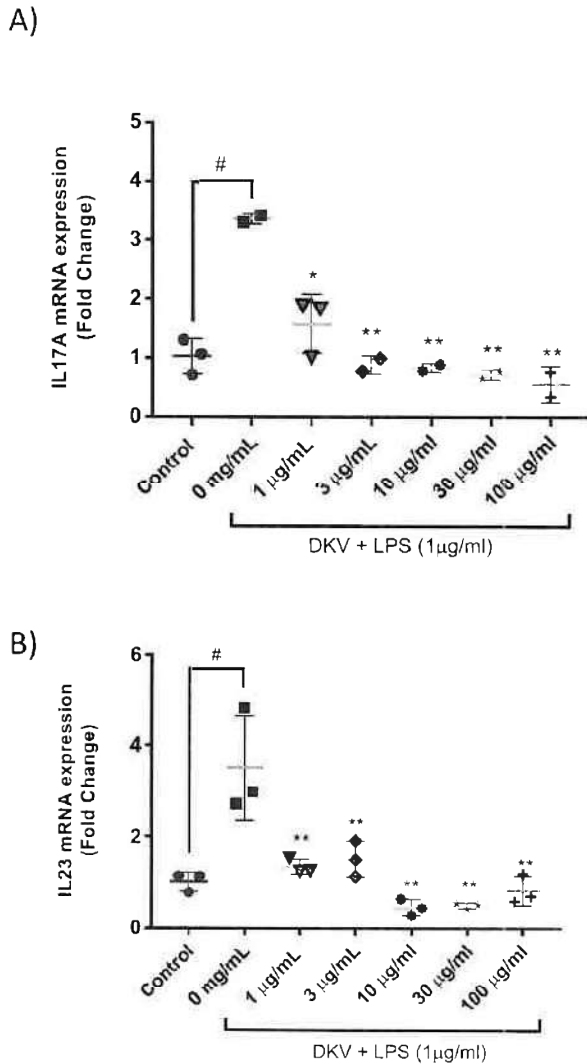


Fig. 6. IL-17A and IL-23 mRNA Expression Changes in LPS-Stimulated THP-1 cells following DKV treatment: LPS (1 µg/ml) stimulation of the PMA-transformed THP-1 cells showed an increase in the mRNA expression levels of A) IL-17a, and B) IL-23 cytokine and their amelioration following treatment with DKV. Results are represented as Mean \pm SEM (n = 3). For statistical analysis, one-way ANOVA followed by Dunnett's post-hoc test was performed. p-value # <0.001 (Control versus LPS only); p-value ** <0.01 (LPS only versus DKV treatments).

inflammation models of λ -carrageenan stimulated Wistar rat paw edema and TPA-stimulated ear edema. The biphasic response of λ -carrageenan in stimulating rat paw-edema and TPA-modulated ear edema is mediated through the release of several pro-inflammatory soluble mediators, such as cytokine, chemokines and growth factors.^{22,51} In our study, the DKV-O combination efficiently reduced the λ -carrageenan and TPA stimulator-induced edema, hyperkeratosis, hyperplasia in the epidermal region, and inflammatory cell influx in the dermal region in the treated animals. TPA is known to induce Ps-like inflammation through the influx of inflammatory cells and modulation of IL-17 cytokine that eventually leads to keratinocyte growth promotion.²⁶ Similarly, carrageenan is known to trigger the release of pro-inflammatory

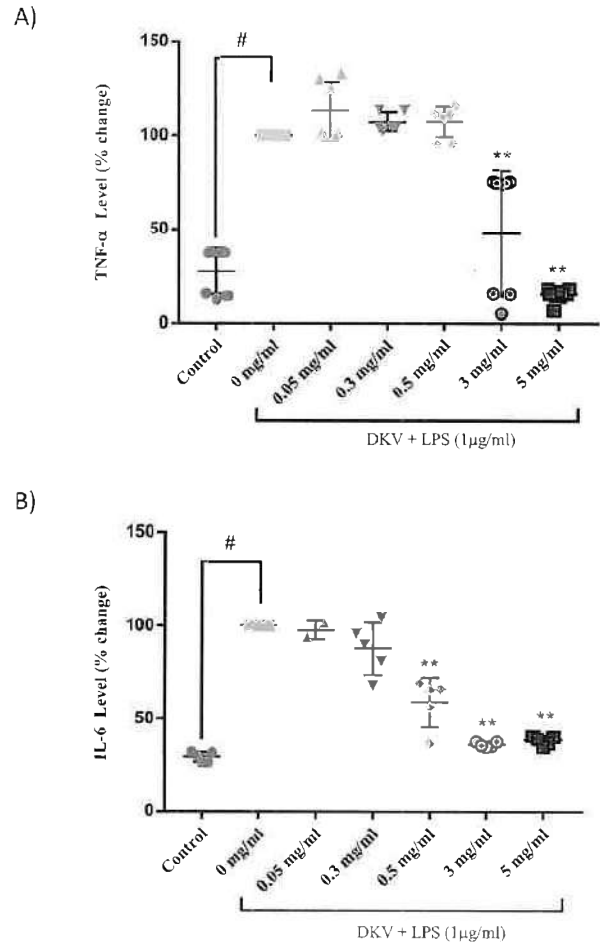


Fig. 7. Release of TNF- α and IL-6 in LPS-Stimulated THP-1 cells following DKV treatment: LPS (1 µg/ml) stimulation of the PMA-transformed THP-1 cells leading to the release of A) TNF- α , and B) IL-6 cytokines and their amelioration following treatment with DKV. Inset showing percent inhibition. Results are represented as Mean \pm SEM (n = 3). For statistical analysis, one-way ANOVA followed by Dunnett's post-hoc test was performed. p-value # <0.001 (Control versus LPS only); p-value ** <0.01 (LPS only versus DKV treatments).

cytokines including IL-6, TNF- α and IL-17 inducing the inflammatory cascade.⁵² Hence, our observed anti-inflammatory activity of DKV-O can be correlated to the observed reduction in the inflammatory cell influx and development of inflammatory epidermal lesions.

Earlier studies on individual plant components used in the preparation of DKV and DKO such as *Cassia tora* L., *Berberis aristata* DC., *Curcuma longa* L., *Caesalpinia bonducella* (L.) Fleming, *Acacia catechu* (L.F.) Willd. and *Azadirachta indica* A. Juss. have shown amelioration of Ps-like inflammation.^{53–62} Phytochemicals such as Berberine, and Curcumin present in DKV-O have individually shown efficacy to reduce carrageenan and TPA stimulated inflammation in animal models through the modulation of the cytokines, nitric oxides, cyclooxygenase and prostaglandins.^{40,63–66} Furthermore, both Berberine and Curcumin have been observed to modulated the IL-17 and IL-23 expression in the immune cells.^{67–69}

5. Conclusion

Taken together, DKV showed good efficacy in the modulation of pro-inflammatory cytokines in LPS-stimulated macrophages. In the λ -carrageenan and TPA-stimulated acute inflammation animal models, DKV-O treatment reduced paw and ear edema, epidermal thickness, and Ps-like inflammatory lesions. Phytochemicals present in the DKV and DKO play an important role through a possible multicentric synergistic effect in the modulation of Ps-like inflammatory response that needs further exploration. Hence, combined treatment of Divya-Kayakalp-Vati and Divya-Kayakalp-Oil can be explored further for the treatment of inflammatory dermal diseases like Psoriasis.

Author contributions

AB provided a broad direction for the study, identified the test formulation, generated resources, and gave final approval for the manuscript. SS conducted the *in-vivo* study, analyzed the data, and performed report writing. KJ assisted in animal handling and in performing *in-vivo* studies. RS and KB performed *in-vitro* experiments and RT-PCR analysis. SV and PN conducted analytical experiments. KB performed data curing and wrote the manuscript. AV supervised overall research project planning, generated resources, and reviewed and finally approved the manuscript.

Funding

This research work was funded internally by Patanjali Research Foundation Trust, Haridwar, India.

Declaration of competing interest

The test article was sourced from Divya Pharmacy, Haridwar, Uttarakhand, India. Acharya Balkrishna is an honorary trustee in Divya Yog Mandir Trust, Haridwar, India. In addition, he holds an honorary managerial position in Patanjali Ayurved Ltd., Haridwar, India. Besides, providing the test article, Divya Pharmacy was not involved in any aspect of this study. All other authors have no conflict of interest to declare.

Acknowledgments

We acknowledge initial support from Professor Paran Gowda and Dr. V.K. Sharma, University of Patanjali, Haridwar, India. We would also like to appreciate Dr. Ravikant Ranjan for *in-vitro* experiments, and Dr. Chandrasekhar Joshi for chemical analysis support, Mr. Bhanu Pratap, Mr. Pushpendra Singh, Mr. Vipin Kumar, and Mr. Sonit Kumar for the excellent animal handling and maintenance. We extend our gratitude to Mr. Brij Kishore, Mr. Tarun Rajput, Mr. Gagan Kumar, and Mr. Lalit Mohan for their swift administrative support. This presented work has been conducted using research funds from Patanjali Research Foundation Trust, Haridwar, India.

Appendix A. Supplementary data

Supplementary data to this article can be found online at <https://doi.org/10.1016/j.jtcme.2021.09.003>.

References

1. Takeshita J, Grewal S, Langan SM, et al. Psoriasis and comorbid diseases: Epidemiology. *J Am Acad Dermatol*. 2017;76(3):377–390.
2. Greb JE, Goldminz AM, Elder JT, et al. Psoriasis. *Nat Rev Dis Primers*. 2016;2:16082.
3. Wagner EF, Schonhaler HB, Guinea-Viniegra J, Tschachler E. Psoriasis: what we have learned from mouse models. *Nat Rev Rheumatol*. 2010;6(12):704–714.
4. Liu YJ. IPC: professional type 1 interferon-producing cells and plasmacytoid dendritic cell precursors. *Annu Rev Immunol*. 2005;23:275–306.
5. Richardson SK, Gelfand JM. Update on the natural history and systemic treatment of psoriasis. *Adv Dermatol*. 2008;24:171–196.
6. Wang Y, Edelmayer R, Wetter J, et al. Monocytes/Macrophages play a pathogenic role in IL-23 mediated psoriasis-like skin inflammation. *Sci Rep*. 2019;9(1):5310.
7. Griffiths CE, Barker JN. Pathogenesis and clinical features of psoriasis. *Lancet*. 2007;370(9583):263–271.
8. Gudjonsson JE, Elder JT. *Fitzpatrick's Dermatology in General Medicine*. seventh ed. seventh ed. New York: McGraw-Hill; 2008.
9. Choi CM, Berson DS. *Cosmeceuticals, Semin Cutan Med Surg*. 2006;25(3):163–168.
10. Sen GD. *Bhaisajya Ratnavali*. 43 ed. Varanasi, India: Chaukhamba Surbharati Prakashan; 2013.
11. Vaidya R. *Ayurveda Sar Sangrah*. 18 ed. Allahabad, India: Shri Baidyanath Ayurveda Bhawan Ltd.; 2009.
12. Afi. *Ayurvedic Formulary of India*. 2003. Part 1 2 ed. Delhi.
13. Upi. *The Unani Pharmacopia of India* Ministry of AYUSH. Government of India 2007.
14. Trikamji J. *Charaka Samhita of Agnivesha, Chikitsa Sthana; Abhaya Amalaki Rasayana Pada*. 1. 1. Varanasi: Chowkhamba Prakashan; 2007:378–379.
15. *Ayurveda_sara_sangraha*. In: *Vaidhya Ramnarayan Sharma*, 5 ed. Kolkata: Shri Baidhnath Ayurveda Bhawan Ltd.; 1964.
16. Bhāvaprakāśa-nighantu. By: bhāvamiśra. In: (NIIMH) NIoIMH, ed. *Bhāvaprakāśa-nighantu India*: NIIMH; 16th Century A.D.
17. Vijayalakshmi A, Madhira G. Anti-psoriatic activity of flavonoids from Cassia tora leaves using the rat ultraviolet B ray photodermatitis model. *Revista Brasileira de Farmacognosia*. 2014;24(3):322–329.
18. Sarafian G, Afshar M, Mansouri P, Asgarpanah J, Raoufinejad K, Rajabi M. Topical turmeric microemulgel in the management of plaque psoriasis: A clinical evaluation. *Iran J Pharm Res (IJPR)*. 2015;14(3):865–876.
19. Muruganatham N, Basavaraj KH, Dhanabal SP, Praveen TK, Shamasundar NM, Rao KS. Screening of Caesalpinia bonduc leaves for antipsoriatic activity. *J Ethnopharmacol*. 2011;133(2):897–901.
20. Patel NK, Khan MS, Bhutani KK. Investigations on Leucas cephalotes (Roth.) Spreng, for inhibition of LPS-induced pro-inflammatory mediators in murine macrophages and in rat model. *EXCLI J*. 2015;14:508–516.
21. Amdekar S, Roy P, Singh V, Kumar A, Singh R, Sharma P. Anti-inflammatory activity of lactobacillus on carrageenan-induced paw edema in male wistar rats. *Int J Inflamm*. 2012;2012, 752015.
22. Kalyan Kumar G, Dhamotharan R, Kulkarni NM, Mahat MY, Gunasekaran J, Ashfaq M. Embelin reduces cutaneous TNF-alpha level and ameliorates skin edema in acute and chronic model of skin inflammation in mice. *Eur J Pharmacol*. 2011;562(1-3):63–69.
23. Patil KR, Patil CR. Anti-inflammatory activity of bartogenic acid containing fraction of fruits of Barringtonia racemosa Roxb. in acute and chronic animal models of inflammation. *J Tradit Complement Med*. 2017;7(1):86–93.
24. Hiranahalli Bhaskarmurthy D, Evan Prince S. Effect of Baricitinib on TPA-induced psoriasis like skin inflammation. *Life Sci*. 2021 Aug 15;279, 119655. <https://doi.org/10.1016/j.lfs.2021.119655>. Epub 2021 May 24. PMID: 34043988.
25. Kulkarni NM, Muley MM, Jaji MS, et al. Topical atorvastatin ameliorates 12-O-tetradecanoylphorbol-13-acetate induced skin inflammation by reducing cutaneous cytokine levels and NF-kappaB activation. *Arch Pharm Res (Seoul)*. 2015;38(6):1238–1247.
26. Madsen M, Hansen PR, Nielsen LB, et al. Effect of 12-O-tetradecanoylphorbol-13-acetate-induced psoriasis-like skin lesions on systemic inflammation and atherosclerosis in hypercholesterolaemic apoE-deficient mice. *BMC Dermatol*. 2016;16(1):9.
27. Ma N, Tang Q, Wu WT, et al. Three constituents of moringa oleifera seeds regulate expression of Th17-relevant cytokines and ameliorate TPA-induced psoriasis-like skin lesions in mice. *Molecules*. 2018;23(12).
28. Yang G, Li S, Yang Y, et al. Nobiletin and 5-Hydroxy-6,7,8,3',4'-pentamethoxyflavone ameliorate 12-O-Tetradecanoylphorbol-13-acetate-Induced psoriasis-like mouse skin lesions by regulating the expression of ki-67 and proliferating cell nuclear antigen and the differentiation of CD4(+) T cells through mitogen-activated protein kinase signaling pathways. *J Agric Food Chem*. 2018;66(31):8299–8306.
29. Kilkenny C, Browne WJ, Cuthill IC, Emerson M, Altman DG. Improving bioscience research reporting: the ARRIVE guidelines for reporting animal research. *PLoS Biol*. 2010;8(6), e1000412.
30. Balkrishna A, Sakat SS, Joshi K, et al. Cytokines driven anti-inflammatory and anti-psoriasis like efficacies of nutraceutical sea buckthorn (Hippophae rhamnoides) oil. *Front Pharmacol*. 2019;10:1186.
31. Kabashima K, Honda T, Ginhoux F, Egawa G. The immunological anatomy of the skin. *Nat Rev Immunol*. 2019;19(1):19–30.
32. Parasuraman S, Thing GS, Dhanaraj SA. Polyherbal formulation: Concept of ayurveda. *Pharmacogn Rev*. 2014;8(16):73–80.
33. Borokini TI, Omotayo FO. Phytochemical and ethnobotanical study of some selected medicinal plants from Nigeria. *J Med Plants Res*. 2012;6(7):1106–1118.
34. Saxena A, Kaur K, Hegde S, Kalekhan FM, Baliga MS, Fayad R. Dietary agents

- and phytochemicals in the prevention and treatment of experimental ulcerative colitis. *J Tradit Complement Med*. 2014;4(4):203–217.
35. Duangjai A, Goh BH, Lee LH, Saokaew S. Relaxant effects of *Azadirachta indica* A. Juss var. *siamensis* Valetton flower extract on isolated rat ileum contractions and the mechanisms of action. *J Tradit Complement Med*. 2018;8(4):515–520.
 36. Chaikul P, Kanlayavattanakul M, Somkumnerd J, Lourith N. *Phyllanthus emblica* L. (amla) branch: a safe and effective ingredient against skin aging. *J Tradit Complement Med*. 2021;11(5):390–399.
 37. Kroes BH, van den Berg AJ, Quarles van Ufford HC, van Dijk H, Labadie RP. Anti-inflammatory activity of gallic acid. *Planta Med*. 1992;58(6):499–504.
 38. Fadus MC, Lau C, Bikhchandani J, Lynch HT. Curcumin: an age-old anti-inflammatory and anti-neoplastic agent. *Journal of Traditional and Complementary Medicine*. 2017;7(3):339–346.
 39. Ohishi T, Goto S, Monira P, Isemura M, Nakamura Y. Anti-inflammatory action of green tea. *Antinflamm Antiallergy Agents Med Chem*. 2016;15(2):74–90.
 40. Kuo CL, Chi CW, Liu TY. The anti-inflammatory potential of berberine in vitro and in vivo. *Canc Lett*. 2004;203(2):127–137.
 41. Farhood B, Mortezaee K, Goradel NH, et al. Curcumin as an anti-inflammatory agent: implications to radiotherapy and chemotherapy. *J Cell Physiol*. 2019;234(5):5728–5740.
 42. Zhang J, Li X, Wei J, et al. Gallic acid inhibits the expression of keratin 16 and keratin 17 through Nrf 2 in psoriasis-like skin disease. *Int Immunopharm*. 2018;65:84–95.
 43. Nimisha Rizvi DA, Fatima Z, Neema, Kaur CD. Antipsoriatic and anti-inflammatory studies of *Berberis aristata* extract Loaded nanovesicular gels. *Phrog Mag*. 2017;13(Suppl 3):S587–S594.
 44. Sun J, Zhao Y, Hu J. Curcumin inhibits imiquimod-induced psoriasis-like inflammation by inhibiting IL-1 beta and IL-6 production in mice. *PLoS One*. 2013;8(6):e67078.
 45. Kim-Park WK, Allam ES, Palasuk J, Kowolik M, Park KK, Windsor LJ. Green tea catechin inhibits the activity and neutrophil release of Matrix Metalloproteinase-9. *Journal of Traditional and Complementary Medicine*. 2016;6(4):343–346.
 46. Amalraj A, Pius A, Gopi S, Gopi S. Biological activities of curcuminoids, other biomolecules from turmeric and their derivatives – a review. *Journal of Traditional and Complementary Medicine*. 2017;7(2):205–233.
 47. Jiang M, Fang H, Shao S, et al. Keratinocyte exosomes activate neutrophils and enhance skin inflammation in psoriasis. *FASEB J*. 2019. f201900642R.
 48. Hawkes JE, Yan BY, Chan TC, Krueger JG. Discovery of the IL-23/IL-17 signaling pathway and the treatment of psoriasis. *J Immunol*. 2018;201(6):1605–1613.
 49. Huang L, Hou L, Xue H, Wang C. Gallic acid inhibits inflammatory response of RAW264.7 macrophages by blocking the activation of TLR4/NF-kappaB induced by LPS. *Xi Bao Yu Fen Zi Mian Yi Xue Za Zhi*. 2016;32(12):1610–1614.
 50. Cheng AW, Tan X, Sun JY, Gu CM, Liu C, Guo X. Catechin attenuates TNF-alpha induced inflammatory response via AMPK-SIRT1 pathway in 3T3-L1 adipocytes. *PLoS One*. 2019;14(5):e0217090.
 51. Afsar T, Khan MR, Razak S, Ullah S, Mirza B. Antipyretic, anti-inflammatory and analgesic activity of *Acacia hydaspica* R. Parker and its phytochemical analysis. *BMC Compl Alternative Med*. 2015;15:136.
 52. Amdekar S, Singh V. Studies on anti-inflammatory and analgesic properties of *Lactobacillus rhamnosus* in experimental animal models. *J Compl Integr Med*. 2016;13(2):145–150.
 53. Antonisamy P, Dhanasekaran M, Kim HR, Jo SG, Agastian P, Kwon KB. Anti-inflammatory and analgesic activity of ononitol monohydrate isolated from *Cassia tora* L. in animal models. *Saudi J Biol Sci*. 2017;24(8):1933–1938.
 54. Kumar R, Gupta YK, Singh S. Anti-inflammatory and anti-granuloma activity of *Berberis aristata* DC. in experimental models of inflammation. *Indian J Pharmacol*. 2016;48(2):155–161.
 55. Rachmawati H, Safitri D, Pradana AT, Adnyana IK. TPGS-stabilized curcumin nanoparticles Exhibit superior effect on carrageenan-induced inflammation in wistar rat. *Pharmaceutics*. 2016;8(3).
 56. Shukla S, Mehta A. In vivo anti-inflammatory, analgesic and antipyretic activities of a medicinal plant, *Caesalpinia bonducella* F. *Pak J Pharm Sci*. 2015;28(4 Suppl):1517–1521.
 57. Umar MI, Asmawi MZ, Sadikun A, et al. Multi-constituent synergism is responsible for anti-inflammatory effect of *Azadirachta indica* leaf extract. *Pharm Biol*. 2014;52(11):1411–1422.
 58. Singhal M, Kansara N. *Cassia tora* Linn Cream inhibits ultraviolet-B-induced psoriasis in rats. *ISRN Dermatol*. 2012;2012:346510.
 59. Nardo VD, Gianfaldoni S, Teherney G, et al. Use of curcumin in psoriasis. *Open Access Maced J Med Sci*. 2018;6(1):218–220.
 60. Reddy S, Aggarwal BB. Curcumin is a non-competitive and selective inhibitor of phosphorylase kinase. *FEBS Lett*. 1994;341(1):19–22.
 61. Heng MC, Song MK, Harker J, Heng MK. Drug-induced suppression of phosphorylase kinase activity correlates with resolution of psoriasis as assessed by clinical, histological and immunohistochemical parameters. *Br J Dermatol*. 2000;143(5):937–949.
 62. Sunil MA, Sunitha VS, Radhakrishnan EK, Jyothis M. Immunomodulatory activities of *Acacia catechu*, a traditional thirst quencher of South India. *J Ayurveda Integr Med*. 2019;10(3):185–191.
 63. Kim S, Kim Y, Kim JE, Cho KH, Chung JH. Berberine inhibits TPA-induced MMP-9 and IL-6 expression in normal human keratinocytes. *Phytomedicine*. 2008;15(5):340–347.
 64. Baradaran S, Hajizadeh Moghaddam A, Khanjani Jelodar S, Moradi-Kor N. Protective effects of curcumin and its nano-phytosome on carrageenan-induced inflammation in mice model: behavioral and biochemical responses. *J Inflamm Res*. 2020;13:45–51.
 65. Lee SY, Cho SS, Li Y, Bae CS, Park KM, Park DH. Anti-inflammatory effect of *Curcuma longa* and *allium hookeri* Co-treatment via NF-kappaB and COX-2 pathways. *Sci Rep*. 2020;10(1):5718.
 66. Kakar SS, Roy D. Curcumin inhibits TPA induced expression of c-fos, c-jun and c-myc proto-oncogenes messenger RNAs in mouse skin. *Canc Lett*. 1994;87(1):85–89.
 67. Zhao G, Liu Y, Yi X, et al. Curcumin inhibiting Th17 cell differentiation by regulating the metabotropic glutamate receptor-4 expression on dendritic cells. *Int Immunopharm*. 2017;46:80–86.
 68. Guo Z, Sun H, Zhang H, Zhang Y. Anti-hypertensive and renoprotective effects of berberine in spontaneously hypertensive rats. *Clin Exp Hypertens*. 2015;37(4):332–339.
 69. Li YH, Xiao HT, Hu DD, et al. Berberine ameliorates chronic relapsing dextran sulfate sodium-induced colitis in C57BL/6 mice by suppressing Th17 responses. *Pharmacol Res*. 2016;110:227–239.

Withanone from *Withania somnifera* Attenuates SARS-CoV-2 RBD and Host ACE2 Interactions to Rescue Spike Protein Induced Pathologies in Humanized Zebrafish Model

AQ1

5

AQ2

AQ3

This article was published in the following Dove Press journal:
Drug Design, Development and Therapy

Acharya Balkrishna^{1,2}
Subarna Pokhrel¹
Hoshiyar Singh¹
Monali Joshi¹
Vallabh Prakash Mulay¹
Swati Halder¹
Anurag Varshney^{1,2}

¹Drug Discovery and Development Division, Patanjali Research Institute, Haridwar, 249405, Uttarakhand, India; ²Department of Allied and Applied Sciences, University of Patanjali, Haridwar, 249405, Uttarakhand, India



Correspondence: Anurag Varshney; Swati Halder
Drug Discovery and Development Division, Patanjali Research Institute, Roorkee-Haridwar Road, Haridwar, 249405, Uttarakhand, India
Tel +91-1334-244107, Ext. 7458;
+91-1334-244107, Ext. 7481
Fax +91-1334-244805
Email anurag@prft.co.in;
swati.halder@prft.in

Purpose: SARS-CoV-2 engages human ACE2 through its spike (S) protein receptor binding domain (RBD) to enter the host cell. Recent computational studies have reported that withanone and withaferin A, phytochemicals found in *Withania somnifera*, target viral main protease (M^{Pro}) and host transmembrane TMPRSS2, and glucose related protein 78 (GRP78), respectively, implicating their potential as viral entry inhibitors. Absence of specific treatment against SARS-CoV-2 infection has encouraged exploration of phytochemicals as potential antivirals.

AQ4

10

AQ5

Aim: This study aimed at *in silico* exploration, along with *in vitro* and *in vivo* validation of antiviral efficacy of the phytochemical withanone.

15

Methods: Through molecular docking, molecular dynamic (MD) simulation and electrostatic energy calculation the plausible biochemical interactions between withanone and the ACE2-RBD complex were investigated. These *in silico* observations were biochemically validated by ELISA-based assays. Withanone-enriched extract from *W. somnifera* was tested for its ability to ameliorate clinically relevant pathological features, modelled in humanized zebrafish through SARS-CoV-2 recombinant spike (S) protein induction.

20

Results: Withanone bound efficiently at the interacting interface of the ACE2-RBD complex and destabilized it energetically. The electrostatic component of binding free energies of the complex was significantly decreased. The two intrachain salt bridge interactions (K31-E35) and the interchain long-range ion-pair (K31-E484), at the ACE2-RBD interface were completely abolished by withanone, in the 50 ns simulation. *In vitro* binding assay experimentally validated that withanone efficiently inhibited (IC₅₀=0.33 ng/mL) the interaction between ACE2 and RBD, in a dose-dependent manner. A withanone-enriched extract, without any co-extracted withaferin A, was prepared from *W. somnifera* leaves. This enriched extract was found to be efficient in ameliorating human-like pathological responses induced in humanized zebrafish by SARS-CoV-2 recombinant spike (S) protein.

25

30

Conclusion: In conclusion, this study provided experimental validation for computational insight into the potential of withanone as a potent inhibitor SARS-CoV-2 coronavirus entry into the host cells.

35

Keywords: ACE2-RBD complex, *Withania somnifera*, withanone, docking and MD simulation, ELISA, SARS-CoV-2 S-protein, humanized zebrafish model

AQ6

Introduction

40

The COVID-19 nightmare began with the report of a pneumonia case of unknown cause in Wuhan, China on December 31, 2019¹ and soon after, in March 2020, WHO declared the disease a pandemic. According to the weekly epidemiological update, until December 27, 2020, the total number of COVID-19 cases crossed 79.2 million with number of deaths being more than 1.7 million since the beginning of the pandemic (<https://www.who.int/publications/m/item/weekly-epidemiological-update-29-december-2020>).

AQ7

SARS-CoV-2, the causative coronavirus responsible for COVID-19 outbreak, is a sister clade of SARS-CoV, that caused severe acute respiratory syndrome (SARS) in 2002.² Resembling SARS-CoV, this virus also exploits ACE-2 receptors to invade host cell, thus, making the high level ACE-2 expressing alveolar type II epithelial cells the primary target.³ Without encouraging outcomes from clinical trials on repurposed drugs,⁴ there is an unmet requirement for newer therapeutics which can specifically act against SARS-CoV-2.

55

During viral infection, entry of the virus into the host cell is a critical step that can be exploited for antiviral

therapy.⁵ Therefore, receptor binding domain (RBD) has been an attractive target for the researchers to abrogate coronavirus infection. Reports suggested that certain human antibodies recognized RBD on the S1 domain of SARS-CoV and inhibited the viral infection by blocking its attachment to ACE2.^{6,7} Three possible mechanisms, namely, targeting the ACE2 receptor, RBD of S protein, and the interaction between ACE2 and RBD have been schematically depicted in Figure 1 through which SARS-CoV-2 entry/infusion can be abrogated. Prime focus is on targeting RBD or ACE2 and less thought is given toward disrupting the RBD-ACE2. Nevertheless, a contingency approach to prevent viral entry in case the first window of opportunity (before RBD gets to interact with ACE2) is missed will be quite valuable. In fact, the observations reported in this study identify a potential candidate for this contingent approach. We are referring to *Withania somnifera* (L.) Dunal (Solanaceae), commonly known as Ashwagandha. It is one of the most valued medicinal plants of the traditional Indian systems of medicines, and has been used in more than 100 Ayurvedic formulations. It is therapeutically equivalent to ginseng, concordant with the

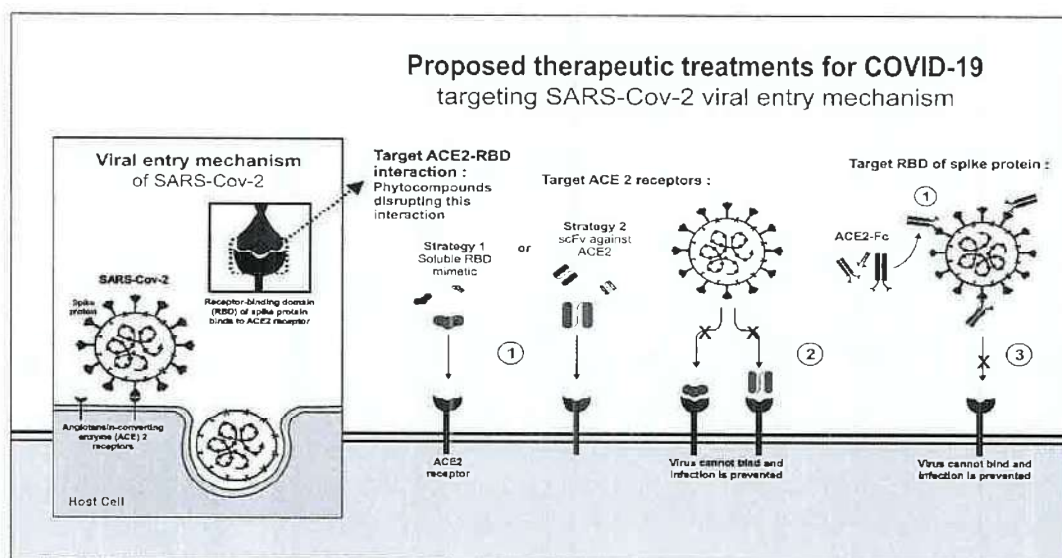
65

70

75

AQ8

80



AQ10

Figure 1 Proposed mechanisms to block the entry of SARS-CoV-2 into host cells.

AQ11

Notes: The mechanism behind SARS-CoV-2 entry into the host cell is schematically represented. Three proposed models are depicted where COVID-19 infection can be abrogated by blocking the interaction of RBD of spike (S) protein and ACE-2. In one of the approaches, ACE2-RBD interaction can be destabilized by small molecules. In the second approach, ACE2 can be blocked with RBD mimetics or single-chain antibody fragment (scFv) against ACE2. In the third approach, RBD of SARS-CoV-2 S protein can be blocked using the ACE-2 extracellular domain. An Fc domain fused to ACE-2 would facilitate prolonged circulation of the biologic (ACE2-Fc). The observations made in this study support the strategy to block or weaken the interaction between RBD and ACE2 by using phytocompounds of natural origin.

observation that medicinal plants with similar bioactivity exhibit phylogenetic clustering.^{8,9} *W. somnifera* is used to treat genital infection by herpes simplex virus among African tribes.¹⁰ It also exhibits anti-influenza properties.¹¹

85 In our preliminary study in March 2020, we observed that withanone binds at the center of the ACE2-RBD interface.¹² A recent computational study has predicted that withanone can also interact with the main protease (M^{Pro}) of SARS-CoV-2, which is responsible for cleaving host transmembrane protease serine 2 (TMPRSS2) required for viral entry

90 into host cell.¹³ In a follow-up study, the same group has shown that withanone and withaferin A can interact with TMPRSS2 and block viral entry into the host cell. Withanone was also shown to downregulate TMPRSS2

95 transcription.¹⁴ Likewise, withaferin A, the second major phytochemical with reported cytotoxicity against cancer cells that co-extracts with withanone from *W. somnifera* leaves, can bind to GRP78 as observed in another docking study.¹⁵ GRP78 was reported to be involved in the MERS

100 infection. Blocking ACE2 with soluble antibodies or RBD of viral S protein with soluble ACE2 are identified as considerable options.^{16–18} Synthetic nanobodies/sybodies to block RBD of SARS-CoV-2 spike (S) protein are reported recently in a preprint.¹⁹ However, all these strategies target either the host cell or viral factors independently. Inhibition of specific host-pathogen interaction will be more preferable, but no report exists to show that this option has been explored yet. So, given the reported antiviral efficacy of *W. somnifera*, we evaluated whether withanone can disrupt host-viral interaction.

The objective of the present study was to evaluate the potential of withanone, the major phytochemical present in *W. somnifera* as an inhibitor of host-pathogen specific interaction between host ACE2 and viral RBD of SARS-

115 CoV-2 S-protein and its efficacy in ameliorating S-protein-induced inflammatory pathologies in a humanized zebrafish model of the disease. We employed computational methods to evaluate the effects of withanone on interaction between viral S-protein RBD and host ACE2 receptor, the rationale being the aforementioned phytochemical could be a disruptor of RBD-ACE2 interaction, a presumption stemming from virtual screening of hundreds of its likes. Through an ELISA-based interaction study, we observed that in the presence of commercially procured withanone, interaction between RBD and ACE2 was significantly reduced. In this regard, it is pertinent to mention that co-extraction of withaferin A with withanone from leaves of *W. somnifera* is unavoidable.²⁰ Withaferin A is cytotoxic

120

AQ12

125

and this property has been explored for treating different types of cancers.²¹ Human equivalent dose (HED) and maximum recommended starting dose (MRSD) for withaferin A have been worked out.²² But one would like to avoid its presence altogether, if possible, particularly when a severe viral infection that leaves the immune system vulnerable is being dealt with. Keeping this, and our subsequent plan for experimental validation of antiviral efficacy of withanone, in perspective, we devised a method to prepare *W. somnifera* leaf extracts enriched only in withanone (WiNeWsE). Furthermore, the antiviral activity of WiNeWsE was checked in a humanized zebrafish (HZF) model of SARS-CoV-2, which was established according to earlier reports.^{23–25} WiNeWsE treatment was found to be effective in ameliorating the characteristic behavioral and phenotypic manifestations associated with SARS-CoV-2 disease induction in zebrafish.

130

135

140

145

Materials and Methods

Computational Study

Structures

We screened 200 different phytochemicals by *in silico* methods. The strategy was to find phytochemicals that bind at the RBD-ACE2 complex interface, and perturb their interactions. In this regard, the phytochemical from *W. somnifera* showed promising results. Nine structurally similar withanolides, namely, 27-hydroxy withanone, 17-hydroxy withaferin A, 17-hydroxy-27-deoxy withaferin A, withaferin A, withanolide D, 27-hydroxy withanolide B, withanolide A, withanone, and 27-deoxy-withaferin A were identified through reverse-phase HPLC in *W. somnifera* root extracts.²⁶ Unpublished data from our laboratory also showed significant concentration of withanolide A, withanolide B, withaferin A, and withanone in 15–20 days old *W. somnifera* sapling. We studied these compounds in detail after preliminary screening. The 3D structures of all the phytochemicals were retrieved from PubChem database (<https://pubchem.ncbi.nlm.nih.gov>).

150

155

160

165

Molecular Docking

The latest structure of SARS-CoV-2 RBD complexed with ACE2 receptor (PDB ID: 6M17, 2.9 Å resolution) was retrieved from protein data bank (<http://rcsb.org>). Clean protease domain of Chain B (ACE2) and chain E (RBD) were selected after editing on PyMol.³⁷ Energy minimization was performed by 100 steps of steepest descent, followed by 500 steps of conjugate gradient using UCSF Chimera-1.13.1²⁷ after adding hydrogens. The

170

175 stereochemical quality of the energy minimized structure was checked using VERIFY3D, ERRAT, PROCHECK, and RAMPAGE (for Ramachandran plot).^{28–31}

The SDF files of all the ligands downloaded from the PubChem database were converted into PDB files using Open Babel 2.4.1.³² Hydrogens were added using UCSF Chimera-1.13.1 (Pettersen et al), and docked against ACE2-RBD complex.²⁷ There is still a challenge in identifying a putative binding site of a ligand on a protein. There are many reports on detecting protein ligand binding sites, but their accuracies only go up to 50–80%.³³ Focused docking is supposed to be better than blind docking in this regard.³⁴ The more accurate method is the molecular-docking binding-site finding (MolSite) method proposed by Fukunishi and Nakamura,³³ which showed 80–99% accuracy in predicting ligand binding sites. In the current study, the ligand binding site in the ACE2-RBD complex was determined by the MolSite method.³³ Briefly, the ACE2-RBD complex was mapped by five-grid center (including the protein interface) of grid size 30×30×30, and was subjected to AutoDock Vina calculations using the PyRx Virtual Screening Tool³⁵ with default parameters. The grid was centered on Ca of five different amino acids (x=166.539, y=105.678, z=256.879; x=178.643, y=126.269, z=220.744; x=165.097, y=119.940, z=247.957; x=150.015, y=122.092, z=213.204; x=150.015, y=122.092, z=213.204; x=130.190, y=136.848, z=221.901); thus, the method helped to map the whole complex surface. The best binding pose was supposed to be the pose with the lowest energy, obtained after comparison of the five independent docking runs, and was aligned with the receptor for the ligand-receptor interaction analysis using Maestro-12.4 (Schrödinger Release 2020–2: Maestro, Schrödinger, LLC, New York, NY, USA). Discovery Studio 2017 R2 Client³⁶ and PyMol³⁷ were used to generate the graphics.

Molecular Dynamics (MD) Simulation

The ligand-ACE2-RBD complex obtained after molecular docking was subjected to MD simulation. The simulation systems for ACE2-RBD complex without or with withanone was prepared using the VMD software.³⁸ Ligand parameterization was done with CHARMM-GUI web interface (<http://www.charmm-gui.org>)³⁹ using CHARMM general force field.³⁹ MD simulation was performed with CHARMM36 force field using the NAMD package.⁴⁰ The protein complex without or with withanone was solvated with TIP3P water molecules 105 Å

from the protein. The systems were ionized and neutralized with 145 mM of NaCl. The systems contained 69,051 and 69,003 water molecules in the protein complex without and with withanone, respectively. NPT ensemble was used with periodic boundary conditions. Pressure was fixed at 1.01325 bar and the temperature at 310 K. The particle-mesh Ewald method was used to evaluate the Coulomb interactions with a grid size of 1 Å. A 2 fs of time step was used in all MD simulations. Initially, water was equilibrated for 0.5 ns at 310 K after fixing the protein and ligand, and energy minimization of 1000 steps. One thousand steps of energy minimization of the whole system were performed, and further equilibration for 5 ns at 310 K, after releasing the protein and ligand, was done. The production run was of 50 ns. The trajectory data were saved at every 50 ps to analyze the change in the dynamics of the ACE2-RBD binding interface. The results for flexibility were analyzed by plotting the RMSD values of backbone atoms (C, Ca, N) against the 1000 conformations, and per residue RMSF was calculated for Ca atoms. For electrostatics calculation, trajectory clustering was performed by UCSF Chimera-1.13.1²⁷ using a step size of one with default parameters.

Salt Bridge Analysis

We considered ion-pair as a salt bridge when side-chain charged group centroids and at least one pair of side-chain nitrogen and oxygen atoms is within 3.2 Å distance, or a longer-range ion pair (up to 7 Å), and was analyzed using VMD.³⁸ Electrostatic free energy upon salt bridge formation was calculated in initial and final trajectories complexed with the withanone. All the computations were performed according to the protocol of Hendsch and Tidor,⁴¹ with slight modifications. Briefly, it was calculated relative to a mutation of its salt-bridging side-chains to their hydrophobic isosteres. They are identical with the charged residue side-chains, with the exception that their partial atomic charges were set to zero. The protonation states of all the charged residues were assigned at pH 7.4 using the ProteinPrepare module in PlayMolecule (<https://www.playmolecule.org>). Continuum electrostatic calculations were performed with the DelPhi v8.4.3.⁴² The PARSE partial atomic charges and atomic radii were used.⁴³ The solvent probe radius used was 1.4 Å. The dielectric constants of the protein and the solvent were 4.0 and 80.0 respectively, and the ionic strength was 0.145 M. The Poisson-Boltzmann equation was solved using the iterative finite difference method, initially

- mapping the molecule on a 3D grid with a grid size of 165 and scale of one, and then focusing with a grid size of 65 and scale of four. DelPhi gives the energy values in units of kT, where k is the Boltzmann constant and T is absolute temperature, and the values were multiplied by 0.5922 to obtain the results in kcal/mol at room temperature (25°C).
- 275 Computation of Electrostatic Component of Binding Free Energy of the ACE2-RBD Complex**
- Quantification of electrostatic interactions is important to study protein-protein interactions in biomolecular systems. We solved the Poisson-Boltzmann equation (PBE) in the implicit solvent model to study the interaction between the receptor ACE2 and the viral RBD.⁴⁴ The electrostatic component of $\Delta\Delta G$, $\Delta\Delta G_{el}$ can be quantified by solving the Poisson-Boltzmann equation (PBE) with the assumption that there are no conformational changes upon binding.
- 285 We used DelPhi v8.4.3⁴² to calculate the electrostatic component of the binding free energies, and in the trajectories obtained after clustering. The term, $\Delta\Delta G_{el}$ can be obtained by subtracting the grid energy of the binding partners from that of the complex (DelPhi manual). Grid size of 165, scale of one and ionic strength of 0.145 M were used for the calculation. Protein and solvent dielectric constants were four and 80, respectively.**
- In vitro Validation of the Inhibitory Effect of Withanone on ACE2-RBD Interaction**
- 295 The effect of withanone on ACE2-RBD interaction was evaluated using the SARS-CoV-2 inhibitor screening kit (ACROBiosystems, Newark, DE, USA) according to the manufacturer's protocol. Briefly, wells of the ELISA plate were coated with recombinant truncated SARS-CoV-2 spike protein expressing only RBD. Subsequently, biotinylated human ACE2 protein was allowed to bind to the immobilized RBD in the ELISA wells in the presence of 47 pg/mL (10 pM)–4.7 µg/mL (10 µM) and absence of commercially procured withanone (Sigma, USA).**
- 300 Efficiency of ACE2 binding to RBD was detected through HRP conjugated streptavidin by measuring the absorbance at 450 nm in EnVision microplate reader (Perkin Elmer Inc, Waltham, MA, USA). The absorbance was used to calculate percent inhibition of ACE2-RBD interaction, relative to the reaction mix without withanone. Reaction mix treated with a known inhibitor (provided with the kit) served as a positive control. The observation was represented as a dose-response curve and IC_{50} calculated using an option built into the GraphPad Prism software.**
- Preparation of Withanone Rich Extract from Leaves of *W. somnifera* (WiNeWsE) and its Compositional Analysis** 315
- Fresh leaves of *W. somnifera* were collected from the medicinal herbal garden of the Patanjali Research Institute, Haridwar, India, washed with water and pulverized. Then, 100 g of this pulverized material was extracted in 1:10 volume of solvent (methanol:water in 80:20 ratio) and agitated three times at 70°C in reflux conditions. Each extraction lasted for two hours. Extracted layers were filtered, pooled, and concentrated to yield 2.7 g of powdered hydro-methanolic extract. For compositional fingerprinting of the leaf extract through HPTLC, 500 mg of the sample was mixed in 5 mL of methanol:water (80:20), sonicated for 20 min and centrifuged. Chromatographic separation was done on silica gel 60 F254 plates in a mobile phase containing toluene, ethylacetate and formic acid in a 5:5:1 ratio. The plates were scanned at 230 nm and derivatized in an anisaldehyde sulfuric acid reagent. Withanone content in the leaf extract was quantified from the regression equation $234.190 * X + 3.043$ using a linearity range from 400–1200 ng having a coefficient of correlation as 0.9997. Limits of detection per spot were 0.30 and 0.90 ng, respectively. Rf value used for detection was 0.40.
- The compositional quantification of this extract was done through high performance liquid chromatography (HPLC) (Waters Corporation, USA) equipped with binary pump (1525), PDAD (2998) and autosampler (2707). Withanone standard was purchased from Natural Remedies Pvt. Ltd (Bangalore, India) and dissolved in methanol to get the appropriate concentration. Next, 0.25 g of *W. somnifera* leaf extract was diluted with 10 mL methanol: water (75:25), sonicated for 30 min and filtered using a 0.45 µm nylon filter before injecting 10 µL of this into the column. Separation was achieved using a Shodex C18-4E (5 µm, 4.6*250 mm) column and elution was carried out at a flow rate of 1.5 mL/min using a defined gradient program of mobile phases A (1 mM KH_2PO_4 , 0.05% H_3PO_4) and B (acetonitrile). Ten microliters of test solution was injected. Column temperature was maintained at 27°C. Wavelength was set at 227 nm for analysis.
- In vivo Preclinical Assessment of the Antiviral Activity of WiNeWsE in Humanized Zebrafish Model of SARS-CoV-2** 355
- Cell Line and Chemicals**
- Human alveolar epithelial cell line (A549) was procured from ATCC certified repository at the National Centre of Cell Science (NCCS), Pune, India. SARS-CoV-2 spike (S) 360

AQ14

Table 1 Zebrafish Selection Criteria and Housing Conditions

| Gender | Male (♂) and Female (♀) |
|-------------------------------|-----------------------------|
| Age | 1 year |
| Body weight | 0.5 g |
| Body length | 25–30 mm |
| Number of fish/group/endpoint | 24 |
| Number of fish per clutch | 12 |
| Tank capacity | 16 L |
| Ambient water temperature | 27±1 °C |
| Light-dark cycle | 14 h light, 10 h dark |
| Feed frequency | 5 mg/g body weight/once/day |

Notes: The above inclusion conditions were considered while selecting the fish for the study. The housing conditions of the selected subjects are also mentioned above.

AQ13

recombinant protein was obtained from Bioss Antibodies (Woburn, MA, USA). H&E stain and PBS were purchased from Sigma Aldrich (St Louis, MO, USA).

Zebrafish Husbandry, Animal Selection, and Group Setting

Zebrafish experiments were in line with the standards of Institutional Animal Ethics Committee (IAEC) in compliance with the guidelines of the Committee for the Purpose of Control and Supervision of Experiments (CPCSEA), India. All zebrafish experiments were conducted according to IAEC approved protocols (approval number 223/Go062062/IAEC). The fish were housed under 14 h light and 10 h dark cycle in 16 L tanks with water temperature maintained at 27±1 °C and were fed with 5 mg of commercial feed (TetraBit, Blacksburg, VA, USA) per gram body weight once per day. One-year-old, 25–30 mm long zebrafish of both the genders, weighing 0.5 g were selected for the study. Selection criteria and housing arrangements are summarized in Table 1. The study subjects were divided into seven groups, each containing 24 fish, maintained in two clutches with 12 each. Different

groups along with the corresponding treatments administered are provided in Table 2.

Xenotransplant Model Establishment

A549 cells, cultured in DMEM with 10% FBS and 1% penicillin-streptomycin at 37 °C, were passaged continuously three times before using the third passage for transplantation. The 1×10² cells in PBS were injected intramuscularly at the junction of the trunk and the caudal region, along the midline to seed them at the posterior lobe of the swim bladder. Postinjection the fish were transferred to their respective clutches and were observed for a period of seven days. Cytology of the swim bladder was studied on day seven to confirm adherence of A549 cells and establishment of humanized zebrafish (HZF) model. A group of 72 HZF without injection of S protein was maintained as the xenotransplant model control (XMC) and studied alongside the normal control (NC). The NC group contained 72 ordinary zebrafish selected as per the criteria mentioned in Table 1.

Induction of Pathological Milieu by SARS-CoV-2 S-protein

Seven days postxenotransplantation, the fish were given intramuscular injections at the site of xenotransplant, with 2.8 µL of 1 ng/µL SARS-CoV-2 recombinant S-protein in PBS using a Hamilton syringe. The fish were anesthetized using gradual cooling of the water to 12 °C. Anesthetization was confirmed through reduced operculum movement and lack of response to touch by the caudal fin. Postrecombinant S-protein injection the zebrafish undergoes a series of immune responses. During this period the fish is housed at 27±1 °C to aid the physiological changes in immunity.

Dosing and Screening

Translational human equivalent doses (HED) were optimized to be 1000X less than the human dose by body weight. Human

Table 2 Experimental Groups, Group Size, and Administered Treatments

| Name of the Group | Group Size ^a | Administered Treatment |
|--------------------------|-------------------------|--|
| NC | 72 | Zebrafish with no xenotransplantation and no SARS-CoV-2 induction |
| XMC | 72 | Zebrafish transplanted with human alveolar epithelial A549 cells on the posterior lobe of swim bladder |
| DC | 72 | XMC injected with SARS-CoV-2 recombinant S-protein |
| 1X ₁ Dexa-HED | 72 | DC administered with 0.08 µg/kg body weight of dexamethasone through feed |
| 0.2X ₁ HED | 72 | DC administered with 6 µg/kg body weight of WiNeWsE through feed |
| 1X ₂ HED | 72 | DC administered with 28 µg/kg body weight of WiNeWsE through feed |
| 5X-HED | 72 | DC administered with 142 µg/kg body weight of WiNeWsE through feed |

Notes: ^aThere were 24 subjects/group/endpoint. There were three endpoints in this study.

Abbreviations: NC, normal control; XMC, xenotransplant model control; DC, disease control; 1₁Dexa-HED, 1 human equivalent dose of dexamethasone; WiNeWsE, withanone enriched *Withania somnifera* extract; 0.2X₁HED, 0.2 human equivalent dose of WiNeWsE; 1X₂HED, 1 human equivalent dose of WiNeWsE; 5X₁HED, 5X human equivalent dose of WiNeWsE.

Table 3 Human Dose Equivalence and Translational Dosing for Zebrafish in Present Study

| Human Dose | | Translational Dose for Zebrafish ^a (µg/kg Body Weight) | | | |
|---------------|---------|---|-----------------------|---------------------|---------------------|
| Dexamethasone | WiNeWsE | Dexamethasone | WiNeWsE | | |
| | | 1 _α -Dexa-HED | 0.2 _α -HED | 1 _α -HED | 5 _α -HED |
| 6 mg/day | 2 g/day | 0.08 | 6 | 28 | 142 |

Note: ^aZebrafish weighing 0.5 g were included in the study.

dose equivalences are provided in Table 3. Oral dosing was adopted over a dilution range of 0.2, 1, 5 relative to HED for a period of 10 days. To prepare the infused oral feeds, a known quantity of the compound was mixed with fish food weighing 2.5 mg per pellet and were extruded in to uniform pellets. The study groups were fed on a 24-h cycle with an estimated number of pellets per fish. During the dosing session the fish were isolated from the respective study groups and were fed individually in the feeding tank. Control fish were fed with unmodified fish food and were fed under similar conditions to that of study groups. Drug screening was done at two screening time points, after three and six days of treatment to understand the acute and subacute pathophysiological changes. Dexamethasone was administered as a positive control.

Endpoint Studies

Behavioral Fever. Zebrafish being an ectotherm exhibits behavioral fever as an adaptive immunity, that is, it migrates to the water at a temperature matching its body temperature. So, if a zebrafish is having a higher body temperature due to immunological reactions, it will migrate and spent more time in water at a higher temperature matching that of its body. To study the behavioral fever an experimental tank with three chambers at different temperatures (23°C, 29°C, and 37°C) was used. The chambers were positioned left to right in order of increasing temperature. Continuous cooling and heating were maintained in the flanking chambers during the study period. A pictorial depiction of this chamber is provided in Figure 2A. The fish from the respective study clutches were introduced individually in to the temperature gradient chamber at 29°C and given opportunity to choose the temperature that supports the physiological change. The time spent by the fish in the temperature gradient chamber was calculated for consecutive three minutes and the readings were recorded.

Screening for Presence of Skin Hemorrhage. Whole animal imaging was performed using a digital single lens reflex (DSLR) camera (D3100 Nikon Corporation,

Tokyo, Japan). Fish with skin hemorrhages, demarcated as red spots, were enumerated.

Dissection of Swim Bladder for Anatomical and Histopathological Observations. The fish were euthanized by putting them in water at 2–4°C and dissected as per ethical guidance by ventral incision in the skin from the lower jaw to the vent. The intestinal tract and gonads were removed to expose the swim bladder. The swim bladder, located ventral to the kidney, was isolated without any damage to the esophagus connected to it through pneumatic duct. Likewise, heart, intestinal cavity, and gonads were removed to expose the kidney attached to the dorsal body wall. The fish was pinned to the dissection board with ventral side up to isolate the kidney intact. The isolated swim bladder and kidney were washed in PBS observed under the Labomed CM4 stereomicroscope at 1_x magnification, using 14 MP Labomed camera. Cytology slides were prepared from whole swim bladder and kidney necropsies and were stained with H&E.

Kaplan–Meier Survival Curve. Mortality was counted on a daily basis and plotted as a Kaplan–Meier survival curve to understand the survival rate of the study groups over therapeutic intervention.

Data Analysis

All graphical data are displayed as mean ± standard error of the mean (SEM). For statistical significance of the variance observed among different means was determined through GraphPad Prism 8.0 software. Two-way ANOVA with Dunnett's multiple comparison test was used to determine the statistical significance.

Result

Computational Studies

Docking and Molecular Dynamic (MD) Simulation

The stereochemical quality of the structure was checked and confirmed. Phytocompounds including withanolides present in roots and leaves of *W. somnifera* were docked with the ACE2-RBD complex. The phytocompounds were bound at the ACE2-RBD complex tightly (see Table 4 for Vina scores).

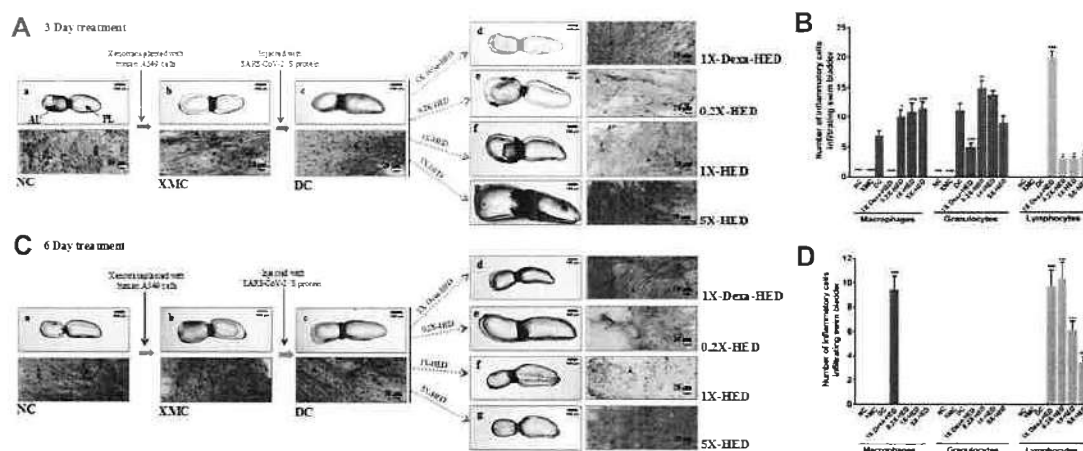


Figure 2 WiNeWsE attenuates viral S protein induced inflammation in zebrafish swim bladder.

Notes: (A and C) Effects of xenotransplantation, subsequent induction of HZF subjects with recombinant viral S protein and successive different ameliorative therapeutic ministrations on the morphology of swim bladders and infiltration of inflammatory cells therein, as monitored through histopathology, are depicted through pictorial flowcharts for three- (A) and six-day (C) treatments. (B and D) Infiltration of different inflammatory cells [macrophages (mud brown arrowheads), granulocytes (green arrowheads) and lymphocytes (blue arrowheads)] in response to xenotransplantation, disease model development and subsequent treatments were quantified and graphically, represented separately for three- (B) and six-day (D) treatments. Data plotted are mean \pm SEM of counts obtained from 24 individual subjects in each group. Statistical significance of the means of different groups was analyzed through one-way ANOVA followed by Dunnett's post hoc test and marked as * $p < 0.01$, ** $p < 0.05$ and *** $p < 0.001$, when compared to disease control (DC). **Abbreviations:** Sm, smooth muscle nuclei; E, epithelial nuclei.

AQ15

The phytocompound which bound to the interface was subjected to further investigation. Only withanone was found to be docked into the ACE2-RBD complex (Figure 3A). It bound at the interface of the ACE2 receptor and RBD, interacted with the residues from both ACE2 and RBD (Figure 3B) and was thus analyzed further to study its role in weakening or blocking the interactions between the ACE2 receptor and RBD. Docking showed efficient binding of withanone (ligand) through two H-bonds (D30 of ACE2 and R403 of RBD to withanone), alkyl, and van der Waals interactions at the ACE2-RBD interface (Figure 3C and D) (Table 5).

The RMSD of the protein complexes without or with withanone was 2.201 Å, and that of ACE2 alone was 1.476 Å, when final trajectories were compared. The RMSD of the simulated molecule (withanone) was 2.166 Å compared to its starting position. At the end of simulation, it moved slightly toward the ACE2 side at the ACE2-RBD interface (Figure 3C–F), revealed by losing contacts (within 4 Å) with the RBD (Figure 3E and F). On analyzing the ligand interaction, it was found that withanone still forms three H-bonds in the protein interface, but with ACE2 only. ACE2 D30, N33 and Q96 form H-bonds with withanone. In addition, withanone was stabilized by alkyl and van der Waals interactions (Figure 3E and F) (Table 5).

We observed that two intrachain (at the protein interface on ACE2 side) salt bridge interactions, K31 NZ-E35 OE1/OE2 (2.73 Å/2.71 Å), and one interchain long-range ion-pair, K31

NZ-E484 OE2 (5.67 Å), were abolished upon incorporation of withanone (Figure 3G–I). The length of the two N-O bridges between K31 and E35 of ACE2 increased by 1.22 and 1.89 Å (Figure 3G and H). We also observed that the occupancy of these N-O bridges reduced by 13.8% upon incorporation of withanone (Figure 3I). The intrachain salt bridge (K31-E35) was destabilizing, as calculated in the trajectory without withanone (5 kcal/mol). This salt bridge was abolished in the presence of withanone. We detected that the length of the interchain salt bridge (ACE2 D30-RBD K417) was 2.6 Å, which increased by 0.4 Å in the final trajectory. Electrostatic contribution of this salt bridge (D30-K417) in the initial trajectory was -2.52 kcal/mol and in the final trajectory it was -1.32 kcal/mol. This salt bridge was not abolished in our study, however, it was found to be destabilizing at the end of 50 ns MD simulation trajectory.

515

520

525

AQ17

Flexibility Analysis and Calculation of the Electrostatic Component of Binding Free Energy of ACE2-RBD Complex




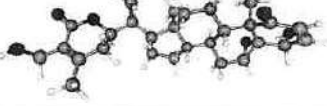
For global flexibility analysis, total RMSDs of backbone atoms (C, CA, N) of the residues in the protein was determined in the trajectories without and with withanone (Figure 4A). The data showed a slight increase in RMSD simulated with the withanone. Figure 4B and C show a C α atom fluctuations of the residues in ACE2 and RBD. Per residue RMSFs of ACE2 trajectories simulated with or

530

535

AQ16

Table 4 Names, Structure Molecular Weight, and Binding Energies (AutoDock Vina Score) of Phytocompounds from *W. somnifera* Docked into ACE2-RBD Complex

| Phytocompounds in <i>W. somnifera</i> | Structure | Molecular Weight (g/mol) | Binding Energy in ACE-RBD Complex (kcal/mol) |
|---------------------------------------|--|--------------------------|--|
| Withanone |  | 470.6 | -9.4 |
| Withanolide A |  | 470.6 | -9.6 |
| Withanolide B |  | 454.6 | -9.4 |
| Withaferin A |  | 470.6 | -9.1 |

Notes: The structures, molecular weights and binding energies (with the ACE2-RBD complex) of major phytocompounds present in *W. somnifera* are provided in the table above. The structures and molecular weights of these phytocompounds were mined from PubChem data sources (<https://pubchem.ncbi.nlm.nih.gov>). The binding energies were obtained from molecular docking studies reported here.

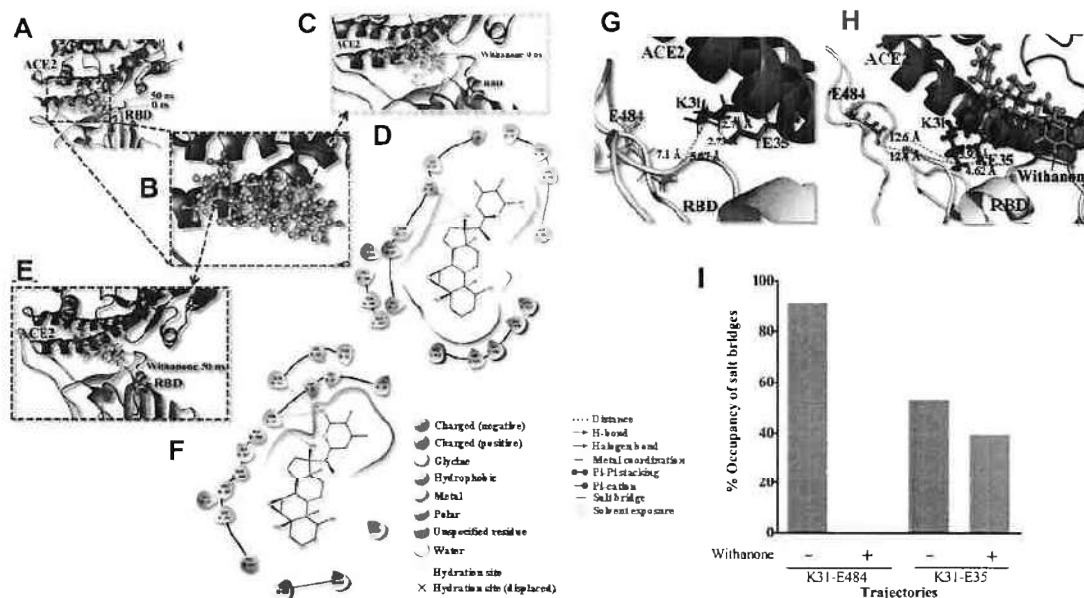
without the withanone were almost similar except for some fluctuations in the noninterfacial region (Figure 4B). Per residue RMSF of RBD shows a sharp increase in the beta hairpin region (a part of the interface region aa468 to aa498), in the trajectories simulated with the withanone (Figure 4C). Other signatures were almost similar in the trajectories without or with the withanone.

In MD simulation, total 96 and 94 clusters were obtained upon clustering analysis of the trajectories with or without Withanone, respectively. The electrostatic component of the binding free energies of ACE2-RBD complex were estimated on the post 25 ns representative trajectories of the cluster (51 trajectories, with the ligand; 43 trajectories, without the ligand) using DelPhi v8.4.3⁴² to assess the hypothesis that the proposed phytocompound weakens the interactions between ACE2 and RBD. The $\Delta\Delta G_{el}$ of the complex simulated with the ligand (17.6 \pm 0.97 kcal/mol) was decreased by 2.85 kcal/mol compared to the ones without the ligand (20.49 \pm 0.57 kcal/mol) (Figure 4D), and was statistically significant at 5% confidence level (Welch's *t*-test

p-value=0.014). This indicates that the binding of withanone at the interface of ACE2 and RBD weakens their interactions.

Withanone Inhibits Interaction Between ACE2 and RBD in *vitro*

Earlier studies have shown that Withanone can target SARS-CoV-2 main protease (M^{pro}) and TMPRSS2.¹⁴ However, experimental validation of that computation prediction has been lacking. In our study, we have checked the effect of commercially available withanone on the interaction between human ACE2 protein and RBD of SARS-CoV-2 viral spike (S) protein, through an ELISA-based biochemical method (Figure 5A). We noted that withanone, dose-dependently, inhibited ACE2-RBD interaction. The dose-response curve exhibited a steep rise over a withanone concentration range of 0.1–1 ng/mL. Concomitantly, the calculated IC_{50} fell in this range and was found to be 0.33 ng/mL. ~100% inhibition of ACE2-RBD interaction was observed with 4.7 ng/mL of withanone (Figure 5B). From these results, we can conclude that



withanone efficiently disrupts the biochemical interaction between the host ACE2 and viral RBD.

Leaf Extract from *W. somnifera* is Enriched in Withanone

As mentioned earlier, 200 phytochemicals were screened before settling down with withanone. We intend to validate the *in silico* findings through detailed *in vitro* and *in vivo*

experiments for which we have optimized a protocol to prepare hydro-methanolic extract enriched in withanone from fresh leaves of *W. somnifera* (WiNeWsE). HPTLC analysis showed that WiNeWsE was indeed enriched with withanone (Figure 6A and B). Quantification of HPTLC data showed that 1.29% w/w of WiNeWsE contained withanone. From the compositional analysis of the extract through HPLC (Figure 6C) we found that 8.93 µg/mg of withanone was

Table 5 Residues of ACE2-RBD Complex Involved Within 4 Å Range of Its Interaction with Withanone Before and After Simulation Runs

| Pre MD | | | Post MD | | |
|---------------------|--------------------------------|---|---------------------------|--------------------------------------|---|
| H-Bond | Alkyl Interaction | Van der Waals | H-Bond | Alkyl Interaction | Van der Waals |
| ACE2: D30 | ACE2: K26, L29, V93, | ACE2: T92, Q96 | ACE2: D30, N33, | ACE2: K26, L29, V93, A387, | ACE2: E37, T92, A386, Q388, P390, |
| RBD: R403 | RBD: P389 | RBD: E405, E406, R408, Q409, G416, K417 | RBD: Q96 | RBD: P389 | RBD: R403, E406, K417 |

Note: The participating residues of the ACE2-RBD complex within 4 Å radial range of its interaction with withanone identified through 50 ns molecular dynamic (MD) simulation of aforementioned complex docked with withanone are provided along with the type of interactions involved.

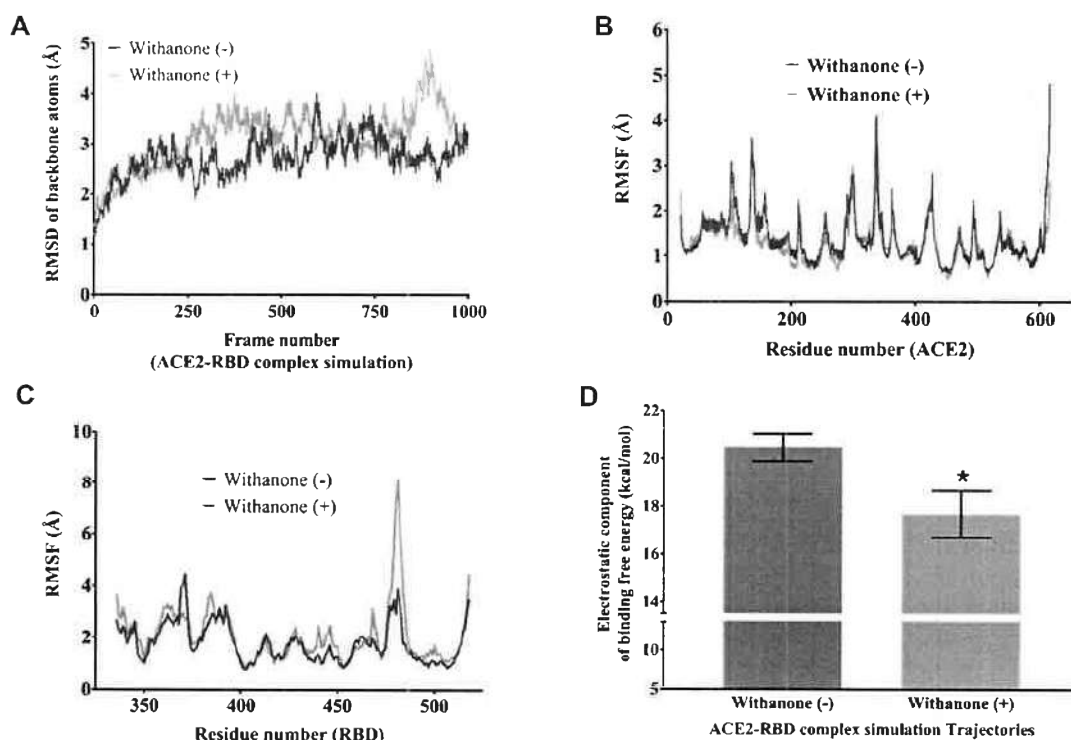


Figure 4 Flexibility analysis of the ACE2-RBD complex docked with withanone.

Notes: RMSD changes of backbone atoms (C, CA, N) of (A) the complex, (B and C) per residue RMSF (C α atom only) of ACE2 (B) and RBD (C) during 50 ns simulation time, as observed in the presence and absence of withanone. (D) Comparison of electrostatic component of binding free energies in the ACE2-RBD complexes with and without withanone. Statistical significance was analyzed through Welch's t-test and represented as * $p < 0.05$.

590 present in WiNeWsE. These observations confirmed the feasibility of preparing *W. somnifera* leaf extract enriched with only withanone. We further validated the antiviral efficacy of WiNeWsE in a humanized zebrafish model of SARS-CoV-2.

595 **In vivo Assessment of Antiviral Efficacy of WiNeWsE in Humanized Zebrafish Model Induced to Reproduce Human Pathological Reactions to SARS-CoV-2 Establishment of Humanized Zebrafish Model and Induction of SARS-CoV-2 Pathological Milieu**

600 The in vivo study comprised of screening the antiviral efficacy of WiNeWsE and assessing its effect on survivability. Accordingly, three endpoints were included in the study plan. The first were for screening the antiviral efficacy after three and six days of treatment, while the last endpoint was to assess the survivability after 10 days of 605 treatment. Posterior lobes of swim bladders of one-year-

old adult zebrafish were transplanted with human alveolar epithelial A549 cells to develop the xenotransplant model (XMC). The A549 cells took seven days to adhere to the bladder epithelium and was confirmed through histological staining. Thereafter, in order to reproduce the human 610 pathological reactions to SARS-CoV-2 in these XMCs, they were injected with recombinant S-protein. Dosing with positive control, dexamethasone, and WiNeWsE at human equivalent doses was administered for three, six, and 10 days. On days four and seven, designated groups of 615 zebrafish were sacrificed to conduct the endpoint studies that included assessment of behavioral fever, skin hemorrhages, swim bladder, and kidney necropsy through gross anatomical and histopathological studies. Survival was analyzed through Kaplan-Meier survival curve. The 620 study consisted of seven groups, namely, NC, XMC, DC, 1X₂Dexa-HED, 0.2X₂HED, 1X₂HED, and 5X₂HED. The details about these groups are provided in Table 3. Briefly,

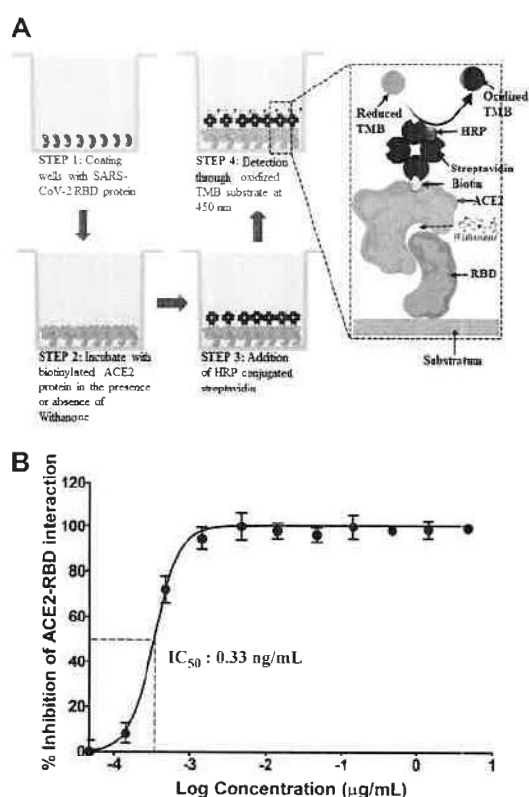


Figure 5 Experimental validation of the computational insights. **Notes:** (A) Schematic representation of the experimental procedure employed in evaluating the inhibitory effect of withanone on the biochemical interaction between host ACE2 and viral RBD. Biotinylated ACE2 bound to RBD, immobilized to the substratum, is detectable through HRP-conjugated streptavidin due to oxidation of 3,3',5,5'-tetramethylbenzidine (TMB). (B) Dose-response curve exhibiting the inhibitory effect of withanone on interaction between human ACE2 and RBD of SARS-CoV-2 S protein. IC_{50} is found to be 0.33 ng/mL.

NC consisted of ordinary adult zebrafish, XMC had xeno-transplanted zebrafish, also referred as humanized zebrafish (HZF), DC is the disease control group, in which the HZF subjects received injections of SARS-CoV-2 recombinant S protein, 1X₂Dexa-HED group subjects were essentially DCs receiving dexamethasone treatment, and serves as a positive control, 0.2X₂HED, 1X₂HED and 5X₂HED are the three experimental groups that received WiNeWsE 0.2 times less than human equivalent dose, human equivalent dose and five times more than human equivalent dose, respectively. The entire experimental plan is depicted in Figure 7 together with the observation of Kaplan-Meier survival analysis. NC and XMC showed 100% survival, whereas, the survivability was reduced to 80% in DC group. Treatment with dexamethasone restored

the survivability to 100%. The groups receiving human equivalent dose of WiNeWsE 1X₂HED and 0.2X₂HED (28 $\mu\text{g/kg}$ body weight) and lesser than it (6 $\mu\text{g/kg}$ body weight), respectively, experienced only slightly better survival (84.8%) than the DC group. However, the survival was found to be 95.2% in the 5X₂HED group which was administered with 142 $\mu\text{g/kg}$ body weight of WiNeWsE.

WiNeWsE Treatment Rescued Zebrafish from Behavioral Fever

The zebrafish elicits many immunological reactions that resemble the ones found in humans and therefore, is considered a more preferable model for immunity research, particularly that pertaining to viral infections. Zebrafish, being an ectotherm, exhibits behavioral fever as an adaptive immunity, that is, increase in their body temperature coaxes them to migrate to an environment at an elevated temperature. Therapeutics that can bring back the body temperature to normal will induce their migration back to the environment at physiological temperature (Figure 8A). An individual study subject from each group was placed in the 29°C water chamber and given sufficient time to migrate to chambers at 23°C and 37°C. Subsequently, durations of their stay in a particular chamber were monitored for three minutes. The recorded durations were plotted as a heat map; longer durations being represented as darker shades of the chosen green color palate (Figure 8B). Normal zebrafish from the NC group and HZFs from the XMC group dwelt in the chamber at 29°C in the case of both three and six-day treatment durations. Zebrafish belonging to the DC group which were injected with SARS-CoV-2 recombinant protein migrated to the chamber at 37°C and spent the entire period monitored there, clearly, indicating that these study subjects were suffering from fever. This, too was observed for both three and six-day treatments. With dexamethasone treatment for six days, the fish started spending almost equal duration in 29°C and 37°C chambers suggesting that dexamethasone could rescue behavioral fever with prolonged administration. But, its effect was not very obvious with three-day treatment. This observation was more pronounced after six days of treatment. The fish treated with 6 $\mu\text{g/kg}$ and 28 $\mu\text{g/kg}$ body weight of WiNeWsE for three days did not show any amelioration in behavioral fever as they spent most of the monitored duration in the chamber at 37°C. However, after receiving 142 $\mu\text{g/kg}$ of WiNeWsE for three days, the fish in the 5X₂HED started spending more time at 29°C compared to

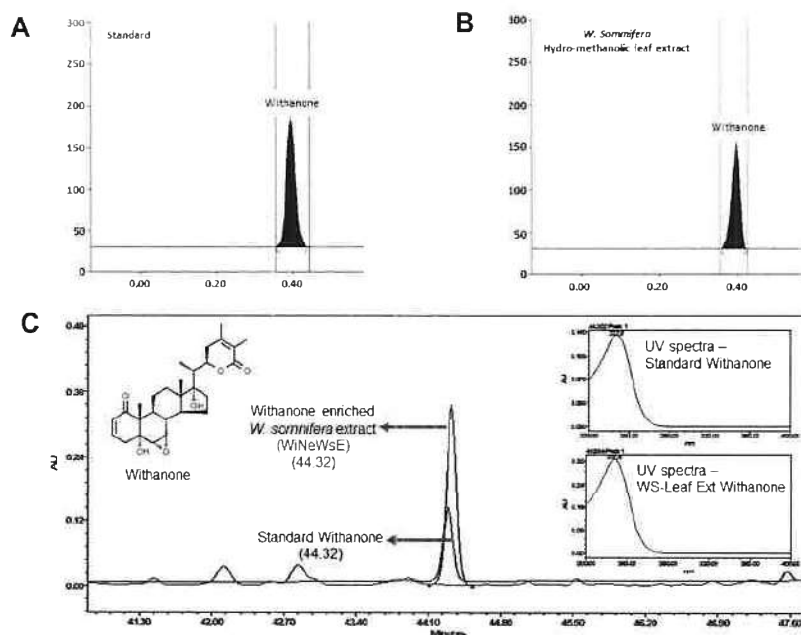


Figure 6 Compositional analysis of extract prepared from leaves of *W. somnifera*.

Notes: (A and B) HPTLC spectra of withanone and *W. somnifera* hydro-methanolic leaf extract both showing peaks at 230 nm. (C) Overlap chromatographs of standard mix (in black) and hydro-methanolic extract of *W. somnifera* leaves (in blue) showing the peak for withanone eluted at 227 nm. Insets show the individual peaks of standard withanone and that present in *W. somnifera* leaf extracts.

those from groups receiving lower doses of WiNeWsE. The effect of WiNeWsE treatment became more prominent after six days of treatment and was clear across all the doses administered, although, the highest dose (142 $\mu\text{g}/\text{kg}$ body weight) exhibited the best outcome, as was evident from the subjects in the 5X₂-HED group spending the entire duration of monitoring at 29°C. Body weight doses of 6 $\mu\text{g}/\text{kg}$ and 28 $\mu\text{g}/\text{kg}$ of WiNeWsE for six days could also ameliorate behavioral fever, but the effect was to a lesser extent compared to the highest dose. Taken together, these observations revealed that WiNeWsE was capable of eliminating one of the manifestations of adaptive immune response mounted against the recombinant S₂ protein of SARS-CoV-2 injected into these fish.

700 WiNeWsE Prevented SARS-CoV-2 Induced Skin Hemorrhaging in Zebrafish

705 Coronavirus infections, including that caused by the current SARS-CoV-2, are associated with blood coagulation.^{49,50} This phenomenon is closely reproduced in zebrafish injected with viral protein as visible skin hemorrhage owing to blood clotting under it. Like behavioral fever, this characteristic manifestation of adaptive

immune response of humanized zebrafish to SARS-CoV-2 induction was monitored subsequent to treatments with dexamethasone and WiNeWsE for three and six days (Figure 9). Earlier, it was ensured that xenotransplantation with human cells did not evoke such outcomes in the zebrafish (Figure 9A and C, compare panels a and b for absence of skin hemorrhage). Distinct red spots pertaining to skin hemorrhage were visible in humanized zebrafish injected with SARS-CoV-2 recombinant S₂-protein, suggesting successful recapitulation of blood coagulation observed in humans with severe SARS-CoV-2 infections (Figure 9A and C, panel c). In fact, every individual subject of the DC group was found to develop such hemorrhagic spots (Figure 9B and D). SARS-CoV-2 S₂-protein-induced fish treated with dexamethasone and different doses of WiNeWsE did not develop these spots. Both three and six-day treatments demonstrated relief from skin hemorrhaging in these groups (Figure 9A and B, panels d-g). Thus, WiNeWsE was able to erase yet another manifestation of adaptive immune reaction in zebrafish against SARS-CoV-2.

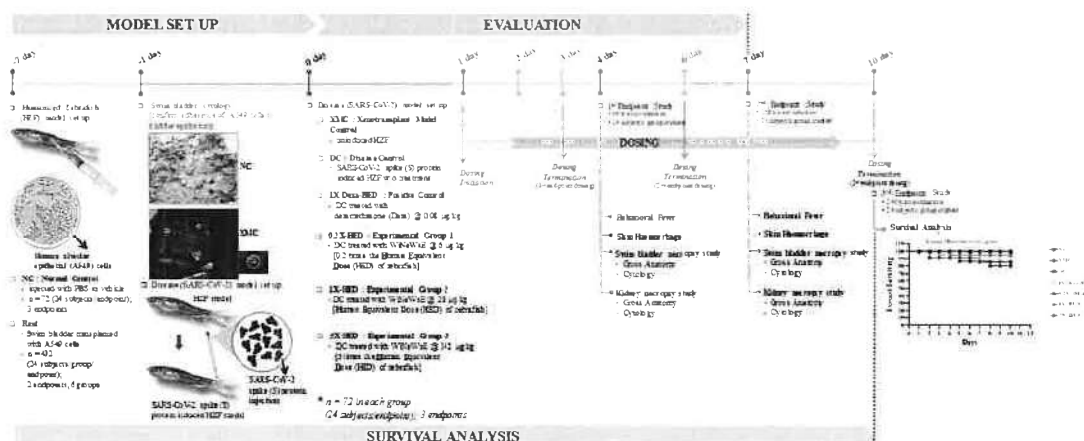


Figure 7 Experimental plan of the in vivo study conducted in xenotransplanted humanized zebrafish model.

Notes: Overall timeline of in vivo experiment has been schematically shown along with the major study steps with corresponding time points. The study included two screenings (at days four and seven) and one survival assay (until day 10) conducted in parallel. The establishment and subsequent, cyclical confirmation of the xenotransplanted humanized zebrafish model (HZF) took seven days from the day of transplantation. Human alveolar epithelial (A549) cells were intramuscularly injected into the posterior lobe of the swim bladder of zebrafish, incubated for seven days, and adherence of the injected human cells to the fish swim bladder epithelium was confirmed through gross cytology of the swim bladder. A group of HZF subjects were maintained throughout the experiment as xenotransplant model control (XMC). Likewise, a group of zebrafish without any xenotransplantation was taken as normal control (NC). Successive to the model confirmation, recombinant SARS-CoV-2 protein was injected at the site of xenotransplantation to establish the disease model. A group of HZF subjects injected with viral S₂ protein without any treatment was included as disease control (DC). Three experimental groups of DC subjects, namely, 0.25X-HED, 1X-HED and 5X-HED, respectively, received 6, 28 and 142 µg/kg of withanone enriched *W. somnifera* extract (WiNeWsE) for three (for first endpoint study), six (for second endpoint study) and 10 (for third endpoint study) days. The group of DC subjects (1X-Dexa-HED) receiving 0.08 µg/kg of dexamethasone for same period as experimental groups was included as a positive control. Doses used in all treatment are shown in Table 3. The screening endpoint studies included monitoring of behavioral fever, skin hemorrhage, and swim bladder and kidney necropsy studies. Survival assay endpoint study included Kaplan-Meier analysis, represented as survival curve.

730 WiNeWsE Modulates Immune Response to SARS-CoV-2 Induction in Zebrafish Swim Bladder

Zebrafishes were humanized by seeding A549 cells on the posterior lobes of their swim bladders. The viral induction was also done at this site. Therefore, signs for anticipated morphological alterations and immune responses were studied in the swim bladders as gross anatomical visualization and tissue histopathology, respectively, for both three- and six-day treatment regimes. Zebrafish swim bladder is a gas filled sac comprising of an anterior lobe (AL) and a posterior lobe (PL) connected by a wide ductus communicans (Figure 2A, panel a). The tunica externa envelops the inner gas gland made out of mesothelium comprising of epithelial cells and musculature formed by smooth muscle cells. The pneumatic duct connects the posterior lobe to the esophagus. Both lobes function under tight coordination with each other. Zebrafish in the NC group which were neither xenotransplanted nor induced with viral protein, had morphologically healthy swim bladders in terms of size, shape and color with continuous tunica externa and mesothelial lining of smooth muscles. Morphology of swim bladders in humanized

zebrafish from XMC groups, from both three- and six-day treatment cohorts, was similar to the normal ones, thereby, confirming that xenotransplantation with human cells did not have any undesirable effects (Figure 2A and C, panel b). But, upon induction with SARS-CoV-2 recombinant S₂ protein, anterior lobes were inflated indicating edema, more prominent in the three-day treatment cohort (Figure 2A and C, panel c). Dexamethasone treated 1X-Dexa-HED group subjects from three-day treatment cohort had slightly inflated swim bladders (Figure 2A, panel d). The observed morphological anomaly in the 1X-Dexa-HED group from six-day treatment cohort was more pronounced as enlarged anterior lobe and narrowed posterior lobe indicating edematous gas gland (Figure 2C, panel d). Subjects in the 0.25X-HED group from three-day treatment cohort receiving 6 µg/kg body weight of WiNeWsE had more inflated lobes, both anterior and posterior when compared to their corresponding NC counterparts. This effect was more obvious in the six-day treatment cohort (Figure 2A and C, panel e). A similar alteration occurred in the fish in the 1X-HED group from three-

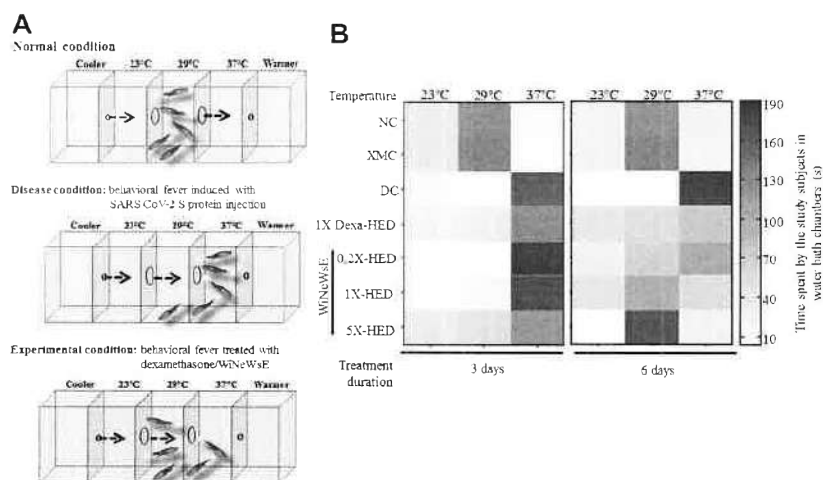


Figure 8 WiNeWsE rescues zebrafish from viral S₂protein induced behavioral fever.

Notes: (A) Pictorial depiction of the chambered water bath maintained at different temperatures with free access between these chambers for zebrafish subjects for migration to conducive temperature zones. The anterior-most and posterior-most chambers are connected to cooling and heating facilities respectively to maintain the temperature gradient along the experimental chambers. In addition, these flanking chambers are designed to prevent access to fish from experimental chambers. As predictive outcome of the treatments, the picture depicts three scenarios. The first scenario pertains to normal condition where the subjects, could be humanized or not, but have not been induced with viral S₂protein and therefore, populate the chamber at 29°C, matching the body temperature of the zebrafish. In the second scenario, where the HZF subjects, injected with recombinant viral S₂protein, experience a rise in their body temperature and thus, migrate to the chamber at 37°C. This phenomenon in which the zebrafish with higher body temperature than their physiological one migrate to a warmer surrounding matching their body temperature is called behavioral fever. In the third scenario, the fevered subjects are treated either with dexamethasone or WiNeWsE, and therefore, are seen migrating back to the chamber at 29°C. The time spent by each treated or untreated subject in a specified chamber is recorded and represented as a color-coded matrix, called a heat map. Increase in time spent is depicted as corresponding darkening of the chosen green color palate. (B) Heat map representing the effect of treatments on behavioral fever.

775 day treatment cohort receiving 28 µg/kg body weight of
WiNeWsE. The same group from six-day cohort showed
shrunken tunica externa and overall reduction of sizes of
the bladder lobes (Figure 2A and C, panel f). Zebrafish
in the 5X-HED group that received 142 µg/kg body
780 weight of WiNeWsE for three days showed visibly sig-
nificant enlargement of bladder lobes with anomalous
AQ20 tunica externa (Figure 2A, panel g). The identical
group from the six-day treatment cohort had overall
shrunken swim bladders (Figure 2C, panel g). These
785 observed morphological alterations, despite the fact that
WiNeWsE treatment supported more than 95% survival
(Kaplan-Meier curve in Figure 7) among the sub-
jects, raising curiosity regarding the underlying possible
reasons. Zebrafish, being a teleost, harbor the features of
790 both innate and adaptive immune responses.^{25,45-48}
Evoked immune reactions quite often manifest them-
selves as transient anomalies in the anatomy of affected
organs. Our histological study revealed that indeed,
these responses were triggered after inducing the huma-
795 nized zebrafish with SARS-CoV-2 recombinant S₂pro-
tein. Histological sections of the swim bladders of fish
from the DC group showed infiltration of macrophages
and granulocytes (Figure 2A, panel DC; Figure 2B and
800 C and D). The xenotransplanted zebrafish did not exhibit any
such infiltration of inflammatory cells, thereby providing
a clean control background for noise-free comparison of
the observations from the DC and treatment groups
(Figure 2A and C, compare panels NC and XMC;
805 Figure 2B and D). In the three-day WiNeWsE treatment
cohort, number of macrophages found to infiltrate the
swim bladders were comparable and, in some cases,
more than that found in the DC group. Dexamethasone
treatment for three days, however, brought down the
810 number of infiltrating macrophages significantly com-
pared to the DC group. A similar observation was
noted for infiltrating granulocytes in the case of dexa-
methasone treatment. Although, infiltrating granulocytes
were found to be trending towards reduction, but the
815 observation was not statistically significant when com-
pared to the DC group. Infiltrating lymphocytes were
not observed in the case of the DC group for both three-
and six-day treatments. However, in fish treated with
dexamethasone over both these periods, significantly,
820 large numbers of lymphocytes were found to infiltrate
when compared to the DC group ($p < 0.001$). With

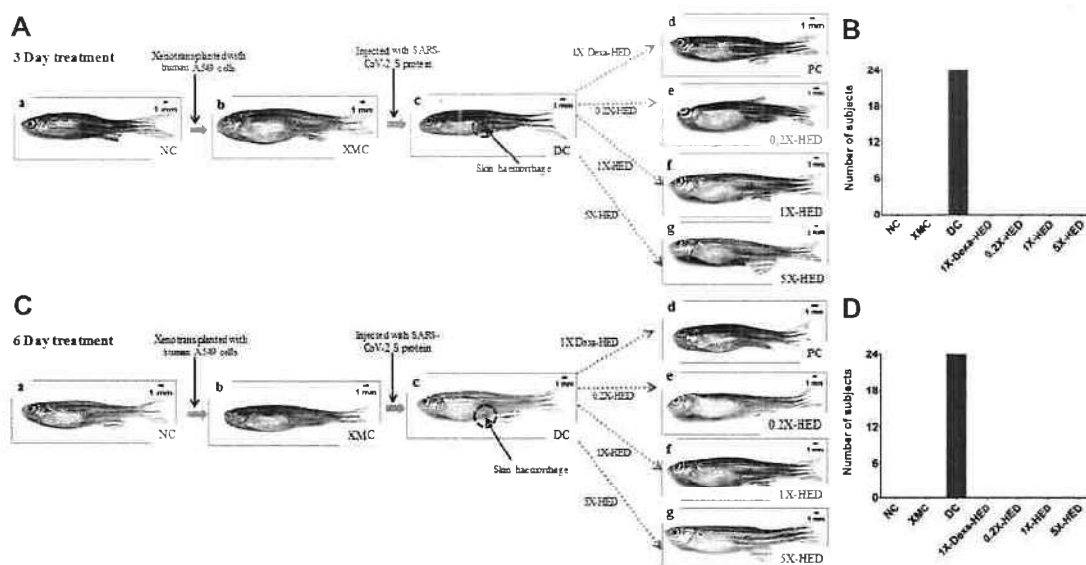


Figure 9 WiNeWsE ameliorates viral S₂ protein induced skin hemorrhages in zebrafish.

Notes: (A and C) Pictorial flowchart depicting the establishment of HZF model (XMC) in normal zebrafish population (NC) and subsequent induction of skin hemorrhage (encircled with open red circles) with intramuscular injections of recombinant viral S₂ protein to develop the disease control (DC), and monitoring the effects of various treatments, namely, 0.08 µg/kg bodyweight of dexamethasone (1X-Dexa-HED) or different concentrations of WiNeWsE (6 µg/kg for 0.2X-HED, 28 µg/kg for 1X-HED and 142 µg/kg for 5X-HED) after three (A) and six (B) days. (B and D) Number of zebrafish subjects developing skin hemorrhages were counted and plotted separately for three-day (C) and six-day (D) cohorts, for a quantitative understanding of the effect of treatments on this disease outcome.

WiNeWsE treatment for three days, the number of lymphocytes infiltrating the swim bladder were greatly reduced. However, a six-day treatment with WiNeWsE showed an increase in infiltrating lymphocytes at lower doses (Figure 2A and C, panels 1X₂-Dexa-HED, 0.2X₂-HED, 1X₂-HED, 5X₂-HED; Figure 2B and D). Knowing that macrophages and granulocytes are part of innate immune response and lymphocytes that of an adaptive response, the overall trend surfacing from the quantification of these cells showed that in the initial phase (three-day treatment), WiNeWsE tends to reduce the innate immune response with complete success through six-day treatment. This is implicative of the capability of WiNeWsE in preventing the innate immune response from going into overdrive. Likewise, WiNeWsE sustains the adaptive immune response in the form of lymphocytes suggesting that it might be helpful in refraining the adaptive immune response from becoming dysfunctional. Interestingly, SARS-CoV-2 infection affects both adaptive and innate immune responses to sustain itself. The inflammatory innate immune response is sent into overdrive and the adaptive immune response is made dysfunctional.⁵¹ So, WiNeWsE might be a solution to

the complex immunomodulation associated with SARS-CoV-2 infection.

845

WiNeWsE Attenuated SARS-CoV-2 S₂ Protein-induced Kidney Necrosis

SARS-CoV-2 infection affects kidneys in humans.⁵² Therefore, the effect of WiNeWsE treatment on fish kidneys was assessed through gross anatomical and cytological studies. The zebrafish kidney is attached to the parenchymal layer of the dorsal wall of the viscera. It is divided into head (H), trunk or saddle (S), and the tail (T) and extends along the anteroposterior length of the body (Figure 10A and B, panel NC). After carefully dissecting out the kidney from the euthanization subject, the whole organ was observed microscopically for anatomical anomalies. In addition, alterations at the tissue level owing to any of the experimental procedure, particularly, administered treatments, was evaluated through cytology. Effects on the kidney were monitored after three and six days of treatments. Zebrafish from the NC groups of both the treatment cohorts, had defined internal arrangements of packed mesonephric nephrons in the head zone of the kidney with glomerular tufts followed by proximal and distal tubule segments. Highly pigmented mesonephros

850

855

860

865

were distributed from head to tail of the kidney (Figure 10A and B, panel NC). Similar, arrangements were observed in the XMC groups with humanized zebrafish from both the treatment cohorts, thus, confirming that xenotransplantation did not affect the kidneys adversely (Figure 10A and B, panel XMC). However, humanized zebrafish induced with SARS-CoV-2 S-protein showed loss of tubular segments and vascular degeneration observed as dark staining bodies indicating renal necrosis (Figure 10A and B, panel DC). Percentage of necrotic cells were also high in this group compared to NC and XMC groups, with normal and humanized zebrafish, respectively (Figure 10B and D). The kidney anatomy after three days of dexamethasone treatment showed an arborized network with packed glomerular tufts and tubular segments indicating normal renal architecture (Figure 10A, panel 1X-Dexa-HED). However, prolonged dexamethasone treatment for six days, showed a disorganized kidney network with irregular glomerular tufts and melanocytic pigmentation indicating structural anomaly (Figure 10B, panel 1X-Dexa-HED). However, anatomical anomaly was not reflected as renal necrosis. In both three- and six-day treatment cohorts, dexamethasone significantly reduced the necrosis ($p < 0.001$) (Figure 10B and D). For all the concentrations of WiNeWsE, in cases of both the treatment cohorts, renal anatomy was found to be anomalous (Figure 10A and C, panels 0.2X-HED, 1X-HED and 5X-HED). However, a three-day WiNeWsE treatment started reducing the renal necrosis which was statistically significant in comparison to the DC group after six-day treatments (Figure 10B and D). Structural anomaly of the kidney could be a manifestation of the SARS-CoV-2 infection at organ level, when the fish are left untreated. The fact that dexamethasone and WiNeWsE treatments were found to attenuate renal necrosis within the span of six days, is indicative of the anatomical rescuing of the kidneys as well, provided longer monitoring is done. Taken together, these observations showed that WiNeWsE is capable of preventing deleterious effects of SARS-CoV-2 infection that percolate to secondary organs, which were not infected directly. In a clinical context, this might be an indication of its ability to prevent multiorgan failure.

910 Discussion

The S₂ protein of SARS-CoV₂ interacts with its cellular receptor, ACE2 via receptor binding motif (RBM; aa 424-494) present in its receptor RBD. Eighteen residues

of the receptor make contact with 14 residues of the viral S₂ protein, mainly through hydrophilic interactions.^{53,54} 915

Molecular dynamic (MD) simulation of the ACE2-RBD complex was performed using NAMD, in the presence and absence of the ligand molecule (withanone). Withanone moved slightly toward the ACE2 side of the protein interface, as revealed by losing H-bond and contact residues with the RBD upon MD simulation. Initially, docking showed 14 residues within 4 Å of withanone. Out of these, seven residues were from ACE2, and seven were from RBD (Table 5). Upon 50 ns MD simulation, R403, E406, and K417 from RBD were within 4 Å of withanone, and rest of the residues were from ACE2 (Figure 3C and D). Furthermore, we explored the ionic interaction at the binding interface of the ACE2 receptor and RBD complex of SARS-CoV-2. The intrachain salt bridge K31-E35 (at the interface on the ACE2 side) was completely abolished (Figure 3G and H). Similarly, the interchain long-range ion-pair K31-E484 (between ACE2 and RBD) was also completely abolished, with a large swing of the residue K31. Percent occupancy of the intrachain salt bridge K31-E35 was also decreased in the simulation trajectories with withanone, compared to the trajectories without withanone (Figure 3I). Similarly, the percent occupancy of the interchain long-range ion-pair K31-E484 was decreased dramatically. Electrostatic component of binding free energy of the ACE2-RBD complex was decreased in the simulation trajectories with withanone (Figure 4D). In simple words, this means withanone prevented stabilization of the interaction between ACE2 and RBD.

Protein surfaces have many hydrophilic residues, and salt bridges present in the surface play an important role in protein-protein association or binding.⁵⁵ Hence the protein interface (binding interface) is generally more hydrophilic than the protein interiors. Electrostatic interactions are thought to be more important for protein-protein or protein-ligand interactions than protein folding.⁵⁶ No wonder the interfacial salt bridges, being the major contributors to the electrostatic interactions between proteins, play a central role in binding events. Generally, the structures of the proteins do not change significantly upon complex formation, but some conformational rearrangements are observed, and most of these are due to side chain movements.⁵⁷ Geometrical complementarity and stability in energetics are the two key driving factors for protein binding while hydrophobic effect, hydrogen 950

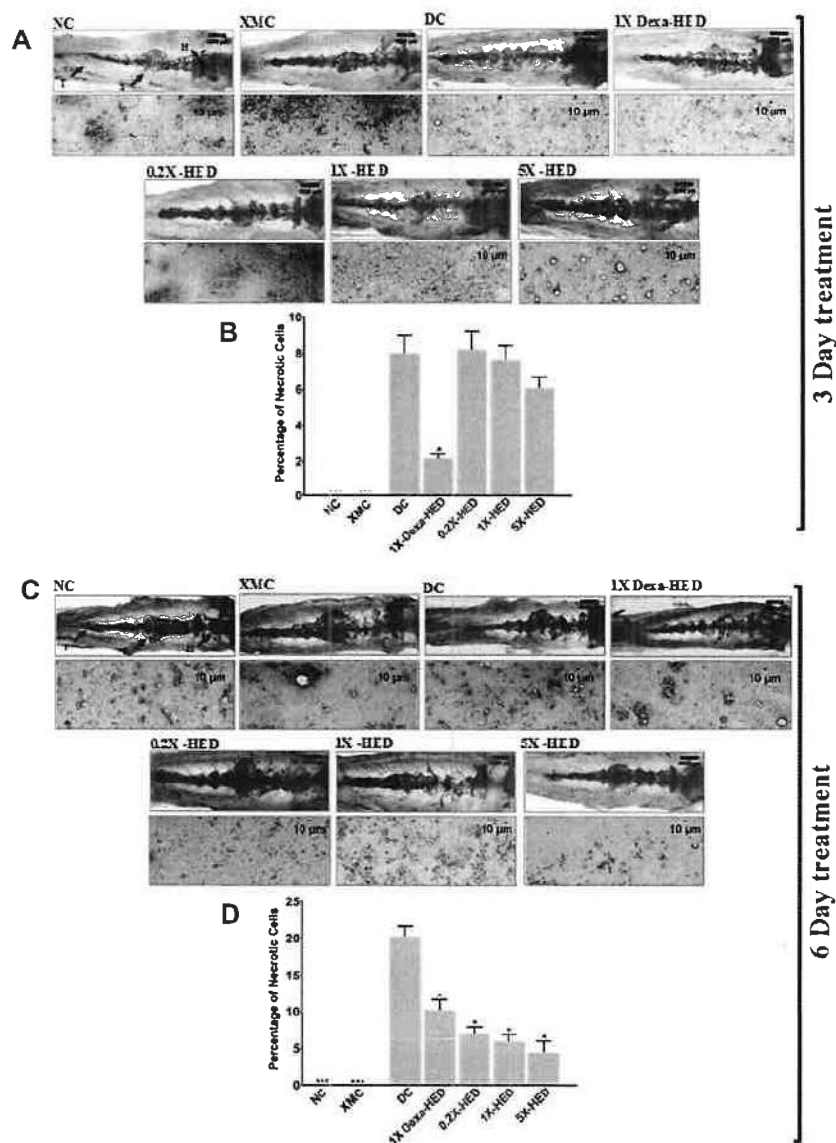


Figure 10 WiNeVsE assuages detrimental effects of viral σ protein on zebrafish kidney.

Notes: (A and C) Effect of experimental model set-up and subsequent therapeutic treatments on zebrafish kidneys was monitored through gross anatomical study and corresponding histopathology for necrosis and degeneration after three (A) and six (C) days. Zebrafish kidney is anatomically divided into head (H), saddle (S) and tail (T). (B and D) Necrotic cells were quantified and separately, plotted as percentage for three (B) and six (D) days of treatments. Data plotted are mean \pm SEM of counts obtained from 24 individual subjects in each group. Statistical significance of the means of different groups was analyzed through one-way ANOVA followed by Dunnett's post hoc test and marked as * $p < 0.001$, x when the comparison was done with the disease control (DC).

bonds, and salt bridges are the key players in energetic. A salt bridge can provide favorable free energy to the binding,⁵⁶ alternatively, an isolated charge without forming a salt bridge, when buried in the protein interface, could substantially destabilize binding through a substantial desolvation cost. We calculated the

energetics of the salt bridges at the interface of ACE2 and RBD. The salt bridge K31_{ACE2}-E35 and ion-pair K31_{ACE2}-E484 were abolished. These results clearly indicated that the incorporation of withanone is likely to decrease protein complex stability by disrupting the factors that build up the favorable binding energetics.

970

Global RMSD changes obtained from MD simulation of the ACE2-RBD complex with and without withanone provided a measure of flexibility (Figure 4A). Per residue RMSF was calculated to assess the flexibility at residue level (Figure 4B and C). Except for some minor fluctuations, a noticeable change was observed in the beta turn in the interfacial region in RBD (aa468-aa498). Generally, residues in the molecular recognition region have higher fluctuations. Reduced electrostatic component of the binding free energies of the ACE2-RBD complex suggests that withanone binding at the interface of ACE2 and RBD weakens the interaction between the latter two. Taken together, these observations reveal that withanone has the potential to disrupt the interaction between ACE2 and RBD of SARS-CoV-2.

Computational observations on withanone targeting SARS-CoV-2 main protease (M^{pro}) and host transmembrane TMPRSS2 have been reported.^{13,14} Likewise, withaferin A is also reported to bind TMPRSS2 and GRP78.^{14,15} While targeting virus-specific factors is encouraging, the same cannot be said for host factors, since that would have associated side effects. Moreover, withaferin A is cytotoxic and this prospect has been widely explored for treating cancer. SARS-CoV-2 sends the immune response into overdrive. It is possible that such an altered physiological condition might not be able to handle cytotoxic assault and lead to other complications. According to the study by Kumar et al,¹³ binding score of withanone to M^{pro} is -4.42 kcal/mol, whereas we obtained a binding score of -9.4 kcal/mol when withanone was docked into the interacting interface of ACE2 and RBD. Kumar et al¹³ have justified the theoretical prospects of functional efficacy of withanone at inhibiting M^{pro} through a comparison with the binding score (-5.6 kcal/mol) of an already reported inhibitor N3 with M^{pro} .^{58,59} Similarly, binding of withanone to TMPRSS2 (-4.30 kcal/mol) was weaker when compared to withanone binding to the ACE2-RBD complex (-9.4 kcal/mol).¹⁴ Employing an identical approach, low binding score in this case was substantiated through comparison with known TMPRSS2 inhibitor camostat mesylate (-5.90 kcal/mol). However, disparity in the binding score calculations between these reported studies and our study, due to the use of different tools, is ruled out as the software programs used are reported to give comparable outputs,⁶⁰ clearly reflecting that withanone shows a tighter binding with the ACE2-RBD complex than with either M^{pro} or TMPRSS2. Using an *in silico* peptide binding approach, Hamza et al attempted identifying the SARS-CoV-2 peptides which could be potential targets for the phytochemicals, hydroxychloroquine, kaempferol and anthraquinone from *Moringa oleifera*.⁶¹ The authors translated the SARS-CoV-2 genome *in silico* (using EMBOSS TRANSEQ server) into peptides which were then used for binding studies with the abovementioned phytochemicals. The maximum binding energies obtained from AutoDock Vina for hydroxychloroquine is -5.1 kcal/mol, kaempferol is -6.2 kcal/mol, and anthraquinone is -6 kcal/mol,⁶¹ which are again less than those observed in the cases of withanone and the ACE2-RBD complex (-9.4 kcal/mol) in this study. Thus, it is possible that withanone might act specifically during viral-host interaction and not target the host factors, sparing the body from side effects. Moreover, the computational findings reported in these studies were not experimentally validated. Although, apparently, our study is on similar lines, however we have demonstrated that withanone targets the ACE2-RBD complex, and have validated our observations from computational studies by wet-lab experiments.

For experimental validation of our computational insights, overexpressed truncated S-protein of SARS-CoV-2 expressing only RBD was used while the human ACE2 (hACE2) used was full length. ELISA wells were coated with viral RBD into which biotinylated hACE2 was added along with different concentrations of withanone. An inhibitor of the ACE2-RBD interaction provided with the kit was used as the positive control, while the reaction without any inhibitor was taken as the negative control. Inhibition of ACE2-RBD interaction was calculated with respect to the negative control assuming the interaction to be 100%. Interaction was detected using HRP-conjugated streptavidin against biotinylated ACE2. Corroborating with the *in silico* observation, we found that in the presence of withanone, ACE2 binding with RBD was less efficient and that the effect was positively correlated to the concentration of withanone used. Withanone efficiently inhibited interaction of ACE2 with RBD ($IC_{50}=333.2$ pg/mL) and this inhibition was found to be dose-dependent.

We have also developed a protocol to prepare leaf extracts enriched in withanone (WiNeWSE). The reason behind choosing extract over isolated phytocompound is to ensure minimum modulation in the chemical milieu of withanone when it is being extracted from the plant. Co-extracting other phytocompound/s along with the one required ensures minimum deviation in the functional set-up of the compound from that present within the

1070 plant. Such an arrangement is likely to modulate the activ-
ity of the phytochemical in vitro or in vivo in a way
similar to what actually happens in nature. To prove this
point, we validated the antiviral activity of WiNeWsE in a
1075 humanized zebrafish xenotransplanted with human alveo-
lar epithelial A549 cells on the posterior lobe of swim
bladder and induced with SARS-CoV-2 recombinant S₂
protein to elicit pathological reactions similar to those
observed in humans.

The zebrafish is a useful and attractive model for
1080 infectious disease and immunity research and is consid-
ered a refinement over the use of mammalian infection
models.²³ The zebrafish model allows the investigation of
specific immune system components at various stages of
immunologic development, and extensive molecular,
1085 genetic, and imaging tools are available for this species.
Zebrafish exhibit both the innate and adaptive arms of the
immune system, including leukocyte populations, inflam-
matory mediators, and signaling molecules that are similar
to those of the mammalian immune system.²⁴ Many com-
1090 ponents of the complement system have been identified in
zebrafish. Similarly, homologs of many mammalian cyto-
kines have been identified in zebrafish, including interleu-
kin 1 β ²⁵ type I⁴⁵ and type II⁴⁶ interferons, tumor necrosis
factor,^{25,47} and several interleukins.⁴⁸ Therefore, zebrafish
1095 have also been used as models of mammalian viral infec-
tion. Zebrafish models for mammalian viral infections
have the advantages of live imaging, whole-organism his-
topathology, and immunohistochemistry. The first zeb-
rafish infection studies using a mammalian virus
1100 demonstrated dose-dependent infection of the adult zeb-
rafish nervous system with herpes simplex virus type 1
(*Herpesviridae*) and its attenuation in response to antiviral
acyclovir.^{23,62} This indicated that the zebrafish model of
human viral diseases can be used to test the efficacies of
1105 antivirals. Observations from the studies conducted in
humanized zebrafish model of SARS-CoV-2 pathology
were compelling regarding the efficacy of WiNeWsE in
relieving fever, managing the immune reactions to thera-
peutic advantage, and preventing spreading of pathological
1110 responses to secondary organs.

Thousands of chemical molecules, already existing as
approved drugs in the market for other diseases, are being
virtually screened for this approach.⁶³ With this strategy of
drug repurposing, the hunt for a COVID-19 cure can be
1115 significantly expedited by foregoing phases I and II of the
clinical trials (the phases dedicated towards establishing
safety and dose of a new drug).⁶⁴ The time constraint

pertaining to the regulatory procedure required for launch-
ing a new drug in the market might limit the scope of
exhaustive exploration for the most suitable cure. 1120
However, cures based on phytochemicals follow naturo-
pathy, thus eliminating the demerit of ensuing toxicity in
the body. Nevertheless, preliminary studies are crucial to
establish the potency of such a treatment. Hence, the
1125 significance of this study which serves as a prefatory for
a phytochemical-based intervention against SARS-CoV-2
entry in the host cell.

Observations made in our present study, sheds light on
our next course of action, a situation arguably better than
repurposing approved drugs. To appreciate the essence of 1130
this study, we have to understand the potential demerits of
repurposing of drugs approved for other diseases. While it
is absolutely logical to adapt such an approach in the face
of the current compounding crisis, yet, we are unaware of
the side effects such repurposed drugs might bring along, 1135
particularly when time is too limited to explore all these
details, which otherwise would have been the most
obvious course of action. Without any intention of down-
playing the contemporary attempts made at finding a cure
for COVID-19, we would like to reiterate that if a cure 1140
from nature herself is showing promise, it is worthwhile
by all means to give it recognition. This study highlights
the importance of natural origin phytochemicals in con-
trolling SARS-CoV-2 entry into host cells, and provides an
attractive and alternative means for the management of 1145
COVID-19 infection.

Conclusion

Through this study we have demonstrated that withanone
has the potential to inhibit the interaction between hACE2
receptor and RBD of SARS-CoV-2 S -protein. Since this 1150
interaction is crucial for viral entry into the host cell, thus,
withanone being able to prohibit it implicates a virus-
specific therapeutic option. More importantly, we have
provided experimental evidence demonstrating the inhibi-
tory effect of withanone against the biochemical interac-
1155 tion between hACE2 and viral RBD proteins. In addition,
we have also shown that extracts enriched with withanone
can be prepared from the leaves of *W. somnifera*. This
report is the first of its kind amidst several others in
which withaferin A unavoidably co-extracts with witha- 1160
none. Last, but not the least, the potential of this extract as
an antiviral was validated in a preclinical set-up using
humanized zebrafish as a model that reliably reproduced
the human pathological responses to SARS-CoV-2. In

1165 conclusion, this study lays the foundation for developing
withanone in to a treatment for COVID-19 as an entry
inhibitor against SARS-CoV-2 coronavirus.

Abbreviations

1170 ACE2, angiotensin-converting enzyme-2; COVID-19, cor-
onavirus disease 2019; MERS, Middle East respiratory
syndrome; MD, molecular dynamics; NAMD, nanoscale
molecular dynamics; PBE, Poisson-Boltzmann equation;
RBD, receptor binding domain; RBM, receptor binding
motif; SARS-CoV, severe acute respiratory syndrome-cor-
onavirus; SARS-CoV-2, severe acute respiratory syn-
drome-coronavirus 2; S-protein, spike protein; VMD,
1175 visual molecular dynamics; RMSD, root mean square
deviation; WiNeWsE, withanone enriched *Withania som-*
nifera extract.

1180 Data Sharing Statement

All data generated or analyzed during this study are
included in this published article.

Ethics Approval

1185 Animal ethics guidelines from the Committee for the
Purpose of Control and Supervision of Experiments
(CPCSEA), Government of India, were followed to con-
duct the zebrafish (*Danio rerio*) experiments. Established
zebrafish protocols were duly approved by the Institutional
Animal Ethics Committee (IAEC study number 223/
1190 Go062020/IAEC).

Acknowledgments

We appreciate the zebrafish test facilities and experimen-
tations at our CRO partner, Pentagrit Labs, Chennai,
India. We thank Mr. Sudeep Verma and Ms. Meenu
1195 Tomer for their help with HPLC; Dr. Pratima Singh, Dr.
Preeti Raj, Mr. Ajeet Chauhan, Mr. Shoor Singh and Mr.
Arun Raturi for their help with visual graphics. We
extend our gratitude to Ms. Priyanka Kandpal, Mr. Tarun
Rajput, Mr. Gagan Kumar and Mr. Lalit Mohan for their
1200 swift administrative support.

Author Contributions

All authors made a significant contribution to the work
reported, whether that is in the conception, study design,
execution, acquisition of data, analysis and interpretation,
1205 or in all these areas; took part in drafting, revising or
critically reviewing the article; gave final approval of the
version to be published; have agreed on the journal to

which the article has been submitted; and agree to be
accountable for all aspects of the work.

Funding

1210 This research received no external funding. This presented
work has been conducted using internal research funds
from the Patanjali Research Foundation Trust, Hardwar,
India.

Disclosure

1215 The authors report no conflicts of interest in this work.

References

1. Lu H, Stratton CW, Tang YW. Outbreak of pneumonia of unknown etiology in Wuhan, China: the mystery and the miracle. *J Med Virol.* 2020;92(4):401–402. doi:10.1002/jmv.25678 1220
2. Gorbalenya AE, Baker SC, Baric RS, et al. The species severe acute respiratory syndrome-related coronavirus: classifying 2019-nCoV and naming it SARS-CoV-2. *Nat Microbiol.* 2020;5(4):536–544. doi:10.1038/s41564-020-0695-z
3. Ni W, Yang X, Yang D, et al. Role of angiotensin-converting enzyme 2 (ACE2) in COVID-19. *Crit Care.* 2020;24(1):1–10. doi:10.1186/s13054-020-03120-0 1225
4. WHO. Solidarity trial consortium. Repurposed antiviral drugs for COVID-19 – interim WHO SOLIDARITY trial results. *medRxiv.* 2020;(October 15). doi:10.1101/2020.10.15.20209817 1230
5. Bupp K, Roth MJ. Alteration and analyses of viral entry with library-derived peptides. *Adv Virus Res.* 2005;65(5):147–172. doi:10.1016/S0065-3527(05)65005-1
6. Dau B, Holodny M. Novel targets for antiretroviral therapy: clinical progress to date. *Drugs.* 2009;69(1):31–50. doi:10.2165/00003495-200969010-00003 1235
7. Anand K, Ziebuhr J, Wadhvani P, Mesters JR, Hilgenfeld R. Coronavirus main proteinase (3CLpro) structure: basis for design of anti-SARS drugs. *Science.* 2003;300(5626):1763–1767. doi:10.1126/science.1085658 1240
8. Sangwan RS, Chaurasiya ND, Misra LN, et al. Phytochemical variability in commercial herbal products and preparations of *Withania somnifera* (Ashwagandha). *Curr Sci.* 2004;86(3):461–465.
9. Zaman W, Saqib S, Ullah F, Ayaz A, Ye J. COVID-19: phylogenetic approaches may help in finding resources for natural cure. *Phytother Res.* 2020;34(11):2783–2785. doi:10.1002/ptr.6787 1245
10. Kambizi L, Goosen BM, Taylor MB, Afolayan AJ. Anti-viral effects of aqueous extracts of *Aloe ferox* and *Withania somnifera* on herpes simplex virus type 1 in cell culture. *S Afr J Sci.* 2007;103:(October):359–362. 1250
11. Cai Z, Zhang G, Tang B, Liu Y, Fu X, Zhang X. Promising anti-influenza properties of active constituent of *Withania somnifera* ayurvedic herb in targeting neuraminidase of H1N1 influenza: computational study. *Cell Biochem Biophys.* 2015;72(3):727–739. doi:10.1007/s12013-015-0524-9 1255
12. Balkrishna A, Pokhrel S, Singh J, Varshney A. Withanone from *Withania somnifera* may inhibit novel coronavirus (COVID-19) entry by disrupting interactions between viral s-protein receptor binding domain and host ACE2 receptor. *Res Sq.* 2020. doi:10.21203/rs.3.rs-17806/v1 1260
13. Kumar V, Dhanjal JK, Kaul SC, Wadhwa R, Sundar D. Withanone and caffeic acid phenethyl ester are predicted to interact with main protease (M^{pro}) of SARS-CoV-2 and inhibit its activity. *J Biomol Struct Dyn.* 2020. doi:10.1080/07391102.2020.1772108

- 1265 14. Kumar V, Dhanjal JK, Bhargava P, et al. Withaferin-A are predicted to interact with transmembrane protease serine 2 (TMPRSS2) and block entry of SARS-CoV-2 into cells. *J Biomol Struct Dyn*. 2020. doi:10.1080/07391102.2020.1775704
- 1270 15. Sudeep H. Molecular docking analysis of Withaferin A from *Withania somnifera* with the glucose regulated protein 78 (GRP78) in comparison with the COVID-19 main protease. *Bioinformation*. 2020;16(5):411–417. doi:10.6026/97320630016411
- 1275 16. Case JB, Rothlauf PW, Chen RE, et al. Neutralizing antibody and soluble ACE2 inhibition of a replication-competent VSV-SARS-CoV-2 and a clinical isolate of SARS-CoV-2. *SSRN Electron J*. 2020. doi:10.2139/ssrn.3606354
- 1285 17. Battle D, Wysocki J, Satchell K. Soluble angiotensin-converting enzyme 2: a potential approach for coronavirus infection therapy? *Clin Sci*. 2020;134(5):543–545. doi:10.1042/CS20200163
- 1280 18. Inal JM. Decoy ACE2-expressing extracellular vesicles that competitively bind SARS-CoV-2 as a possible COVID-19 therapy. *Clin Sci*. 2020;134(12):1301–1304. doi:10.1042/CS20200623
- 1285 19. Walter JD, Hutter CAJ, Zimmermann I, et al. Sybodies targeting the SARS-CoV-2 receptor-binding domain. *bioRxiv*. 2020. doi:10.1101/2020.04.16.045419
- 1290 20. Kaul SC, Ishida Y, Tamura K, et al. Novel methods to generate active ingredients-enriched *Ashwagandha* leaves and extracts. *PLoS One*. 2016;11(12):1–15. doi:10.1371/journal.pone.0166945
- 1290 21. Dutta R, Khalil R, Green R, Mohapatra SS, Mohapatra S. *Withania somnifera* (*Ashwagandha*) and withaferin a: potential in integrative oncology. *Int J Mol Sci*. 2019;20(21):21. doi:10.3390/ijms20215310
- 1295 22. Pires N, Gota V, Gulia A, Hingorani L, Agarwal M, Puri A. Safety and pharmacokinetics of Withaferin-A in advanced stage high grade osteosarcoma: a Phase I trial. *J Ayurveda Integr Med*. 2020;11(1):68–72. doi:10.1016/j.jaim.2018.12.008
- 1300 23. Burgos JS, Ripoll-gomez J, Alfaro JM, Sastre I, Valdivieso F. Zebrafish as a new model for herpes simplex virus type 1 infection. *Zebrafish*. 2008;5(4):323–333. doi:10.1089/zeb.2008.0552
- 1300 24. Crim MJ, Riley LK. Viral diseases in zebrafish: what is known and unknown. *ILAR J*. 2012;53(2):135–143. doi:10.1093/ilar.53.2.135
- 1305 25. Pressley ME, Phelan PE, Witten PE, Mellon MT, Kim CH. Pathogenesis and inflammatory response to *Edwardsiella tarda* infection in the zebrafish. *Dev Comp Immunol*. 2005;29(6):501–513. doi:10.1016/j.dci.2004.10.007
- 1305 26. Das CN, Uniyal GC, Lal P, et al. Analysis of withanolides in root and leaf of *Withania somnifera* by HPLC with photodiode array and evaporative light scattering detection. *Phytochem Anal*. 2008;19(2):148–154. doi:10.1002/pca.1029
- 1310 27. Pettersen EF, Goddard TD, Huang CC, et al. UCSF chimera - a visualization system for exploratory research and analysis. *J Comput Chem*. 2004;25(13):1605–1612. doi:10.1002/jcc.20084
- 1315 28. Luthy R, Bowie JU, Eisenberg D. Assessment of protein models with three-dimensional profiles. *Nature*. 1992;356(6364):83–85. doi:10.1038/356083a0
- 1315 29. Colovos C, Yeates TO. Verification of protein structures: patterns of nonbonded atomic interactions. *Protein Sci*. 1993;2(9):1511–1519. doi:10.1002/pro.5560020916
- 1320 30. Laskowski RA, MacArthur MW, Moss DS, Thornton JM. PROCHECK: a program to check the stereochemical quality of protein structures. *J Appl Crystallogr*. 1993;26(2):283–291. doi:10.1107/s0021889892009944
- 1325 31. Lovell SC, Davis IW, Adrendall WB, et al. Structure validation by C alpha geom basic local alignment search tool. *J Mol Biol*. 2003;50(August2002):437–450. doi:10.1002/pro.10286
- 1325 32. O'Boyle NM, Banck M, James CA, Morley C, Vandermeersch T, Hutchison GR. Open babel: an open chemical toolbox - 1758-2946-3-33.pdf. *J Cheminform*. 2011;3(33):1–14. doi:10.1186/1758-2946-3-33
- 1330 33. Fukunishi Y, Nakamura H. Prediction of ligand-binding sites of proteins by molecular docking calculation for a random ligand library. *Protein Sci*. 2011;20(1):95–106. doi:10.1002/pro.540
34. Ghersi D, Sanchez R. Improving accuracy and efficiency of blind protein-ligand docking by focusing on predicted binding sites. *Proteins*. 2009;74(2):417–424. doi:10.1002/prot.22154
35. Dallakyan S, Olson AJ. Small-molecule library screening by docking with PyRx. In: Hempel JE, Ai E, editors. *Chemical Biology: Methods in Molecular Biology*. Vol. 1263. New York, NY: Humana Press; 2015: 243–250. doi:10.1007/978-1-4939-2269-7_19
36. Dassault. *Dassault Systèmes BIOVIA, Discovery Studio 2017 R2 Client, Release 2017*. San Diego: Dassault Systèmes; 2017.
37. DeLano WL. Pymol: an open-source molecular graphics tool. *CCP4 News! Protein Crystallogr*. 2002;40:82–92.
38. Humphrey W, Dalke A, Theoretical KS. VMD: visual molecular dynamics. *J Mol Graph*. 1996;14(1):33–38. doi:10.1016/j.carbon.2017.07.012
39. Jo S, Kim T, Iyer VG, Im W. CHARMM-GUI: a web-based graphical user interface for CHARMM. *J Comput Chem*. 2008;29(11):1859–1865. doi:10.1002/jcc
40. Phillips JC, Braun R, Wang W, et al. Scalable molecular dynamics with NAMD. *J Comput Chem*. 2005;26(16):1781–1802. doi:10.1002/jcc.20289
41. Hendsch ZS, Tidor B. Do salt bridges stabilize proteins? A continuum electrostatic analysis. *Protein Sci*. 1994;3(2):211–226. doi:10.1002/pro.5560030206
42. Li L, Li C, Sarkar S, et al. DelPhi: a comprehensive suite for DelPhi software and associated resources. *BMC Biophys*. 2012;5(1):9. doi:10.1186/2046-1682-5-9
43. Sitkoff D, Sharp KA, Honig B. Accurate calculation of hydration free energies using macroscopic solvent models. *J Phys Chem*. 1994;98(7):1978–1988. doi:10.1021/j100058a043
44. Fogolari F, Brigo A, Molinari H. The Poisson-Boltzmann equation for biomolecular electrostatics: a tool for structural biology. *J Mol Recognit*. 2002;15(6):377–392. doi:10.1002/jmr.577
45. Altmann SM, Mellon MT, Distel DL, Kim CH. Molecular and functional analysis of an interferon gene from the zebrafish, *danio rerio*. *J Virol*. 2003;77(3):1992–2002. doi:10.1128/JVI.77.3.1992
46. Igawa D, Sakai M, Savan R. An unexpected discovery of two interferon gamma-like genes along with interleukin (IL) -22 and -26 from teleost: IL-22 and -26 genes have been described for the first time outside mammals. *Mol Immunol*. 2006;43(7):999–1009. doi:10.1016/j.molimm.2005.05.009
47. Praveen K, Evans DL, Jaso-friedmann L. Constitutive expression of tumor necrosis factor-alpha in cytotoxic cells of teleosts and its role in regulation of cell-mediated cytotoxicity. *Mol Endocrinol*. 2006;43:279–291. doi:10.1016/j.molimm.2005.01.012
48. Sullivan C, Kim CH. Zebrafish as a model for infectious disease and immune function. *Fish Shellfish Immunol*. 2008;25(4):341–350. doi:10.1016/j.fsi.2008.05.005
49. Vinayagam S, Sattu K. SARS-CoV-2 and coagulation disorders in different organs. *Life Sci*. 2020;260:118431. doi:10.1016/j.lfs.2020.118431
50. Giannis D, Ziogas IA, Gianni P. Coagulation disorders in coronavirus infected patients: COVID-19, SARS-CoV-1, MERS-CoV and lessons from the past. *J Clin Virol*. 2020;127:104362. doi:10.1016/j.jcv.2020.104362
51. Catanzaro M, Fagiani F, Racchi M, Corsini E, Govoni S, Lanni C. Immune response in COVID-19: addressing a pharmacological challenge by targeting pathways triggered by SARS-CoV-2. *Signal Transduct Target Ther*. 2020;5(84):1–10. doi:10.1038/s41392-020-0191-1
52. Soleimani M. Acute kidney injury in SARS-CoV-2 infection: direct effect of virus on kidney proximal tubule cells. *Int J Mol Sci*. 2020;21(3275):2–6. doi:10.3390/ijms21093275
53. Prabakaran P, Gan J, Feng Y, et al. Structure of severe acute respiratory syndrome coronavirus receptor-binding domain complexed with neutralizing antibody. *J Biol Chem*. 2006;281(23):15829–15836. doi:10.1074/jbc.M600697200

- 1400 54. Li F, Li W, Farzan M, Harrison SC. Structural biology: structure of SARS coronavirus spike receptor-binding domain complexed with receptor. *Science*. 2005;309(5742):1864–1868. doi:10.1126/science.1116480
55. Barlow DJ, Thornton JM. The distribution of charged groups in proteins. *Biopolymers*. 1986;25(9):1717–1733. doi:10.1002/bip.360250913
- 1405 56. Xu D, Lin SL, Nussinov R. Protein binding versus protein folding: the role of hydrophilic bridges in protein associations. *J Mol Biol*. 1997;265(1):68–84. doi:10.1006/jmbi.1996.0712
57. Norel R, Wolfson HJ, Nussinov R. Small molecule recognition: solid angles surface representation and molecular shape complementarity. *Comb Chem High Throughput Screen*. 1999;2(4):223–236.
- 1410 58. Jin Z, Du X, Xu Y, et al. Structure of M^{pro} from SARS-CoV-2 and discovery of its inhibitors. *Nature*. 2020;582(7811):289–293. doi:10.1038/s41586-020-2223-y
- 1415 59. Yang H, Xie W, Xue X, et al. Design of wide-spectrum inhibitors targeting coronavirus main proteases. *PLoS Biol*. 2005;3:10. doi:10.1371/journal.pbio.0030324
60. Castro-Alvarez A, Costa AM, Vilarrasa J. The performance of several docking programs at reproducing protein-macrolide-like crystal structures. *Molecules*. 2017;22(1):1. doi:10.3390/molecules22010136
61. Hamza M, Ali A, Khan S, et al. nCoV-19 peptides mass fingerprinting identification, binding, and blocking of inhibitors flavonoids and anthraquinone of *Moringa oleifera* and hydroxychloroquine. *J Biomol Struct Dyn*. 2020:1–11. doi:10.1080/07391102.2020.1778534. 1420
62. Hubbard S, Darmani NA, Thrush GR, Dey D, Burnham L. Zebrafish-encoded 3-O-sulfotransferase-3 isoform mediates herpes simplex virus type 1 entry and spread. *Zebrafish*. 2010;7(2):181–187. doi:10.1089/zeb.2009.0621. 1425
63. Wu C, Liu Y, Yang Y, et al. Analysis of therapeutic targets for SARS-CoV-2 and discovery of potential drugs by computational methods. *Acta Pharm Sin B*. 2020;10(5):766–788. doi:10.1016/j.apsb.2020.02.008. 1430
64. Gautret P, Lagier J-C, Parola P, et al. Hydroxychloroquine and azithromycin as a treatment of COVID-19: results of an open-label non-randomized clinical trial. *Int J Antimicrob Agents*. 2020;56(1):105949. doi:10.1016/j.ijantimicag.2020.105949. 1435

Drug Design, Development and Therapy

Dovepress

Publish your work in this journal

Drug Design, Development and Therapy is an international, peer-reviewed open-access journal that spans the spectrum of drug design and development through to clinical applications. Clinical outcomes, patient safety, and programs for the development and effective, safe, and sustained use of medicines are a feature of the journal, which has also

been accepted for indexing on PubMed Central. The manuscript management system is completely online and includes a very quick and fair peer-review system, which is all easy to use. Visit <http://www.dovepress.com/testimonials.php> to read real quotes from published authors.

Submit your manuscript here: <https://www.dovepress.com/drug-design-development-and-therapy-journal>



Article

Validation of a Novel Zebrafish Model of Dengue Virus (DENV-3) Pathology Using the Pentaherbal Medicine Denguenil Vati

Acharya Balkrishna ^{1,2}, Siva Kumar Solleti ¹, Sudeep Verma ¹ and Anurag Varshney ^{1,2,*}

¹ Drug Discovery and Development Division, Patanjali Research Institute, NH-58, Haridwar 249 405, Uttarakhand, India; pyp@divyayoga.com (A.B.); siva.kumar@prft.co.in (S.K.S.); sudeep.verma@prft.co.in (S.V.)

² Department of Allied and Applied Sciences, University of Patanjali, Patanjali Yog Peeth, Roorkee-Haridwar Road, Haridwar 249 405, Uttarakhand, India

* Correspondence: anurag@prft.co.in; Tel.: +91-13-3424-4107 (ext. 7458)

Received: 18 May 2020; Accepted: 22 June 2020; Published: 28 June 2020

Abstract: Dengue is a devastating viral fever of humans, caused by dengue virus. Using a novel zebrafish model of dengue pathology, we validated the potential anti-dengue therapeutic properties of pentaherbal medicine, Denguenil Vati. At two different time points (at 7 and 14 days post infection with dengue virus), we tested three translational doses (5.8 µg/kg, 28 µg/kg, and 140 µg/kg). Dose- and time-dependent inhibition of the viral copy numbers was identified upon Denguenil Vati treatment. Hepatocyte necrosis, liver inflammation, and red blood cell (RBC) infiltration into the liver were significantly inhibited upon Denguenil treatment. Treatment with Denguenil Vati significantly recovered the virus-induced decreases in total platelet numbers and total RBC count, and concomitantly increasing hematocrit percentage, in a dose- and time-dependent manner. Conversely, virus-induced white blood cell (WBC) counts were significantly normalized. Virus-induced hemorrhage was completely abrogated by Denguenil after 14 days, at all the doses tested. Gene expression analysis identified a significant decrease in disease-induced endothelial apoptotic marker Angiopoietin2 (*Ang-2*) and pro-inflammatory chemokine marker *CCL3* upon Denguenil treatment. Presence of gallic acid, ellagic acid, palmetin, and berberine molecules in the Denguenil formulation was detected by HPLC. Taken together, our results exhibit the potential therapeutic properties of Denguenil Vati in ameliorating pathological features of dengue.

Keywords: dengue virus; DENV; zebrafish model; gene expression; Denguenil Vati

1. Introduction

Dengue is an important mosquito-transmitted viral hemorrhagic fever of humans caused by the infection of dengue virus (DENV) primarily in tropical and subtropical countries [1]. As per the Center for Disease Control, USA, dengue is endemic in more than 100 countries, with an estimated 400 million infections each year [2], of which approximately 100 million people get sick from infection [3]. It has been predicted that more than 40% of the world's population are at risk of dengue infection [4]. With the rapid spread of DENV, which is now prevalent in Asia, Africa, and the Americas, dengue has become a major public health threat worldwide [5].

DENV is an enveloped positive-sense ssRNA virus of the Flaviviridae family [5]. There are four serotypes of the virus exist (DENV-1, 2, 3, and 4) [6] and all elicit a similar range of disease manifestations during infection [7]. The first infection with dengue virus typically results in either no symptoms or a mild illness that can be mistaken for the flu or another viral infection. Dengue viral infection causes a spectrum of illnesses ranging from asymptomatic to causing mild dengue Fever

(DF), joint pains, rashes, and other mild symptoms [8]. The feature of DF includes vascular leakage, thrombocytopenia, and coagulopathy [9].

Upon inoculation, DENV is thought to infect Langerhans cells, and then migrate through the lymphatic system and the infection spreads to various cells of hematopoietic lineages, including macrophages, monocytes, before spreading systemically [10]. Liver is an important target for DENV infection [11]. DENV induces both innate and acquired immune responses upon infection. Innate immune response, includes complement and type I Interferon (IFN) [12] and acquired immune response involves serotype-specific CD8+ and CD4+ T cells, lysis of DENV-infected cells and production of various cytokines, such as IFN- γ , TNF- α , CCL3, and lymphotoxin [6,13,14].

Development of an appropriate animal model for DENV infection has been hindered by lack of replication of DENV clinical isolates in wild-type (WT) mice; and the lack of clinical disease in nonhuman primates. Nonhuman primates can sustain DENV replication even after inoculation with the presumed mosquito inoculation in humans [15] and occasionally display only low platelet counts and no other overt clinical signs of DENV infection [16], such as fever, anorexia, or lethargy [17]. Further, mouse models of dengue did not show human clinical signs of dengue viral infection, but developed neurotropic disease, which is not generally observed in humans [18]. While few strains of mice support minimal replication of DENV, other strains show signs of paralysis and DENV infection induces limited DENV pathogenesis, such as liver damage, increased white blood cell counts, and thrombocytopenia [19]. Further, lack of a suitable small-animal model of dengue infection has greatly hindered the study of dengue pathogenesis and the development of novel therapeutics [20,21].

Zebrafish (*Danio rerio*) is an excellent model organism to investigate complex biological processes [22]. Besides traditional host models such as mice, zebrafish offers a well-developed immune system with both innate and adaptive immune responses. Further, its remarkable similarities to the human system and signaling pathways involved in the immune response has made zebrafish a greatly used model to research host–pathogen interactions, including viral infections and antiviral drug screening, hence providing original therapeutic avenues [23]. Further, use of zebrafish for disease modelling of rare genetic blood diseases and for drug discovery in Parkinson's disease and other movement disorders is apparent [24,25]. In the context of viral infections, zebrafish models have unexpected idiosyncrasies among organs that may apply to the human situation [22].

Imbalance of host response to the infection results in severe dengue. Currently, there is no licensed therapeutic drug available to treat dengue [26]. Therapeutic modulation to inhibit or mitigate the progression of the disease has been investigated for many decades. However, these intensive efforts to develop antiviral drugs as well as clinical trials using repurposing drugs or with natural products to prevent the plasma leakage have not been encouraging so far. While the development of vaccines has been held back for a while due to the lack of a good animal model and the complexity of disease [27], the FDA has recently approved Dengvaxia® [3], the only available vaccine against dengue.

Despite being an old disease, therapeutic options available for prevention and control of DENV infection are severely limited. Hence, developments of cost effective, efficacious prophylactic/therapeutic drugs against DENV are needed. Many plant-derived herbal medicines and purified natural compounds have been shown to exert antiviral effects in animal studies and human clinical trials [28]. Natural products are a potent source of combinatorial chemicals as they contain structurally diverse bioactive chemicals, thus making them a valuable resource for novel drug discovery. Natural products and their derivatives accounted for 34 % of new medicines approved by the US Food and Drug Administration (FDA) between 1981 and 2010 [29]. Further, natural products are more likely to reach the site of action and have better coverage of biologically relevant chemical space [29,30]. Uses of several natural products against dengue viral infection have been reported [31–33].

Denguenil Vati is a pentaherbal Indian traditional formulation that has been prescribed by ayurvedic practitioners for the treatment of dengue infection in India. However, its anti-dengue viral properties have not yet been explored scientifically. Denguenil consists of extracts from *Tinospora cordifolia* (Willd.) Miers, *Aloe vera* (L.) Burm.f, *Carica papaya* L., *Punica granatum* L., and *Ocimum*

sanctum L. The aim of the present research work is to validate potential antidengue therapeutic properties of Denguenil *in vivo* using the zebrafish model of disease. In addition, HPLC analysis was undertaken to quantify chemical fingerprints present in the Denguenil and their correlation with observed biological responses.

2. Materials and Methods

2.1. Ethics Statement

All the animal experiments were performed according to ethical guidelines as per the Committee for the Purpose of Control and Supervision of Experiments (CPCSEA), Government of India; and the established zebrafish protocols were approved (IAEC study number- 218/Go062019/IAEC) by Institutional Animal Care and Ethics Committee. Informed written consent was obtained from all patients. The collection and storage of patient serum samples were also approved by the institute's ethical committee (Approval number- 218/IEC/062019/Pent/TN). All methods were carried out in accordance with relevant guidelines and regulations of the relevant ethical committee.

2.2. Zebrafish Care and Maintenance

Zebrafish were maintained in the dedicated zebrafish research facility according to IAEC standards. IAEC approved guidelines for zebrafish care followed the standard procedures of a 14 h light, 10 h dark cycle at 28 °C. Zebrafish of similar bodyweight were selected for the experimental study and were housed in polycarbonate tank at a stocking density of 2 liters of water per fish.

2.3. Propagation of Dengue Virus (Serotype, DENV-3) in Zebrafish

Human serum samples were collected with informed patient consent at the source clinic and transferred to the laboratory for the study. The samples were obtained from a total of three male dengue-positive subjects, within age groups of 21 to 45 who had fever accompanied with joint and muscle pain. All the patients confirmed to not having other comorbid conditions. Fresh serum samples from these dengue-positive patients (Serotype, DENV-3) were maintained at 4 °C under controlled conditions and were used within 96 h of collection. Briefly, samples were brought to room temperature in a water-bath just before use. Zebrafish were anesthetized by placing them in ice water (18 °C). The fish were held intact with a wet sponge, and an aliquot of 3 µL dengue-infected human serum was injected intramuscularly into the proximo-distal region of adult zebrafish (n = 10) as primary carrier and to propagate the virus. Fish receiving same volume of 0.1 % saline served as control. After injection, fish were transferred to water tank for recovery. After 14 days of viral induction, 1 µL each of serum samples were harvested from five primary carriers and diluted to 100 µL with sterile PBS for the study. From this, 3 µL of diluted serum from primary carriers were injected into the study fish.

2.4. Blood Collection Harvesting Serum from Carrier Zebrafish

Fish were euthanized in ice water and the fish surface was wiped dry. A sharp slit was made between the anal fin and the caudal fin region, thus isolating the caudal fin, and the fish was held with the wound facing down. Whole blood was collected at the dorsal aorta using a P20 micropipette fitted with an elongated tip and aspirated into prechilled microcentrifuge tubes. Both pipette tips and tubes were precoated with EDTA by submerging in 18 mg/mL EDTA solution for 24 h and then dried prior to use. The samples were centrifuged with 2% EDTA at high speed of 7000 rpm for 10 min. Following centrifugation, the serum was collected very carefully from the top layer, without disturbing the layers.

2.5. Dengue Viral Infection Study Design

After viral infection, the study groups (n = 24) were cotreated with Denguenil from day 7 for effective dose (ED) screening. Two time points were chosen for the effective dose screening after 7 and 14 days of Denguenil dosing (i.e., on the 8th day and 15th day) of viral-serum-infected zebrafish. Virus-infected zebrafish receiving serum plus PBS served as the disease control; fish receiving only PBS without any virus served as the normal control.

2.6. Preparation of Zebrafish Test Feed and Dosing

The study compound, Denguenil, was mixed and ground with a known volume of fish feed, then extruded to pellets of standard size weighing 4 mg per pellet for dosing. A 24 h feeding cycle was followed throughout the study period. Test article information for each study group was blind coded for investigators and fish-handlers. In the present study, Denguenil was crushed and diluted with PBS. For preparing fish feed, the required volume of Denguenil was mixed with feed and extruded. For control group, fish feed was mixed with an equal volume of PBS without drug and extruded. Hence, fish feed containing Denguenil was used to treat disease model, whereas fish receiving normal feed without Denguenil served as the control.

2.7. Harvesting Liver Tissue and Caudal Fins for Histopathology

On the last day of the experiment, zebrafish were euthanized with cold water and an incision was made in the viscera to harvest the livers. Livers were divided into two parts, for RNA isolation and for cell smear preparation. For RNA isolation, liver tissues were frozen in liquid nitrogen immediately after sectioning and stored at -80°C till further use. The caudal fin isolated was mounted on a slide for further observation.

2.8. RNA Isolation and Gene Expression Analysis

The total RNA was extracted from fresh tissue using RNAqueous[®]-Micro Kit (Thermo Fisher Scientific, Waltham, MA, USA) as per the manufacturer's instruction and rendered DNA free, quantified, and subsequently storing at -80°C . cDNA synthesis was performed using SuperScript II reverse transcriptase (Thermo Fisher Scientific, Waltham, MA, USA) employing Oligo(dT) primers and the target cDNA templates were amplified by PCR using gene specific primers with 2X PCR Master mix (Thermo Fisher Scientific, Waltham, MA, USA). After 40–50 cycles, the amplified products were quantified by mean absorbance using a standard 10 nanomoles reference. A total of 200 μL of QuantiFluor[®] ONE dsDNA System (Promega Corporation, Madison, WI, USA) was added to 10 μL of amplified cDNA, incubated at room temperature for 5 min and readings were made at (504 nm Ex/531 nm Em) using a Robonik microplate reader. The following primers for zebrafish sequences were used for the study.

DENV-3: Forward 5'-CGGGAAAACCGTCTATCAATATGC-3'

Reverse 5'-TGAGAATCTCTTCGCCAACTGTG-3'

CCL3: Forward 5'-CCGCGGATCCGACGATTTA-3'

Reverse 5'-AATGACTCCAGGCAGAGTGC-3'

ANG2: Forward 5'-TATTTGTGAGGTTTTCCGTTCCCATCGGGCT-3'

Reverse 5'-AGAGGACTATGAGAAGTCGGCTCCTCGGATCAT-3'.

2.9. Complete Blood Count

For complete blood analysis, whole blood was collected from each fish separately using heparinized microhematocrit tubes, and samples were centrifuged at 14,000 rpm for 13 min, resuspended in 1 mL phosphate buffered saline (PBS), and counted using a hemocytometer, before smears were made and stained with Hematoxylin and Eosin (H&E).

2.10. Hematoxylin and Eosin (H&E) Staining, Imaging, and Cell Counting

Fixed glass slides with sample smears were stained with H&E for 2 min each, followed by three PBS washes and allowed to dry at room temperature. Slides were viewed under microscope (Labomed 1× 400 microscope) at 45× magnification and bright field images were captured by Future Winjoe image capture system. One hundred cells were counted per field for quantification.

2.11. Cell Culture

The cell lines used in this study included human liver cancer cell lines, HepG2 cells, and human epidermoid carcinoma cell lines, A431 cells (purchased from ATCC licensed cell repository, National Centre for Cell Science (NCCS), Pune, India). Both of these cell lines were maintained in DMEM (Dulbecco's modified Eagle's medium; Invitrogen, USA) supplemented with 10% FCS and antibiotics. Cells were placed in a humidified incubator at 5% CO₂ at 37 °C. For in vitro experiments, cells were seeded at 2 × 10⁴ cells/well in 96-well plates and experimental treatments with Denguenil Vati was carried out for 24 h in DMEM + 1% FBS media at 70% confluence.

2.12. Cell Viability Assay

HepG2 and A431 cell viabilities were measured using Alamar blue reagent (Hi Media, India). Briefly, both HepG2 and A431 cells (2 × 10⁴ cells/well) were seeded in 96-well plates and treated for 24 h with various concentrations of Denguenil Vati (1–1000 µg/mL). Two hours before termination, 10 µL of Alamar blue (0.15 mg/mL) was added to each well. Cytotoxicity was measured by reading fluorescence at Ex. 540/Em. 590, using an Envision microplate reader (Perkin Elmer, Waltham, MA, USA).

2.13. Reactive Oxygen Species (ROS) Measurement

The intracellular ROS levels were quantified by a fluorescent probe, 2,7-dichlorofluorescein diacetate (DCFH-DA, Sigma, St. Louis, MO, USA). HepG2 and A431 cells were seeded in 96 well plates and treatment with various concentrations of Denguenil Vati (1–1000 µg/mL) for 24 h. Cells were washed with PBS and incubated with DCF-DA (10 µg/mL) in serum free DMEM for 1 h in dark. The ROS production was quantified by measuring DCF fluorescence intensity at Ex. 495/Em. 527 using Envision microplate reader (Perkin Elmer, Waltham, MA, USA). Results were expressed as the percentage of ROS generation, as compared to untreated control cells.

2.14. Malondialdehyde (MDA) Estimation

Lipid peroxidation was estimated by measuring the levels of malondialdehyde (MDA) in cell culture spent medium. MDA estimation assay was based on the reaction of MDA with Thio-Barbituric acid (TBA); forming an MDA–TBA adduct [34]. Its absorption at 532 nm was measured using an Envision microplate reader (Perkin Elmer, Waltham, MA, USA) and normalized with untreated control cells.

2.15. Preparation of Denguenil Sample for HPLC

Denguenil was sourced from Divya Pharmacy, Haridwar, India (Batch number A-DNV014). Tablets were crushed into fine powder; 10 mL methanol was added to 0.5 gm of powdered sample; and sonicated (Thermo Fisher Scientific, Waltham, MA, USA) for 30 min. The samples were centrifuged at 8000 rpm for 5 min; filtered using 0.45 µm nylon filter (Sol A); and used for the analysis of chemical signatures present. The samples were analyzed using gallic acid, and ellagic acid (Sigma Aldrich); palmetin and berberine (Natural Remedies, Bengaluru, India) as reference standards with purity ≥ 98.0%.

The quantification of signature compounds was performed using High Performance Liquid Chromatography (Waters Corporation, Milford, MA, USA) equipped with binary pump (1525), PDAD (2998) and autosampler (2707) using a Shodex C18-4E (4.6 mm ID × 250 mm L) column at a

flow rate of 1.0 mL/min. The filtered solution (Sol A) was used for the analysis of palmetin and berberine. Next, 2.0 mL of Sol A was diluted to 5 mL with same solvent and used for the analysis of ellagic acid and gallic acid. The chromatographs were recorded at 270 nm (gallic acid and ellagic acid) and 346 nm (palmetin and berberine) wavelengths.

2.16. Statistical Analysis

All in vivo experiments were conducted with multiple replicates ($n = 24$), and in vitro experiments were conducted at least thrice in triplicates and data are expressed as means \pm SEM. Comparisons between experimental groups were made by one-way ANOVA, followed by Dunnett's multiple comparison post hoc test. Differences in mean values were considered significant at $p < 0.05$. Significance of data were analyzed using GraphPad Prism 7.03.3.

3. Results

3.1. Study Design for Translational Dosing

Dengue is a mosquito-borne viral fever of humans with limited therapeutic options [26]. In the present investigation, we screened for the translational effective dose (ED) of ayurvedic herbal formulation, Denguenil. Considering the body weights and body surface area of adult zebrafish and human, the translational dose of Denguenil was determined to be 1000 times less than the relative human dose, as described [35,36]. Human serum infected with dengue virus (DENV-3) was propagated in primary carrier fish. After 14 days, the serum was harvested from carrier fish, diluted, and injected into study fish. A week after injection, the study fish were cotreated with Denguenil-impregnated feed until the termination of the study (Figure 1A). At first, 50% tissue culture infective dose (TCID₅₀) for DENV-3 was titrated using an end point neutralization assay employing VeroE6 cell lines and calculated using the Reed–Muench method to be 420 TCID₅₀/mL. For induction of the disease model, 1 μ L of serum from carrier zebrafish was diluted with PBS to a final concentration of 1 TCID₅₀/mL and a total of 3 TCID₅₀ was used as the induction dose. In the present investigation, fish were fed with the indicated doses individually in separated tanks, and once the dosing was complete, they were put back into the original tank for housing.

In an effort to identify the maximum therapeutic efficacy of Denguenil in dengue model of zebrafish, a wide range of translational effective doses were tested in the present study with 0.2 \times (ED-1, 5.6 μ g/kg), 1 \times (ED-2, 28 μ g/kg), and 5 \times (ED-3, 140 μ g/kg) dose of the Denguenil translated from the human prescribed dose (1000 mg/day, BID); these were used to identify the effective dose with maximum therapeutic efficacy. Further, two time points were chosen for the effective dose screening after 7 and 14 days of Denguenil dosing (i.e., on the 8th day and 15th day) of viral-serum-infected zebrafish (Figure 1A). The course of dengue infection included disease initiation, in which hypoactivity, body discoloration, and RBC infiltration were noticed. The critical progression phase showed vascular hemorrhage, hepatocyte necrosis, elevated expression of DENV-3 viral transcripts, and concomitant increase in Ang-2 and CCL3 expression.

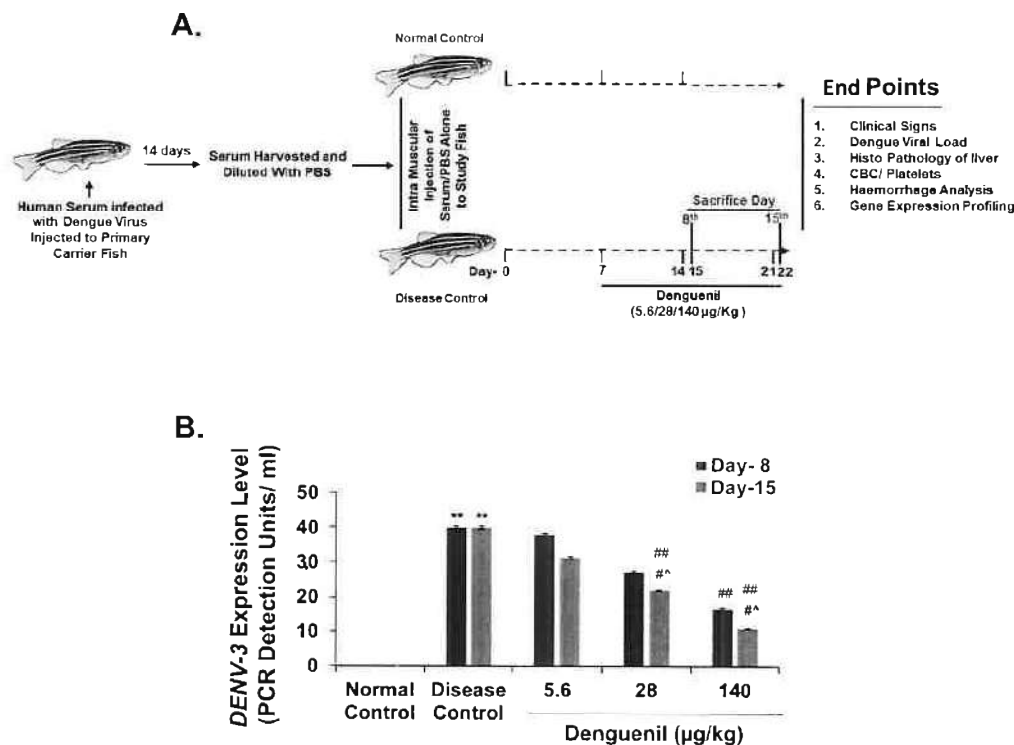


Figure 1. Denguenil inhibits dengue virus (DENV) transcript levels. **(A)** Schematic representation of zebrafish model of dengue viral pathology. Human serum infected with dengue virus was propagated in primary carrier fish. Study zebrafish ($n = 24$) were injected with dengue virus (DENV-3) (Disease Control) or PBS as in control (Normal Control) and treated with three different effective doses (5.6 µg/kg, 28 µg/kg, and 140 µg/kg Denguenil) for various time points. **(B)** Whole RNA from liver tissue was analyzed by quantitative real-time PCR (qPCR) for the dengue viral load. Virus induced increases in the DENV-3 copy number were decreased upon Denguenil treatment. $n = 24$, data are presented as means \pm SEM. **, ##, #^ $p < 0.001$, * Represents significant compared to Normal Control; ##, # Represents significant compared to their respective Disease Controls; #^ Represents significant among two time points.

3.2. Denguenil Inhibited DENV-3 Viral Transcript Copy Numbers

We screened for the expression of dengue viral biomarker (DENV-3) in the liver samples. The results indicated an active viral infection in the Disease Control. Dengue viral infection resulted in forty-fold increased DENV-3 transcript copy number (Figure 1B) in both the 8th day group (Normal Control, 0 PDU/mL vs. 40 PDU/mL, Disease Control, $p < 0.0001$) and 15th day group (Normal Control, 0 PDU/mL vs. 40 PDU/mL, Disease Control, $p < 0.0001$), whereas no DENV3 copies were detected in Normal Control. Irrespective of time point, Denguenil administration resulted in a dose-dependent decrease in DENV-3 transcript copy numbers (Figure 1B). While a 58% decrease (40 PDU/mL vs. 17 PDU/mL, $p < 0.0001$) in DENV-3 copy number was detected on the 8th day at 140 µg/kg dose, the copy number further decreased to 72% on the 15th day (40 PDU/mL vs. 11 PDU/mL, $p < 0.0001$) (Figure 1B).

3.3. Denguenil Inhibited Dengue Virus Induced Hepatocyte Necrosis

We examined the hepatopathological features using hematoxylin and eosin staining of the liver smears. Control liver smears from both 8th and 15th day group showed normal and intact hepatocytes with well-defined cellular architectures (Figure 2A, F). Dengue viral infection in Disease Control fish resulted in a 39% increase in cell necrosis by the 8th day, with a majority of shrunken cells (Figure 2B). Further, the necrosis was significantly increased to 41% by 15th day with shrunken and darkly stained necrotic hepatic cells (Figure 2G), (Disease Control, 8th day group, 39% vs. 41%, 15th day group, $p < 0.0001$) (Figure 3A). Conversely, Denguenil treatment significantly inhibited the hepatocyte necrosis at both time points in a dose-dependent manner (Figures 2C–E, H–J and 3A). At 5.6 $\mu\text{g}/\text{kg}$ Denguenil, a modest decrease in the necrosis was identified on both 8th and 15th days compared to the disease controls (8th day group, Disease Control, 39% vs. 33%, 5.6 $\mu\text{g}/\text{kg}$ Denguenil, $p < 0.0001$; 15th day group, Disease Control, 41% vs. 40%, 5.6 $\mu\text{g}/\text{kg}$ Denguenil, $p < 0.05$) (Figures 2C, H and 3A). While drug treatment decreased necrosis to 29% on the 8th day (Disease Control, 39% vs. 29%, 28 $\mu\text{g}/\text{kg}$ Denguenil, $p < 0.0001$), the necrosis was further decreased to 22% by the 15th day (Disease Control, 41% vs. 22%, 28 $\mu\text{g}/\text{kg}$ Denguenil, $p < 0.0001$), suggesting a significant inhibition of hepatic cell necrosis by 45% upon receiving 28 $\mu\text{g}/\text{kg}$ Denguenil in the 15th day group (Figures 2D, I and 3A). Denguenil at 140 $\mu\text{g}/\text{kg}$ has been found to be the effective dose with maximum protection (86%) from dengue viral damage in the 15th day group. In fish receiving 140 $\mu\text{g}/\text{kg}$ Denguenil, while 16% sparsely scattered necrotic cells were identified in the 8th day group (8th day group, Disease Control, 39% vs. 16%, 140 $\mu\text{g}/\text{kg}$ Denguenil, $p < 0.0001$), the necrosis was significantly attenuated to 6% in the 15th day group, indicating 86% inhibition of hepatocyte necrosis compared to Disease Control (15th day, Disease Control, 41% vs. 6%, 140 $\mu\text{g}/\text{kg}$ Denguenil, $p < 0.0001$) (Figures 2E, J and 3A).

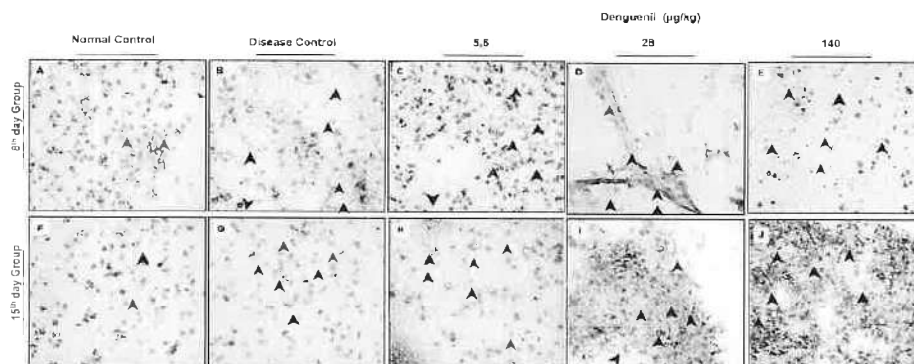


Figure 2. Smear pathology examination of liver showing the protective effect of Denguenil. Hematoxylin and eosin (H&E) staining and analysis was performed on liver smears from different groups containing various doses to assess the anatomy and cellular damage upon DENV-3 infection, and protective effect of Denguenil on cellular phenotypes. (A, F) Normal Control. (B, G) Disease Control. (C, H) 5.6 $\mu\text{g}/\text{kg}$ Denguenil. (D, I) 28 $\mu\text{g}/\text{kg}$ Denguenil. (E) 140 $\mu\text{g}/\text{kg}$ Denguenil, 8th day group. (J) 140 $\mu\text{g}/\text{kg}$ Denguenil, 15th day group. Black arrowheads indicate normal and intact cells; red arrowheads indicate necrotic cells, and blue arrowheads indicate inflammatory cells. Representative images from each group ($n = 24$) are shown. Original magnification, 40 \times .

3.4. Denguenil Inhibited Dengue-Virus-Induced Liver Inflammation

Inflammatory cell accumulation is a hallmark of viral infection. We therefore examined the inflammatory cell accumulation in liver upon dengue viral infection. Normal Control liver smears showed no inflammatory cell accumulation (Figure 3B). However, dengue-virus-induced inflammatory cell accumulation was observed in the livers of Disease Control fish with 19% inflammation on the 8th day; this active inflammation significantly progressed to 22% ($p < 0.0001$) by the 15th day. The Denguenil treatment groups showed a decrease in liver inflammation compared to Disease Control (Figure 3B). In the 5.6 $\mu\text{g}/\text{kg}$ Denguenil group, the inflammation was significantly

decreased by 15% in the 8th day group (Disease Control, 19% vs. 16%, 5.6 $\mu\text{g}/\text{kg}$ Denguenil, $p < 0.0001$) and 9% in the 15th day group (Disease Control, 22% vs. 20%, 5.6 $\mu\text{g}/\text{kg}$ Denguenil, $p < 0.0001$) respectively. In the 28 $\mu\text{g}/\text{kg}$ Denguenil group, while the inflammation was reduced by 37% in the 8th day group (Disease Control, 19% vs. 12%, 28 $\mu\text{g}/\text{kg}$ Denguenil, $p < 0.0001$), the inflammation was further decreased to 56% in the 15th day group (Disease Control, 22% vs. 9%, 28 $\mu\text{g}/\text{kg}$ Denguenil, $p < 0.0001$) (Figure 3B). Interestingly, 140 $\mu\text{g}/\text{kg}$ Denguenil at both time points exhibited significantly abrogated inflammation compared to Disease Control in both the 8th day group (Disease Control, 19% vs. 0%, 140 $\mu\text{g}/\text{kg}$ Denguenil, $p < 0.0001$) and the 15th day group (Disease Control, 22% vs. 0%, 140 $\mu\text{g}/\text{kg}$ Denguenil, $p < 0.0001$) (Figure 3B), suggesting the therapeutic benefit of Denguenil and complete protection at this dose from dengue-virus-induced liver inflammation.

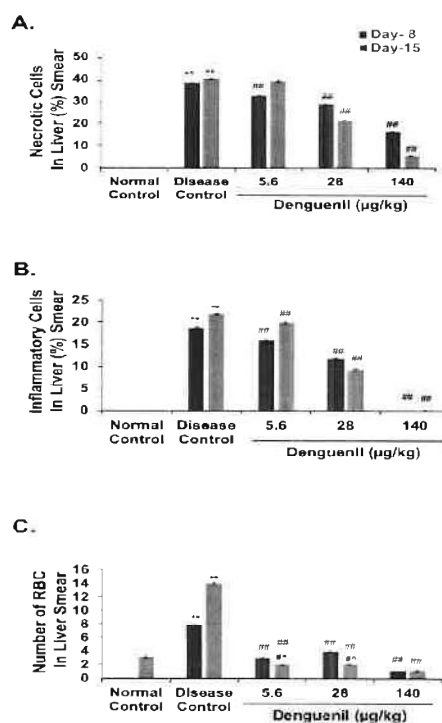


Figure 3. Denguenil treatment inhibits hepatic cell necrosis and inflammation, and red blood cell (RBC) infiltration into liver. H&E staining and analysis was performed on liver smears from different groups at the 8th day and 15th day time points. Percentage necrosis, inflammation, and RBCs present in liver smear were quantified. (A) Denguenil treatment inhibited the dengue-virus-induced hepatic cell necrosis in a dose-dependent manner with the maximum protection at 15th day time point in the 140 $\mu\text{g}/\text{kg}$ group. (B) Denguenil treatment inhibited the dengue virus induced liver inflammation in a dose-dependent manner. (C) RBC infiltration into liver was inhibited upon Denguenil treatment. $n = 24$, data are presented as means \pm SEM. **, ##, #^ $p < 0.001$. ** Represents significant compared to Normal Control; ## Represents significant compared to their respective Disease Controls; #^ Represents significant among two time points.

3.5. Denguenil Attenuated Dengue-Virus-Induced RBC Infiltration into Liver

We measured virus-induced RBC infiltration in the liver (Figure 3C). The results indicated that the virus induced RBC infiltration in both the 8th day group (Normal Control, 0 vs. 8, Disease Control, $p < 0.0001$) and the 15th day group (Normal Control, 3 vs. 14, Disease Control, $p < 0.0001$) and treatment with Denguenil attenuated vascular leakage and RBC infiltration at both time points. The 140 $\mu\text{g}/\text{kg}$ dose of Denguenil showed a maximum attenuation of RBC infiltration compared to Disease Control on both the 8th day (Disease Control, 8 vs. 1, 140 $\mu\text{g}/\text{kg}$ Denguenil, $p < 0.0001$) and 15th day (Disease Control, 14 vs. 1, 140 $\mu\text{g}/\text{kg}$ Denguenil $p < 0.0001$) (Figure 3C). Further, the maximum percentage of protective response was observed on the 15th day compared to the 8th day (140 $\mu\text{g}/\text{kg}$ Denguenil, 8th day, 87% vs. 92%, 15th day, $p < 0.0001$) (Figure 3C).

3.6. Dengue-Virus-Infected Zebrafish Blood Phenotyping Identified Protective Effects of Denguenil

Blood phenotyping was performed to assess the accumulation of various inflammatory cells. Normal Control group showed intact and well-defined healthy cells along with very few enlarged and swollen WBCs (Figure 4A. a, f). While dengue viral infection resulted in increased WBC count, a dose-dependent decrease in WBC was observed at both time points, with the highest percentage of protection in 140 $\mu\text{g}/\text{kg}$ Denguenil after 15 days (Figure 4B). Compared to Normal Control, dengue viral infection resulted in accumulation of poorly stained, swollen WBC (Figure 4A. b, g), in a time-dependent manner (Normal Control, 2.8×10^3 vs. 3.1×10^3 , 8th day, Disease Control, $p < 0.0001$; Normal Control, 2.8×10^3 vs. 3.3×10^3 , 15th day, Disease Control, $p < 0.0001$). The treatment with 5.6 $\mu\text{g}/\text{kg}$ Denguenil on the 8th day did not show protective response and was comparable to Disease Control (Disease Control, 3.1×10^3 vs. 3.1×10^3 , 5.6 $\mu\text{g}/\text{kg}$ Denguenil) (Figure 4B); Conversely, the WBC count was significantly reduced in the 15th day group upon receiving 5.6 $\mu\text{g}/\text{kg}$ Denguenil (Disease Control, 3.1×10^3 vs. 2.9×10^3 , 5.6 $\mu\text{g}/\text{kg}$ Denguenil, $p < 0.0001$) (Figure 4A. c, h and 4B). The WBC count was further decreased in the 28 $\mu\text{g}/\text{kg}$ Denguenil group on the 15th day compared to the 8th day (28 $\mu\text{g}/\text{kg}$ Denguenil, 8th day 3.0×10^3 vs. 2.9×10^3 , 15th day, $p < 0.0001$) (Figure 4A. d, i and 4B). Among the two time points, fish receiving 140 $\mu\text{g}/\text{kg}$ Denguenil showed significantly reduced WBC count on the 15th day compared to Disease Control (Disease Control, 3.1×10^3 vs. 2.8×10^3 , $p < 0.0001$) (Figure 4A. e, j and 4B).

Further, RBC counts indicated that viral infection induced a decrease in total RBC count on both the 8th day (Figure 4C) (Normal Control, 3.0×10^6 vs. 2.7×10^6 , Disease Control, $p < 0.0001$), and 15th day (Normal Control, 3×10^6 vs. 2.6×10^6 , Disease Control, $p < 0.0001$) (Figure 4C); whereas drug treatment induced hemopoiesis in a dose- and time-dependent manner (Figure 4C), with a maximum RBC production after 15 days in fish receiving 140 $\mu\text{g}/\text{kg}$ drug (15th day, Disease Control, 2.6×10^6 vs. 3.0×10^6 , 140 $\mu\text{g}/\text{kg}$ Denguenil, $p < 0.0001$), restoring the RBC number to the Normal Control level (Figure 4C).

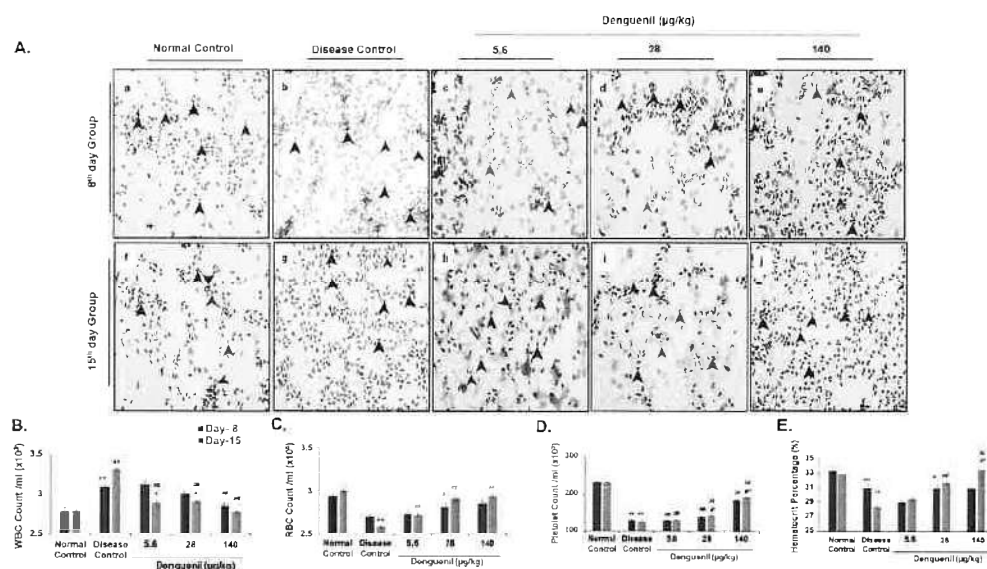


Figure 4. Pharmacological treatment with Denguenil reverses virus-induced serological dynamics. Whole blood was collected and analyzed using H&E staining of blood smears and differential blood cell counts. (4A) Blood smear analysis. (a, f) Normal Control. (b, g) Disease Control. (c, h) 5.6 µg/kg Denguenil. (d, i) 28 µg/kg Denguenil. (e, j) 140 µg/kg Denguenil. (4B) Whole blood WBC count. (4C) Whole blood RBC count. (4D) Whole blood platelet count. (4E) Hematocrit percentage analysis. Black arrowheads indicate RBC; blue arrowheads indicate WBC, and red arrowhead indicates platelets. $n = 24$, data are presented as means \pm SEM. **, ##, #[^] $p < 0.001$ and *, #, [^] $p < 0.05$ by one-way ANOVA. **, * Represents significant compared to Normal Control; ##, # Represents significant compared to their respective Disease Controls; #[^], [^] Represents significant among two time points. Original magnification, 40 \times .

Decrease in platelet count is a hallmark of dengue viral infection. From the results, it is evident that dengue virus induced a 50% decrease in platelet count in a time-dependent manner on both the 8th day (Normal Control, 230×10^3 vs., 128×10^3 , Disease Control, $p < 0.0001$) and 15th day (Normal Control, 231×10^3 vs. 125×10^3 , Disease Control, $p < 0.0001$) (Figure 4D). The platelet numbers were restored upon Denguenil treatment in a dose- and time-dependent manner, with 140 µg/kg Denguenil showing the maximum platelet induction (8th day, Disease Control, 128×10^3 vs. 182×10^3 , 140 µg/kg Denguenil, $p < 0.0001$; 15th day, Disease Control, 125×10^3 vs. 191×10^3 , 140 µg/kg Denguenil, $p < 0.0001$) (Figure 4D).

In line with blood phenotyping, hematocrit analysis identified a decrease in hematocrit percentage upon dengue viral infection, compared to Normal Control on both the 8th day (Normal Control 33% vs. Disease Control, 31%, $p < 0.0001$) and 15th day (Normal Control 33% vs. Disease Control, 28%, $p < 0.0001$) (Figure 4E). Change in blood cell types upon Denguenil treatment translated as a dose- and time-dependent increase in hematocrit percentage, with the 15th day time point showing the maximum percent of restoration in fish receiving 140 µg/kg Denguenil (Normal Control 33% vs. 33%, 140 µg/kg Denguenil, $p < 0.0001$) (Figure 4E). No significant increase in hematocrit percentage was noticed at the 8th day time point (Disease Control 31% vs. 31%, 140 µg/kg Denguenil, NS) (Figure 4E).

3.7. Denguenil Attenuated Dengue-Virus-Induced Hemorrhage

We analyzed caudal fins for signs of virus-induced hemorrhage and presence of blood clots. While clear, unimpaired, and distinct caudal fins were present in normal control (Figure 5A. f), dengue viral infection resulted in hemorrhage and formation of clot, along with ripped edges of caudal fins, indicating impairment of peripheral cells (Figure 5A. b, g). In the 8th day group,

hemorrhage and well stained thick blood clots were identified in 5.6 $\mu\text{g}/\text{kg}$ Denguenil (Figure 5A. c). At 28 $\mu\text{g}/\text{kg}$ Denguenil, palely stained blood clots and hemorrhage with completely fringed caudal tip were present (Figure 5A. d). At 140 $\mu\text{g}/\text{kg}$ Denguenil, partial hemorrhage with small clots and clear blastema cells were observed (Figure 5A. e). This suggests a partial recovery from hemorrhage at 140 $\mu\text{g}/\text{kg}$ dose in 8th day time point. Interestingly in 15th day point, all the three doses (5.6 $\mu\text{g}/\text{kg}$ –140 $\mu\text{g}/\text{kg}$) showed substantial recovery from dengue infection induced hemorrhage. In 5.6 $\mu\text{g}/\text{kg}$ Denguenil, palely stained hemorrhage clots were noticed (Figure 5A. h) and at 28 $\mu\text{g}/\text{kg}$ Denguenil dose, very few clots were identified with normal looking caudal fin (Figure 5A. i). At 140 $\mu\text{g}/\text{kg}$ dose in 15th day time point, hemorrhage and blood clots were very few with normal, clear and unimpaired caudal fins (Figure 5A. j). These results indicate that zebrafish receiving Denguenil for 15 days recovered from virus induced hemorrhage, completely as indicated by a dose-dependent decrease in the size of hemorrhage clot (Figure 5B).

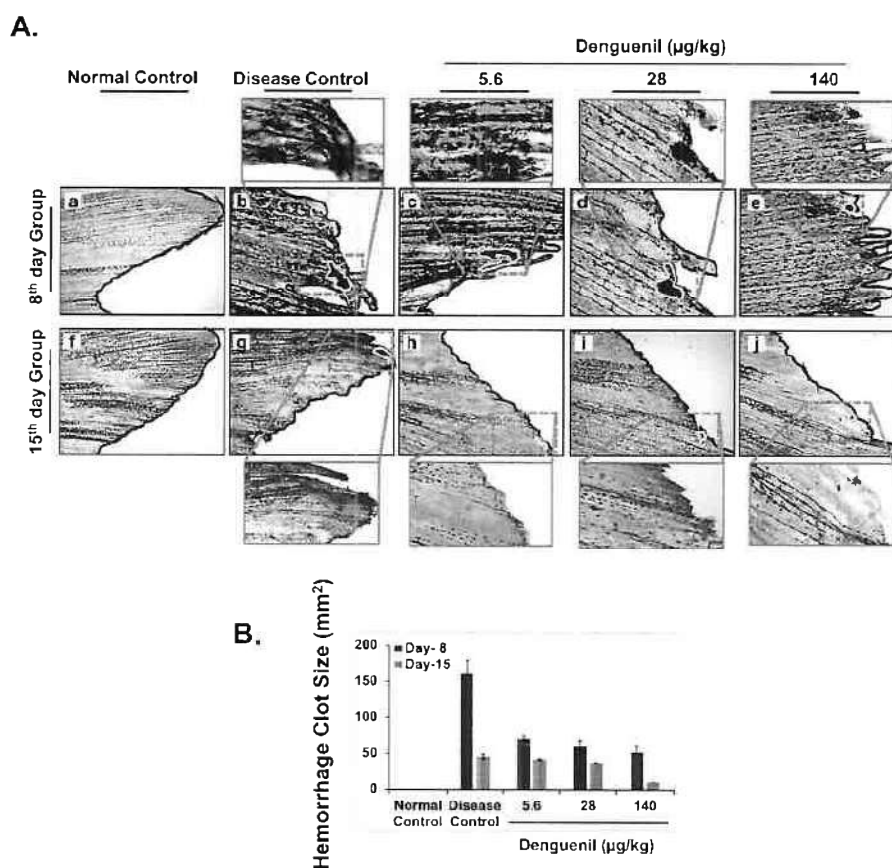


Figure 5. Pharmacological treatment with Denguenil inhibits dengue-virus-induced hemorrhage. Zebrafish caudal fins were harvested from all the groups at the end of the experiment and analyzed for dengue-virus-induced hemorrhage, at the 8th day and 15th day time points. (A) H&E stained caudal fin anatomy. 5A. (a, f) Normal Control. 5A. (b, g) Disease Control. 5A. (c, h) 5.6 $\mu\text{g}/\text{kg}$ Denguenil. 5A. (d, i) 28 $\mu\text{g}/\text{kg}$ Denguenil. 5A. (e, j) 140 $\mu\text{g}/\text{kg}$ Denguenil. The Caudal fin areas with observed hemorrhage and clots (marked in yellow) have been zoomed expanded for clarity. Original magnification, 10 \times , zoomed in magnification, 40 \times . (B) Quantification of hemorrhage clot size, averaged across each treatment group and respective time points.

3.8. Denguenil Normalized Expression of Endothelial Apoptotic Marker, Angiopoietin-2

Next, we tested for the expression of the endothelial cell apoptotic marker Angiopoietin-2 (Ang-2). ANG-2 is an important proangiogenic factor that has recently been implicated in mediating inflammatory processes [37]. Parallel to DENV-3 expression, *Ang-2* expression levels exhibited a 4.6-fold increase on the 8th day (Normal Control, 1.5-fold vs. 7.4-fold, Disease Control, $p < 0.0001$) and 4-fold increase on the 15th day (Normal Control, 2-fold vs. 8-fold, Disease Control, $p < 0.0001$) (Figure 6A). Denguenil treatment resulted in a dose-dependent decrease in *Ang-2* expression levels at both time points tested, with the 140 $\mu\text{g}/\text{kg}$ dose exhibiting more than 50% decrease in *Ang-2* expression (8th day group, Disease Control, 7.4-fold vs. 3.3-fold in 140 $\mu\text{g}/\text{kg}$ Denguenil, $p < 0.0001$; 15th day group, Disease Control, 8-fold vs. 3-fold in 140 $\mu\text{g}/\text{kg}$ Denguenil, $p < 0.0001$) (Figure 6A).

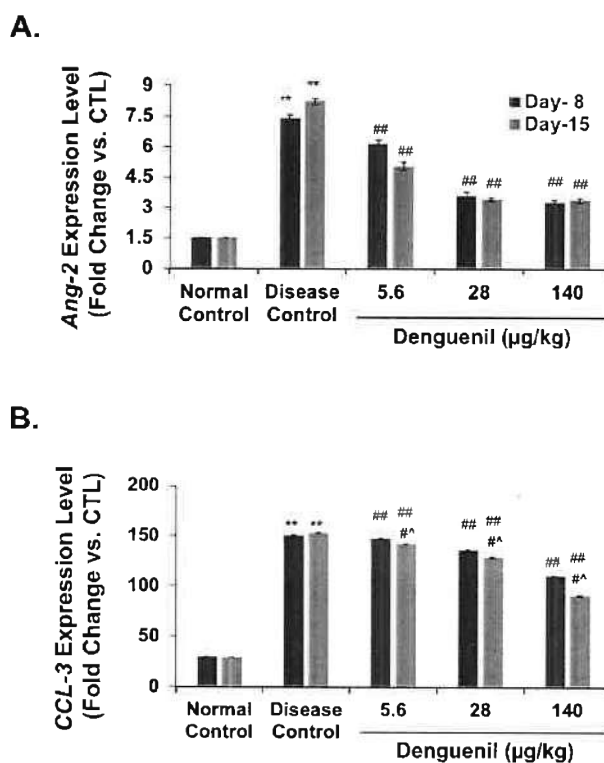


Figure 6. Denguenil treatment normalizes expression of *Ang2* and chemokine *CCL3*. Virus-induced increases in (A) *Ang-2* expression and (B) *CCL3* levels were attenuated upon Denguenil treatment in a dose-dependent manner. $n = 24$, data are presented as means \pm SEM. **, ##, #^ $p < 0.001$. ** Represents significant compared to Normal Control; ##, Represents significant compared to their respective Disease Controls; #^ Represents significant difference between the two time points.

3.9. Denguenil Inhibited Upregulation of the *CCL3* Gene

Chemokines are involved in leucocyte trafficking during infection and inflammation. Gene expression analysis of *CCL3* indicated a 5-fold increase at the 8th day time point (Normal Control, 30-fold vs. 150-fold, Disease Control, $p < 0.0001$) and 15th day time point (Normal Control, 30-fold

vs. 153-fold, Disease Control, $p < 0.0001$) (Figure 6B) upon dengue infection. While a moderate dose-dependent response in the expression of *CCL3* was detected on the 8th day, a robust dose-dependent decrease was identified in the 15th day group upon Denguenil treatment (Figure 6B). In line with this, 140 $\mu\text{g}/\text{kg}$ Denguenil in the 8th day group displayed only a 26% decrease in *CCL3* expression compared to Disease Control (Disease Control, 150-fold vs. 110-fold in 140 $\mu\text{g}/\text{kg}$ of Denguenil, $p < 0.0001$), whereas a robust 40% decrease in *CCL3* expression was identified in 140 $\mu\text{g}/\text{kg}$ of Denguenil after 15 days (Disease Control, 153-fold vs. 91-fold in 140 $\mu\text{g}/\text{kg}$, $p < 0.0001$) (Figure 6B).

3.10. Cytosafety of Denguenil in Human Cell Lines

In order to test the cytosafety profile of Denguenil Vati, we first measured cell viability using human hepatic cell line HepG2 and human skin cell line A431. The results indicated that in HepG2 cells, Denguenil did not exert any cytotoxicity up to 300 $\mu\text{g}/\text{mL}$ (Figure 7A). In HepG2, very minimal cytotoxicity was observed at 1000 $\mu\text{g}/\text{mL}$. No cytotoxicity was noticed in A431 cells (Figure 7B).

Next, Denguenil-induced oxidative stress was evaluated by measuring the reactive oxygen species (ROS) generation and malondialdehyde (MDA) levels. Treatment with Denguenil did not induce any ROS generation in either HepG2 and A431 cells (Figure 7C, D) even at the highest dose tested. Malondialdehyde (MDA), the major end product of lipid peroxidation and indicator of damage to membrane lipids had no significant changes in either HepG2 or A431 cells even at the highest tested dose of Denguenil (Figure 7E, F). Taken together, Denguenil exhibited an acceptable cytosafety profile in human cell lines under in vitro conditions.

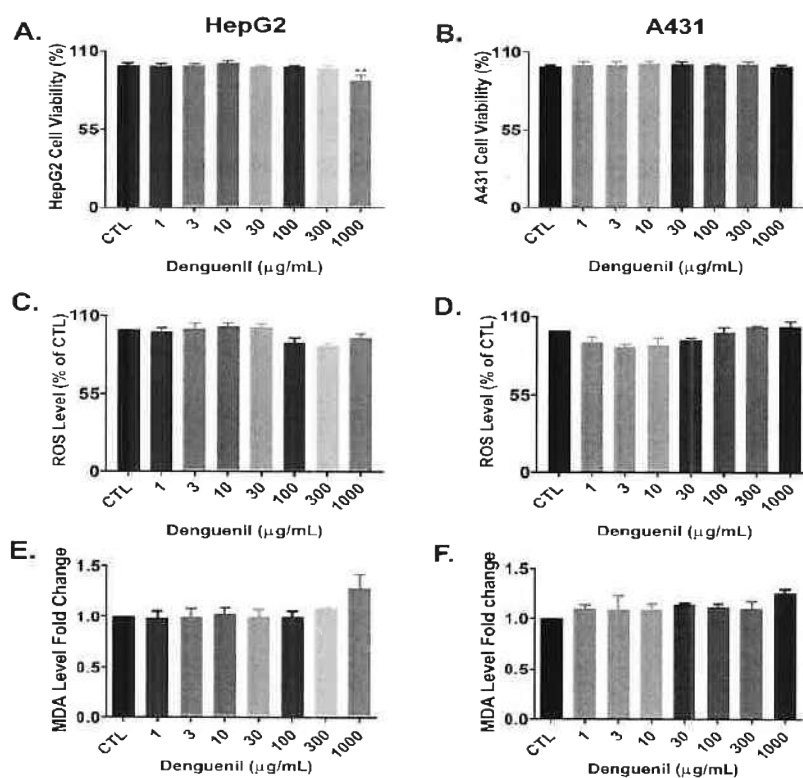


Figure 7. Cytosafety of Denguenil in human cell lines. HepG2 and A431 cells were treated with a series of Denguenil concentrations for 24 h and tested for various endpoints. In (A) HepG2 cells and in (B) A431 cells, Denguenil exerted no cytotoxicity up to the highest tested concentration of 1000 $\mu\text{g}/\text{mL}$. Reactive oxygen species (ROS) generation was measured (C) In HepG2 and (D) A431 cells. MDA secretion in cell culture supernatant was estimated in (E) HepG2 and (F) A431 cells. $n = 3$, data are presented as means \pm SEM. **, $p < 0.001$, represents statistically significant as compared to untreated control (CTL).

3.11. HPLC Analysis of Denguenil

HPLC analysis identified the active ingredients present in the Denguenil. Comparing the chromatograms obtained from the pure substances used to prepare the standard curve identified the presence of gallic acid, ellagic acid, palmetin, and berberine as active ingredients. The analytical curve showed linearity in the concentration range used as standard (data not shown). Gallic acid, ellagic acid, palmetin, and berberine were separated within 40 min. Gallic acid, ellagic acid, palmetin, and berberine were eluted at 7.187 min, 21.240 min, 24.722 min, and 25.036 min retention time, respectively (Figure 8A, B). HPLC analysis revealed that 0.86 $\mu\text{g}/\text{mg}$ gallic acid, 1.87 $\mu\text{g}/\text{mg}$ ellagic acid, 0.03 $\mu\text{g}/\text{mg}$ palmetin, and 0.04 $\mu\text{g}/\text{mg}$ berberine were present in Denguenil.

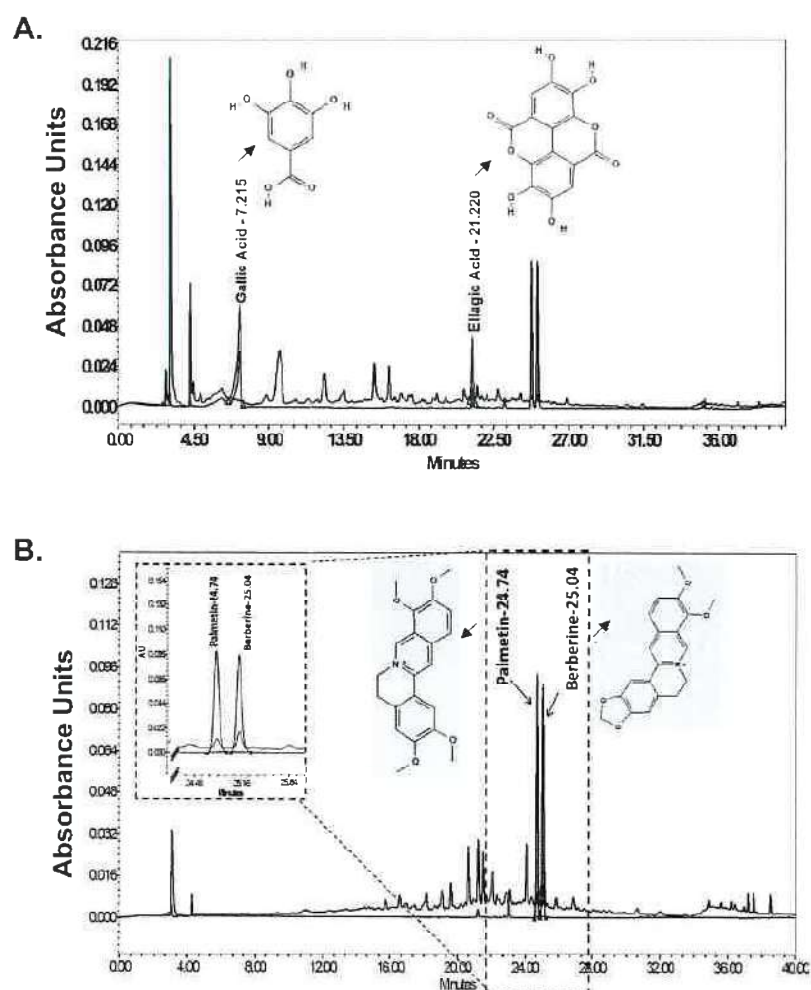


Figure 8. HPLC analysis identification of active ingredients in Denguenil. The Denguenil sample was crushed into a fine powder and analyzed on HPLC using reference standards. The chromatographs were recorded at 270 nm (gallic acid and ellagic acid) and 346 nm (palmetin and berberine) wavelength. By comparing with chromatographs of pure standards, HPLC analysis identified the presence of bioactive compounds, namely, (A) gallic acid and ellagic acid and (B) palmetin and berberine in the Denguenil. The chemical structures of the identified compounds have been appended in the chromatogram.

4. Discussion

Dengue is an acute febrile illness caused by dengue virus (DENV) and is a major cause of morbidity and mortality in tropical and subtropical regions of the world [2]. However, effective antiviral therapy is lacking. With the absence of an effective anti-dengue viral drug, dengue fever has become a major public health threat worldwide [5]. In the present research, we have successfully demonstrated the therapeutic efficacy and disease-modifying properties of an ayurvedic herbal formulation, Denguenil, on dengue-virus-induced pathology. Further, we have also demonstrated that translational dose of Denguenil is effective in modifying various cellular, molecular, and

biochemical diagnostic endpoints of human dengue infection using a physiologically relevant zebrafish model (Table 1).

Table 1. The course of dengue infection and pathological changes. Various pathological features of dengue infection in zebrafish, its comparison with human dengue clinical signs, and subsequent therapeutic modulation by Denguenil treatment.

| Course of Dengue Illness. | Zebrafish Aetiology. | | | Human Dengue Endpoints |
|-----------------------------|--------------------------------------|--|---|---|
| | Disease Initiation | Critical Progression | Recovery by Denguenil Vati | |
| Phenotypic Changes | Hypoactivity and Body discolouration | Vascular Hemorrhage of blood vessels in the caudal extremities | Caudal tip with no fringes | Lethargy, Restlessness, Endothelial dysfunction, Vascular leak and Hemorrhage development |
| Pathological Changes | RBC infiltration | Hepatocyte necrosis | Normal hepatocytes and Reduction in RBC infiltration | Hepatocellular necrosis and Cellular infiltration |
| Molecular Changes | | Dengue biomarker <i>DENV-3</i> expression | No expression | <i>DENV</i> transcript expression |
| | | Expression of <i>Ang-2</i> | Low expression of <i>Ang-2</i> | Elevated <i>Ang-2</i> expression |
| | | Increased <i>CCL3</i> expression | Low <i>CCL3</i> expression | Elevated <i>CCL3</i> levels associated with disease severity |
| Blood Counts | | Decline in RBC count Increase in WBC count Decline in Platelet count | Restoration of Blood count for RBC- 3×10^6 WBC- 2.8×10^3 Platelet- 191×10^3 | Anemia Elevated lymphocytes Decrease in platelet counts |

Zebrafish has been used as model for studying various human diseases and host–pathogen interactions [23]. Further, it has been used to study a number of virus-induced human diseases [22], identify drug leads, and explore new applications for known drugs [38]. In the present investigation, we were successful in exploring the therapeutic benefit of Denguenil against dengue viral infection by using a series of effective doses of Denguenil (5.6–140 µg/kg) more than 1000-fold lower than the human therapeutic dose. Effective dose screening indicated a dose-dependent decrease in various parameters tested, with the maximum response at 140 µg/kg Denguenil after 15 days.

Denguenil is an ayurvedic herbal formulation consisting of extracts from *Tinospora cordifolia* (Giloy or Guduchi), *Aloe vera* (Aloe), *Carica papaya* (Papaya), *Punica granatum* (Pomegranate), *Ocimum sanctum* (Holy Basil). The immunomodulatory property of *Tinospora cordifolia* includes reported anti-human immunodeficiency virus (HIV) activity [31]. In silico analysis identified that it is a potent inhibitor of the NS2B-NS3 receptor in dengue virus [39]. The acemannan carbohydrate polymers present in *Aloe vera* facilitate phagocytosis by acting as a bridge between foreign proteins, such as virus particles and macrophages [40], and reduce hepatic damage by inhibiting necrosis and mononuclear cell infiltration [25,41]. *Carica papaya* leaf extracts exert antidengue properties by decreasing intracellular viral load [42]. Further, it improves platelet and RBC counts [42,43]. However, the exact phytochemicals responsible for boosting thrombopoiesis and erythropoiesis have not been identified. *Punica granatum* seeds contain a high content of punical acid. It increases peripheral blood mononuclear cell (PBMC) count and inhibits apoptosis in splenocytes and PBMCs [44]. Further, its use as antiviral therapy has been reported against herpes simplex virus (HSV) infection [45] and as an HIV entry inhibitor [46]. *Ocimum sanctum* has been recommended for the treatment of chronic fever, respiratory diseases, and skin diseases. It has antimicrobial, and hepatoprotective properties due to the presence of Eugenol as an active constituent [47], and exerts modest inhibitory activity against DENV-1 [48].

HPLC analysis revealed the presence of gallic acid, ellagic acid, palmetin, and berberine as active chemicals present in Denguenil. Mechanistically, how Denguenil and its active ingredients protect against DENV infection is not very clear at present. However, ellagic acid and gallic acid have been found to inhibit entry of infectious ebolavirus into host cells, and have exhibited potent antifiloviral activity [49]. Further, gallic acid has also been reported to inhibit attachment and entry of human rhinoviruses and HSV type 1 [50,51]. Berberine has been in use for hepatitis [27,52] and as an anti-inflammatory compound [53]. Further, berberine has been shown to inhibit Chikungunya Virus (CHIKV) replication and downregulation of viral protein expression [54]. Palmetin has been found to inhibit respiratory syncytial virus (RSV) replication, along with possessing immunomodulatory properties.

The diagnosis of dengue fever is carried out based on various parameters, including clinical, epidemiological, and laboratory data. Among laboratory tests, the nonspecific tests include blood count, platelet count, prothrombin time (PT), liver function tests, and serum albumin concentration, whereas specific tests include viral isolation tests and serology for antibody examination [55,56]. Keeping these parameters as standard, in a translational approach, we have successfully replicated dengue viral pathology in zebrafish. After the onset of dengue viral illness, the virus can be detected in serum, plasma, circulating blood cells, and other tissues for four to five days. In the present investigation, we used infected serum to propagate the virus in zebrafish and for subsequent studies. Dengue viral infection resulted in a significant increase in total WBC count, whereas the total RBC number was decreased. Hematologically, dengue fever causes early neutropenia, with subsequent lymphocytosis and a decrease in platelet count and hypocellular marrow with abnormal megakaryocytopoiesis in the early stage [57]. In the present investigation, increased WBC number could be due to the presence of active and ongoing dengue viral infection. Decreased RBC number upon infection is indicative of poor hemopoiesis and vascular leakage induced upon viral infection. Conversely, increased platelet counts in zebrafish receiving drug suggests the restoration of hemopoiesis upon Denguenil treatment.

Upon infection, the dengue virus can infect various cell types and cause diverse clinical and pathological effects. Histopathology suggests that various organs, including the lymph nodes, spleen, liver, and bone marrow, are affected by dengue viral replication, and a variety of cell types, including macrophages, lymphocytes, dendritic cells (DCs), monocytes, and endothelial cells become infected at varying rates during the course of disease [58]. In the present study, we have observed a severe liver pathology in the zebrafish model, including hepatic cell necrosis and inflammation. The observed liver damage in our model could be due to dysregulated host immune response and its products (e.g., cytokines and chemokines) or the direct dengue viral infection of the cells [59]. Previous reports suggest that liver damage in dengue includes microvascular steatosis, hepatocellular necrosis, and cellular infiltrates at the portal tract [11]. In the present investigation, we have demonstrated that therapeutic administration of Denguenil has protective effects on virus-induced liver damage as evidenced by reduced necrosis and inflammation in a dose- and time-dependent manner. Further, liver pathological symptoms were abrogated by Denguenil. This indicates that the drug itself does not induce inflammatory responses and has no toxic effect on liver, as shown by its acceptable cytosafety profile in human cells. Involvement of JNK1/2 signaling, ERK1/2 pathway, and p38 MAPK signaling pathways in liver damage were reported, and use of their inhibitors reduced hepatic cell apoptosis and liver injury in DENV-infected mice; however, these inhibitors were not able to restrict virus replication in the liver [60–62].

The dengue virus can replicate in both hepatocytes and Kupffer cells [63]. In the present study, we have observed an increase in the transcript copies of DENV-3 by 40-fold upon infection with serum-containing active viruses. The copy number did not change after the 8th day until the end of the experiment in the Disease Control. Significantly increased copy number is indicative of active viral replication, multiplication, and propagation of disease. Use of various replication and transcription inhibitors, such as nucleoside analogs [64,65], helicase [66], and protease inhibitors [67] have been tested as potential dengue therapy. However, they either failed in *in vivo* models or human

trials, suggesting their development is still in infancy [26]. A significant attenuation of viral copy number upon Denguenil treatment indicates its efficacy as a therapeutic agent.

Thrombocytopenia is one of the simple diagnostic criteria proposed by the World Health Organization (WHO) for diagnosis of dengue hemorrhagic fever (DHF) [68]. Dengue complications are frequently preceded by a rapid drop in platelet counts, often to very low numbers [69]. Decrease in platelet count in the zebrafish model is in line with the severe dengue fever symptomatology in humans. Further dose-dependent increase in platelet count in effective dose screening at both 8th and 15th day time points indicates the superior role of Denguenil on DENV-induced thrombocytopenia. Interestingly, *Carica papaya* leaf extract has been found to be an antidengue agent, and resulted in platelet augmentation and significant decrease in erythrocyte damage [42]. In the present study, while we have demonstrated the restoration of platelet count upon Denguenil treatment, the mechanism leading to protective response from thrombocytopenia is yet to be ascertained.

Vascular leakage, which is a hallmark of DHF, has been found to be associated with derangement of the normal regulatory function of endothelial cells, rather than endothelial cell death, and underlies the hemorrhagic diathesis of dengue [70]. Numerous studies have established ANG-2 and CCL3 as biomarkers that serve as reference standards for sensitive and early indicators of disease [14,71–73]. Hence, even with minute onset of viral replication and pathology, these genes show changes in their steady-state mRNA levels. In the present study, we have used these two genes to establish the fact that abrogation of ANG-2 and CCL3 mRNA levels to baseline is a strong indicator of drug efficacy. This also indicates the pathways that may be inhibited at the early stage of the disease. In the present research, the observed decrease in RBC count could be due to vascular leakage, and coincides with the expression of apoptotic marker *ANG2*. Previous reports suggest that *ANG2* is pro-apoptotic and that its expression is associated with endothelial breakdown and apoptosis of vascular cells during injury [74]. Interestingly, significant attenuation of *ANG2* expression and restoration of RBC number upon Denguenil treatment is indicative of anti-apoptotic and anti-dyserythropoietic properties of Denguenil. In line with WBC, RBC, and platelet counts, dengue virus induced a decrease in hematocrit percentage, which was restored upon drug Denguenil treatment. Dose-dependent decrease in dengue parameters without any overt pathological features further indicates the beneficial effect of this ayurvedic herbal formulation.

In the present study, the clinical course of hemorrhage was established as per the WHO (2009) [9], CDC, and previous reports [75]. We observed hemorrhage during the initial phase of the study, i.e., from day zero to seven. This is due to the leaky vessels at the initial stage of the infection with visible RBC. After seven days, the hemorrhage stopped and the Disease Control survived. However, blood clotting was still observed in the periphery of the caudal fin with indicative darkly stained blotches and uneven fringes in the caudal fin tip clearly visible. Treatment with Denguenil resulted in recovery of DC from dengue-virus-induced hemorrhage as evident by minimal blotches and decreased peripheral vascular damage.

Previous reports indicate that CCL3 levels are increased in liver and spleen of DENV-infected mice [76] and elevated CCL3 concentrations in plasma of patients with DENV infection may be associated with disease severity [77]. Further, reports suggest that CCL2 and CCL3 may play a role in early recruitment of leukocyte [78] subsets and may have a strong influence in patient clinical outcome [79].

Use of natural compounds have been found to be effective in inhibiting DENV infection and have the potential to be developed as anti-dengue drugs [32,80]. However, many natural products that have shown potent inhibitory activity against certain viruses in vitro have failed to progress to clinical trials because of their poor in vivo activity [81]. In addition, several natural products, such as Quercetin and Narasin, have also been observed to possess significant anti-DENV properties [82,83].

5. Conclusions

In the present study, we successfully developed a novel zebrafish model of dengue virus pathology and demonstrated the therapeutic efficacy and disease-modifying properties of the Indian traditional pentaherbal formulation, Denguenil Vati, on dengue-virus-induced pathology using

various cellular, molecular, and biochemical diagnostic endpoints. Our zebrafish model of dengue viral pathology would help in early screening of potential anti-dengue drugs and aid in proof-of-concept studies, thereby reducing the gap in drug development and increasing overall drug success rates. Use of Denguenil Vati formulation as a complementary or alternative medicine in dengue treatment could alleviate dengue pathological features. The present preclinical study warrants clinical trials of Denguenil Vati in human subjects of dengue and other viral diseases.

Author Contributions: A.B. provided broad direction for the study, identified and prepared the test formulations, generated resources and gave final approval for the manuscript; S.V. performed analytical chemistry experiments; S.K.S. analyzed the data, performed data curing, and wrote the manuscript; A.V. conceptualized and supervised overall studies, generated resources, critically reviewed and finally approved the manuscript. All authors have read and agreed to the published version of the manuscript.

Funding: This research received no external funding. This presented work has been conducted using internal research funds from Patanjali Research Foundation Trust, Haridwar, India.

Acknowledgments: We appreciate the zebrafish test facilities and experimentations at our CRO partner, Pentagrit Labs, Chennai, India. We thank Mr Hoshiyar singh for his expert assistance in in-vitro experiments; and Dr Rajesh Mishra and translation team for fantastic Sanskrit translations. We extend our gratitude to Ms Priyanka Kandpal, Mr Pradeep Nain, Mr Tarun Rajput, Mr Gagan Kumar and Mr Lalit Mohan for their swift administrative supports.

Conflicts of Interest: The authors declare no competing interests in the publication of the data in this manuscript.

References

1. WHO. Global Strategy for Dengue Prevention and Control 2012–2020. In *World Health Organization*; WHO: Geneva, Switzerland, 2012; p. 43, ISBN 978 92 4 150403 4.
2. Bhatt, S.; Gething, P.W.; Brady, O.J.; Messina, J.P.; Farlow, A.W.; Moyes, C.L.; Drake, J.M.; Brownstein, J.S.; Hoen, A.G.; Sankoh, O.; et al. The global distribution and burden of dengue. *Nature* **2013**, *496*, 504–507, doi:10.1038/nature12060.
3. Centers for Disease Control and Prevention National Center for Emerging and Zoonotic Infectious Diseases. Available online: <https://www.cdc.gov/dengue/about/index.html> (accessed on 5 May 2020).
4. Brady, O.J.; Gething, P.W.; Bhatt, S.; Messina, J.P.; Brownstein, J.S.; Hoen, A.G.; Moyes, C.L.; Farlow, A.W.; Scott, T.W.; Hay, S.I. Refining the Global Spatial Limits of Dengue Virus Transmission by Evidence-Based Consensus. *PLoS Negl. Trop. Dis.* **2012**, *6*, e1760, doi:10.1371/journal.pntd.0001760.
5. Guzman, M.G.; Harris, E. Dengue. *Lancet* **2015**, *385*, 453–465, doi:10.1016/S0140-6736(14)60572-9.
6. Rothman, A.L. Immunity to dengue virus: A tale of original antigenic sin and tropical cytokine storms. *Nat. Rev. Immunol.* **2011**, *11*, 532–543, doi:10.1038/nri3014.
7. Sayce, A.C.; Miller, J.L.; Zitzmann, N. Targeting a host process as an antiviral approach against dengue virus. *Trends Microbiol.* **2010**, *18*, 323–330, doi:10.1016/j.tim.2010.04.003.
8. Halstead, S.B. Dengue. *Lancet* **2007**, *370*, 1644–1652, doi:10.1016/S0140-6736(07)61687-0.
9. WHO. *Dengue: Guidelines for Diagnosis, Treatment, Prevention and Control 2009*; WHO: Geneva, Switzerland 2013.
10. Noisakran, S.; Onlamoon, N.; Songprakhon, P.; Hsiao, H.M.; Chokephaibulkit, K.; Perng, G.C. Cells in dengue virus infection in vivo. *Adv. Virol.* **2010**, *2010*, 164878, doi:10.1155/2010/164878.
11. Bhamarapravati, N. Hemostatic Defects in Dengue Hemorrhagic Fever. *Rev. Infect. Dis.* **1989**, *11*, 826–829, doi:10.1093/clinids/11.Supplement_4.S826.
12. Green, A.M.; Beatty, P.R.; Hadjilaou, A.; Harris, E. Innate immunity to dengue virus infection and subversion of antiviral responses. *J. Mol. Biol.* **2014**, *426*, 1148–1160, doi:10.1016/j.jmb.2013.11.023.
13. Gagnon, S.J.; Ennis, F.A.; Rothman, A.L. Bystander target cell lysis and cytokine production by dengue virus-specific human CD4(+) cytotoxic T-lymphocyte clones. *J. Virol.* **1999**, *73*, 3623–3629.
14. Tolfvenstam, T.; Lindblom, A.; Schreiber, M.J.; Ling, L.; Chow, A.; Ooi, E.E.; Hibberd, M.L. Characterization of early host responses in adults with dengue disease. *BMC Infect. Dis.* **2011**, *11*, 209, doi:10.1186/1471-2334-11-209.

15. Marchette, N.J.; Halstead, S.B.; Falkler, W.A.; Stenhouse, A.; Nash, D. Studies on the pathogenesis of dengue infection in monkeys. III. sequential distribution of virus in primary and heterologous infections. *J. Infect. Dis.* **1973**, *128*, 23–30, doi:10.1093/infdis/128.1.23.
16. Halstead, S.B.; Shotwell, H.; Casals, J. Studies on the pathogenesis of dengue infection in monkeys. I. clinical laboratory responses to primary infection. *J. Infect. Dis.* **1973**, *128*, 7–14, doi:10.1093/infdis/128.1.7.
17. Onlamoon, N.; Noisakran, S.; Hsiao, H.M.; Duncan, A.; Villinger, F.; Ansari, A.A.; Perng, G.C. Dengue virus - Induced hemorrhage in a nonhuman primate model. *Blood* **2010**, *115*, 1823–1834, doi:10.1182/blood-2009-09-242990.
18. Raut, C.G.; Deolankar, R.P.; Kolhapure, R.M.; Goverdhan, M.K. Susceptibility of laboratory-bred rodent to the experimental infection with dengue virus type 2. *Acta Virol.* **1996**, *40*, 146.
19. Paes, M.V.; Pinhão, A.T.; Barreto, D.F.; Costa, S.M.; Oliveira, M.P.; Nogueira, A.C.; Takiya, C.M.; Farias-Filho, J.C.; Schatzmayr, H.G.; Alves, A.M.B.; et al. Liver injury and viremia in mice infected with dengue-2 virus. *Virology* **2005**, *338*, 236–246, doi:10.1016/j.virol.2005.04.042.
20. Zompi, S.; Harris, E. Animal models of dengue virus infection. *Viruses* **2012**, *4*, 62–82.
21. Krishnakumar, V.; Durairajan, S.S.K.; Alagarasu, K.; Li, M.; Dash, A.P. Recent updates on mouse models for human immunodeficiency, influenza, and dengue viral infections. *Viruses* **2019**, *11*, 252, doi:10.3390/v11030252.
22. Levraud, J.P.; Palha, N.; Langevin, C.; Boudinot, P. Through the looking glass: Witnessing host-virus interplay in zebrafish. *Trends Microbiol.* **2014**, *22*, 490–497, doi:10.1016/j.tim.2014.04.014.
23. Varela, M.; Figueras, A.; Novoa, B. Modelling viral infections using zebrafish: Innate immune response and antiviral research. *Antiviral Res.* **2017**, *139*, 59–68, doi:10.1016/j.antiviral.2016.12.013.
24. Vaz, R.L.; Outeiro, T.F.; Ferreira, J.J. Zebrafish as an animal model for drug discovery in Parkinson's disease and other movement disorders: A systematic review. *Front. Neurol.* **2018**, *9*, 347.
25. Rissone, A.; Burgess, S.M. Rare genetic blood disease modeling in zebrafish. *Front. Genet.* **2018**, *9*, 348.
26. Chan, C.Y.; Ooi, E.E. Dengue: An update on treatment options. *Future Microbiol.* **2015**, *10*, 2017–2031, doi:10.2217/fmb.15.105.
27. Rothman, A.L.; Ernis, F.A. Dengue Vaccine: The Need, the Challenges, and Progress. *J. Infect. Dis.* **2016**, *214*, 825–827, doi:10.1093/infdis/jiw068.
28. Lin, L.T.; Hsu, W.C.; Lin, C.C. Antiviral natural products and herbal medicines. *J. Tradit. Complement. Med.* **2014**, *4*, 24–35, doi:10.4103/2225-4110.124335.
29. Harvey, A.L.; Edrada-Ebel, R.; Quinn, R.J. The re-emergence of natural products for drug discovery in the genomics era. *Nat. Rev. Drug Discov.* **2015**, *14*, 111–129, doi:10.1038/nrd4510.
30. Hert, J.; Irwin, J.J.; Laggner, C.; Keiser, M.J.; Shoichet, B.K. Quantifying biogenic bias in screening libraries. *Nat. Chem. Biol.* **2009**, *5*, 479–483, doi:10.1038/nchembio.180.
31. Zandi, K.; Teoh, B.T.; Sam, S.S.; Wong, P.F.; Mustafa, M.R.; AbuBakar, S. Novel antiviral activity of baicalein against dengue virus. *BMC Complement. Altern. Med.* **2012**, *12*, 214, doi:10.1186/1472-6882-12-214.
32. Frabasile, S.; Koishi, A.C.; Kuczera, D.; Silveira, G.F.; Verri, W.A.; Dos Santos, C.N.D.; Bordignon, J. The citrus flavanone naringenin impairs dengue virus replication in human cells. *Sci. Rep.* **2017**, *7*, 41864, doi:10.1038/srep41864.
33. Lin, L.T.; Chen, T.Y.; Lin, S.C.; Chung, C.Y.; Lin, T.C.; Wang, G.H.; Anderson, R.; Lin, C.C.; Richardson, C.D. Broad-spectrum antiviral activity of chebulagic acid and punicalagin against viruses that use glycosaminoglycans for entry. *BMC Microbiol.* **2013**, *13*, 187, doi:10.1186/1471-2180-13-187.
34. Heath, R.L.; Packer, L. Photoperoxidation in isolated chloroplasts. I. Kinetics and stoichiometry of fatty acid peroxidation. *Arch. Biochem. Biophys.* **1968**, *125*, 189–198, doi:10.1016/0003-9861(68)90654-1.
35. Ducharme, N.A.; Reif, D.M.; Gustafsson, J.A.; Bondesson, M. Comparison of toxicity values across zebrafish early life stages and mammalian studies: Implications for chemical testing. *Reprod. Toxicol.* **2015**, *55*, 3–10, doi:10.1016/j.reprotox.2014.09.005.
36. Shin, J.; Seol, I.; Son, C. Interpretation of Animal Dose and Human Equivalent Dose for Drug Development. *J. Korean Orient. Med.* **2010**, *31*, 1–7.
37. Scholz, A.; Plate, K.H.; Reiss, Y. Angiopoietin-2: A multifaceted cytokine that functions in both angiogenesis and inflammation. *Ann. N. Y. Acad. Sci.* **2015**, *1347*, 45–51, doi:10.1111/nyas.12726.
38. Taylor, K.L.; Grant, N.J.; Temperley, N.D.; Patton, E.E. Small molecule screening in zebrafish: An in vivo approach to identifying new chemical tools and drug leads. *Cell Commun. Signal.* **2010**, *8*, 11, doi:10.1186/1478-811X-8-11.

39. Bency, B.J.; Helen, P.A.M. In silico identification of dengue inhibitors in Giloy (*Tinospora cordifolia*) and Papaya. *J. Emerg. Technol. Innov. Res.* **2018**, *5*, 506–511.
40. Eshun, K.; He, Q. Aloe Vera: A Valuable Ingredient for the Food, Pharmaceutical and Cosmetic Industries – A Review. *Crit. Rev. Food Sci. Nutr.* **2004**, *44*, 91–96, doi:10.1080/10408690490424694.
41. Chandan, B.K.; Saxena, A.K.; Shukla, S.; Sharma, N.; Gupta, D.K.; Suri, K.A.; Suri, J.; Bhadauria, M.; Singh, B. Hepatoprotective potential of Aloe barbadensis Mill. against carbon tetrachloride induced hepatotoxicity. *J. Ethnopharmacol.* **2007**, *111*, 560–566, doi:10.1016/j.jep.2007.01.008.
42. Sharma, N.; Mishra, K.P.; Chanda, S.; Bhardwaj, V.; Tanwar, H.; Ganju, L.; Kumar, B.; Singh, S.B. Evaluation of anti-dengue activity of Carica papaya aqueous leaf extract and its role in platelet augmentation. *Arch. Virol.* **2019**, *164*, 1095–1110, doi:10.1007/s00705-019-04179-z.
43. Dharmarathna, S.L.C.A.; Wickramasinghe, S.; Waduge, R.N.; Rajapakse, R.P.V.J.; Kularatne, S.A.M. Does Carica papaya leaf-extract increase the platelet count? An experimental study in a murine model. *Asian Pac. J. Trop. Biomed.* **2013**, *3*, 720–724, doi:10.1016/S2221-1691(13)60145-8.
44. Zhao, F.; Pang, W.; Zhang, Z.; Zhao, J.; Wang, X.; Liu, Y.; Wang, X.; Feng, Z.; Zhang, Y.; Sun, W.; et al. Pomegranate extract and exercise provide additive benefits on improvement of immune function by inhibiting inflammation and oxidative stress in high-fat-diet-induced obesity rats. *J. Nutr. Biochem.* **2016**, *32*, 20–28, doi:10.1016/j.jnutbio.2016.02.003.
45. Houston, D.M.J.; Bugert, J.J.; Denyer, S.P.; Heard, C.M. Potentiated virucidal activity of pomegranate rind extract (PRE) and punicalagin against Herpes simplex virus (HSV) when coadministered with zinc (II) ions, and antiviral activity of PRE against HSV and aciclovir-resistant HSV. *PLoS ONE* **2017**, *12*, e0179291, doi:10.1371/journal.pone.0179291.
46. Neurath, A.R.; Strick, N.; Li, Y.Y.; Debnath, A.K. Punica granatum (pomegranate) juice provides an HIV-1 entry inhibitor and candidate topical microbicide. *Ann. N. Y. Acad. Sci.* **2005**, *1056*, 311–327, doi:10.1196/annals.1352.015.
47. Pattanayak, P.; Behera, P.; Das, D.; Panda, S. Ocimum sanctum Linn. A reservoir plant for therapeutic applications: An overview. *Pharmacogn. Rev.* **2010**, *4*, 95–105, doi:10.4103/0973-7847.65323.
48. Tang, L.I.C.; Ling, A.P.K.; Koh, R.Y.; Chye, S.M.; Voon, K.G.L. Screening of anti-dengue activity in methanolic extracts of medicinal plants. *BMC Complement. Altern. Med.* **2012**, *12*, 3, doi:10.1186/1472-6882-12-3.
49. Cui, Q.; Du, R.; Anantpadma, M.; Schafer, A.; Hou, L.; Tian, J.; Davey, R.A.; Cheng, H.; Rong, L. Identification of ellagic acid from plant rhodiola rosea l. as an anti-ebola virus entry inhibitor. *Viruses* **2018**, *10*, 152, doi:10.3390/v10040152.
50. Kratz, J.M.; Andrighetti-Fröhner, C.R.; Kolling, D.J.; Leal, P.C.; Cirne-Santos, C.C.; Yunes, R.A.; Nunes, R.J.; Trybala, E.; Bergström, T.; Frugulhetti, I.C.P.P.; et al. Anti-HSV-1 and anti-HIV-1 activity of gallic acid and pentyl gallate. *Mem. Inst. Oswaldo Cruz* **2008**, *103*, 437–442, doi:10.1590/S0074-02762008000500005.
51. Choi, H.J.; Song, J.H.; Bhatt, L.R.; Baek, S.H. Anti-human rhinovirus activity of gallic acid possessing antioxidant capacity. *Phyther. Res.* **2010**, *24*, 1292–1296, doi:10.1002/ptr.3101.
52. Li, H.L.; Han, T.; Liu, R.H.; Zhang, C.; Chen, H.S.; Zhang, W.D. Alkaloids from Corydalis saxicola and their anti-hepatitis B virus activity. *Chem. Biodivers.* **2008**, *5*, 777–783, doi:10.1002/cbdv.200890074.
53. Zou, K.; Li, Z.; Zhang, Y.; Zhang, H.Y.; Li, B.; Zhu, W.L.; Shi, J.Y.; Jia, Q.; Li, Y.M. Advances in the study of berberine and its derivatives: A focus on anti-inflammatory and anti-tumor effects in the digestive system. *Acta Pharmacol. Sin.* **2017**, *38*, 157–167, doi:10.1038/aps.2016.125.
54. Varghese, F.S.; Kaukinen, P.; Gläsker, S.; Bespalov, M.; Hanski, L.; Wennerberg, K.; Kümmerer, B.M.; Ahola, T. Discovery of berberine, abamectin and ivermectin as antivirals against chikungunya and other alphaviruses. *Antiviral Res.* **2016**, *126*, 117–124, doi:10.1016/j.antiviral.2015.12.012.
55. De Paula, S.O.; Fonseca, B.A.L. da Dengue: A review of the laboratory tests a clinician must know to achieve a correct diagnosis. *Braz. J. Infect. Dis.* **2004**, *8*, 390–398, doi:10.1590/S1413-86702004000600002.
56. Srichaikul, T.; Nimmannitya, S. Haematology in dengue and dengue haemorrhagic fever. *Bailliere's Best Pract. Res. Clin. Haematol.* **2000**, *13*, 261–276, doi:10.1053/beha.2000.0073.
57. Bierman, H.R.; Nelson, E.R. Hematodepressive Virus Diseases of Thailand. *Ann. Intern. Med.* **1965**, *62*, 867–884, doi:10.7326/0003-4819-62-5-867.
58. Bente, D.A.; Rico-Hesse, R. Models of dengue virus infection. *Drug Discov. Today Dis. Model.* **2006**, *3*, 97–103, doi:10.1016/j.ddmod.2006.03.014.

59. Seneviratne, S.L.; Malavige, G.N.; de Silva, H.J. Pathogenesis of liver involvement during dengue viral infections. *Trans. R. Soc. Trop. Med. Hyg.* **2006**, *100*, 608–614, doi:10.1016/j.trstmh.2005.10.007.
60. Sreekanth, G.P.; Chuncharunee, A.; Cheunsuchon, B.; Noisakran, S.; Yenchtsomanus, P.T.; Limjindaporn, T. JNK1/2 inhibitor reduces dengue virus-induced liver injury. *Antiviral Res.* **2017**, *141*, 7–18, doi:10.1016/j.antiviral.2017.02.003.
61. Sreekanth, G.P.; Chuncharunee, A.; Sirimontaporn, A.; Panaampon, J.; Srisawat, C.; Morchang, A.; Malakar, S.; Thuwajit, P.; Kooptiwut, S.; Suttiheptumrong, A.; et al. Role of ERK1/2 signaling in dengue virus-induced liver injury. *Virus Res.* **2014**, *188*, 15–26, doi:10.1016/j.virusres.2014.03.025.
62. Sreekanth, G.P.; Chuncharunee, A.; Sirimontaporn, A.; Panaampon, J.; Noisakran, S.; Yenchtsomanus, P.T.; Limjindaporn, T. SB203580 modulates p38 MAPK signaling and Dengue virus-induced liver injury by reducing MAPKAPK2, HSP27, and ATF2 phosphorylation. *PLoS ONE* **2016**, *11*, e0149486, doi:10.1371/journal.pone.0149486.
63. Huerre, M.R.; Lan, N.T.; Marianneau, P.; Hue, N.B.; Khun, H.; Hung, N.T.; Khen, N.T.; Drouet, M.T.; Huong, V.T.Q.; Buisson, Y.; et al. Liver histopathology and biological correlates in five cases of fatal dengue fever in Vietnamese children. *Virchows Arch.* **2001**, *438*, 107–115, doi:10.1007/s004280000329.
64. Nguyen, N.M.; Tran, C.N.B.; Phung, L.K.; Duong, K.T.H.; Huynh, H.L.A.; Farrar, J.; Nguyen, Q.T.H.; Tran, H.T.; Nguyen, C.V.V.; Merson, L.; et al. A randomized, double-blind placebo controlled trial of balapiravir, a polymerase inhibitor, in Adult dengue patients. *J. Infect. Dis.* **2013**, *207*, 1442–1450, doi:10.1093/infdis/jis470.
65. Yin, Z.; Chen, Y.L.; Schul, W.; Wang, Q.Y.; Gu, F.; Duraiswamy, J.; Kondreddi, R.R.; Niyomrattanakit, P.; Lakshminarayana, S.B.; Goh, A.; et al. An adenosine nucleoside inhibitor of dengue virus. *Proc. Natl. Acad. Sci. USA* **2009**, *106*, 20435–20439, doi:10.1073/pnas.0907010106.
66. Gu, B.; Liu, C.; Lin-Goerke, J.; Maley, D.R.; Gutshall, L.L.; Feltenberger, C.A.; Del Vecchio, A.M. The RNA Helicase and Nucleotide Triphosphatase Activities of the Bovine Viral Diarrhea Virus NS3 Protein Are Essential for Viral Replication. *J. Virol.* **2000**, *74*, 1794–1800, doi:10.1128/jvi.74.4.1794-1800.2000.
67. Phong, W.Y.; Moreland, N.J.; Lim, S.P.; Wen, D.; Paradkar, P.N.; Vasudevan, S.G. Dengue protease activity: The structural integrity and interaction of NS2B with NS3 protease and its potential as a drug target. *Biosci. Rep.* **2011**, *31*, 399–409, doi:10.1042/BSR20100142.
68. Leangpibul, P.; Thongcharoen, P. Monograph on dengue/dengue haemorrhagic fever. In *World Health Organization. No. Regional Publication No. 22*. WHO Regional Office for South-East Asia: New Delhi, India. 1993; pp. 62–71.
69. Lam, P.K.; Ngoc, T. Van; Thu Thuy, T.T.; Hong Van, N.T.; Nhu Thuy, T.T.; Hoai Tam, D.T.; Dung, N.M.; Hanh Tien, N.T.; Thanh Kieu, N.T.; Simmons, C.; et al. The value of daily platelet counts for predicting dengue shock syndrome: Results from a prospective observational study of 2301 Vietnamese children with dengue. *PLoS Negl. Trop. Dis.* **2017**, *11*, e0005498, doi:10.1371/journal.pntd.0005498.
70. Dewi, B.E.; Takasaki, T.; Kurane, I. In vitro assessment of human endothelial cell permeability: Effects of inflammatory cytokines and dengue virus infection. *J. Virol. Methods* **2004**, *121*, 171–180, doi:10.1016/j.jviromet.2004.06.013.
71. Mapalagamage, M.; Handunnetti, S.M.; Wickremasinghe, A.R.; Premawansa, G.; Thillainathan, S.; Fernando, T.; Kanapathippillai, K.; de Silva, A.D.; Premawansa, S. High levels of serum angiotensin 2 and angiotensin 2/1 ratio at the critical stage of dengue hemorrhagic fever in patients and association with clinical and biochemical parameters. *J. Clin. Microbiol.* **2020**, *58*, doi:10.1128/JCM.00436-19.
72. Malavige, G.N.; Ogg, G.S. Pathogenesis of vascular leak in dengue virus infection. *Immunology* **2017**, *151*, 261–269.
73. John, D.V.; Lin, Y.S.; Perng, G.C. Biomarkers of severe dengue disease—A review. *J. Biomed. Sci.* **2015**, *22*, 83.
74. Nag, S.; Papneja, T.; Venugopalan, R.; Stewart, D.J. Increased angiotensin2 expression is associated with endothelial apoptosis and blood-brain barrier breakdown. *Lab. Investig.* **2005**, *85*, 1189–1198, doi:10.1038/labinvest.3700325.
75. Soukaloun, D. Dengue infection in Lao PDR. *Southeast. Asian J. Trop. Med. Public Health* **2014**, *45*, 113–119.
76. Guabiraba, R.; Marques, R.E.; Besnard, A.G.; Fagundes, C.T.; Souza, D.G.; Ryffel, B.; Teixeira, M.M. Role of the Chemokine Receptors CCR1, CCR2 and CCR4 in the Pathogenesis of Experimental Dengue Infection in Mice. *PLoS ONE* **2010**, *5*, e15680, doi:10.1371/journal.pone.0015680.

77. Lok, S.M.; Ng, M.L.; Aaskov, J. MIP-1 α and MIP-1 β induction by dengue virus. *J. Med. Virol.* **2001**, *65*, 324–330, doi:10.1002/jmv.2037.
78. Rothman, A.L. Immunology and Immunopathogenesis of Dengue Disease. *Adv. Virus Res.* **2003**, *60*, 397–419, doi:10.1016/S0065-3527(03)60010-2.
79. Moreno-Altamirano, M.M.B.; Romano, M.; Legorreta-Herrera, M.; Sánchez-García, F.J.; Colston, M.J. Gene expression in human macrophages infected with dengue virus serotype-2. *Scand. J. Immunol.* **2004**, *60*, 631–638, doi:10.1111/j.0300-9475.2004.01519.x.
80. Ocazonez, R.E.; Meneses, R.; Torres, F.Á.; Stashenko, E. Virucidal activity of Colombian Lippia essential oils on dengue virus replication in vitro. *Mem. Inst. Oswaldo Cruz* **2010**, *105*, 304–309, doi:10.1590/S0074-02762010000300010.
81. Kurokawa, M.; Shimizu, T.; Watanabe, W.; Shiraki, K. Development of New Antiviral Agents from Natural Products *Open Antimicrob. Agents J.* **2010**, *2*, 49–57, doi:10.2174/1876518101002020049.
82. Zandi, K.; Teoh, B.T.; Sam, S.S.; Wong, P.F.; Mustafa, M.; Abubakar, S. Antiviral activity of four types of bioflavonoid against dengue virus type-2. *Virol. J.* **2011**, *8*, 560, doi:10.1186/1743-422X-8-560.
83. Low, J.S.Y.; Wu, K.X.; Chen, K.C.; Ng, M.M.L.; Chu, J.J.H. Narasin, a novel antiviral compound that blocks dengue virus protein expression. *Antivir. Ther.* **2011**, *16*, 1203–1218, doi:10.3851/IMP1884.



© 2020 by the authors. Licensee MDPI, Basel, Switzerland. This article is an open access article distributed under the terms and conditions of the Creative Commons Attribution (CC BY) license (<http://creativecommons.org/licenses/by/4.0/>).



सत्यमेव जयते

वैद्य राजेश कोटेचा
Vaidya Rajesh Kotecha



सचिव

भारत सरकार

आयुर्वेद, योग व प्राकृतिक चिकित्सा

यूनानी, सिद्ध, सोवा रिग्पा एवं होम्योपैथी (आयुष) मंत्रालय
आयुष भवन, 'बी' ब्लॉक, जी.पी.ओ. कॉम्प्लेक्स,

आई.एन.ए. नई दिल्ली-110023

SECRETARY

GOVERNMENT OF INDIA

MINISTRY OF AYURVEDA, YOGA & NATUROPATHY

UNANI, SIDDHA, SOWA-RIGPA AND HOMOEOPATHY (AYUSH)

AYUSH BHAWAN, B-BLOCK, GPO COMPLEX

INA, NEW DELHI-110023

Tel. : 011-24651950, Fax : 011-24651937

E-mail : secy-ayush@nic.in

D.O. No. S. 16030/18/2019 -NAM

Dated: 06th March, 2020

As you are aware, incidences of Corona Virus (COVID-19) have been reported worldwide and 30 Positive cases of Corona Virus have also been reported in India till date. Even though there is no panic response warranted, AYUSH being one of the important Ministry equipped for providing appropriate response to the circumstances arose due to this public health challenge, it is worthwhile to associate with other Stake holders in eliciting AYUSH based public health response considering the strength and evidences of these systems. In the past also, interventions under AYUSH systems had been varyingly used for making an effective public health response in similar situations faced in many States/UTs.

Keeping in view, Ministry of AYUSH with the recommendations from Research Councils under its administrative control has come out with an advisory (Copy enclosed as **Annexure-I**) which may be communicated /implemented through AYUSH personnel and facilities as per the prevailing system of medicine in your State/UT.

These interventions from different AYUSH systems of medicine are supported with evidences for promotion of immunity and help in improving the respiratory symptoms in similar diseases. In this regard, a separate list of references is also enclosed at **Annexure-II** for your ready reference.

Therefore, I request you to do the needful for appropriate roll out of this strategy in consultation with other stake holder departments responsible for Public Health in your State/UT.

Encl: as above

Yours sincerely,

-Sd/-

(Rajesh Kotecha)

To,

Chief Secretaries of all States/UTs.

Copy to:

- 1) Principal Secretary AYUSH/Health of all States/UTs
- 2) Director/Commissioner/Mission Director (AYUSH) of all States/UTs.

TRUE COPY

(Rajesh Kotecha)

ANNEXURE-IADVISORY FROM MINISTRY OF AYUSH FOR MEETING THE CHALLENGE
ARISING OUT OF SPREAD OF CORONA VIRUS (COVID-19) IN INDIA

Corona viruses (CoV) are a large family of viruses that cause illness ranging from the common cold to more severe diseases such as Middle East Respiratory Syndrome (MERS-CoV) and Severe Acute Respiratory Syndrome (SARS-CoV). The new Corona virus disease (COVID-19) was first reported from Wuhan, China, on 31 December 2019. 72 countries reported COVID-19 incidence with 90,870 confirmed cases and 3112 deaths as per WHO factsheet as on 03.03.2020. As on 03.03.2020, 05 confirmed cases are reported in India from various parts.

Common signs of infection include fever, cough, myalgia, fatigue and breathing difficulties. In more severe cases, infection can cause pneumonia, severe acute respiratory syndrome, kidney failure and even death.

The function of the immune system is critical in the human response to infectious disease. Viral infections induce oxidative stress and cause damage to airway epithelial cells. A growing body of evidence identifies stress, nutrition and immunity as a cofactor in infectious disease susceptibility and outcomes. The mainstay in management of corona viral infections has been supportive care, nutrition and preventing further progression in the absence of any antiviral agent or vaccine.

During Ebola outbreak in 2014 expert group of WHO has recommended that "it is ethical to offer unproven interventions with as yet unknown efficacy and adverse effects, as potential treatment or prevention" keeping in view no vaccine or anti-virals were available.

Approach of AYUSH systems:

The holistic approach of AYUSH systems of medicine gives focus on prevention through lifestyle modification, dietary management, prophylactic interventions for improving the immunity and simple remedies based on presentations of the symptoms.

TRUE COPY

For instance, emphasis on avoidance of causative factors and enhancing the immunity against host of infections are characteristics of Ayurveda management. The preventive aspect of Homoeopathy is well known, and historically, Homoeopathy has reportedly been used for prevention during the epidemics of Cholera, Spanish Influenza, Yellow fever, Scarlet fever, Diphtheria, Typhoid etc. The genus epidemicus (GE) is the remedy found to be most effective for a particular epidemic once data have been gathered from several cases. It was reported that, during recent past GE had been used during various disease outbreak for preventing the spreading of diseases like Chikungunya, Dengue Fever, Japanese Encephalitis and Cholera with good results. As detail accounts of use of homoeopathy in control of epidemics are given in recent publications.

The AYUSH approach to manage the outbreak broadly comprise of:

- i. Preventive and prophylactic
- ii. Symptom management of COVID-19 like illnesses
- iii. Add on Interventions to the conventional care

Based on potential & strength of AYUSH systems supported by evidences for promotion of immunity and help in improving the respiratory symptoms in similar diseases and as per the recommendations from the research councils under Ministry of AYUSH following system wise approach is recommended:

i. Preventive and prophylactic:

Ayurveda:

Samshamani Vati 500 mg. twice a day with warm water for 15 days. The medicine contains aqueous extract of *Tinospora cordifolia*.

Siddha:

Nilavembu Kudineer decoction 60 ml. twice a day for 14 days. The medicine contains aqueous extract of *Andrographis paniculata* & others.

Unani:

Preparation of decoction by boiling Behidana (*Cydonia oblonga*) 3 gm, Unnab (*Zizyphus jujube*) 5 in number. Sapistan (*Cordia myxa*) 9 in number in water. (Boil these in 250 ml water- boil it till it remains half- filter it – keep in a glass bottle and use it lukewarm). The drugs used in the preparation of this decoction have been reported to have

Antioxidant activity, Immuno-modulatory, antiallergic, smooth muscle relaxant activity and Anti-influenza activity. This decoction may be taken twice a day for 14 days.

Homoeopathy:

Arsenicum album 30, daily once in empty stomach for three days. The dose should be repeated after one month by following the same schedule till Corona virus infections prevalent in the community.

In one of the studies Arsenic album as one of the constituents in a formulation affected HT29 cells and human macrophages. Also, it showed ↓NF-κB hyperactivity (reduced expression of reporter gene GFP in transfected HT29 cells), ↓TNF-α release in macrophages. More over Arsenic album is a common prescription in the cases of respiratory infections in day to day practice.

ii. Symptom management of COVID-19 like illnesses

Ayurveda

1. AYUSH-64 : 02 tablets twice a day
2. Agasthya Hareetaki : 05 gm twice a day with warm water
3. Anuthaila/ Sesame oil 02 drops in each nostril daily in the morning

Siddha

1. Nilavembu Kudineer /Kaba Sura Kudineer – decoction 60ml twice a day
2. Adathodai Manapagu – Syrup 10 ml twice a day

Homoeopathy

Various medicine which found to be effective in treating flu like illness are *Arsenicum album*, *Bryonia alba*, *Rhus toxico dendron*, *Belladonna* *Gelsemium* *Eupatorium perfoliatum*.

All these medicines should be taken in consultation with qualified physicians of respective AYUSH systems.

iii. Add on Interventions to the conventional care

Ayurveda

1. AYUSH-64 : 02 tablets twice a day
2. Agastya Hareetaki : 05 gm twice a day with warm water

Siddh

1. Vishasura Kudineer : decoction 60ml twice a day
2. Kaba Sura Kudineer – decoction 60ml twice a day

Homoeopathy

Medicine mentioned Symptom management of COVID-19 like illnesses” under subhead Homoeopathy can also be given as add on to the conventional care.

All these medicines should be taken in consultation with qualified physicians of respective AYUSH systems.

General preventive measures (already notified):

- i. Observe good personal hygiene.
- ii. Practice frequent hand washing with soap.
- iii. Follow respiratory etiquettes - cover your mouth when coughing or sneezing.
- iv. Avoid close contact with people who are unwell or showing symptoms of illness, such as cough, runny nose etc.
- v. Avoid contact with live animals and consumption of raw/undercooked meats.
- vi. Avoid travel to farms, live animal markets or where animals are slaughtered.
- vii. Wear a mask if you have respiratory symptoms such as cough or runny nose.

In addition, the following AYUSH specific measures may be adopted:

The diet should be fresh, warm, easy to digest, containing whole cereals, seasonal vegetables etc. Frequent sipping of water boiled with Tulsi leaves, crushed ginger, and turmeric would be beneficial. Honey with a pinch of pepper powder is also beneficial in case cough. Cold, frozen and heavy foods may be best avoided. It is always beneficial to avoid direct exposure to cold breeze. Appropriate rest and timely sleep are advisable. The practice of Yogasana and Pranayama under the guidance of qualified Yoga instructor is recommended.

Common medicinal plants useful in similar symptoms are Tulsi (*Ocimum sanctum*), Guduchi (*Tinospora cordifolia*), Ginger (*Zingiber officinale*) and Turmeric (*Curcuma longa*)

ANNEXURE-II

References for Interventions of different AYUSH systems of medicines for promotion of immunity and help in improving the respiratory symptoms

1. Pedersen A, Zachariae R, Bovbjerg DH. Influence of Psychological Stress on Upper Respiratory Infection—A Meta-Analysis of Prospective Studies. *Psychosom Med* [Internet]. 2010 Oct [cited 2020 Mar 4];72(8):823–32. Available from: <http://journals.lww.com/00006842-201010000-00014>.
2. JENSEN MM, RASMUSSEN AF. Stress and susceptibility to viral infections. II. Sound stress and susceptibility to vesicular stomatitis virus. *J Immunol* [Internet]. 1963 Jan 1 [cited 2020 Mar 4];90(1):21–3. Available from: <http://www.ncbi.nlm.nih.gov/pubmed/13957641>.
3. WHO. Ethical considerations for use of unregistered interventions for Ebola virus disease (EVD) <https://www.who.int/media/centre/news/statements/2014/ebola-ethical-review-summary/en/>.
4. Dinesh Kumar *et al.* A review of immunomodulators in the Indian traditional health care system *Journal of Microbiology, Immunology and Infection*, Volume 45, Issue 3, June 2012, Pages 165-184.
5. Winston J. *The Faces of Homeopathy*. Wellington, New Zealand: Great Auk Publishing; 1999.
6. Dewey W. A.. Homeopathy in influenza—A chorus of fifty in harmony. *Journal of the American Institute of Homeopathy* 1920-21; 13: 1038-1043.
7. Sharma, A.; Chadha, N.K.; Das, S.K.; Sen, A.; Roy, S.D.; Chanu, T.I.; Sawant, P.B.; Prakash, C. *Tinospora cordifolia* extract induced effects on cellular immune reactions of *labeorohita* (hamilton) challenged against *aeromonas hydrophila*. *Int. J. Pure Appl. Biosci.* 2017,5,765–775. [Cross Ref].
8. Kalikar MV, Thawani VR, Varadpande UK, Sontakke SD, Singh RP, Khiyani RK. Immunomodulatory effect of *Tinospora cordifolia* extract in human immuno-deficiency virus positive patients. *Indian J Pharmacol* 2008;40 (3):107-10.
9. More, P.; Pai, K. Immunomodulatory effects of *Tinospora cordifolia* (Guduchi) on macrophage activation. *Biol. Med.* 2011, 3, 134–140.

10. G.S.Lekha *et al.* An Interventional Cohort Study in Dengue Prevalent Area by Using Nilavembu Kudineer and Awareness Programme "IOSR Journal of Dental and Medical Sciences (IOSR-JDMS), Volume 17, Issue 2(2018),PP (19-23).
11. Christian GJ *et al.* Protective Effect of Poly Herbal Siddha Formulation – Nilavembu Kudineer against common Viral Fevers Including Dengue – A case Control Approach. *Int J Pharm Sci Res* 2015; 6(4):1656-60.
12. Kalaiarasi *et al.* A combination of Nilavembu Kudineer and Adathodai Manapagu in the Management of Dengue Fever. *International Journal of Current Research*, Vol 5, Issue 4, PP 978-981 2013.
13. The medical importance of *Cydonia oblonga*- A review Prof Dr Ali Esmail Al-Snafi Department of Pharmacology, College of Medicine, Thi qar University, Nasiriyah, P O Box 42, Iraq *IOSR Journal Of Pharmacy* www.iosrphr.org (e)-ISSN: 2250-3013, (p)- ISSN: 2319-4219 Volume 6, Issue 6 Version. 2 (June 2016), PP. 87-99.
14. Hamauzu Y, Yasui H, Inno T, Kume C, Omanyuda M. Phenolic profile, antioxidant property, and anti-influenza viral activity of Chinese quince (*Pseudocydonia sinensis* Schneid.), quince (*Cydonia oblonga* Mill.), and apple (*Malus domestica* Mill.) fruits. *J Agric Food Chem.* 2005 Feb 23;53(4):928-34.
15. Hong EH, Song JH, Kang KB, et al. Anti-influenza activity of betulinic acid from on influenza A/PR/8 virus. *Biomol Ther.* 2015;23(4):345–349. doi:10.4062/biomolther.2015.019.
16. Chi A, Kang C, Zhang Y, Tang L, Guo H, Li H, Zhang K. Immunomodulating and antioxidant effects of polysaccharide conjugates from the fruits of *Ziziphus Jujube* on Chronic Fatigue Syndrome rats. *Carbohydr Polym.* 2015 May 20;122:189-96. doi: 10.1016/j.carbpol.2014.12.082. Epub 2015 Jan 14.
17. Ali WR, Al-Asady ZT and Ibrahim AA. Immunomodulatory of *Cordia myxa* (L.) aqueous extract fruit in immunized mice with hydatid cyst fluid. *Journal of Natural Science Research* 2015; 5(10): 75-83.
18. Ad-Dahhan HAA. Detection of Immunomodulatory activity of alcoholic extract of *Cordia myxa* (L.) fruit. *AL-Qadisyia Journal of Applied Sciences* 2010; 15(4): 1-8.

19. Al-Bayaty MAA and Al-Tahan FJ. Mechanism of the tracheal smooth muscle relaxant activity of the *Cordia myxa* plant extract in sheep. *Iraqi Journal of Veterinary Medicine* 2008; 32(2): 214-226.
20. Afzal M, Obuekwe C, Khan AR and Barakat H. Antioxidant activity of *Cordia myxa* L. and its hepato protective potential. *EJEAF Che* 2007; 8(6): 2236-2242.
21. Bellavite P, Signorini A, Marzotto M, Moratti E, Bonafini C, Olioso D. Cell sensitivity, non-linearity and inverse effects. *Homeopathy*. 2015 Apr;104(2):139-60.
22. Srikanth Narayanam & K.D.Sharma, &R.K.Shingal, &G.Veluchamy, Effect of AYUSH-64 in the treatment of Malaria. 2001.
23. Divya Kajaria, Nasreen Ahmed and Deepak Bhati. Evaluating Clinical Efficacy of Ayurvedic Inhalation Therapy (Aerosol) and Rasayan Therapy in the Management of COPD - A Randomized Cohort Control Clinical Study. *The Lancet Respiratory Medicine*. The lancetrm-D-19-00759.
24. Dalvi *et al.* LITERARY REVIEW OF ANU TAILA NASYA, *UJAHM* 2015, 03 (02): Page 42-45.
25. Saravanan J *et.al.* Anti – Inflammatory, Anti – Pyretic and Anti bacterial Study of *Kabasura kudineer Chooranam*. *International Journal of Current Advanced Research*, Vol 7; Issue 2,2018.
26. Shailaja *et.al.* A Review on Poly herbal Formulation – *Visha Sura Kudineer Chooranam* – A Classical Anti –Viral Used in Siddha System, *European Journal of Pharmaceutical and Medical Research*,2017,4 (9),184-192.
27. Chakraborty P S, Lamba C D, Nayak D, John M D, Sarkar D B, Poddar A, Arya J S, Raju K, Vivekanand K, Singh H B, Baig H, Prusty A K, Singh V, Nayak C. Effect of individualized homoeopathic treatment in influenza like illness: A multicenter, single blind, randomized, placebo controlled study. *Indian J Res Homoeopathy* 2013;7:22-30.
28. Shailaja *et.al.* A Review on Polyherbal Formulation – *Visha Sura Kudineer Chooranam* – A Classical Anti –Viral Used in Siddha System, *European Journal of Pharmaceutical and Medical Research*,2017,4 (9),184-192.
29. Marc Maurice Cohen. *Tulsi – Ocimum sanctum: A herb for all reasons*. *J Ayurveda Integr Med*. 2014 Oct-Dec; 5(4): 251–259.

30. Sharma *et al.* Therapeutic Vistas of Guduchi (*Tinospora cordifolia*): a medico-historical memoir. The Journal of research and education in Indian medicine XX(2):113-28 · April 2014.
31. Dr Anant Saznam, Dr Satyendra Kumar Singh. Review of Shunthi (*Zingiber officinale* Rosc.) in Ayurvedic Literature. Journal of medical science and clinical research. Volume 05 Issue 09 September 2017.
32. Krup V, Prakash LH, Harini A (2013). Pharmacological Activities of Turmeric (*Curcuma longa* linn): A Review. J Homeo Ayurv Med 2:133. Doi: 10.4172/2167-1206.1000133.
33. Chandrasekaran, C. V., Sundarajan, K., Edwin, J. R., Gururaja, G. M., Mundkinajeddu, D., & Agarwal, A. (2013). Immune-stimulatory and anti-inflammatory activities of *Curcuma longa* extract and its polysaccharide fraction. Pharmacognosy research, 5(2), 71-9.

↓
TRUE COPY

(To be published in the Extraordinary Gazette of India)



F.No. L.11011/8/2020/AS
Government of India
Ministry of AYUSH

Date: 21st April, 2020.
New Delhi

NOTIFICATION

No. L.11011/8/2020/AS: In the wake of COVID-19 caused by SARS CoV 2, there has been surge in proposals received by Ministry of AYUSH for claiming possible treatment of COVID19. At present, there is no approved treatment for COVID 19 infection. Indian Traditional Medicines have wide potential for usage in such conditions owing to their longstanding use in the community, huge number of ancient references and large number of publications in scientific journals on their phyto-chemical constituents, mode of action, clinical efficacy etc. At the same time, it is also essential to have scientific evidence on use of any Ayurveda, Unani, Siddha or Homeopathy formulation on prevention/ management of COVID 19. Therefore, it is felt necessary to make serious efforts for development of drugs based on any of AYUSH systems recognized under Drugs and Cosmetics Act, 1940.

2. There are no specific regulatory provisions in the Drugs & Cosmetics Rules 1945, for conduct of clinical trials of Ayurveda, Siddha, Unani and Homeopathy drugs. At the same time it is also necessary that the clinical data generated is scientifically valid and credible. In this context the Ministry has undertaken consultation with DCGI, CDSCO as well as other research experts.

3. In the above background and based on the consultation of CDSCO, the Ministry of AYUSH with the approval of Minister of State Independent Charge for AYUSH notifies that scientists, researchers, clinicians of any of recognized systems of medicine under IMCC Act, 1970, HCC Act 1973 and NMC Act 2019 (formerly IMC Act 1956) can undertake research on COVID19 through Ayurveda, Siddha, Unani and Homeopathy systems including prophylactic measures, intervention during the quarantine, asymptomatic and symptomatic cases of COVID -19, public health research, survey, lab based research etc. to generate evidence.

4. While undertaking research, it is mandatory for the organizations to comply with the following conditions:

- i) The proposals should be approved by their scientific advisory bodies and Institutional Ethics Committees.
- ii) If it is clinical trial, the project should be registered with CTRI.
- iii) The sample size should be based on statistical justification.

L
TRUE COPY



WHO recommends against the use of remdesivir in COVID-19 patients

20 November 2020



WHO has updated its recommendation on remdesivir for the treatment of COVID-19.

On 22 April 2022, following publication of new data from a clinical trial looking at the outcome of admission to hospital, WHO now suggests the use of remdesivir in mild or moderate COVID-19 patients who are at high risk of hospitalization.

[Latest information on COVID-19 therapeutics.](#)

WHO has issued a conditional recommendation against the use of remdesivir in hospitalized patients, regardless of disease severity, as there is currently no evidence that remdesivir improves survival and other outcomes in these patients.

This recommendation, released on 20 November, is part of a living guideline on clinical care for COVID-19. It was developed by an international guideline development group, which includes 28 clinical care experts, 4 patient-partners and one ethicist.

The guidelines were developed in collaboration with the non-profit Magic Evidence Ecosystem Foundation (MAGIC), which provided methodologic support. The guidelines are an innovation, matching scientific standards with the speed required to respond to an ongoing pandemic.

Work on this began on 15 October when the WHO Solidarity Trial published its interim results. Data reviewed by the panel included results from this trial, as well as 3 other randomized controlled trials. In all, data from over 7000 patients across the 4 trials were considered.

The evidence suggested no important effect on mortality, need for mechanical ventilation, time to clinical improvement, and other patient-important outcomes.

The guideline development group recognized that more research is needed, especially to provide higher certainty of evidence for specific groups of patients. They supported continued enrollment in trials evaluating remdesivir.

Updated 20 November 2020

* A conditional recommendation is issued when the evidence around the benefits and risks of an intervention are less certain. In this case, there is a conditional recommendation against the use of remdesivir. This means that there isn't enough evidence to support its use.

Want to read more?

[Subscribe to newsletter →](#)



Why Remdesivir Failed: Preclinical Assumptions Overestimate the Clinical Efficacy of Remdesivir for COVID-19 and Ebola

Victoria C. Yan,^a Florian L. Muller^b

^aCopycat Sciences, Boston, Massachusetts, USA

^bSporos Bioventures, Houston, Texas, USA

ABSTRACT Remdesivir is a nucleoside monophosphoramidate prodrug that has been FDA approved for coronavirus disease 2019 (COVID-19). However, the clinical efficacy of remdesivir for COVID-19 remains contentious, as several trials have not found statistically significant differences in either time to clinical improvement or mortality between remdesivir-treated and control groups. Similarly, the inability of remdesivir to provide a clinically significant benefit above other investigational agents in patients with Ebola contrasts with strong, curative preclinical data generated in rhesus macaque models. For both COVID-19 and Ebola, significant discordance between the robust preclinical data and remdesivir's lackluster clinical performance have left many puzzled. Here, we critically evaluate the assumptions of the models underlying remdesivir's promising preclinical data and show that such assumptions overpredict efficacy and minimize toxicity of remdesivir in humans. Had the limitations of *in vitro* drug efficacy testing and species differences in drug metabolism been considered, the underwhelming clinical performance of remdesivir for both COVID-19 and Ebola would have been fully anticipated.

KEYWORDS GS-441524, GS-5734, *in vitro* models, *in vivo* models, nonhuman primates, pharmacokinetics, prodrug, remdesivir

Remdesivir (RDV) is a nucleoside monophosphoramidate prodrug that has been FDA approved for coronavirus disease 2019 (COVID-19) principally on the basis of one double-blind, randomized control trial (RCT) (1), which demonstrated a faster median time to recovery in RDV-treated patients by about 5 days (10 days) than in the placebo group (15 days). However, the clinical efficacy of RDV remains contentious, as a smaller double-blind RCT showed no statistical difference in clinical improvement between RDV- and placebo-treated patients (2); interim results from a larger RCT conducted by the WHO revealed no significant difference in mortality between patients treated with RDV and those treated with the standard of care (SOC) (3, 4), prompting the organization to recommend against using RDV for COVID-19 (4). Such clinical results diametrically oppose the impressive preclinical data, which showcased RDV's strong, broad-spectrum antiviral activity in cell culture (5–7) and in preclinical species (8–11). Here, we show that overestimations of RDV's clinical performance arise from several preclinical assumptions made at both the *in vitro* and *in vivo* levels, with the principal assumption being that the conventional drug development framework is relevant to prodrugs such as RDV. We show that this preconceived notion fails to account for the significant differences between “soft” drugs (those that are subject to metabolic transformation) such as RDV and “hard” drugs (those that are metabolically inert) which permeate the FDA-approved drug landscape (12). By reassessing key data on RDV at the cell culture and preclinical organismal levels, we elucidate the predictability of RDV's underwhelming clinical performance and provide insights for future development of phosphate prodrugs.

Citation Yan VC, Muller FL. 2021. Why remdesivir failed: preclinical assumptions overestimate the clinical efficacy of remdesivir for COVID-19 and Ebola. *Antimicrob Agents Chemother* 65:e01117-21. <https://doi.org/10.1128/AAC.01117-21>.

Copyright © 2021 American Society for Microbiology. All Rights Reserved.

Address correspondence to Victoria C. Yan, victoria.yan@copycatsciences.com.

Dedicated to Tomas Cihlar, Richard Mackman, and Bill Lee.

Accepted manuscript posted online

12 July 2021

Published 17 September 2021

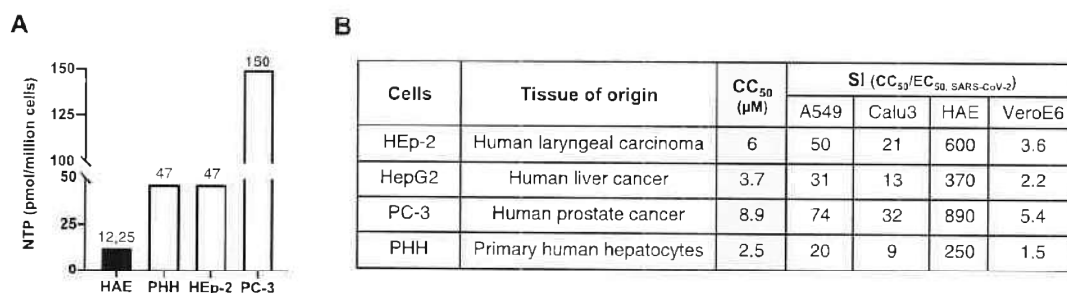


FIG 1 Remdesivir is preferentially bioactivated in hepatocytes. (A) RDV NTP (GS-443902) formation in PHH and HEp-2 cells is about 4-fold higher than in HAE cells and about 12-fold higher in PC-3 cells than in HAE cells. Data are means of data replotted from references 5 (HAE) and 28 (PHH, HEp-2, and PC-3). Cells were seeded at approximately 1×10^6 cells/well and were incubated with $1 \mu\text{M}$ RDV for 24 h. Levels of NTP in HAE cells represent the average of quadruplicate technical replicates from 2 donors. (B) Comparison of selectivity indices (SIs) for CC₅₀s of RDV in HEp-2, HepG2, PC-3, and PHH and RDV EC₅₀s obtained in A549, Calu3, HAE, and Vero E6 cells infected with SARS-CoV-2. EC₅₀s used were obtained from references 37 (A549) and 5 (Calu3, HAE, and Vero E6).

REMDESIVIR IS A McGUIGAN PRODRUG THAT PREDOMINANTLY DEPOSITS BIOACTIVE TRIPHOSPHATE IN THE LIVER

RDV is a phosphoramidate prodrug of the McGuigan (ProTide) class that was originally designed to deliver a membrane-impermeable nucleoside triphosphate (NTP) analogue (GS-443902) for the treatment of hepatitis C (HCV) (13–16). McGuigan prodrugs such as RDV, which contain a phosphate protected by aryloxy and amino acid ester moieties, are intended for intracellular conversion of the active NTP through bioactivation by carboxylesterase 1 (CES1), cathepsin A (CTSA), and histidine triad nucleotide binding protein 1 (HINT1) (16, 17). During RDV's development, several other nucleoside and nucleotide analogues were also being investigated for their anti-HCV efficacy, with the most advanced compounds being pyrimidine analogues (NCT00120835, NCT00869661, and NCT01096576). As purine analogues, RDV and its sibling compounds (14) were thus developed against the backdrop of pyrimidine analogues. Application of the McGuigan prodrug strategy onto anti-HCV pyrimidine analogues had two aims: (i) rapid loading of the active NTP in the liver, where HCV is trophic, and (ii) overcoming the rate-limiting initial phosphorylation step observed for some pyrimidine analogues (18). While the former reason is generally applicable to multiple phosphate prodrugs, the latter reasoning has yet to be explicitly demonstrated for purine (adenosine) analogues such as RDV and its parent nucleoside, GS-441524. In fact, the prohibitively slow initial phosphorylation step appears to be limited to some uridine analogues, such as RO2433 (parent nucleoside of sofosbuvir) (18), with many cytidine and thymidine analogues appearing to undergo initial phosphorylation quite readily (19, 20). Multiple studies have already demonstrated the ability of GS-441524 to undergo conversion to the active NTP through direct measurement of GS-443902 levels or through indirect assessment of the low-micromolar 50% effective concentration (EC₅₀) of GS-441524 against virus-infected cells; varying EC₅₀s for GS-441524 and RDV in head-to-head comparisons further suggest that the cellular potency of either compound is cell line and cell type dependent (see Data Set S1) (5, 7, 8, 21, 22), despite the fact that the exquisite specificity of GS-443902 for the SARS-CoV-2 RNA-dependent RNA polymerase (RdRp) is undisputed (K_m ~9 nM) (23–25). Thus, as an artifact of its initial HCV indication, the primary function of the McGuigan prodrug on RDV is preferential hepatic bioactivation (26).

Much of the initial excitement around the potency of RDV in cell culture models of SARS-CoV-2 centered on its low-micromolar potency in a variety of cell lines and cell types, including primary human airway epithelial (HAE) cells, in which the lowest reported EC₅₀ for RDV against severe acute respiratory syndrome coronavirus 2 (SARS-CoV-2) was obtained (5). Against Ebola virus (EBOV)-infected cells in culture, treatment with RDV yielded similarly impressive, nanomolar EC₅₀s (6, 8, 27) (Data Set S1). Among other oversights discussed subsequently, these superficially impressive *in vitro* efficacy data were assessed in isolation—without considering how such data compare to RDV's

TABLE 1 Assumptions in standard cell culture procedures do not reflect the *in vivo* behavior for prodrugs like RDV

| Standard procedure | Incorrect assumption | <i>In vivo</i> reality |
|---|--|--|
| Incubate cells with virus for 30–60 min | Viral load is constant | Viral load is not always constant |
| Incubate cells with drug for 48–72+ h | Target population of cells is constantly exposed to prodrug for 48–72+ hours at supraphysiological [drug] [Drug]:target cell population is high <i>in vivo</i> Preferential extraction by other organs or cell types is negligible | Prodrug exposure can be short and is influenced by the $t_{1/2}$ of the prodrug [Drug]:target cell population is low <i>in vivo</i> Drug distribution can be uneven due to preferential metabolism by certain tissue over others |

cytotoxicity in hepatocytes. Placed in the context of primary human hepatocytes (PHH) *in vitro*, the levels of active NTP formed by primary HAE cells are unambiguously dominated by those formed in PHH (Fig. 1). Simply put, even in the cell model where RDV performs best against SARS-CoV-2, levels of active NTP are still approximately 4-fold higher in PHH than in primary HAE cells when both cell types are subjected to identical culturing and treatment conditions (5, 28).

CONVENTIONAL CELL CULTURE PROTOCOLS FAIL TO ACCOUNT FOR THE COMPLEX PHARMACOKINETICS OF REMDESIVIR *IN VIVO*

Discrepancies between the *in vitro* and *in vivo* conditions are exacerbated for prodrugs that are susceptible to extracellular metabolism, such as RDV. Key considerations that are particularly pertinent for (phosphate) prodrugs but tend to be overlooked under standard cell culturing protocols include magnitude of exposure, exposure time, and distribution patterns incurred by route of administration. One could argue that such shortcomings could be accounted for in subsequent *in vivo* evaluations. Nevertheless, it appears that decisions to advance or halt the development of certain prodrugs are contingent upon *in vitro* and *ex vivo* data without consideration of the assumptions inherent in standard cell culture protocols or without revision to the way in which cell culture assessments are performed even after observing the prodrug's pharmacokinetic behavior *in vivo*. For instance, a typical cell-based screening assay involves incubating cells with virus for approximately 30 to 60 min before removing virus-containing medium, washing the cells, and then incubating the cells with drug for 48 to 72 h (5, 6, 29). While appropriate for drugs with long half-lives ($t_{1/2}$) (i.e., most hard drugs), such conditions skew efficacy results for soft drugs with short $t_{1/2}$, such as RDV. Under standard screening conditions, 4 assumptions are made (Table 1): (i) viral load is constant, (ii) the target population of cells is constantly exposed to drug for 48 to 72 h at supraphysiological concentrations of drug, (iii) the ratio of drug concentration to the number of target cells is high, (iv) preferential extraction by other organs or cell types is negligible. Using RDV as an example, such assumptions are inconsistent with its clinical pharmacokinetics, given that it has a $t_{1/2}$ of less than 1 h in humans (30, 31). For the brief time that intact RDV is present in systemic circulation, it is both unclear and unlikely that tissue distribution is uniform, despite RDV's large apparent volume of distribution during terminal phase (V_z) (32); preferential hepatic extraction (Fig. 1) and competing plasma esterase hydrolysis undermine the ability of RDV to durably reach the primary site of SARS-CoV-2 infection (type II alveolar cells) and exert its antiviral activity (30, 31).

A set of experiments by Wang and colleagues demonstrated that the magnitude of SARS-CoV-2 inhibition by RDV in Vero E6 cells was largely contingent upon the duration of drug exposure (29). Seeking to probe the mechanism of SARS-CoV-2 inhibition by RDV and chloroquine (CQ), Wang et al. performed a series of "prophylactic," "entry," and "postentry" experiments (Fig. 2A and B). Of the 3 conditions tested, the entry experiment most closely resembled the *in vivo* pharmacokinetics of RDV, as cells were pulsed with drug for just 3 h before being washed and allowed to incubate with fresh medium for the duration of the experiment. Like RDV, CQ is subject to metabolism to

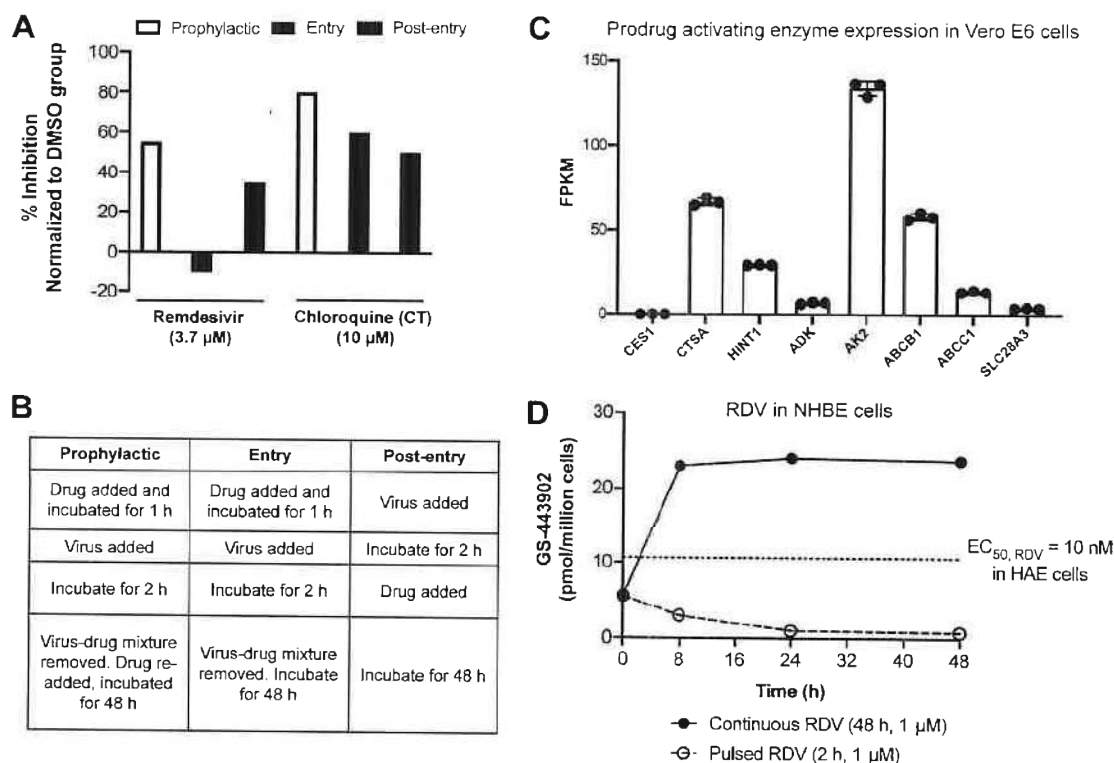


FIG 2 Duration of drug exposure impacts the antiviral efficacy of remdesivir. (A) Continuous exposure to RDV leads to durable *in vitro* inhibition of SARS-CoV-2, but pulsed treatment with RDV results in diminished antiviral activity in Vero E6 cells. Data are means of triplicate data replotted from reference 29. Across the three experiments, RDV was tested at $3.7 \mu\text{M}$ and CQ was tested at $10 \mu\text{M}$. Due to its long *in vivo* $t_{1/2}$, CQ serves as a positive control. (B) Corresponding treatment procedures for prophylactic, entry, and postentry experiments described for panel A. Pulsed experiments correspond to the entry trial. (C) Transcriptome sequencing (RNA-seq) data showing expression of relevant prodrug bioactivating enzymes for RDV in Vero E6 cells, presented as means and standard deviations (SD) from 3 experiments (see the supplemental material). ADK, adenosine kinase; AK2, adenylate kinase 2. AK2 and SLC29A3 were found to mediate RDV potency and toxicity in a genome-wide CRISPR screen (55). (D) Formation of active triphosphate (GS-443902) in normal human bronchial epithelial (NHBE) cells following pulsed (open circles) and continuous (filled circles) incubation. Data are adapted from reference 36 and are presented as means for at least 2 independent replicates. The dotted line at $10.6 \text{ pmol/million cells}$ corresponds to the mean C_{24} of triphosphate formed by RDV in SARS-CoV-2-infected HAE cells when the EC_{50} was determined to be 10 nM , as reported in reference 5.

its main metabolite, *N*-desethylchloroquine (DCQ). However, unlike RDV, with its short $t_{1/2}$ (<1), the $t_{1/2}$ of CQ is approximately 18 to 30 days (33, 34). Thus, the short pulsing experiment more accurately reflects the *in vivo* pharmacokinetic situation for RDV but not CQ. Noting differences in the tested concentrations of RDV and CQ, RDV demonstrated no inhibition of SARS-CoV-2 after a 3-h drug pulse at $3.7 \mu\text{M}$; in contrast, CQ maintained similar levels of SARS-CoV-2 inhibition across all 3 conditions (Fig. 2A, Entry). Discordant inhibitory values for RDV across the 3 conditions suggest that the antiviral efficacy of RDV is considerably diminished when target cells are pulsed rather than continuously exposed to RDV. One potential confounder to this interpretation could be that these experiments were performed in Vero E6 cells, which have rather high expression of *p*-glycoprotein (*p*-gp) (Fig. 2C, ABCB1). It has been reported that RDV is a substrate for ABCB1 (32); in contrast, CQ has been shown to be a substrate for ABCC1 (35), which is expressed at lower levels in Vero E6 than ABCB1 (Fig. 2C). Thus, while pulsed experiments in Vero E6 may exaggerate the reduced anti-SARS-CoV-2 activity of RDV, the totality of these data points to the dependency of RDV's antiviral activity in the target cell population on duration of exposure.

In a more recent publication, Mackman et al. compared the formation of GS-443902 when normal human bronchial epithelial (NHBE) cells were incubated with either pulsed (2 h) or continuous (48 h) concentrations ($1 \mu\text{M}$) of drug in an attempt to better recapitulate the transient *in vivo* $t_{1/2}$ of RDV (Fig. 2D) (36). Expectedly, concentrations of

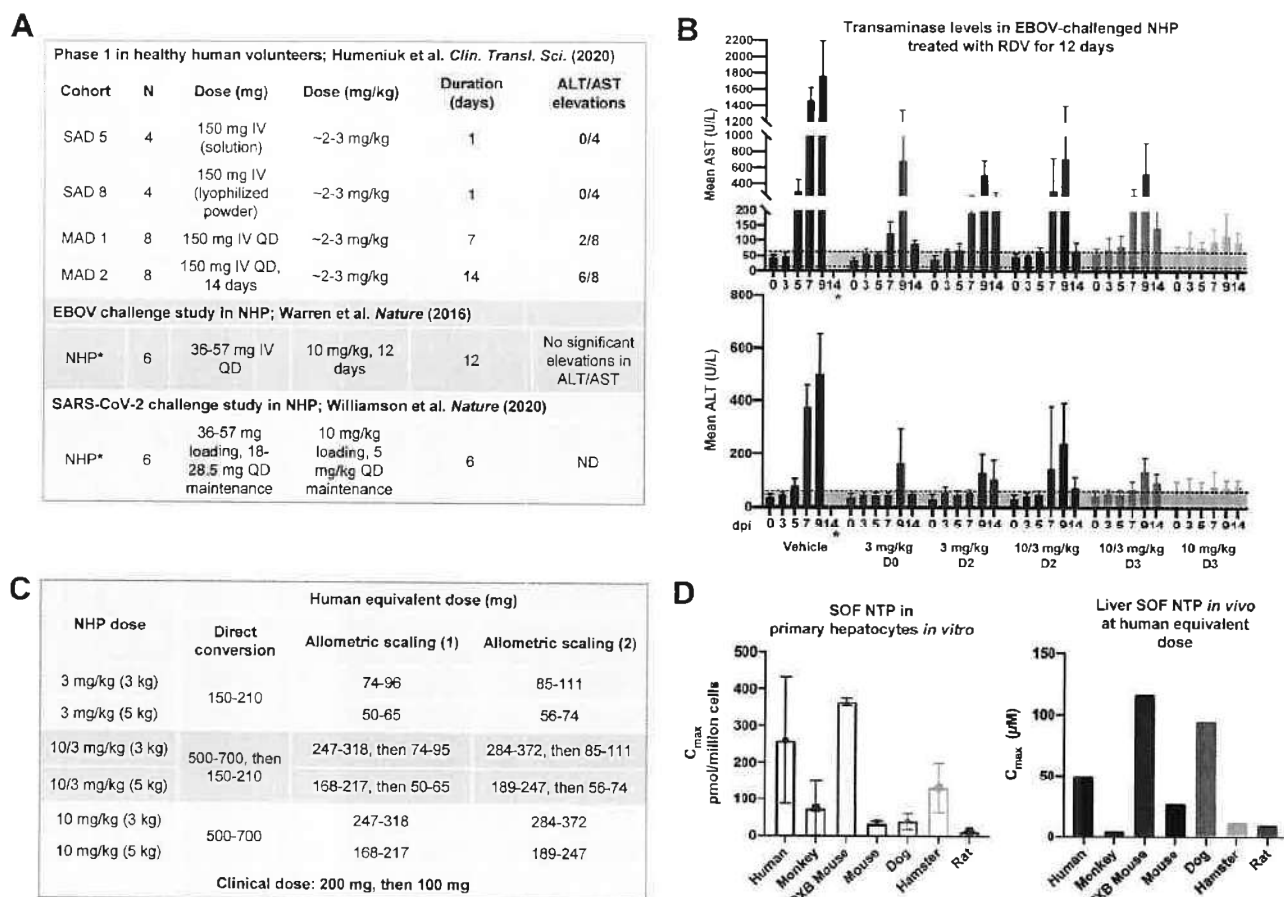


FIG 3 Humans exhibit higher hepatic extraction of McGuigan prodrugs than nonhuman primates. (A) Doses of RDV trialed in the single ascending dose (SAD) and multiple ascending dose (MAD) arms of the phase 1 trial for a 50- to 70-kg human compared to the dose administered in a 3.6- to 5.7-kg NHP. The human and NHP doses have been converted to milligrams per kilogram and milligrams, respectively. Values were obtained from references 8, 30, and 11. (B) ALT and AST levels in NHP (rhesus macaques; 6 per group) challenged with EBOV and treated with RDV for a total of 12 days (adapted from reference 8). Regions shaded in gray correspond to normal ALT/AST ranges in NHP (ALT, 5 to 61 U/liter; AST, 12 to 63 U/liter) (56). NHPs treated at 10 mg/kg for 12 days (light blue) did not experience significant elevations in ALT/AST. *, No ALT/AST values were obtained at 14 days postinfection (dpi) in vehicle control animals because 100% of animals had died. (C) Human equivalent dose (HED) of NHP RDV doses tested in reference 8 via direct conversion and allometric scaling as described in reference 40. Allometric scaling (1) uses an exponent of 0.75, while allometric scaling (2) uses an exponent of 0.80. HEDs were calculated for rhesus macaques weighing 3 kg (light gray) and 5 kg (dark gray) using the Clymer allometric scaling calculator. (D) Sofosbuvir (SOF) is another McGuigan prodrug that is more readily metabolized in PHH than primary monkey hepatocytes *in vitro* (left) and *in vivo* (right). (Left) Levels of SOF NTP in primary hepatocytes following a 2-h pulse of 10 μ M SOF. (Right) Levels of SOF NTP in human explanted livers and in preclinical model species at the allometrically scaled human dose (400 mg). Open bars, C_{max} ; shaded bars, C_{24} . C_{24} in primary monkey livers was below the detection threshold. Values were replotted from references 43 and 42. Formation of SOF NTP is higher in PHH than primary monkey hepatocytes *in vitro* and *in vivo*, suggesting more efficient metabolism of McGuigan prodrugs in human than monkey livers.

GS-443902 were considerably diminished under pulsed conditions (Fig. 2D), which supports reduced antiviral activity by RDV observed by Wang et al. (29) under entry conditions (Fig. 2A). In fact, when the levels of GS-443902 generated by RDV under pulsed and continuous conditions are compared to the concentration at 24 h (C_{24}) of GS-443902, corresponding to an EC_{50} of 10 nM in SARS-CoV-2-infected HAE cells (5), it becomes apparent that short exposure to RDV is insufficient to achieve the desired, low-nanomolar antiviral effects *in vitro* (Fig. 2D). This supports the dramatically reduced antiviral activity observed by Wang et al. in Vero E6 cells (29).

While the aforementioned experiments address the second assumption (drug exposure), they do not resolve the third (ratio of drug concentration to cell number) and fourth (preferential extraction by other organs) assumptions and thus must be taken with grains of salt rather than as definitive extrapolations of *in vivo* behavior (Table 1). The pulsed experiments described by Wang et al. (29) and by Mackman et al. (36) assume the ratio of drug concentration to cell number is high (Table 1, third

assumption), which opposes the *in vivo* reality where the ratio of drug concentration to cell number is low and is exacerbated by uneven drug distribution due to preferential metabolism in cell types such as the liver (Table 1, fourth assumption) (26). It is admittedly difficult to account for these *in vivo* factors in cell culture; however, the challenge of modeling them does not give license to disregard their significance. Indeed, Mackman et al. demonstrated that a 10-mg/kg single intravenous (i.v.) dose of RDV in African green monkeys and cynomolgus macaques resulted in high accumulation of GS-443902 and RDV metabolites in the liver and kidney, suggesting nonuniform distribution of the prodrug (Table 1, fourth assumption; Fig. S1) and reemphasizing the inability of conventional cell culture protocols to account for this important *in vivo* reality (36). As is apparent in the stark contrast between the *in vitro* potency of RDV and its modest clinical efficacy (2, 3, 27, 37), results from *in vitro* experiments offer an incomplete portrayal of the *in vivo* situation; data obtained from such studies should thus be reconsidered in light of the 4 key assumptions (Table 1) when judgments are made regarding which compounds to advance to the clinic.

PROLONGED TREATMENT WITH REMDESIVIR IN NONHUMAN PRIMATES FAILS TO ANTICIPATE CLINICALLY SIGNIFICANT HEPATOTOXICITY

While biochemical and immunohistological data suggest that preferential hepatic metabolism of RDV could result in liver related dose-limiting toxicities (DLTs) in the clinic, such shortcomings were not accounted for in nonhuman primates (NHPs) subjected to repeated dosing of RDV. During a 28-day EBOV challenge study, rhesus macaques were subject to various dosing regimens of RDV for 12 days (8). There were two particularly outstanding findings from this study. First, only the continuous 10-mg/kg dose resulted in "profound suppression of EBOV replication and protected 100% of EBOV-infected animals against lethal disease, ameliorating clinical disease signs and pathophysiological markers, even when treatments were initiated 3 days after virus exposure when systemic viral RNA was detected in two out of six treated animals." Second, 12-day treatment with RDV at 10 mg/kg did not lead to significant elevations in the ratio of alanine aminotransferase to aspartate transaminase (ALT/AST) (Fig. 3B). The latter is particularly surprising, as a 10-mg/kg dose in a 50- to 70-kg human directly equates to 500 to 700 mg of RDV, which is more than 2 times higher than the amount of RDV used clinically and more than twice the duration of RDV currently recommended for COVID-19 (1–3, 38, 39). Even with allometric scaling (40), 10 mg/kg RDV in NHPs translates to about 168 to 284 mg of RDV in humans (Fig. 3C), which exceeds the recommended loading dose of 200 mg followed by 100 mg for 5 to 10 days. Unlike NHPs, which can tolerate 10 mg/kg RDV for 12 days without significant transaminase elevations, humans would not be able to withstand the allometrically scaled dose for the same duration, given that duration-dependent, low-grade transaminase elevations had already emerged in 25% and 75% of healthy human volunteers administered 150 mg once a day (QD) for 7 and 14 days, respectively (Fig. 3A and B) (30, 41). Allusions to higher hepatic extraction of McGuigan prodrugs in human than in monkey hepatocytes had been demonstrated in another Gilead study with sofosbuvir (SOF), another McGuigan prodrug (42). Following a 2-h pulse with 10 μ M SOF in primary hepatocytes across species, human hepatocytes formed about 3-fold-higher levels of active SOF NTP than monkey hepatocytes (Fig. 3D). Likewise, maximum concentrations (C_{max}) of SOF NTP *in vivo* were found to be much higher in human liver (\sim 50 μ M) (43) than in monkey liver (\sim 5 μ M) when SOF was administered at the allometrically scaled dose (400 mg in humans) (Fig. 3D) (42). Coupled with the observation that 12-day dosing with RDV at 10 mg/kg does not yield significant ALT/AST elevations in NHP (8), these data strongly suggest there is preferential hepatic extraction of McGuigan prodrugs in humans compared to NHP.

As a result of model-specific disparities in the hepatic extraction of McGuigan prodrugs, the dose escalation that would likely be required to clarify RDV's antiviral activity in COVID-19 (2) and Ebola (44, 45) patients is prohibited due to on-target

hepatotoxicity (30). Thus far, the largest clinical study that examined the relationship between RDV treatment and reduction of SARS-CoV-2 titers was published by Wang and colleagues in *The Lancet* (2). Although it was criticized for its small trial size ($n = 237$), this study showed that RDV was unable to demonstrate (i) a statistically significant time to improvement compared to placebo controls and (ii) reduction in viral loads in the upper and lower airways compared to controls (2). Since that study was published, some unique case reports have described the ability of RDV to reduce viral loads in the upper airway (46, 47). Still, the bulk of available data suggest that the current recommended dose (200 mg loading, 100 mg maintenance for 5 to 10 days [48]) is insufficient (41) to yield the robust antiviral activity to which many *in vitro* studies have alluded (5, 37, 49). Insufficient dosing in humans is corroborated by data on RDV in EBOV-infected patients, in which RDV was unable to demonstrate significant reductions in viral loads at the standard dose (200 mg loading, 100 mg maintenance for 9 to 12 days) in hospitalized patients (45) or at a lower dose (100 mg for 5 days) during treatment in patients with viral persistence in semen (44).

Preclinical evaluation of RDV at the allometrically scaled dose (10 mg/kg loading, 5 mg/kg maintenance for 6 days postinfection [dpi]) in rhesus macaque models with mild COVID-19 (11, 50) found that there was no significant reduction in viral titers in the upper airway by RDV compared to untreated animals, with the exception of the trachea (Fig. 4A and B) at 7 dpi. Treatment with RDV yielded a global reduction in viral load in all examined lobes of the lung; however, this dose was unable to exert a more profound reduction in viral titers during the treatment period (Fig. 4A). The underwhelming nature of these data is underscored by the close relationship between viral load and disease severity (51).

Likewise, the relationship between RDV dose and degree of viral reduction was readily observed in a rigorous study designed to investigate the optimal RDV dose for the treatment of EBOV in NHPs. Among the 12-day dosing regimens investigated in EBOV-challenged NHPs, two schedules initiated at 3 dpi yielded a 100% survival rate at 28 dpi: (i) 10 mg/kg and (ii) 10 mg/kg loading followed by 3 mg/kg maintenance for 11 days. Despite the fact that both schedules yielded the same survival efficacy, the authors note that "antiviral effects were consistently greater in animals administered repeated 10 mg/kg GS-5734 [RDV] doses (8)" (Fig. 4D). In fact, the direct relationship between drug dose, reduction in antiviral activity, and improved disease outcomes is most apparent in a comparison of the outcomes between the lowest (3 mg/kg beginning at 2 dpi) and highest (10 mg/kg beginning at 3 dpi) dosing regimens tested (Fig. 4D, light purple versus light blue): whereas the former yielded 66% survival by 28 dpi and moderate reductions in viral titers early in treatment, the latter yielded 100% survival by 28 dpi and robust reductions in viral titers early in treatment. In contrast to the large, unexplained disparities in survival for the 10/3-mg/kg dosing regimen (Fig. 4E, dark purple versus light purple), frank reductions in viral titers and 100% survival were unique to the 10-mg/kg D3 cohort (Fig. 4D and E, light blue). Viewed in totality, these data demonstrate that the antiviral effects of RDV can be augmented by up-dosing. As RDV had already been investigated for EBOV before SARS-CoV-2, knowledge of its safety and tolerability in healthy human volunteers had already been established (30) well before preclinical studies into its *in vivo* efficacy against SARS-CoV-2 had begun, and 10-mg/kg/day dosing was not evaluated (11). However, the dose-dependent decreases in viral titers with EBOV (8), coupled with the higher affinity of GS-443902 for the SARS-CoV-2 RdRp compared to the EBOV RdRp (23), strongly suggest that 10-mg/kg/day dosing would have demonstrated a more obvious antiviral benefit in NHP models.

Inadequate dosing of RDV in humans likely explains suboptimal antiviral effects for both COVID-19 and EBOV. Though Warren et al. concluded that 10-mg/kg/day dosing offered the best response in EBOV-challenged NHPs (8), liver-related DLTs in healthy human volunteers (Fig. 3) ultimately precluded administration at the human equivalent dose (HED) for the duration required for more dramatic reductions in viral titers in NHPs

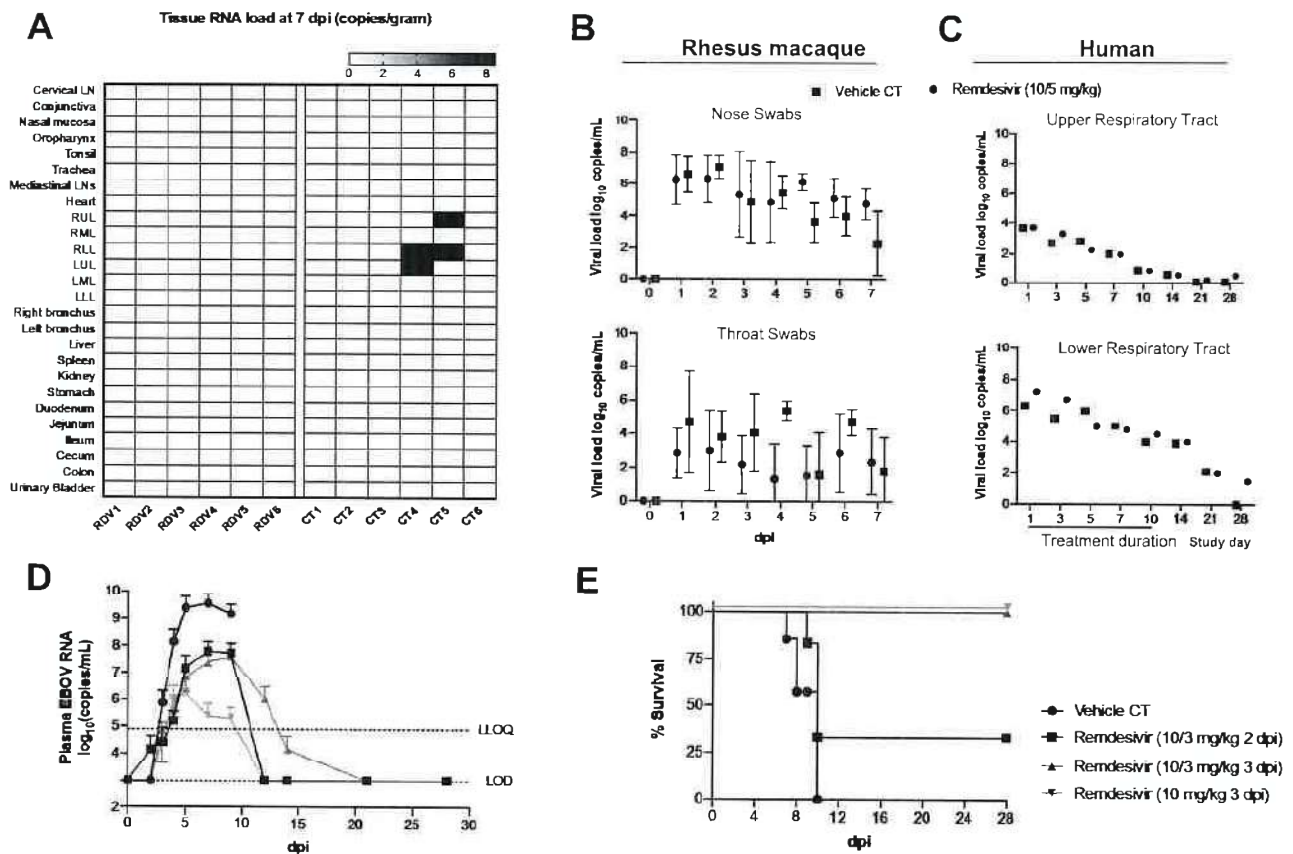


FIG 4 Human equivalent dose of RDV in rhesus macaque models of COVID-19 or EBOV does not yield robust reductions in viral titers. (A and B) SARS-CoV-2-infected rhesus macaques (2.6×10^6 50% tissue culture infective doses [TCID₅₀] of nCoV-WA1-2020) treated with the allometrically scaled dose of 10 mg/kg 1 dpi followed by 5 mg/kg 2 to 6 dpi yields a modest global reduction in SARS-CoV-2 viral titers. Data are adapted from the supplemental information in reference 11. (A) Heat map of organs profiled for the presence of SARS-CoV-2 RNA in RDV-treated ($n=6$) and control (CT) ($n=6$) animals. LN, lymph node; UL, upper lobe; ML, middle lobe; LL, lower lobe. (B) Viral loads in nose swabs and throat swabs between RDV-treated and CT animals. (C) No significant decrease in viral loads in the upper and lower respiratory tracts in patients treated with RDV (200 mg on day 1, 100 mg on days 2 to 10) was seen compared to placebo. Data are adapted from reference 2 and are presented as means ($n=107$ [RDV] and 52 [placebo]). (D) Rhesus macaques were infected with EBOV (1,000 PFU; EBOV *H. sapiens-tc/COD/1995/Kikwit*) and treated i.v. with either 10 mg/kg RDV at 2 dpi for 12 days (light blue), a 10-mg/kg loading dose at 3 dpi and then 3 mg/kg for 11 days (dark purple), a 10-mg/kg loading dose at 3 dpi and then 3 mg/kg for 11 days (light purple), or vehicle (black). Animals (6 per group) were monitored for a total of 28 days. The most distinct reductions in viral titers occurred for NHPs in the 10-mg/kg treatment group (light blue). (E) Survival curves for NHPs at 28 dpi for treatment groups indicated. Though viral titers dropped to the limit of detection (LOD) for the 10/3-mg/kg D2 group (D, dark purple D) by day 12, only 2/6 NHPs in this group survived (E, dark purple), skewing viral titer data. At the same time, this reinforces the close relationship between stark reductions in viral titers and improved disease outcomes, as the remaining 2/6 animals in the 10/3-mg/kg D2 (2 days postinfection) group survived at 28 dpi. Data are adapted from reference 8.

(30). If the 10-mg/kg RDV dose regimen had been directly translated in humans, an HED of 168 to 284 mg RDV for 12 days would have been administered. Instead, RDV was instead administered at 200 mg on day 1, followed by 100 mg from day 2 and continuing to days 9 to 13 for EBOV or days 2 to 10 for COVID-19 (1, 2, 45). These dosing schedules resemble the 10/3-mg/kg schedule used for NHPs challenged with EBOV or the 10/5-mg/kg schedule used for NHPs challenged with SARS-CoV-2, neither of which resulted in stark reductions in viral titers for their respective virus (Fig. 4B and D) (8, 11).

Viewed together, these data suggest that reductions in viral titers—and the closely related improvements in disease outcomes (Fig. 4D and E)—are dose dependent. Stronger antiviral effects by RDV would likely be observed in humans if it were possible to safely escalate the dose (41, 52). Considering the dose recommendations for RDV, large-scale studies on the relationship between up-dosing RDV and reductions in viral titers have thus not been conducted. However, there exists a single notable case report from 2015 documenting the effects of high-dose RDV in reducing EBOV titers in a Scottish nurse who relapsed with EBOV—the first time RDV had been administered in

an EBOV patient (52). While she had received other agents during her hospitalization, there was a period in which only RDV was administered on a compassionate-use basis—before safety in humans had been fully characterized. This patient received a daily i. v. infusion of 150 mg RDV for 3 days, which was then increased to 225 mg for 11 days. In addition to being the highest reported dosing schedule for any human, it most closely resembles the 12-day 10-mg/kg dosing schedule that was found to be most effective in the rhesus model of EBOV (8). While the report indicates that the first reported decline in viral RNA occurred 1 day before RDV treatment began, it is interesting that a sharp, sustained reduction in viral titers in cerebrospinal fluid (CSF) and plasma occurred during RDV treatment. Ultimately, clinical recovery was observed when RDV was supplemented with dexamethasone on day 4 of 14 of RDV treatment (52). Despite the inherent limitations of a case report, these data hint that up-dosing could clarify the magnitude of antiviral activity by RDV and could warrant further investigation into the dose-dependent nature of its antiviral activity in humans. Due to the low-grade transaminase elevations observed in healthy human volunteers treated with RDV (30), constraints on the RDV dose have understandably prevented larger-scale studies from being initiated to support initial observations made in the Scottish nurse case report (52). Both *in vitro* and phase 1 data indicate that the up-dosing that would be required to boost the presently questionable antiviral effects of RDV (2, 3) is precluded by its nephro- and hepatotoxicity (28, 30).

Against liver-derived cell lines and PHH *in vitro* (Fig. 1b), RDV demonstrated uniquely low 50% cytotoxic concentrations (CC_{50}) (2.5 to 6 μM) compared to $>100 \mu\text{M}$ for its parent nucleoside, GS-441524, which demonstrates similar anti-SARS-CoV-2 activity (28); this concurs with its putative mechanism of bioactivation by enzymes that are highly expressed in the liver (16). These *in vitro* data explain the dose duration-dependent emergence of low-grade transaminitis observed in the phase 1 dose escalation study in healthy human volunteers: administration of RDV at 150 mg for 7 or 14 days resulted in 25% and 75% of volunteers experiencing grade 1 and 2 ALT/AST elevations, respectively (Fig. 3A) (30). Likewise, the *in vitro* CC_{50} against renal proximal tubule epithelial cells (RPTECs), while not as low as that observed in liver cell lines, is considerably lower (12.9 μM) than that observed for its parent nucleoside ($>100 \mu\text{M}$) (Fig. S1) (28). Coupled with the documented renal elimination of the solubilizing excipient Captisol (53), the lower CC_{50} of RDV observed in kidney cells *in vitro* could partly explain observations of exacerbated kidney injury in patients with compromised renal function treated with RDV (41, 54). The latter explanation concurs with tissue distribution studies of the total nucleoside (GS-441524) and nucleotide metabolites (mono- and diphosphates of GS-441524 and the triphosphate, GS-443902) in NHPs following 10-mg/kg single-dose i.v. administration of RDV formulated with the Captisol-containing solution used in the clinic (36). Compared to NHP administered 20 mg/kg i.v. GS-441524 formulated without Captisol, a significantly higher proportion of total nucleoside and nucleotide metabolites were observed in the kidneys of NHPs dosed with RDV (Supplemental Fig. S1) (36). Thus, the unique sensitivity of liver and kidney cells to RDV due to its identity as a hydrophobic McGuigan prodrug (28)—reinforced by the liver- and kidney-related exclusion criteria in its clinical trials (1–3)—indicates that the up-dosing that would be required to boost RDV's antiviral effects would be likely to broadly result in concomitant hepato- and nephrotoxicity.

CONCLUSION

Preclinical evaluation of compounds should be dynamic. Especially in the case of prodrugs with short *in vivo* $t_{1/2}$, such as RDV, cell culture protocols should be revised upon receipt of *in vivo* data to better reflect the prodrug's pharmacokinetics *in vivo* (Table 1). Standard workflows appear to overemphasize low EC_{50} s while underappreciating the contributions of drug exposure, tissue-specific localization, and a drug's CC_{50} . While it is true that the exigency of the COVID-19 pandemic made RDV amenable to rapid investigation into its utility as a therapeutic, its underwhelming clinical

performance ought to have incited a meticulous investigation to identify reasons for RDV's discordant preclinical strength and clinical weakness. Assumptions inherent in cell-based screening protocols—while perhaps adequate for hard drugs—are poorly suitable for esterase-labile prodrugs such as RDV, in which transient exposure to the target cell population is exacerbated by uneven tissue metabolism (Table 1, assumptions 2 to 4) (26, 30, 31).

At the *in vivo* level, an overreliance on NHP models when studying McGuigan prodrugs fails to anticipate RDV's hepatotoxicity in humans at dosing intervals that are well tolerated in NHP, presumably due to species differences in hepatic extraction of McGuigan prodrugs (Fig. 3B and D). Based on studies spearheaded by Wang et al. with SOF (42), it appears that the efficiency of McGuigan prodrug metabolism in human hepatocytes is greater than that in NHPs but less than that in PXB mice and dogs (Fig. 3D). This would suggest that the contribution of dog models for safety and tolerability should not be underappreciated in favor of NHP models when considering the *in vivo* behavior of McGuigan prodrugs such as RDV. Stated simply, these data together indicate that conventional approaches to *in vitro* and *in vivo* studies for hard drugs are poorly suited to complex prodrugs like RDV. If the logic and interpretation of RDV preclinical data were correct, then a more distinct clinical benefit would be anticipated. This is not the case. The gap between the strong preclinical data (6, 8, 27) with RDV across many virus models and its questionable clinical activity (2, 3) suggests that assumptions are being made at the preclinical level that do not reflect the conditions observed in patients. In light of RDV's clinical performance, we have attempted to explain the causes for such a discordance by parsing the nuances of typical preclinical models used to judge RDV's efficacy. Our careful analysis offers insight that should be considered when selecting (phosphate) prodrugs for clinical advancement.

SUPPLEMENTAL MATERIAL

Supplemental material is available online only.

SUPPLEMENTAL FILE 1, PDF file, 0.1 MB.

SUPPLEMENTAL FILE 2, XLSX file, 0.04 MB.

ACKNOWLEDGMENTS

V.C.Y. is the CEO of Copycat Sciences, a company developing antiviral nucleoside analogues.

V.C.Y. performed research and analysis and wrote the manuscript. F.L.M. provided critical comments and assisted in the preparation of the manuscript.

REFERENCES

1. Beigel JH, Tomashek KM, Dodd LE, Mehta AK, Zingman BS, Kalil AC, Hohmann E, Chu HY, Luetkemeyer A, Kline S, Lopez de Castilla D, Finberg RW, Dierberg K, Tapson V, Hsieh L, Patterson TF, Paredes R, Sweeney DA, Short WR, Touloumi G, Lye DC, Ohmagari N, Oh M, Ruiz-Palacios GM, Benfield T, Fätkenheuer G, Kortepeter MG, Atmar RL, Creech CB, Lundgren J, Babiker AG, Pett S, Neaton JD, Burgess TH, Bonnett T, Green M, Makowski M, Osinusi A, Nayak S, Lane HC. 2020. Remdesivir for the treatment of Covid-19—final report. *N Engl J Med* 383:1813–1826. <https://doi.org/10.1056/NEJMoa2007764>.
2. Wang Y, Zhang D, Du G, Du R, Zhao J, Jin Y, Fu S, Gao L, Cheng Z, Lu Q, Hu Y, Luo G, Wang K, Lu Y, Li H, Wang S, Ruan S, Yang C, Mei C, Wang Y, Ding D, Wu F, Tang X, Ye X, Ye Y, Liu B, Yang J, Yin W, Wang A, Fan G, Zhou F, Liu Z, Gu X, Xu J, Shang L, Zhang Y, Cao L, Guo T, Wan Y, Qin H, Jiang Y, Jaki T, Hayden FG, Horby PW, Cao B, Wang C. 2020. Remdesivir in adults with severe COVID-19: a randomised, double-blind, placebo-controlled, multicentre trial. *Lancet* 395:1569–1578. [https://doi.org/10.1016/S0140-6736\(20\)31022-9](https://doi.org/10.1016/S0140-6736(20)31022-9).
3. WHO Solidarity Trial Consortium. 2020. Repurposed antiviral drugs for Covid-19—interim WHO Solidarity Trial results. *N Engl J Med* 384:497–511. <https://doi.org/10.1056/NEJMoa2023184>.
4. WHO. 2020. WHO recommends against the use of remdesivir in COVID-19 patients.
5. Pruijssers AJ, George AS, Schäfer A, Leist SR, Galinski LE, Dinnon KH, Yount BL, Agostini ML, Stevens LJ, Chappell JD, Lu X, Hughes TM, Gully K, Martinez DR, Brown AJ, Graham RL, Perry JK, Du Pont V, Pitts J, Ma B, Babusis D, Murakami E, Feng JY, Bilello JP, Porter DP, Cihlar T, Baric RS, Denison MR, Sheahan TP. 2020. Remdesivir inhibits SARS-CoV-2 in human lung cells and chimeric SARS-CoV expressing the SARS-CoV-2 RNA polymerase in mice. *Cell Rep* 32:107940. <https://doi.org/10.1016/j.celrep.2020.107940>.
6. Lo MK, Jordan R, Arvey A, Sudhamsu J, Shrivastava-Ranjan P, Hotard AL, Flint M, McMullan LK, Siegel D, Clarke MO, Mackman RL, Hui HC, Perron M, Ray AS, Cihlar T, Nichol ST, Spiropoulou CF. 2017. GS-5734 and its parent nucleoside analog inhibit filo-, pneumo-, and paramyxoviruses. *Sci Rep* 7:43395. <https://doi.org/10.1038/srep43395>.
7. Agostini ML, Andres EL, Sims AC, Graham RL, Sheahan TP, Lu X, Clinton Smith E, Brett Case J, Feng JY, Jordan R, Ray AS, Cihlar T, Siegel D, Mackman RL, Clarke MO, Baric RS, Denison MR, Agostini CM, Gallagher T. 2018. Coronavirus susceptibility to the antiviral remdesivir (GS-5734) is mediated by the viral polymerase and the proofreading exoribonuclease. *mBio* 9:e00221-18. <https://doi.org/10.1128/mBio.00221-18>.
8. Warren TK, Jordan R, Lo MK, Ray AS, Mackman RL, Soloveva V, Siegel D, Perron M, Bannister R, Hui HC, Larson N, Strickley R, Wells J, Stuthman KS, Van Tongeren SA, Garza NL, Donnelly G, Shurtleff AC, Retterer CJ, Gharaibeh D, Zamani R, Kenny T, Eaton BP, Grimes E, Welch LS, Gomba L, Wilhelmsen CL, Nichols DK, Nuss JE, Nagle ER, Kugelman JR, Palacios G, Doerffler E, Neville S, Carra E, Clarke MO, Zhang L, Lew W, Ross B, Wang Q,

- Chun K, Wolfe L, Babusis D, Park Y, Stray KM, Trancheva I, Feng JY, Barauskas O, Xu Y, Wong P, Braun MR, Flint M, et al. 2016. Therapeutic efficacy of the small molecule GS-5734 against Ebola virus in rhesus monkeys. *Nature* 531:381–385. <https://doi.org/10.1038/nature17180>.
9. Sheahan TP, Sims AC, Graham RL, Menachery VD, Gralinski LE, Case JB, Leist SR, Pyrc K, Feng JY, Trancheva I, Bannister R, Park Y, Babusis D, Clarke MO, Mackman RL, Spahn JE, Palmiotti CA, Siegel D, Ray AS, Cihlar T, Jordan R, Denison MR, Baric RS. 2017. Broad-spectrum antiviral GS-5734 inhibits both epidemic and zoonotic coronaviruses. *Sci Transl Med* 9:eal3653. <https://doi.org/10.1126/scitranslmed.aal3653>.
 10. de Wit E, Feldmann F, Cronin J, Jordan R, Okumura A, Thomas T, Scott D, Cihlar T, Feldmann H. 2020. Prophylactic and therapeutic remdesivir (GS-5734) treatment in the rhesus macaque model of MERS-CoV infection. *Proc Natl Acad Sci U S A* 117:6771–6776. <https://doi.org/10.1073/pnas.1922083117>.
 11. Williamson BN, Feldmann F, Schwarz B, Meade-White K, Porter DP, Schulz J, Van Doremalen N, Leighton I, Yinda CK, Pérez-Pérez L, Okumura A, Lovaglio J, Hanley PW, Saturday G, Bosio CM, Anzick S, Barbian K, Cihlar T, Martens C, Scott DP, Munster VJ, De Wit E. 2020. Clinical benefit of remdesivir in rhesus macaques infected with SARS-CoV-2. *Nature* 585:273–276. <https://doi.org/10.1038/s41586-020-2423-5>.
 12. Rautio J, Meanwell NA, Di L, Hageman MJ. 2018. The expanding role of prodrugs in contemporary drug design and development. *Nat Rev Drug Discov* 17:559–587. <https://doi.org/10.1038/nrd.2018.46>.
 13. Butler T, Cho A, Kim C, Saunders OL, Zhang L. October 2009. 1'-substituted carba-nucleoside analogues for antiviral treatment. Patent WO2009132135. World Intellectual Property Organization.
 14. Lawitz E, Hill J, Marbury T, Hazan D, Gruener D, Webster L, Majauskas R, Morrison R, DeMicco M, German P, Stefanidis D, Svarovskaia E, Arterburn S, Ray A, Rossi S, McHutchinson J, Rodriguez-Torres M. 2012. GS-6620, a liver-targeted nucleotide prodrug, exhibits antiviral activity and favorable safety profile over 5 days in treatment naïve chronic HCV genotype 1 subjects. *EASL 47th Annual Meeting*, Barcelona, Spain.
 15. Cho A, Zhang L, Xu J, Lee R, Butler T, Metobo S, Aktoudianakis V, Lew W, Ye H, Clarke M, Doerffler E, Byun D, Wang T, Babusis D, Carey AC, German P, Sauer D, Zhong W, Rossi S, Fenaux M, McHutchinson JG, Perry J, Feng J, Ray AS, Kim CU. 2014. Discovery of the first C-nucleoside HCV polymerase inhibitor (GS-6620) with demonstrated antiviral response in HCV infected patients. *J Med Chem* 57:1812–1825. <https://doi.org/10.1021/jm400201a>.
 16. Murakami E, Wang T, Babusis D, Lepist E-I, Sauer D, Park Y, Vela JE, Shih R, Birkus G, Stefanidis D, Kim CU, Cho A, Ray AS. 2014. Metabolism and pharmacokinetics of the anti-hepatitis C virus nucleotide prodrug GS-6620. *Antimicrob Agents Chemother* 58:1943–1951. <https://doi.org/10.1128/AAC.02350-13>.
 17. Mehellou Y, Rattan HS, Balzarini J. 2018. The ProTide prodrug technology: from the concept to the clinic. *J Med Chem* 61:2211–2226. <https://doi.org/10.1021/acs.jmedchem.7b00734>.
 18. Ma H, Jiang WR, Robledo N, Leveque V, Ali S, Lara-Jaime T, Masjedizadeh M, Smith DB, Cammack N, Klump K, Symons J. 2007. Characterization of the metabolic activation of hepatitis C virus nucleoside inhibitor β -D-2'-deoxy-2'-fluoro-2'-C-methylcytidine (PSI-6130) and identification of a novel active 5'-triphosphate species. *J Biol Chem* 282:29812–29820. <https://doi.org/10.1074/jbc.M705274200>.
 19. Perrone P, Daverio F, Valente R, Rajyaguru S, Martin JA, Lévêque V, Le Pogam S, Najera I, Klump K, Smith DB, Mcguigan C. 2007. First example of phosphoramidate approach applied to a 4'-substituted purine nucleoside (4'-azidoadenosine): conversion of an inactive nucleoside to a submicromolar compound versus hepatitis C virus. *J Med Chem* 50:5463–5470. <https://doi.org/10.1021/jm070362i>.
 20. Heinemann V, Hertel LW, Grindey GB, Plunkett W. 1988. Comparison of the cellular pharmacokinetics and toxicity of 2',2'-difluorodeoxycytidine and 1- β -D-arabinofuranosylcytosine. *Cancer Res* 48:4024–4031.
 21. Li Y, Cao L, Li G, Cong F, Li Y, Sun J, Luo Y, Chen G. 2021. Remdesivir metabolite GS-441524 effectively inhibits SARS-CoV-2 infection in mouse models. *J Med Chem* <https://doi.org/10.1021/acs.jmedchem.0c01929>
 22. Murphy BG, Perron M, Murakami E, Bauer K, Park Y, Eckstrand C, Liepnieks M, Pedersen NC. 2018. The nucleoside analog GS-441524 strongly inhibits feline infectious peritonitis (FIP) virus in tissue culture and experimental cat infection studies. *Vet Microbiol* 219:226–233. <https://doi.org/10.1016/j.vetmic.2018.04.026>.
 23. Gordon CJ, Tchesnokov EP, Woolner E, Perry JK, Feng JY, Porter DP, Götte M. 2020. Remdesivir is a direct-acting antiviral that inhibits RNA-dependent RNA polymerase from severe acute respiratory syndrome coronavirus 2 with high potency. *J Biol Chem* 295:6785–6797. <https://doi.org/10.1074/jbc.RA120.013679>.
 24. Tchesnokov EP, Gordon CJ, Woolner E, Kocincova D, Perry JK, Feng JY, Porter DP, Gotte M. 2020. Template-dependent inhibition of coronavirus RNA-dependent RNA polymerase by remdesivir reveals a second mechanism of action. *J Biol Chem* 295:16156–16165. <https://doi.org/10.1074/jbc.AC120.015720>.
 25. Yin W, Mao C, Luan X, Shen DD, Shen Q, Su H, Wang X, Zhou F, Zhao W, Gao M, Chang S, Xie YC, Tian G, Jiang HW, Tao SC, Shen J, Jiang Y, Jiang H, Xu Y, Zhang S, Zhang Y, Xu HE. 2020. Structural basis for inhibition of the RNA-dependent RNA polymerase from SARS-CoV-2 by remdesivir. *Science* 368:1499–1504. <https://doi.org/10.1126/science.abc1560>.
 26. Yan VC, Muller FL. 2020. Advantages of the parent nucleoside GS-441524 over remdesivir for Covid-19 treatment. *ACS Med Chem Lett* 11:1361–1366. <https://doi.org/10.1021/acsmchemlett.0c00316>.
 27. Siegel D, Hui HC, Doerffler E, Clarke MO, Chun K, Zhang L, Neville S, Carra E, Lew W, Ross B, Wang Q, Wolfe L, Jordan R, Soloveva V, Knox J, Perry J, Perron M, Stray KM, Barauskas O, Feng JY, Xu Y, Lee G, Rheingold AL, Ray AS, Bannister R, Strickley R, Swaminathan S, Lee WA, Bavari S, Cihlar T, Lo MK, Warren TK, Mackman RL. 2017. Discovery and synthesis of a phosphoramidate prodrug of a pyrrolo[2,1-f][triazin-4-amino] adenine C-nucleoside (GS-5734) for the treatment of Ebola and emerging viruses. *J Med Chem* 60:1648–1661. <https://doi.org/10.1021/acsmchem.6b01594>.
 28. Xu Y, Barauskas O, Kim C, Babusis D, Murakami E, Kornyejev D, Lee G, Stepan G, Perron M, Bannister R, Schultz BE, Sakowicz R, Porter D, Cihlar T, Feng JY. 2021. Off-target in vitro profiling demonstrates that remdesivir is a highly selective antiviral Agent. *Antimicrob Agents Chemother* 65:e02237-20. <https://doi.org/10.1128/AAC.02237-20>.
 29. Wang M, Cao R, Zhang L, Yang X, Liu J, Xu M, Shi Z, Hu Z, Zhong W, Xiao G. 2020. Remdesivir and chloroquine effectively inhibit the recently emerged novel coronavirus (2019-nCoV) in vitro. *Cell Res* 30:269–271. <https://doi.org/10.1038/s41422-020-0282-0>.
 30. Humeniuk R, Mathias A, Cao H, Osinusi A, Shen G, Chng E, Ling J, Vu A, German P. 2020. Safety, tolerability, and pharmacokinetics of remdesivir, an antiviral for treatment of COVID-19, in healthy subjects. *Clin Transl Sci* 13:896–906. <https://doi.org/10.1111/cts.12840>.
 31. Tempestilli M, Caputi P, Avataneo V, Notari S, Forini O, Scorzolini L, Marchioni L, Bartoli TA, Castillette C, Lalle E, Capobianchi MR, Nicastrì E, D'Avolio A, Ippolito G, Agrati C. 2020. Pharmacokinetics of remdesivir and GS-441524 in two critically ill patients who recovered from COVID-19. *J Antimicrob Chemother* 75:2977–2980. <https://doi.org/10.1093/jac/dkaa239>.
 32. European Medicines Agency. 2020. Remdesivir: summary on compassionate use EMA/178637/2020 - Rev. 1.
 33. Frisk-Holmberg M, Bergqvist Y, Termond E, Domeij-Nyberg B. 1984. The single dose kinetics of chloroquine and its major metabolite desethylchloroquine in healthy subjects. *Eur J Clin Pharmacol* 26:521–530. <https://doi.org/10.1007/BF00542151>.
 34. Vries PJ, Oosterhuis B, Bostel CJ. 1994. Single-dose pharmacokinetics of chloroquine and its main metabolite in healthy volunteers. *Drug Invest* 8:143–149. <https://doi.org/10.1007/BF03259430>.
 35. Oerlemans R, Van Der Heijden J, Vink J, Dijkmans BAC, Kaspers GJL, Lems WF, Scheffer GL, Ifergan I, Scheper RJ, Cloos J, Assaraf YG, Jansen G. 2006. Acquired resistance to chloroquine in human CEM T cells is mediated by multidrug resistance-associated protein 1 and provokes high levels of cross-resistance to glucocorticoids. *Arthritis Rheum* 54:557–568. <https://doi.org/10.1002/art.21569>.
 36. Mackman RL, Hui HC, Perron M, Murakami E, Palmiotti C, Lee G, Stray K, Zhang L, Goyal B, Chun K, Byun D, Siegel D, Simonovich S, Du Pont V, Pitts J, Babusis D, Vijayapurapu A, Lu X, Kim C, Zhao X, Chan J, Ma B, Lye D, Vandersteent A, Wortman S, Barrett KT, Toteva M, Jordan R, Subramanian R, Bilello JP, Cihlar T. 2021. Prodrugs of a 1'-CN-4-aza-7,9-dideazaadenosine C-nucleoside leading to the discovery of remdesivir (GS-5734) as a potent inhibitor of respiratory syncytial virus with efficacy in the African green monkey model of RSV. *J Med Chem* 64:5001–5017. <https://doi.org/10.1021/acs.jmedchem.1c00071>.
 37. Xie X, Muruato AE, Zhang X, Lokugamage KG, Fontes-Garfias CR, Zou J, Liu J, Ren P, Balakrishnan M, Cihlar T, Tseng CTK, Makino S, Menachery VD, Bilello JP, Shi PY. 2020. A nanoluciferase SARS-CoV-2 for rapid neutralization testing and screening of anti-infective drugs for COVID-19. *Nat Commun* 11:5214. <https://doi.org/10.1038/s41467-020-19055-7>.
 38. Goldman JD, Lye DCB, Hui DS, Marks KM, Bruno R, Montejano R, Spinner CD, Galli M, Ahn M-Y, Nahass RG, Chen Y-S, SenGupta D, Hyland RH, Osinusi AO, Cao H, Blair C, Wei X, Gaggari A, Brainard DM, Towner WJ, Muñoz J, Mullane KM, Marty FM, Tashima KT, Diaz G, Subramanian A, GS-

- US-540–5773 Investigators. 2020. Remdesivir for 5 or 10 days in patients with severe Covid-19. *N Engl J Med* 383:1827–1837. <https://doi.org/10.1056/NEJMoa2015301>.
39. Spinner CD, Gottlieb RL, Criner GJ, Arribas López JR, Cattelan AM, Soriano Viladomiu A, Ogbuagu O, Malhotra P, Mullane KM, Castagna A, Chai LYA, Roestenberg M, Tsang OTY, Bernasconi E, Le Turnier P, Chang S-C, SenGupta D, Hyland RH, Osinusi AO, Cao H, Blair C, Wang H, Gaggar A, Brainard DM, McPhail MJ, Bhagani S, Ahn MY, Sanyal AJ, Huhn G, Marty FM, GS-US-540–5774 Investigators. 2020. Effect of remdesivir vs standard care on clinical status at 11 days in patients with moderate COVID-19. *JAMA* 324:1048–1057. <https://doi.org/10.1001/jama.2020.16349>.
 40. West GB, Brown JH. 2005. The origin of allometric scaling laws in biology from genomes to ecosystems: towards a quantitative unifying theory of biological structure and organization. *J Exp Biol* 208:1575–1592. <https://doi.org/10.1242/jeb.01589>.
 41. Yan VC, Muller FL. 2021. Remdesivir for COVID-19: why not dose higher? *Antimicrob Agents Chemother* 65:e2713–20. <https://doi.org/10.1128/AAC.02713-20>.
 42. Wang T, Babusis D, Park Y, Niu C, Kim C, Zhao X, Lu B, Ma B, Muench RC, Sperger D, Ray AS, Murakami E. 2020. Species differences in liver accumulation and metabolism of nucleotide prodrug sofosbuvir. *Drug Metab Pharmacokinet* 35:334–340. <https://doi.org/10.1016/j.dmpk.2020.04.333>.
 43. Babusis D, Curry MP, Kirby B, Park Y, Murakami E, Wang T, Mathias A, Afdhal N, McHutchison JG, Ray AS. 2018. Sofosbuvir and ribavirin liver pharmacokinetics in patients infected with hepatitis C virus. *Antimicrob Agents Chemother* 62:e02587–17. <https://doi.org/10.1128/AAC.02587-17>.
 44. Higgs ES, Gayedyu-Dennis D, Fisher W, Nason M, Reilly C, Beavogui AH, Aboulhab J, Nordwall J, Lobbo P, Wachekwa I, Cao H, Cihlar T, Hensley L, Lane HC. 2021. PREVAL IV: a randomized, double-blind, two-phase, phase 2 trial of remdesivir versus placebo for reduction of Ebola virus RNA in the semen of male survivors. *Clin Infect Dis* <https://doi.org/10.1093/cid/ciab215>. Epub ahead of print.
 45. Mulangu S, Dodd LE, Davey RT, Tshiani Mbaya O, Proschan M, Mukadi D, Lusakibanza Manzo M, Nzolo D, Tshomba Oloma A, Ibanda A, Ali R, Coulibaly S, Levine AC, Grais R, Diaz J, Lane HC, Muyembe-Tamfum J-J, Sivahera B, Camara M, Kojan R, Walker R, Dighero-Kemp B, Cao H, Mukumbayi P, Mbala-Kingebeni P, Ahuka S, Albert S, Bonnett T, Crozier I, Duvenhage M, Proffitt C, Teitelbaum M, Moench T, Aboulhab J, Barrett K, Cahill K, Cone K, Eckes R, Hensley L, Herpin B, Higgs E, Ledgerwood J, Pierson J, Smolskis M, Sow Y, Tierney J, Sivapalasingam S, Holman W, Gettinger N, Vallée D, the PALM Writing Group, et al. 2019. A randomized, controlled trial of Ebola virus disease therapeutics. *N Engl J Med* 381:2293–2303. <https://doi.org/10.1056/NEJMoa1910993>.
 46. Buckland MS, Galloway JB, Fhogartaigh CN, Meredith L, Provine NM, Bloor S, Ogbe A, Zelek WM, Smielewska A, Yakovleva A, Mann T, Bergamaschi L, Turner L, Mescia F, Toonen EJM, Hackstein CP, Akther HD, Vieira VA, Cerón-Gutiérrez L, Periseleris J, Kiani-Alikhan S, Grigoriadou S, Vaghela D, Lear SE, Török ME, Hamilton WL, Stockton J, Quick J, Nelson P, Hunter M, Coulter Ti, Devlin L, Bradley JR, Smith KGC, Ouwehand WH, Estcourt L, Harvala H, Roberts DJ, Wilkinson IB, Screation N, Loman N, Doffinger R, Lyons PA, Morgan BP, Goodfellow IG, Klenerman P, Lehner PJ, Matheson NJ, Thaventhiran JED, MRC-Toxicology Unit COVID-19 Consortium. 2020. Treatment of COVID-19 with remdesivir in the absence of humoral immunity: a case report. *Nat Commun* 11:6385. <https://doi.org/10.1038/s41467-020-19761-2>.
 47. Boshier FAT, Pang J, Penner J, Hughes J, Parker M, Shepherd J, Alders N, Bamford A, Grandjean L, Grunewald S, Hatcher J, Best T, Dalton C, Bynoe PD, Frauenfelder C, Köeglmeier J, Myerson P, Roy S, Williams R, Thomson EC, de Silva TI, Goldstein RA, Breuer J. 2020. Remdesivir induced viral RNA and subgenomic RNA suppression, and evolution of viral variants in SARS-CoV-2 infected patients. medRxiv <https://doi.org/10.1101/2020.11.18.20230599>.
 48. Food and Drug Administration. 2020. VEKLURY (remdesivir). https://www.accessdata.fda.gov/drugsatfda_docs/label/2020/214787Orig1s000lbl.pdf.
 49. Fiege JK, Thiede JM, Nanda HA, Matchett WE, Moore PJ, Montanari NR, Thielen BK, Daniel J, Stanley E, Hunter RC, Menachery VD, Shen SS, Bold TD, Langlois RA. 2021. Single cell resolution of SARS-CoV-2 tropism, antiviral responses, and susceptibility to therapies in primary human airway epithelium. *PLoS Pathog* 17:e1009292. <https://doi.org/10.1371/journal.ppat.1009292>.
 50. Munster VJ, Feldmann F, Williamson BN, van Doremalen N, Pérez-Pérez L, Schulz J, Meade-White K, Okumura A, Callison J, Brumbaugh B, Avanzato VA, Rosenke R, Hanley PW, Saturday G, Scott D, Fischer ER, de Wit E. 2020. Respiratory disease in rhesus macaques inoculated with SARS-CoV-2. *Nature* 585:268–272. <https://doi.org/10.1038/s41586-020-2324-7>.
 51. Fajnzylber J, Regan J, Coxen K, Corry H, Wong C, Rosenthal A, Worrall D, Giguél P, Piechocka-Trocha A, Atyeo C, Fischinger S, Chan A, Flaherty KT, Hall K, Dougan M, Ryan ET, Gillespie E, Chishti R, Li Y, Jilg N, Hanidziar D, Baron RM, Baden L, Tsibris AM, Armstrong KA, Kuritzkes DR, Alter G, Walker BD, Yu X, Li JZ, Abayneh B(B), Allen P, Antille D, Balazs A, Bals J, Barbash M, Bartsch Y, Boucau J, Boyce S, Braley J, Branch K, Broderick K, Carney J, Chevalier J, Choudhary MC, Chowdhury N, Cordwell T, Daley G, Davidsons S, Desjardins M, The Massachusetts Consortium for Pathogen Readiness, et al. 2020. SARS-CoV-2 viral load is associated with increased disease severity and mortality. *Nat Commun* 11:5493. <https://doi.org/10.1038/s41467-020-19057-5>.
 52. Jacobs M, Rodger A, Bell DJ, Bhagani S, Cropley I, Filipe A, Gifford RJ, Hopkins S, Hughes J, Jabeen F, Johannessen I, Karageorgopoulos D, Lackenby A, Lester R, Liu RSN, MacConnachie A, Mahungu T, Martin D, Marshall N, Mephram S, Orton R, Palmarini M, Patel M, Perry C, Peters SE, Porter D, Ritchie D, Ritchie ND, Seaton RA, Sreenu VB, Templeton K, Warren S, Wilkie GS, Zambon M, Gopal R, Thomson EC. 2016. Late Ebola virus relapse causing meningoencephalitis: a case report. *Lancet* 388:498–503. [https://doi.org/10.1016/S0140-6736\(16\)30386-5](https://doi.org/10.1016/S0140-6736(16)30386-5).
 53. Stella V, He Q. 2008. Cyclodextrins. *Toxicol Pathol* 36:30–42. <https://doi.org/10.1177/0192623307310945>.
 54. Lê MP, Le Hingrat Q, Jaquet P, Wicky PH, Bunel V, Massias L, Visseaux B, Messika J, Descamps D, Mal H, Timsit JF, Peytavin G. 2020. Removal of remdesivir's metabolite GS-441524 by hemodialysis in a double lung transplant recipient with COVID-19. *Antimicrob Agents Chemother* 64:e01521–20. <https://doi.org/10.1128/AAC.01521-20>.
 55. Akinci E, Cha M, Lin L, Yeo G, Hamilton MC, Donahue CJ, Bermudez-Cabrera HC, Zanetti LC, Chen M, Barkal SA, Khowpinitchai B, Chu N, Velimirovic M, Jodhani R, Fife JD, Sovrovic M, Cole PA, Davey RA, Cassa CA, Sherwood RI. 2020. Elucidation of remdesivir cytotoxicity pathways through genome-wide CRISPR-Cas9 screening and transcriptomics. *bioRxiv* 2020.08.27.270819.
 56. Brunetti-Pierri N, Liou A, Patel P, Palmer D, Grove N, Finegold M, Piccolo P, Donnachie E, Rice K, Beaudet A, Mullins C, Ng P. 2012. Balloon catheter delivery of helper-dependent adenoviral vector results in sustained, therapeutic hFIX expression in rhesus macaques. *Mol Ther* 20:1863–1870. <https://doi.org/10.1038/mt.2012.143>.

Minireview

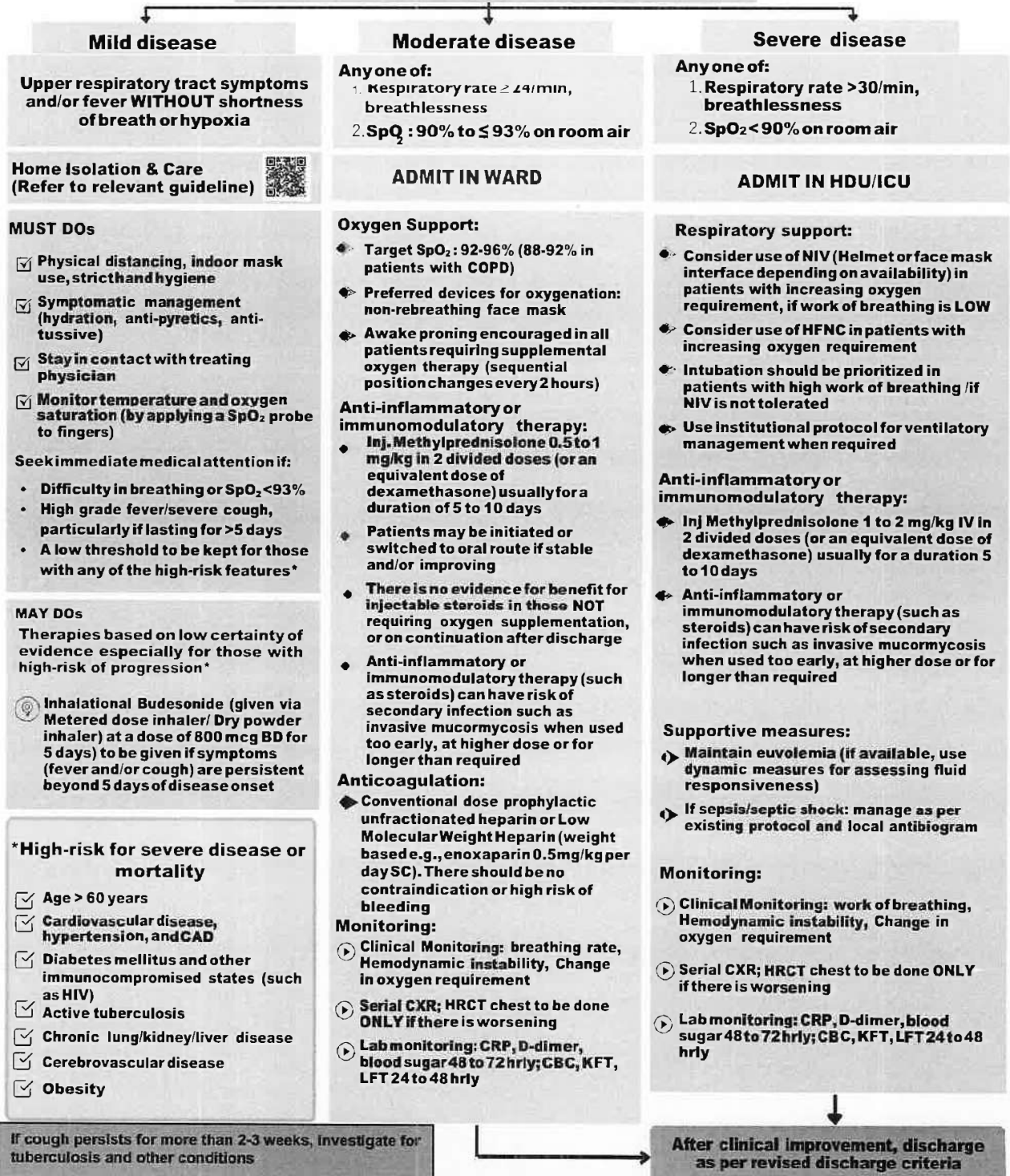
Victoria C. Yan, M.S. received her undergraduate degree in biochemistry from Mount Holyoke College in 2018 and her M.S. in therapeutics & pharmacology from the University of Texas Health Science Center at Houston/MD Anderson Cancer Center in 2020. As a master's student in the lab of Florian Muller, she developed novel methods for the synthesis of phosphoramidate prodrugs and synthesized several prodrugs of a phosphonate-containing inhibitor of enolase 2 for the treatment of cancers harboring deletions of enolase 1. During the COVID-19 pandemic, she directed her knowledge of phosph(on)ate prodrug metabolism to remdesivir and has been advocating the use of its parent nucleoside, GS-441524, for COVID-19 treatment. Ms. Yan is the first to report the safety, tolerability, and pharmacokinetics of orally administered GS-441524 in women. As an extension of her graduate work, she founded Copycat Sciences, a phosph(on)ate prodrug company, with foci in virology, precision oncology, and inborn errors of metabolism.



Florian L. Muller, Ph.D., received his undergraduate degree from Washington State University and his Ph.D. from the University of Texas Health Science Center at San Antonio in 2007. His undergraduate and graduate careers were dedicated to the study of mitochondrial reactive oxygen species in aging and neurodegenerative disease. During his postdoctoral training, Dr. Muller joined the lab of Ron DePinho, where he applied his training in basic biochemistry to precision oncology, demonstrating the utility of passenger genomic deletions of metabolic enzymes, as pharmacologically targetable vulnerabilities in cancer. As an assistant professor at M.D. Anderson Cancer Center, he brought this concept closer to the clinic by synthesizing small molecules exploiting such vulnerabilities. This led to the development of novel phosphonate prodrugs, the knowledge of which became relevant during COVID-19 given remdesivir's identity as a phosphate prodrug. Dr. Muller is currently a senior director at Sporos Bioventures, a venture capital firm specializing in early oncology startups.



Adult patient diagnosed with COVID-19



Scan QR Code to access Clinical guidance for management of adult COVID-19 patients

EUA/Off label use (based on limited available evidence and only in specific circumstances):

Remdesivir (EUA) may be considered ONLY in patients with

- 10 days of onset of symptoms, in those having moderate to severe disease (requiring supplemental oxygen), but who are NOT on IMV or ECMO
- Consider remdesivir for 5 days to treat hospitalized patients with COVID-19 (No evidence of benefit for treatment more than 5 days)
- NOT to be used in patients who are NOT on oxygen support or in home setting
- Monitor for RFT and LFT (remdesivir not recommended if eGFR <30 ml/min/m²; AST/ALT >5 times UNL) (not an absolute contraindication)
- Recommended dose: 200 mg IV on day 1 followed by 100 mg IV OD for next 4 days

Tocilizumab may be considered when ALL OF THE BELOW CRITERIA ARE MET

- Rapidly progressing COVID-19 needing oxygen supplementation or IMV and not responding adequately to steroids (preferably within 24-48 hours of onset of severe disease/ ICU admission)
- Preferably to be given with steroids
- No active TB, fungal, systemic bacterial infection
- Long term follow up for secondary infections (such as reactivation of TB, Flaring of Herpes etc.)
- Significantly raised inflammatory markers (CRP and/or IL-6)
- Recommended single dose: 4 to 6 mg/kg (400 mg in 60 kg adult) in 100 ml NS over 1 hour

